Investigating the Environmental Fate of Iodinated X-ray Contrast Media in the Urban Water Cycle:

Identification, Characterization, and Occurrence of Biotransformation Products

Dissertation

Zur Erlangung des akademischen Grades

eines Doktors der Naturwissenschaft

Fachbereich 3:

Mathematik/Naturwissenschaften Universität Koblenz-Landau

Vorgelegt

am 28.05.2010

von Jennifer Lynne Kormos, M.Sc.

geb. am. 13.11.1979 in St. John's, Canada

Referent: PD Dr. Thomas A. Ternes

Koreferent: Prof. Dr. Joachim Scholz

Acknowledgments

This thesis is the result of a collaborative effort from many people! First of all I would like to thank the Marie Curie Research Training Network KEYBIOEFFECTS for funding this research and more importantly providing opportunities for me to network with other graduate students and research scientists in a number of scientific disciplines within Europe and internationally.

I would like to thank and acknowledge Dr. Thomas Ternes, my supervisor, or as they say in German my "Doktor Vater," for giving me the opportunity to complete my PhD in his research group at the Federal Institute of Hydrology (Bundesanstalt für Gewässerkunde, BfG). It was an honour for me to work with an internationally-known researcher investigating the occurrence and fate of emerging organic micropollutants. His dedication, guidance, support, enthusiasm and extensive knowledge are just a few of his qualities that helped me to strive in completing my PhD degree.

I would like to thank Prof. Dr. Joachim Scholz for agreeing to be one of the evaluators of my PhD thesis and the University of Koblenz-Landau for allowing me to defend my dissertation in the Department of Chemistry.

Collaborations with Dr. Manfred Wagner and Dr. Hans-Peter Kohler give me opportunity to extend my knowledge in NMR analysis and microbial pathways. These two researchers provided fruitful discussions in their area of interest and I thank them for providing their expertise to this thesis.

I want to say a big thank-you to my colleagues in G2, who really became my family and support system away from home! My G2 family includes Angela, Anne, Arne, Burkhard, Carsten,

Conny, Dennis, Dirk, Guido, Harald, Jelena, Michael, Olena, and Thomas. I would also like to acknowledge the "G2 Alumni" including Bianca, Karoline, Marco, Steffi, Stefan, and Uta. I really was fortunate to work with a great bunch of people! I hope most of them will make a trip to Canada some day!

I would like to especially thank Carmen, my office mate for the last 3 years. I enjoyed chatting with her and definitely made my time sitting in front of the computer more enjoyable! I also want to say a special thanks to Corinna who was the social planner of the group, who allowed me to experience different things outside of work!

I do not know how I could have accomplished everything in the last 3 years, if it was not for Manoj. Thanks so much Manoj for your generosity, hard work and willingness to help me with my research.

I do not think I can fully express how much Jessica, my Superstar, was involved in supporting, motivating, guiding me and being a great friend during my time in Germany. She was my shoulder and my rock during the good times and bad times. I will always cherish our friendship…I think I would have been lost with her!

Even though, I did not get to know Saskia until the end of my time in Germany, we became friends quite quickly. She has such a positive energy about her…this is one of the things that really helped me to continue and finish my thesis.

I would like to thank my girls back home, Anne, Brianne, Patricia, Marwah, Natasha and Tejal, for being so supported when I told them that I was moving to Germany, and being understanding about the 6 hour time difference phone calls.

Of course none of my accomplishments within the last 3 years would have happened if it was not for the support and love I received from friends and family members in Canada. I especially want to thank my parents, who provided me with the strength and motivation to successfully complete this adventure….

Table of Contents

Summary

Iodinated X-ray contrast media (ICM) are a group of emerging contaminants which have been detected at elevated concentrations in the aquatic environment. These compounds are excreted unmetabolized into hospital wastewater, and eventually treated at wastewater treatment plants (WWTPs). The removal of ICM in WWTPs has not been very effective and therefore the ICM enter the aquatic environment via WWTP effluent discharges. Research has investigated the removal of selected ICM via abiotic and biotic processes, however limited work has attempted to determine the fate of these compounds once released into the environment.

This thesis investigates the biotransformation of four selected ICM (diatrizoate, iohexol, iomeprol, and iopamidol) in aerobic soil-water and sediment-water systems as well as in different environmental matrices. Iohexol, iomeprol and iopamidol were biotransformed to several TPs in the aerobic batch systems, while no biotransformation was observed for the ionic ICM, diatrizoate. In total 34 biotransformation products (TPs) of the three non-ionic ICM were identified. The combination of semi-preparative HPLC-UV, hybrid triple quadrupole-linear ion trap mass spectrometry (Qq-LIT-MS) was found to be an accurate approach for the structural elucidation of ICM TPs. The ICM TPs resulted in microbial transformation occurring at the side chains of the parent ICM, with the iodinated aromatic ring unmodified.

Biotransformation rate constants were calculated for the parent ICM in different batch systems and it was found that zero-order reactions could be used to explain the biotransformation observed in the different aerobic systems. Lower rate constants were reported for iopamidol compared to iohexol and iomeprol. The slower biotransformation of iopamidol could be related to the increase in steric hindrance of branched hydroxylated side chains of iopamidol. The

elevated concentrations of iopamidol detected in real environmental samples correlates well to the slow transformation observed in the aerobic batch systems.

Based on the chemical structures and the sequence of TP formation in the batch systems three reactions types were suggested which could be responsible for non-ionic ICM biotransformation. It appears that that the primary hydroxylated moieties are oxidized first, followed by decarboxylation and cleavage of the N-C bond (i.e. deacetylation and removal of hydroxylated propanoic acids). The microbial transformation pathways were proposed for all three non-ionic.

A LC tandem MS method was developed to investigate the occurrence of the identified TPs in WWTPs, surface water, groundwater and drinking water. It was found that up to 80% of iohexol, iomeprol and iopromide could be transformed during biological treatment in WWTPs resulting in the formation of ICM TPs. Minimal removal was observed for diatrizoate as well as iopamidol. ICM TPs were also found in surface waters at concentrations > 100 ng/L for some TPs (i.e. iomeprol TP687 and TP629). In addition, stable TPs were formed during soil passage and bank filtration, suggesting a potential removal option for the parent ICM, but resulting in the formation of stable TPs. The presence of these stable TPs in groundwater or ground water influenced by surface water is of concern if these water resources are use for drinking water production. Samples collected from selected drinking water production facilities show that certain ICM TPs are not effectively removed by flocculation, sand filtration, ozonation and in some cases GAC filtration.

The results presented in this thesis provide an example of how important it is to investigate the fate of compounds when assessing the environmental risk. For the case of ICM, the parent compounds were not found at high concentrations in raw water or treated drinking water, but the

formation of stable TPs resulted in contamination of groundwater and drinking water supplies. The impact of these TPs in drinking water supplies is not currently known, but in order to provide a comprehensive risk assessment of ICM, TPs should be considered to some extent when determining the risk.

1 General Introduction

1.1 Iodinated X-ray Contrast Media (ICM)

X-ray contrast media, also referred to as radiopaque agents or diagnostic aids, are a class of pharmaceuticals used for the imaging of internal organs, blood vessels and soft tissues during radiological and medical diagnostic procedures (Pérez and Barceló, 2007). The main objective of contrast media is to effectively absorb X-radiation, and therefore enhance visualization between internal structures of interest and the surrounding tissues during diagnostic testing (Christiansen, 2005). As earlier as the 1930s it was discovered that iodine, having a high electron density, could be attached to aromatic rings to produce stable compounds for use as diagnostic agents (Wallingford, 1953). In the 1950s, the first tri-iodinated benzene derivatives, also known as iodinated X-ray contrast media (ICM), were introduced (Wallingford, 1953).

1.1.1 Consumption and Application of ICM

Currently, iodinated X-ray contrast media (ICM) are the dominant contrast media used in human medicine. By weight, these radiological agents are the most frequently used pharmaceuticals in hospitals (Hirsch *et al.* 2000), and are reported to be the most widely used pharmaceuticals for intravascular administration (Christiansen, 2005; Busetti *et al.* 2008). A 2003 publication by BLAC (Bund/Länderausschuss für Chemikaliensicherheit) reported the consumption of diatrizoate, iomeprol, iopamidol, and iopromide to be approximately 60669, 83377, 42994 and 64056 kg/a, respectively, in Germany (BLAC, 2003). The worldwide consumption of ICM has been reported to be approximately 3.5×10^6 kg/a (Pérez and Barceló, 2007). It has been estimated that 600 million X-ray examinations are conducted on an annual basis, with 75 million of these tests involving the application of contrast media (Christiansen 2005).

ICM can be used in a number of different diagnostic medical procedures. Some of the most common applications of ICM include: computerized tomography (CT) for head and body imaging, angiography of the cardiovascular system (cerebral and peripheral arteriography, coronary arteriography, aortography), venography, myelography (lumbar, cervical and thoracic), and urography (Steger-Hartmann *et al.* 1999; Dooley and Jarvis, 2000). In addition, ICM can be used in the examination of the gastrointestinal tract, shoulder and knee joints, and female reproductive organs. In most cases, ICM are injected intravenously or intra-arterially, but can also be administered by the intrathecal (spinal canal) or oral route. ICM are administrated at high concentrations and large volumes, which can result in a single dose containing up to 200 g of active substance or approximately 100 g of iodine (Steger-Hartmann *et al.* 1999). The formulations of common ICM approved for use in Europe and North America can vary between 140 mg iodine/mL up to 370 mg iodine/mL with possible injection volumes up to 200 mL depending on specific use (Gallotti *et al.* 1994). It can be expected that the consumption of ICM will continue to increase as the medical profession move towards early screening tools and examinations for proper diagnosis of health problems experienced by individuals.

1.1.2 Physical and Chemical Properties

Most ICM are derivatives of 2,4,6-triiodobenzoic acid, and therefore have a simple basic structure of three iodine atoms attached to an aromatic ring. The functional groups at the other ring positions make each ICM distinct, in addition to increasing water solubility, hydrophilicity, and lowering the chemotoxicity and osmolality of an injection solution (i.e. minimizing adverse reactions) (Christiansen 2005). ICM have a relatively high molecular weight (600 to 1300 Da) compared to other pharmaceuticals. They have been described as chemically inert, and have

shown limited biodegradability in short-term degradation experiments (Steger-Hartmann *et al.* 1999; Steger-Hartmann *et al.* 2002).

Commercially available ICM are usually categorized by four types: ionic monomers, non-ionic monomers, ionic dimers, and non-ionic dimers. Currently, most of the contrast media available on the market are non-ionic monomers, which have a lower frequency of adverse reactions in patients. In fact, non-ionic ICM are at least a factor of 5 less toxic than the ionic ICM (Steger-Hartmann *et al.* 2002; Christiansen, 2005).

The difference between ionic and non-ionic ICM is based on the functional groups attached to positions 1, 3, and 5 of the aromatic ring. Ionic ICM, such as diatrizoate, ioxaglic acid, iodipamide and iothalamic acid, have side chains with one or more free carboxylic moieties attached to the iodinated aromatic ring. Iohexol, iomeprol, iopamidol and iopromide are examples of non-ionic ICM, and have hydroxylated amide functional groups as their side chains. The non-ionic ICM usually have two identical side chains resulting in a divalent structure (Christiansen, 2005; Pérez and Barceló, 2007).

The chemical structures and physicochemical properties for five common ICM (diatrizoate, iohexol, iomeprol, iopamidol and iopromide) are summarized in Table 1.1.

Table 1.1: Chemical and physical properties of selected iodinated X-ray contrast media

Compound	Structure	LogK$_d$	pK$_a$	LogK$_{ow}$	Molecular Weight (g/mol)
Diatrizoate (ionic monomer) CAS no. 117-96-4		-3.76[1]	3.4[1]	1.37[1]	613.92[4]
Iohexol (non-ionic monomer) CAS no. 66108-95-0				-3.05[2]	821.15[4]
Iomeprol (non-ionic monomer) CAS no. 78649-41-9		4.17[1]		-2.79[1]	777.09[4]
Iopamidol (non-ionic monomer) CAS no. 60166-93-0		-3.90[1]		-2.42[2]	777.09[4]
Iopromide (non-ionic monomer) CAS no. 73334-07-3				-2.33[3] -2.05[4]	791.12[4]
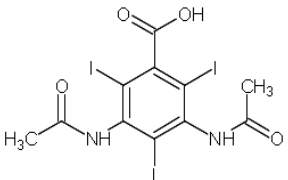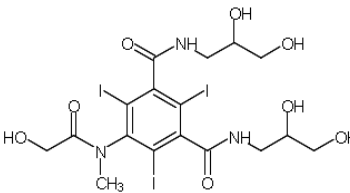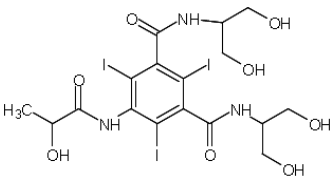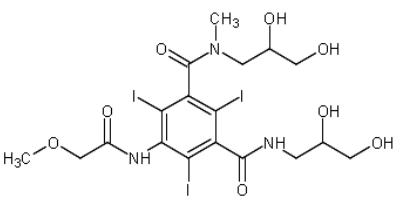
[1] Ternes et al. 2007; [2] ChemIDplus, United States National Library of Medicine, http://toxnet.nlm.nih.gov/cgi-bin/sis/htmlgen?CHEM; [3] Steger-Hartmann et al. 2002; [4] Syracuse SRC Interactive PhysProp Database. http://www.syrres.com/ (accessed May 24, 2010)

1.1.3 Pharmacokinetics

In contrast to most pharmaceuticals, ICM are not designed to have a specific therapeutic activity. These compounds are metabolically stable and are eliminated quickly from the human body (Ternes and Joss, 2006; Pérez and Barceló, 2007). The average half-life time of ICM in the body was estimated to be approximately 2 h based on emission and consumption data of selected ICM in a hospital in Switzerland (Weissbrodt *et al.* 2009). In most cases, > 90 % of the administered dose is recovered unmetabolized in the urine within 24 h (Steger-Hartmann *et al.* 2002; Christiansen, 2005; Weissbrodt *et al.* 2009).

Following intravascular injection, ICM are mixed with the circulating plasma volume, and can cross blood vessel walls into the extracellular space. In most cases, the ICM do not enter cells, which eliminates the possibility of ICM undergoing extensive human metabolism (Dooley and Jarvis, 2000; Christiansen, 2005).

In general, there are very few adverse reactions observed in patients administered ICM. However, the high doses applied may result in nausea, vomiting, fever and different skin reactions. In addition, renal impairment, severe skin eruptions and anaphylactic reactions in the cardiovascular and respiratory system may result (Dooley and Jarvis, 2000; Christiansen, 2005).

1.2 Sources of ICM

It has been well documented that the major point sources of ICM entering the domestic sewage system, and indirectly the aquatic environment, are wastewaters from hospitals and radiological clinics. Gartiser *et al.* (1996) found elevated concentrations of absorbable organic halogens (AOX) in hospital wastewaters. When comparing the consumption of several pharmaceutical products, it was found that ICM represented a dominant proportion of the AOX load in hospital

wastewaters. Other studies have shown that the high concentrations of absorbable organic iodine (AOI) in hospital and clinical wastewater can be partly explained by the presence of ICM (Drewes *et al.* 2001; Putschew *et al.* 2001). Therefore, one can assume that the remaining amount of AOI is represented by metabolites and transformation products.

The fluctuation of the AOI loads in hospital wastewater and wastewater treatment plants (WWTPs) receiving wastewater from hospitals corresponds well to the consumption pattern of ICM. Higher loads and concentrations of ICM have been detected in samples collected from hospital wastewaters and municipal WWTPs on weekdays compared to weekends (Ternes and Hirsch, 2000; Drewes *et al.* 2001). In contrast to other emerging contaminants, the loads of ICM entering the WWTP and therefore the aquatic environment fluctuate over a week with concentration peaks occurring Monday to Friday. This can be explained by the fact that ICM are applied sporadically at high doses for relatively few patients, and most radiological examinations take place in hospitals and clinics predominately on weekdays (Joss *et al.* 2006; Ternes and Joss, 2006; Weissbrodt *et al*. 2009).

1.3 Analytical Methods and Instrumentation

The application of liquid chromatography tandem mass spectrometry (LC tandem MS) has become the analytical tool of choice for the determination and quantification of pharmaceuticals, personal care products, and other emerging polar organic compounds in aqueous environmental samples. Therefore, it is not surprising that LC tandem MS has been used extensively in investigating the presence of ICM in different environmental samples (Santos *et al.* 2010). The application of solid phase extraction (SPE) cartridges has been effective in removing matrix components, and extracting ICM in complex environmental samples. However, some published

LC tandem MS methods developed for ICM have omitted the use of SPE for sample clean-up and extraction (Seitz et al. 2006a). Although, the amount of time required for sample preparation was reduced and matrix effects for the ICM were low to moderate, the sensitivity of the method decreased significantly by omitting a sample extraction step.

One of the first analytical methods published for determining the presence of ICM in the environment was reported by Hirsch *et al.* (2000). The authors developed a method using Isolute ENV+ cartridges and LC tandem MS with electrospray ionization (ESI) for the detection of eight ICM in aqueous samples. A similar analytical method was applied for investigating the occurrence and fate of ICM in WWTPs and surface waters (Ternes and Hirsch, 2000). Putschew *et al.* (2000) also developed a LC ESI MS method for determining the presence of selected ICM in aqueous environmental samples, but different SPE cartridges (LiChrolut EN and Envi-Carb cartridges) were selected to achieve a more efficient extraction. Recently, Busetti *et al.* (2008 and 2010) developed a method using direct injection LC tandem MS for quantifying selected ICM in aqueous samples, however the authors reported lower sensitivity compared to other methods.

Sacher *et al.* (2005) validated an analytical method for measuring six ICM in water samples by coupling ion chromatography and inductively-coupled plasma mass spectrometry (IC-ICP-MS). When comparisons were made between the use of IC-ICP-MS and LC tandem MS, higher sensitivity and specificity were found for the latter. However, the IC-ICP-MS method had the advantage of no sample clean-up, and iodate and iodide could be measured concomitantly.

1.4 Occurrence of ICM in the Environment

The application of LC tandem MS instrumentation has been intensively used to determine the presence of ICM in different environmental samples. The concentrations of selected ICM in different environmental samples are been summarized in Table 1.2, and are also reported by Santos *et al.* (2010). ICM can be detected at concentrations >10 µg/L, and are found throughout the urban water cycle. In comparison to other pharmaceuticals, these particular organic contaminants are found at higher concentrations, and can be explained by their high stability during different treatment processes as well as "natural" removal processes (i.e. riverbank infiltration).

Table 1.2: Concentrations [µg/L] of Selected ICM in Different Environmental Matrices

ICM	WWTP influent	WWTP effluent	Surface water	Groundwater	Bank filtrate	Drinking water	Reference
Diatrizoate		1.14	0.11; 0.14			0.06	Hirsch et al. 2000
Iomeprol		2.06	0.04				
Iopamidol		0.59	0.30; 0.18			0.07	
Iopromide		3.07	0.15			0.04	
Diatrizoate	3.3	4.1 0.25 (median); 8.7 (max.)	0.23 (median); 100 (max.)	0.03 (median); 0.17 (max.)			Ternes and Hirsch 2000
Iomeprol	1.6	1.3 0.37 (median); 3.8 (max.)	0.10 (median); 0.89 (max.)				
Iopamidol	4.3	4.7 0.66 (median); 15 (max.)	0.49 (median); 2.8 (max.)	0.16 (median); 2.4 (max.)			
Iopromide	7.5	8.1 0.75 (median); 11 (max.)	0.10 (median); 0.91 (max.)	<LOQ (median); 0.21 (max.)			
Diatrizoate		13 - 15	6 – 8 (receiving channel) 1.5 – 3 (lake)				Putschew et al. 2001
Iohexol		7	2 (receiving channel) 0.5 (lake)				
Iopromide		20 - 21	8.5 - 11 (receiving channel) 2 – 4 (lake)				

ICM	WWTP influent	WWTP effluent	Surface water	Groundwater	Bank filtrate	Drinking water	Reference
Diatrizoate			0.960 (lake)		0.298 – 0.632	0.166 (raw drinking water)	Schittko et al. 2004
Iopromide			0.860 (lake)		0.037 – 0.219	<0.02	
Diatrizoate			0.13 – 0.44				Sacher et al. 2005
Iohexol			0.03 – 0.09				
Iomeprol			0.05 – 0.12				
Iopamidol			0.09 – 0.22				
Iopromide			0.09 – 0.20				
Diatrizoate		5.2[1]	0.089 – 0.155[2] (median)				Seitz et al. 2006a[1]
Iohexol		2.6[1]	0.04 – 0.086 [2] (median)				Seitz et al. 2006b[2]
Iomeprol		6.6[1]	0.100 – 0.160[2] (median)				
Iopamidol		7.0[1]	0.210[2] (median)				
Iopromide		2.4[1]	0.076 – 0.100[2] (median)				
Diatrizoate			0.080 – 0.208			0.129 – 0.149	Seitz et al. 2006c
Iohexol			0.106 – 0.253			0.038 – 0.040	
Iomeprol			0.081 – 0.092			0.081 – 0.092	
Iopamidol			0.307 – 0.399			0.072 – 0.098	
Iopromide			0.232 – 0.287			0.069 – 0.077	
Iopromide	0.017	0.0046 (tertiary effluent); 2.67 (secondary effluent)	0.0022			0.0046	Trenholm et al. 2006 (cited in Santos et al. 2010)

ICM	WWTP influent	WWTP effluent	Surface water	Groundwater	Bank filtrate	Drinking water	Reference
Iopromide		2.63 (1.17 – 4.03)	0.134 (0.020 – 0.361)			0.143 – 0.177	Kim et al. 2007
Diatrizoate	3.3	3.3		3.2 – 9.6 (wells) 1.4 – 3.5 (lysimeters)			Ternes et al. 2007
Iohexol	9.0	1.0					
Iomeprol	10	1.1					
Iopamidol	2.3	1.9					
Iopromide	18	3.0					
Iopromide	3.7 – 31	1.2 – 7.0		0.075			Schulz et al. 2008
Iopromide biotransformation products (TPs)		1.6 – 11.9 (sum of TPs)		0.18 (TP731) – 4.6 (TP701A)	0.013 (TP643) – 0.045 (TP759)		
Iopromide			0.033 – 1.8 (river) 0.78 – 8.1 (creeks)				Yoon et al. 2010

1.4.1 Wastewater Treatment Plants (WWTPs)

A number of studies have investigated the presence of selected ICM in wastewater samples collected from various treatment facilities (Ternes and Hirsch, 2000; Putschew *et al.* 2001; Busetti *et al.* 2010; Yoon *et al.* 2010). The limited removal of ICM during wastewater treatment has been intensely investigated (Ternes and Hirsch, 2000; Carballa *et al.* 2004; Carballa *et al.* 2007), and can be attributed to the high stability and hydrophilic properties of these compounds. In most cases, maximum concentrations in influent and effluent samples have been greater than 1 µg/L for commonly applied ICM (Hirsch *et al.* 2000; Ternes and Hirsch 2000; Putschew *et al.* 2001; Carballa *et al*. 2004).

Some results have shown that certain ICM can be effectively transformed (> 80%) during wastewater treatment (Ternes *et al.* 2007). Iohexol, iomeprol and iopromide were eliminated by 80 to 90% in a conventional German WWTP. The high sludge retention time (SRT) of 12 – 14 d could be responsible for the increase in removal efficiency of iopromide since it allows more time for the slow-growing bacteria to transform or degrade the ICM during activated sludge treatment (Batt *et al.* 2006). The high removal efficiency was not observed for diatrizoate or iopamidol with elimination reported to be 0% and 17%, respectively (Ternes *et al*. 2007). Clara *et al.* (2005) reported that iopromide was not detected in samples collected from a membrane bioreactor (MBR) pilot plant with high SRT and hydraulic retention time s (HRT). However, it was detected in wastewater samples collected from two conventional WWTPs operating at low SRT and HRT.

1.4.2 Surface Water

The concentrations reported in surface waters, mostly in river water, were lower than the concentrations reported in WWTPs, however, concentrations were still found above 1 µg/L. Since WWTPs are an important source of ICM contamination in the aquatic environment, it is not unexpected that higher concentrations of ICM are found downstream of WWTP discharges (Seitz *et al.* 2006b; Yoon *et al.* 2010). For example, higher concentrations of diatrizoate, iohexol and iopromide were detected in a channel directly receiving WWTP effluent compared to concentrations detected in a nearby lake (Putschew *et al.* 2001). Other studies have shown that higher percentages of wastewater effluent in surface waters results in higher concentrations of ICM (Ternes and Hirsch, 2000; Seitz *et al.* 2006b; Yoon *et al.* 2010).

1.4.3 Groundwater and Bank Filtration

The presence of ICM in groundwater and at bank filtration sites has been studied, but to a lesser extent compared to other matrices. Sacher *et al.* (2001) investigated the presence of four ICM in groundwater as part of a groundwater well monitoring program in Germany. Iopamidol was detected in five wells with a maximum concentration of 0.3 µg/L, while diatrizoate was detected in 21 wells with a maximum concentration of 1.1 µg/L. The authors concluded that the presence of ICM in groundwater is due to the indirect or direct input from WWTPs, and mostly likely groundwater is influenced by surface water to a certain extent. Ternes and Hirsch (2000) reported a maximum concentration of 2.4 µg/L for iopamidol in groundwater samples, and lower concentrations for diatrizoate and iopromide. Schittko *et al.* (2004) illustrated that ICM can be removed during anoxic bank filtration. For example, high concentrations (> 0.8 µg/L) of iopromide and diatrizoate in lake water were reduced as water passed through the soil.

Concentrations detected in the observation wells over 100 m from the lake were 0.298 µg/L (diatrizoate) and 0.045 µg/L (iopromide), and in raw water used for drinking water purposes concentrations were below 0.2 µg/L. The concentration of AOI was eliminated by 64% during anoxic bank filtration, therefore suggesting partial deiodination took place in addition to transformation of ICM to partly deiodinated organic compounds.

A study by Oppel *et al.* (2004) showed that iopromide or its TPs have a high mobility in soils, with close to 50% of the initial amount detected in soil leachate samples. The mobility of ICM in soil raises concerns about their potential to contaminate groundwater, and suggests that significant transformation of iopromide is possible during soil passage.

The presence of diatrizoate at relatively high concentrations in groundwater wells and lysimeters after irrigation of secondary effluent and sludge onto agricultural land, suggests this ICM is not effectively eliminated by soil-aquifer passage (Ternes *et al.* 2007). In some cases, irrigation of treated effluent leads to contamination of groundwater with ICM. Iopamidol was also detected a low concentrations in groundwater wells, suggesting the stability of this nonionic ICM during soil-aquifer passage.

When surface water and bank filtrate samples were measured for ICM, iopromide was found to decrease after bank filtration suggesting a potential removal mechanism (1.6 µg/L to non-detectable levels). However, the same conclusion could not be drawn for diatrizoate in which the concentrations were comparable between surface water and bank filtrate samples (Putschew *et al.* 2000).

Recently, Patterson *et al.* (2010) investigated the fate of certain pharmaceuticals during the passage of aerobic treated reverse-osmosis (RO) water through an anaerobic aquifer system in

sediment columns. Iohexol was selected for these experiments and was found to degrade slowly under anaerobic conditions (i.e. half-life was > 100 d). The authors concluded that biodegradation during soil-aquifer passage may not occur, especially under anaerobic conditions.

The presence of ICM in groundwater samples and during bank filtration suggests that ICM infiltrate into groundwater aquifers, and can contaminate groundwater supplies used for drinking water production (Putschew *et al.* 2000; Oppel *et al.* 2004; Ternes *et al.* 2007).

1.4.4 Drinking Water Treatment Plants (DWTPs)

There have been limited studies focusing on the presence of ICM in DWTPs. However, published research clearly illustrates that these polar compounds are found in drinking water (Seitz *et al.* 2006c; Hirsch *et al.* 2000). Seitz *et al.* (2006c) investigated the presence and elimination of diatrizoate, iohexol, iomeprol, iopamidol and iopromide in a German DWTP, in which river water is used for drinking water production. Diatrizoate was not removed during the various treatment steps including flocculation, biological removal (bio-reactor), ozonation, granular activated carbon (GAC) filtration, and by chlorine dioxide disinfection. Flocculation as well as biological removal did not have an impact on non-ionic ICM elimination. However, removal of the non-ionic ICM was observed during ozonation as well as GAC filtration. The non-ionic ICM were transformed by 46% to 85%, with an average of 30% removal by ozonation, and 50% by GAC filtration. Comparable results were observed for the removal of iopromide in a DWTP in South Korea which used lake water for drinking water production. The authors reported coagulation and ultra-filtration were not effective, but GAC filtration resulted in concentrations below the limit of quantification (LOQ) (Kim *et al.* 2007).

1.5 Impact of Chemical and Biological Processes on ICM Removal

Numerous studies have focused the elimination of ICM when applying various abiotic and biotic processes. In addition, few studies have investigated what intermediates and products are formed from the application of these processes.

1.5.1 Chemical Treatment

The elimination of ICM by ozonation and advanced oxidation processes (AOPs) has been investigated. In general, ICM were more resistant to oxidation compared to other pharmaceuticals (Ternes *et al.* 2003). Oxidation of ICM did not result in mineralization suggesting the formation of oxidation products (OPs) (Ning *et al.* 2007; Putschew *et al.* 2007; Ning *et al.* 2008; Seitz *et al.* 2008). In some cases, the application of ozone (O_3) as a possible treatment option for the removal of selected ICM was effective. The actual mechanism of how ICM are degraded by ozone and AOPs is not completely understood, but it has been suggested that a direct reaction of molecular O_3 with ICM is unlikely, and therefore ICM are attacked by OH radicals (Huber *et al.* 2003; Huber *et al.* 2005; Ning *et al.* 2007; Seitz *et al.* 2008). This non-selective oxidant probably attacks the iodine-carbon bond resulting in partial or complete deiodination of the ICM. The deiodinated ICM is then more susceptible to further degradation by other oxidants (Seitz *et al.* 2006b; Seitz *et al.* 2008; Knitt *et al.* 2008).

Seitz *et al.* (2008) investigated the removal of selected ICM by applying different ozone doses. Oxidation of diatrizoate by ozone was not effective. However, iomeprol and iopromide were partly oxidized by ozone. As expected, ozonation did not result in complete mineralization of ICM, and oxidation products of iomeprol were formed. Initial identification of one OP showed

that it had a molecular weight of 775 Da. The authors suggested that this OP was the result of an aldehyde or carbonyl group being formed on a side chain of iomeprol.

Non-ionic ICM (iomeprol, iopamidol and iopromide) were effectively oxidized (> 80%) with an ozone dose of 15 mg/L or the combination of O_3/H_2O_2 and O_3/UV at ozone doses higher than 10 mg/L. (Ternes *et al.* 2003). However, diatrizoate exhibited limited oxidation with only 14% oxidized with 15 mg/L O_3, and 25% to 36% with O_3/H_2O_2 and O_3/UV, respectively (Ternes *et al.* 2003).

Huber *et al*. (2003 and 2005) showed that ICM are not effectively oxidized by ozonation in water or wastewater samples. The oxidation of iopromide in water samples was approximately 40% for applied O_3 doses up to 5 mg/L (Huber *et al*. 2003). The oxidation percentage of ICM by ozone was found to be independent of the wastewater matrix. Iopromide, iomeprol and iopamidol in conventional activated sludge (CAS) effluent did not react with O_3 doses of 0.5 to 5 mg/L. At higher doses limited oxidation was observed for these non-ionic ICM, and likely a result of non-selective oxidation. Diatrizoate was resistant to oxidation by ozone, and had a relatively low reactivity to OH radicals (Huber *et al.* 2005).

Studies have also investigated the transformation of ICM by stimulated solar irradiation, photochemical reactions (i.e. ultra-violent radiation and hydrogen peroxide, UV/H_2O_2) and photocatalytic processes (i.e. use of titanium dioxide and metal catalysts). Doll and Frimmel (2003) concluded that iomeprol photodegrades by stimulated UV solar radiation. The increase in iodide concentration and the slow decrease in AOI concentration during degradation suggested that iodinated or partly iodinated intermediates are formed. Canonica *et al.* (2008) showed that

iopromide is partly removed (15%) during UV-C irradiation, and therefore this ICM can be phototransformed during UV disinfection to a limited extent.

Pereira *et al.* (2007) investigated the photolysis and UV/H_2O_2 oxidation of iohexol using a low- and medium-pressure UV system. The transformation of iohexol was less than 25% using the low- and medium-pressure lamps as well as applying UV/H_2O_2 treatment. Sprehe et al. (2001) concluded that photochemical oxidation is a possible technique for decreasing AOX concentrations and increasing the degradation potential of ICM in hospital wastewaters. ICM degradation was observed in an UV reactor with UV/H_2O_2. It was reported that iodine atoms were released and partial mineralization took place.

Ning *et al.* (2007 and 2009) investigated the removal of ICM by sonolysis (ultrasound irradiation) by itself and in combination with O_3 and H_2O_2. The authors reported that the application of gaseous O_3/ultrasound irradiation and H_2O_2/ultrasound irradiation showed better oxidation performance compared to only O_3 or pure ultrasound irradiation. The oxidation of ICM resulted in an increase of iodine being released (Ning *et al.* 2007).

Pérez *et al.* (2009) investigated the degradation of iopromide by artificial sunlight. A total of eight photodegradation products were identified using ultra performance liquid chromatography/quadrupole time-of-flight mass spectrometry (UPLC-QqTOF MS). Photodegradation of iopromide could be explained by one or more of four main reactions; deiodination, replacement of iodine with a hydroxyl group, *N*-dealkylation of amide in the hydroxylated side chain, and oxidation of the hydroxylated side chain with the methylene group being converted to a ketone. These identified TPs were not the same as the ones observed during

biological degradation in activated sludge systems or in aerobic soil-water systems (Batt *et al.* 2006; Schulz *et al*. 2008).

Some studies have shown that photocatalytic processes are useful for oxidizing ICM. Benotti *et al.* (2009) showed > 70% of iopromide was oxidized in a photocatalytic reactor with UV radiation and titanium dioxide (TiO_2), however high treatment levels were required. A similar result was reported by Doll and Frimmel (2004), who revealed that iomeprol and iopromide were degraded with simulated solar irradiation and two types of TiO_2 material. However, complete mineralization of iomeprol and iopromide did not occur based on the concentrations of AOI and DOC measured during the experiments. It is likely that deiodination occurred resulting in the formation of partly iodinated degradation products (Doll and Frimmel, 2004; Doll and Frimmel, 2005).

Knitt *et al.* (2008) showed that reductive catalysis, a treatment process using metal catalysts (nickel and palladium) to convert hydrogen gas to atomic hydrogen, results in complete hydrodehalogenation of diatrizoate and iopromide. However, further experiments need to be conducted to investigate the influence of matrix components on the efficiency and activity of the metal catalysts.

Zwiener *et al*. (2009) reported that electrochemical reduction (potentiostatic electrolysis) is a promising technique for the deiodination of ICM. Electrochemical reduction resulted in the formation of four products of iomeprol. Three of the products were identified as the sequential loss of one, two or three iodine atoms. The fourth product (*m/z* 342) was proposed to be a completely deiodinated structure with the loss of C(=O)=CHOH from the non-identical side chain of iomeprol.

Putschew *et al.* (2007) and Stieber *et al.* (2008) showed that the use of zero-valent iron (i.e. reductive dehalogenation treatment) at a pH of 2 is effective in the removal of iopromide. The degradation of this ICM could be explained by first-order kinetics.

Hennebel *et al.* (2010) used biogenic palladium nanoparticles (bio-Pd) to deiodinate diatrizoate. It was found that the dominant precursor ions in the samples collected after removal of diatrizoate by bio-Pd was the sequential deiodination of diatrizoate. Diatrizoate was also removed in bio-catalytically active membrane systems (i.e. high concentration of bio-Pd nanoparticles and polyvinylidene fluoride membranes), with a removal efficiency of 77% after 2 d.

In addition to oxidation techniques, ICM can be removed by other treatment processes including reverse osmosis (RO). Busetti *et al.* (2008 and 2010) investigated the presence of eight ICM in a water reclamation plant which uses microfiltration and reverse osmosis (RO) treatment for supplying water to industrial areas. It was found that RO treatment effectively removed ICM to below the limit of detection (LOD), with elimination percentages of > 90%. This can be explained by the high molecular weights of the ICM (i.e. RO membrane rejection), and suggests RO treatment is an option for ICM removal.

1.5.2 Biological Treatment

Most research looking at microbial degradation of pharmaceuticals has focused on characterizing their elimination during wastewater treatment as opposed to degradation in fresh water systems or marine environments. In either case, microbial degradation is an important removal pathway in WWTPs as well as natural systems, especially when compounds are resistant to hydrolysis, photolysis, and various chemical oxidation processes (Kunkel *et al.* 2008). Löffler *et al.* (2005)

investigated the degradation of iopromide in laboratory water-sediment systems. Iopromide showed resistance to degradation, resulting in a lag phase of two weeks and a DT_{50} value of 29 d. Complete transformation occurred after 100 d of incubation and resulted in the formation of four unknown products. Since most of the initial concentration of iopromide was detected in the water phase, sorption of iopromide to sediment was minimal. This correlates well to the hydrophilic nature of ICM, and the low $logK_d$ values estimated in activated sludge systems (Carballa *et al.* 2008; Joss *et al.* 2006).

Schulz *et al.* (2008) identified 12 biotransformation products (TPs) of iopromide in aerobic water-soil systems using semi-preparative HPLC, mass fragmentation experiments, and nuclear magnetic resonance (NMR) to structurally elucidate the chemical structures. The TPs resulted from modifications to the hydroxylated side chains, while the triiodinated aromatic ring remained intact.

Batt *et al.* (2006) reported biodegradation of iopromide in nitrifying activated sludge systems to be 97 % when the nitrifying bacteria were not inhibited, and 86% when nitrification was inhibited in laboratory-based studies. The degradation half-lives were estimated to be 20 h during nitrification and 34 h if nitrification was inhibited. The authors suggested that nitrifying bacteria (ammonia oxidizing and nitrite-oxidizing bacteria) play an important role in the degradation of iopromide in activated sludge systems. These bacteria are slow-growing microbes and tend to be dominant in WWTPs with a longer SRT. Two metabolites of iopromide were identified (i.e. *m/z* 760 and *m/z* 806) in the batch systems. A TP with *m/z* 760 was detected in the batch system, in which nitrification was not inhibited, while a TP with *m/z* 806 was detected in the batch system in which nitrification was inhibited.

Joss *et al.* (2006) investigated the biological degradation of a number of PPCPs, including selected ICM, and estimated the degradation rate constants in batch systems with activated sludge from two WWTPs focusing on nutrient removal (i.e. CAS and MBR facilities). The authors classified the biodegradability in WWTPs based on their rate constants. For iohexol, iomeprol and iopromide rate constants were calculated to be between 0.5 to 2.5 $Lg^{-1}ssd^{-1}$. The rate constants for diatrizoate and iopamidol were not calculated, since the lower limit was beyond experimental resolution. The authors classified substances with biological rate constants between 0.1 and $10Lg^{-1}ssd^{-1}$ to be partially removed.

Lecouturier *et al.* (2003) investigated the reductive deiodination of a precursor molecule of ICM, 5-amino-2,4,6-triiodophthalic acid. It was found that this compound was converted to three metabolites (deiodinated metabolites) by an enriched mixed culture sludge system performed under anaerobic conditions. Deiodination was only found to take place when an electron donor was added (i.e. ethanol). The di-iodinated and deiodinated metabolites were detected at higher levels compared to the mono-iodinated metabolite. The authors showed deiodination being coupled to microbial growth, proposing that the microbes might somehow obtain energy from dehalogenation of certain compounds. Lecouturier *et al.* (2008) illustrated that the same ICM precursor molecule can be mineralized to a great extent in an anaerobic-aerobic fixed-bed reactor. As expected, deiodination of this compound took place mostly in the anaerobic reactor while carbon removal was higher in the aerobic reactor. The removal of iodine allowed the aerobic microbes to degrade the deiodinated compounds more effectively.

Iopromide was removed by approximately 80 % in laboratory-conducted wastewater batch systems (OECD 303A test), and resulted in the formation of a "free amino" metabolite of iopromide (Steger-Hartmann *et al.* 2002). The authors proposed the product was formed by

cleavage of the N-C bond, the same nitrogen atom in which the methylene group is attached. Further biotransformation batch experiments (i.e. light-exposed and dark-exposed systems) showed that the free amino product of iopromide was degraded. Degradation was faster in the dark-exposed systems with the formation of partly iodinated products. In the light-exposed batch systems degradation was slower and the free amino iopromide was photodegraded to deiodinated compounds.

Both Kalsch (1999) and Haiß and Kümmerer (2006) reported degradation of diatrizoate, and proposed that diatrizoate was degraded to metabolites in which the acetyl groups were removed. Kalsch (1999) observed degradation of diatrizoate in water-sediment systems, while Haiß and Kümmerer (2006) reported degradation in the Zahn-Wellens test system (i.e. type of activated sludge test). Both studies reported that under very specific conditions diatrizoate is transformed, but not completely mineralized. Kalsch (1999) also reported degradation of iopromide in activated sludge as well as water-sediment systems. The metabolites were not identified, but were different between the two systems based on the retention times during the LC analyses. The one metabolite observed in the water-sediment system was likely the result of deiodination, due to the increase in iodide concentrations.

Perez *et al.* (2006) investigated the transformation of iopromide in activated sludge systems as well of nitrifying activated sludge systems. The degradation of iopromide was faster in the nitrifying system compared to the CAS system. Three metabolites of iopromide in the CAS system were identified by LC ion trap MS. One product had a molecular weight of 819 Da and the other two products a weight of 805 Da. All three products resulted from oxidation of the primary hydroxyl groups of iopromide. In the batch systems conducted with the nitrifying activated sludge, a different TP (m/z 760) was observed resulting from dehydoxylation of a

secondary hydroxyl group. Schulz et al. (2008) reported a TP with a *m/z* of 760 in water-soil batch systems. This TP was identified as the result of oxidative decarboxylation of the hydroxylated side chain and not dehydroxylation of the secondary hydroxyl groups. However, the same three TPs in the CAS were also detected in the water-soil systems.

In general, limited research has tried to identify the enzymes that might be responsible for the biotransformation observed in natural aquatic environments as well as in activated sludge systems. Rode and Müller (1998) illustrated that white rot fungi (*Trametes versicolor*) are capable of degrading diatrizoate and other tri-iodinated benzoates under aerobic conditions. Three metabolites were detected in the extracellular fluid of this microbe, and likely resulted from the cleavage of C-I bonds. The authors proposed that initial deiodination of diatrizoate is likely the result of extracellular peroxidases and/or laccases and mostly likely a non-specific reaction. These results show that diatrizoate can undergo reductive dehalogenation by certain microbes.

1.6 Ecotoxicology of ICM

Currently, there is limited ecotoxicological information available for ICM. The results from the limited toxicity tests conducted for iopromide suggest that it has low toxicity towards aquatic organisms (Santos *et al*. 2010; Steger-Hartmann *et al*. 2002). Steger-Hartmann *et al*. (2002) reported that iopromide showed no inhibition of luminescence in *Vibrio fisheri* (anaerobic bacterium), and no growth inhibition of green algae (*Scenedesmus subspicatus*) or a bacterium (*Pseudomonas putida*) with effect concentration values (EC_{50} values) estimated to be > 10 g/L. Acute and chronic toxicity tests using *Daphnia magna* showed the iopromide did not effect the immobilization of these species and no significant differences were observed between exposed

and control groups in a reproduction test. In addition, no mortality was reported for two fish species, *Danio rerio* and *Leuciscus idus,* exposed to iopromide. Lethal concentrations (LC_{50}) were reported to be > 10 g/L for these fish species exposed to iopromide (Steger-Hartmann *et al.* 2002; Santos *et al*. 2010). Similar results were reported for a metabolite of iopromide (free amino iopromide metabolite), in which low toxicity was reported in a growth inhibition test with green algae, an immobilization test using *Daphnia magna*, and an acute mortality test with zebra fish. For an early life stage 28 d test with zebra fish, a no-observed-effect-concentration (NOEC) of > 100 mg/L was reported based on four endpoints (i.e. body weight and length, hatchability and post-hatch survival).

Steger-Hartmann *et al.* (2002) conducted a screening environmental risk assessment for iopromide, in which the risk was based on the comparison of the predicted environmental concentration (PEC) (or measured concentration) to the lowest predicted no effect concentration (PNEC). The authors estimated a PEC to be 2 µg/L, and a PNEC of 10 mg/L, and concluded iopromide would pose a minimal risk to the aquatic environment based on the PEC/PNEC ratio of < 0.0002. Busetti *et al*. (2010) and Webb *et al.* (2003), used a slightly different approach for estimating the risk of ICM. Both compared the predicted or measured concentrations to either health based values (Busetti *et al*. 2010) or therapeutic doses (Webb *et al*. 2003). In both cases, the authors indicated a negligible or low risk to humans.

Although research has focused on different treatment processes to remove the ICM, and has clearly shown that mineralization of these compounds is rare, limited information is available on what products are formed during treatment and the fate of ICM once they have enter the environment. In order to accurately assess the risk of these ICM in the environment, identification of products formed during chemical and biological treatment is needed.

1.7 Objectives

The overall objective of this thesis was to investigate the environmental fate of iodinated X-ray contrast media (ICM). In particular, to investigate the biotransformation (microbial degradation) of diatrizoate, iohexol, iomeprol and iopamidol in aerobic laboratory batch systems as well as in the environment.

A literature review (***Chapter 1***) illustrated that hospital and radiological clinics are major sources of ICM, and their presence in wastewaters contributes to elevated concentrations of AOI. In most cases, ICM enter the aquatic environment via discharges of treated wastewater. Studies have shown that ICM are not effectively removed during wastewater treatment and as a result ICM have been detected at high concentrations in surface waters. In addition, their presence in groundwater, during bank filtration, and even in treated drinking water illustrates their potential resistance to certain biotic and abiotic processes. In general, limited information is available on the environmental fate of ICM once they have entered aquatic ecosystems.

The specific objectives of this study include:

1.   To determine if selected ICM (diatrizoate, iohexol, iomeprol and iopamidol) are microbially degraded, under aerobic conditions, in contact with soil and to elucidate the chemical structures of biotransformation products (TPs) of selected ICM shown to be biotransformed in laboratory aerobic water-soil batch systems (***Chapter 2***).

2.   To compare and characterize the differences in biotransformation of the selected ICM in different aerobic soil-water and sediment system batch systems. In particular, to determine the biotransformation rate constants of the parent ICM and sequence of TP formation for the selected ICM and the different batch systems. Additionally, to

propose microbial transformation pathways of the selected ICM and possible enzymes and biochemical reactions responsible for the observed ICM biotransformation (**Chapter 3**).

3. To investigate the occurrence and fate of ICM and their newly identified TPs in various environmental matrices (i.e. raw and treated wastewater, surface waters, ground water and drinking water) using a recently developed LC tandem MS method. In particular, to illustrate the formation and changes in TP composition between different environmental compartments (**Chapter 4**).

1.8 Structure of Thesis

The thesis is divided into five chapters:

Chapter 1 provides a comprehensive overview of the application and consumption of ICM, the occurrence of these compounds in the environment, the removal efficiencies of ICM during chemical as well as biological treatment processes, and the current knowledge about the environmental fate and toxicity of ICM.

Chapter 2 presents a multistep approach to structurally elucidate TPs of three non-ionic ICM (iohexol, iomeprol and iopamidol) formed in aerobic soil-water batch systems. This approach involved the use of various analytical techniques, including semi-preparative HPLC-UV, LC tandem/ion trap MS, and ^{1}H- and ^{13}C-NMR analyses.

Chapter 3 investigates the biotransformation of diatrizoate, iohexol, iomeprol and iopamidol in different aerobic water-soil and water-sediment systems. In particular, the characterization and formation of the ICM TPs during incubation (i.e. sequence of TP formation, dominant ICM TPs),

as well as estimating biotransformation rate constants was performed. This chapter also reports on possible biochemical reactions and enzymes involved in the microbial transformation pathways of ICM.

Chapter 4 focuses on the development and optimization of a LC tandem MS method to quantify the presence of five parent ICM and 46 TPs in the urban water cycle. Samples were collected from WWTPs, surface water, groundwater influenced by surface water, natural groundwater and drinking water. The concentrations of the ICM TPs detected in the different environmental samples were reported, and changes observed in the composition of the parent ICM and the TPs throughout the urban water cycle were determined to establish the extent of ICM TPs found in the environment.

Chapter 5 discusses the results presented in other chapters and summarizes the major conclusions. In addition, future research initiatives are presented.

1.9 Literature Cited

Batt, A. L.; Kim, S.; Aga, D. Enhanced biodegradation of iopromide and trimethoprim in nitrifying sludge. *Environ. Sci. Technol.* **2006**, *40* (23), 7367-7373.

Benotti, M. J.; Stanford, B. D.; Wert, E. C.; Snyder, S. A. Evaluation of a photocatalytic reactor membrane pilot system for the removal of pharmaceuticals and endocrine disrupting compounds from water. *Water Res.* 2009, *43* (6), 1513-1522.

BLAC, Bund/Länderausschuss für Chemikaliensicherheit. Arzneimittel in der Umwelt Auswertung der Untersuchungsergebnisse. 2003. Hamburg, Germany, www.blac.de/servlet/is/2146/P-2c.pdf.

Busetti, F.; Linge K. L.; Blythe, J. W.; Heitz, A. Rapid analysis of iodinated X-ray contrast media in secondary and tertiary wastewater by direct injection liquid chromatography-tandem mass spectrometry. *J Chromatogr A*. **2008**, *1213* (2), 200-208.

Busetti, F.; Linge, K L.; Rodriguez, C.; Heitz, A. Occurrence of iodinated X-ray contrast media in indirect potable reuse systems. *J. Environ. Sci. Health., Part A. Toxic/Hazard. Subst. Environ. Eng.* **2010**, *45*, (5) 542-548.

Canonica, S.; Meunier, L.; von Gunten, U. Phototransformation of selected pharmaceuticals during UV treatment of drinking water. *Water Res.* **2008**, *42* (1-2), 121-128.

Carballa, M.; Omil, F.; Lema, J. M.; Llompart, M.; García-Jares, C.; Rodriguez, I.; Gómez, M.; Ternes, T. Behavior of pharmaceuticals, cosmetics and hormones in a sewage treatment plant. *Water Res.* **2004**, *38* (12), 2918-2926.

Carballa, M.; Omil, F.; Ternes, T. A.; Lema, J. M. Fate of pharmaceuticals and personal care products (PPCPs) during anaerobic digestion of sewage sludge. *Water Res.* **2007**, *41* (10), 2139-2150.

Carballa, M.; Fink, G.; Omil, F.; Lema, J. M.; Ternes, T. A. Determination of the solid-water distribution coefficient (K_d) for pharmaceuticals, estrogens and musk fragrances in digested sludge. *Water Res.* **2008**, *42* (1-2), 287-295.

Christiansen, C. X-ray contrast media – an overview. *Toxicol.* **2005**, *209* (2), 185-187.

Clara, M.; Strenn, B.; Gans, O.; Martinez, E.; Kreuzinger, N.; Kroiss, H. Removal of selected pharmaceuticals, fragrances and endocrine disrupting compounds in a membrane bioreactor and conventional wastewater treatment plants. *Water Res.* **2005**, *39* (19), 4797-4807.

Doll, T. E.; Frimmel, F. H. Fate of pharmaceuticals-photodegradation by stimulated solar UV-light. *Chemosphere.* **2003**, *52* (10), 1757-1769.

Doll, T. E.; Frimmel, F. H. Kinetic study of photocatalytic degradation of carbamazepine, clofibric acid, iomeprol and iopromide assisted by different TiO_2 materials – determination of intermediates and reaction pathways. *Water Res.* **2004,** *38* (4), 955-964.

Doll, T. E.; Frimmel, F. H. Cross-flow microfiltration with periodical back-washing for photocatalytic degradation of pharmaceuticals and diagnostic residues-evaluation of the long-term stability of the photocatalytic activity of TiO_2. *Water Res.* **2005**, *39* (5), 847-854.

Dooley, M.; Jarvis, B. Iomeprol a review of its use as a contrast medium. *Drugs.* 2000, *59* (5), 1169-1186.

Drewes, J. E.; Fox, P.; Jekel, M. Occurrence of iodinated X-ray contrast media in domestic effluents and their fate during indirect potable reuse. *J. Environ. Sci. Health.* **2001**, *36* (9), 1633-1645.

Gallotti, A.; Uggeri, F.; Favilla, A.; Cabrini, M.; de Haën, C. The chemistry of iomeprol and physico-chemical properties of is aqueous solutions and pharmaceutical formulations. *Eur J. Radiol.* **1994**, *18* (suppl. 1), S1-S12.

Gartiser, St.; Brinker, L.; Erbe, T.; Kümmerer, K.; Willmund, R. Contamination of hospital wastewater with hazardous compounds as defined by §7a WHG. *Acta hydroch. hydrob.* **1996**, *24* (2). 90-97.

Haiß, A.; Kümmerer, K. Biodegradability of the X-ray contrast compound diatrizoic acid, identification of aerobic degradation products and effects of against sewage sludge micro-organisms. *Chemosphere.* **2006**, *62* (2), 294-302.

Hennebel, T.; De Corte, S. Vanhaecke, L.; Vanherck, K.; Forrez, I; De Gusseme, B.; Verhagen, P.; Verbeken, K.; Van der Bruggen, B.; Vankelecom, I.; Boon, N.; Verstraete, W. Removal of diatrizoate with catalytically active membranes incorporating microbially produced palladium nanoparticles. *Water Res.* **2010**, *44* (5), 1498-1506.

Hirsch, R.; Ternes, T. A.; Lindart, A.; Haberer, K.; Wilken, R-D. A sensitive method for the determination of iodine containing diagnostic agents in aqueous matrices using LC-electrospray-tandem-MS detection. *Fresenius J Anal Chem.* **2000**, *366* (8), 835-841.

Huber, M.; Canonica, S.; Park, G.-Y.; von Gunten, U. Oxidation of pharmaceuticals during ozonation and advanced oxidation processes. *Environ. Sci. Technol.* **2003**, *37* (5), 1016-1024.

Huber, M.; Göbel, A.; Joss, A.; Hermann, N.; Löffler, D.; McArdell, C. S.; Ried, A.; Siegrist, H.; Ternes, T. A.; von Gunten, U. Oxidation of pharmaceuticals during ozonation of municipal wastewater effluents: A pilot study. *Environ. Sci. Technol.* **2005**, *39* (11), 4290-4299.

Joss, A.; Keller, E.; Alder, A. C.; Göbel, A.; McArdell, C. S.; Ternes, T.; Siegrist, H. Removal of pharmaceuticals and fragrances in biological wastewater treatment. *Water Res.* **2005**, *39* (14), 3139-3152.

Joss, A.; Zabczynski, S.; Göbel, A.; Hoffmann, B.; Löffler, D.; McArdell, C. S.; Ternes, T. A.; Thomsen, A.; Siegrist, H. Biological degradation of pharmaceuticals in municipal wastewater treatment: proposing a classification scheme. *Water Res.* **2006**, *40* (8), 1686-1696.

Kalsch, W. Biodegradation of the iodinated X-ray contrast media diatrizoate and iopromide. *Sci. Total Environ.* **1999**, *225* (1-2), 143-153.

Kim, S. D.; Cho, J.; Kim, I. S.; Vanderford, B, J,; Snyder, S. A. Occurrence and removal of pharmaceuticals and endocrine disruptors in South Korean surface, drinking, and waste waters. *Water Res.* **2007**, *41* (5), 1013-1021.

Knitt, L. E.; Sharply, J. R.; Strathmann, T. J. Rapid metal-catalyzed hydrodehalogenation of iodinated X-ray contrast media. *Environ. Sci. Technol.* **2008**, *42* (2), 577-583.

Kunkel, U.; Radke, M. Biodegradation of acidic pharmaceuticals in bed sediments: Insight from a laboratory experiment. *Environ. Sci. Technol.* **2008**, *42* (19), 7273-7279.

Lecouturier, D.; Rochex, A.; Lebeault, J.-M. Enrichment and properties of an anaerobic mixed culture that reductively deiodinated 5-amino-2,4,6-triiodophthalic acid, an X-ray contrast agent precursor. *Appl. Microbiol. Biotechnol.* **2003**, *63* (5-6), 550-556.

Lecouturier, D.; Rochex, A.; Lebeault, J.-M. The mineralization of 5-amino-2,4,6-triiodoisophthalic acid by a two-stage fixed-bed reactor. *Water Res.* **2008**, *42* (10-11), 2491-2498.

Löffler, D.; Römbke, J.; Meller, M.; Ternes, T. A. Environmental fate of pharmaceuticals in water/sediment systems. *Environ. Sci. Technol.* **2005**, *39* (14), 5209-5218.

Ning, B.; Graham N. J. D.; Lickiss, P. D. Degradation of X-ray contrast media compounds by combined ozone and ultrasound. *Water Environ. Res.* **2007**, *79* (12). 2427-2436.

Ning, B.; Graham N. J. D. Ozone degradation of iodinated pharmaceutical compounds. *J. Environ. Eng.* **2008**, *134* (12), 944-953.

Ning, B.; Graham, N. J. D. A comparison of ultrasound-based advanced oxidation processes for the removal of X-ray contrast media. *Water Sci. Technol.* **2009**, *60* (9), 2383-2390.

Oppel, J.; Broll, G.; Löffler, D.; Meller, M.; Römbke, J.; Ternes, Th. Leaching behaviour of pharmaceuticals in soil-testing-systems: a part of an environmental risk assessment for groundwater protection. *Sci. Total Environ.* **2004**, *328* (1-3), 265-273.

Patterson, B. M.; Shackleton, M.; Furness, A. J.; Pearce, J.; Descourvieres, C.; Linge, K. L.; Busetti, F.; Spadek, T. Fate of nine recycled water trace organic contaminants and metal(loids) during managed aquifer recharge into a anaerobic aquifer: Column studies. *Water Res.* **2010**, *44* (5), 1471-1481.

Pereira, V. J.; Linden, K. G.; Weinberg, H. S. Evaluation of the UV irradiation for photolytic and oxidative degradation of pharmaceutical compounds in water. *Water Res.* **2007**, *41* (19), 4413-4423.

Pérez, S.; Eichhorn, P.; Celiz, M. D.; Aga, D. S. Structural characterization of metabolites of the x-ray contrast agent iopromide in activated sludge using ion trap mass spectrometry. *Anal. Chem.* **2006**, *78* (6), 1866-1874.

Pérez, S.; Barceló, D. Fate and occurrence of X-ray contrast media in the environment. *Anal. Bioanal. Chem.* **2007**, *387* (4), 1235-1246.

Pérez, S.; Eichhorn, P.; Ceballos, V.; Barceló, D. Elucidation of phototransformation reactions of the X-ray contrast medium iopromide under simulated solar radiation using UPLC-ESI-QqTOF-MS. *J. Mass Spectrom.* **2009**, *44* (9), 1308-1317.

Putschew, A.; Wischnack, S.; Jekel, M. Occurrence of triiodinated X-ray contrast agents in the aquatic environment. *Sci. Total Environ.* **2000**, *255* (1), 129-134.

Putschew, A.; Schittko, S.; Jekel, M. Quantification of triiodinated benzene derivatives and x-ray contrast media in water samples by liquid chromatography-electrospray tandem mass spectrometry. *J. Chromatogr. A.* **2001**, *930* (1-2), 127-134.

Putschew, A.; Miehe, U.; Tellez, A. S.; Jekel, M. Ozonation and reductive deiodination of iopromide to reduce the environmental burden of iodinated X-ray contrast media. *Water Sci. Technol.* **2007**, *56* (11), 159-165.

Rode, U.; Müller, R. Transformation of the ionic X-ray contrast agent diatrizoate and related triiodinated benzoates by *Trametes versicolor*. *Appl. Environ. Microbiol.* **1998**, *64* (8), 3114-3117.

Sacher, F.; Lange, F. T.; Brauch, H.-J.; Blankenhorn, I. Pharmaceuticals in groundwaters Analytical methods and results of a monitoring program in Baden-Württemberg, Germany. *J. Chromatogr. A.* **2001**, *938* (1-2), 199-210.

Sacher, F.; Raue, B., Brauch, H.-J. Analysis of iodinated X-ray contrast agent in water samples by ion chromatography and inductively-coupled plasma mass spectrometry. *J. Chromatogr. A.* **2005**, *1085* (1), 117-123.

Santos, L. H.M.L.M.; Araújo, A. N.; Fachini, A.; Pena, A.; Delerue-Matos, C.; Montenegro, M.C.B.S.M. Ecotoxicological aspects related to the presence of pharmaceuticals in the aquatic environment. *J. Hazard. Mater.* **2010**, *175* (1-3), 45-95.

Schittko, S.; Putschew, A.; Jekel, M. Bank filtration: a suitable process for the removal of iodinated X-ray contrast media? *Water Sci. Technol.* **2004**, *50* (5), 261-268.

Schulz, M.; Löffler, D.; Wagner, M.; Ternes, T. A. Transformation of the X-ray contrast medium iopromide in soil and biological wastewater treatment. *Environ. Sci. Technol.* **2008**, *42* (19), 7207-7217.

Seitz, W.; Schulz, W.; Weber, W. H. Novel applications of highly sensitive liquid chromatography/mass spectrometry/mass spectrometry for the direct detection of ultra-trace levels of contaminants in water. *Rapid Commun. Mass Spectrom.* **2006a**, *20* (15), 2281-2285.

Seitz, W.; Weber, W. H.; Jiang, J.-Q.; Lloyd B. J.; Maier, M.; Maier, D.; Schulz, W. Monitoring of iodinated X-ray contrast media in surface water. *Chemosphere.* **2006b**, *64* (8), 1318-1324.

Seitz, W.; Jiang, J.-Q.; Weber, W. H.; Lloyd B. J.; Maier, M.; Maier, D. Removal of iodinated X-ray contrast media during drinking water treatment. *Environ. Chem.* **2006c**, *3* (1), 35-39.

Seitz, W.; Jiang, J.-Q.; Schulz, W.; Weber, W. H.; Maier, D.; Maier, M. Formation of oxidation by-products of the iodinated X-ray contrast medium iomeprol during ozonation. *Chemosphere.* **2008**, *70* (7), 1238-1246.

Sprehe, M.; Geiβen, S.-U.; Vogelpohl, A. Photochemical oxidation of iodized X-ray contrast media (XRC) in hospital wastewater. *Water Sci. Technol.* **2001**, *44* (5), 317-323.

Steger-Hartmann, T.; Länge, R.; Schweinfurth, H. Environmental risk assessment for the widely used iodinated X-ray contrast agent iopromide (Ultravist). *Ecotoxicol. Environ. Saf.* **1999**, *42* (3), 274-281.

Steger-Hartmann, T.; Länge, R.; Schweinfurth, H.; Tschampel, M., Rehmann, I. Investigations into the environmental fate and effects of iopromide (ultravist), a widely used iodinated X-ray contrast medium. *Water Res.* **2002**, *36* (1), 266-274.

Stieber, M.; Putschew, A., Jekel, M. Reductive dehalogenation of iopromide by zero-valent iron. *Water Sci. Technol.* **2008**, *57* (12), 1969-1975.

Syracuse SRC Interactive PhysProp Database. http://www.syrres.com (accessed on May 24th, 2010).

Ternes, T. A.; Hirsch, R. Occurrence and behavior of X-ray contrast media in sewage facilities and the aquatic environment. *Environ. Sci. Technol.* **2000**, *34* (13), 2741-2748.

Ternes, T. A.; Stüber, J.; Herrmann, N.; McDowell, D.; Ried, A.; Kampmann, M.; Teiser, B. Ozonation: a tool for removal of pharmaceuticals, contrast media and musk fragrances from wastewater? *Water Res.* **2003**, *37* (8), 1976-1982.

Ternes, T. A., Joss, A., Eds. *Human Pharmaceuticals, Hormones and Fragrances: The challenge of micropollutants in urban water management*; IWA Publishing: London, **2006**.

Ternes, T. A.; Bonerz, M.; Hermann, N.; Teiser, B.; Andersen, H. R. Irrigation of treated wastewater in Braunschweig, Germany: An option to remove pharmaceuticals and musk fragrances. *Chemosphere*. **2007**, *66* (5), 894-904.

Trenholm, R. A.; Vanderford, B. J.; Holady, J. C; Rexing, D. J.; Snyder, S. A. Broad range analysis of endocrine disruptors and pharmaceuticals using gas chromatography and liquid chromatography tandem mass spectrometry. *Chemosphere*. **2006**, *65* (11), 1990-1998.

Wallingford. V. H. The development of organic iodine compounds as x-ray contrast media. *J. Am. Pharm. Assoc. (Baltim)*. **1953**, *42* (12), 721-728.

Webb, S.; Ternes, T.; Gibert, M.; Olejniczak, K. Indirect human exposure to pharmaceuticals via drinking water. *Toxicol. Lett*. **2003**, *142* (3), 157-167.

Weissbrodt, D.; Kovalova, L.; Ort, C.; Pazhepurackel, V.; Moser, R.; Hollender, J.; Siegrist, H.; McArdell, C. S. Mass flows of X-ray contrast media and cytostatics in hospital wastewater. *Environ. Sci. Technol*. **2009**, *43* (13), 4810-4817.

Yoon, Y.; Ryu, J.; Oh, J.; Choi, B.-G.; Snyder, S. A. Occurrence of endocrine disrupting compounds, pharmaceuticals and personal care products in the Han River (Seoul, South Korea). *Sci. Total Environ*. **2010**, *408* (3), 636-643.

Zwiener, C.; Glauner, T.; Sturm, J.; Wörner, M.; Frimmel, F. H. Electrochemical reduction of the iodinated contrast medium iomeprol: iodine mass balance and identification of transformation products. *Anal. Bioanal. Chem*. **2009**, *395* (6), 1885-1892.

Chapter 2:

Multistep Approach for the Structural Identification of Biotransformation Products of Iodinated X-ray Contrast Media by Liquid Chromatography/Hybrid Triple Quadrupole Linear Ion Trap Mass Spectrometry and ^{1}H and ^{13}C Nuclear Magnetic Resonance

Jennifer Lynne Kormos,[1] Manoj Schulz,[1] Manfred Wagner,[2] and Thomas A. Ternes[1]

[1]*Federal Institute of Hydrology (BfG), Am Mainzer Tor 1, D-56068, Koblenz, Germany*

[2]*Max Planck Institute for Polymer Research, Ackermannweg 10, D-55128, Mainz, Germany*

Abstract

This study investigated the application of a hybrid triple quadrupole-linear ion trap mass spectrometer (Qq-LIT-MS) in combination with NMR to elucidate the chemical structures of 27 biotransformation products (TPs) of the nonionic iodinated X-ray contrast media (ICM), iohexol, iomeprol, and iopamidol, formed in contact with soil. The combination of MS^2 and MS^3 spectra with Qq-LIT-MS was essential to determine the MS fragmentation pathways crucial for structural elucidation. ^{1}H-NMR and ^{13}C-NMR analyses were needed to confirm the chemical structures of TPs proposed by MS fragmentation. Biotransformation occurred exclusively at the side chains of the iodinated X-ray contrast media, while the iodinated benzene ring remained unaltered. Several of the newly identified TPs of the ICM were found in surface water, groundwater and even drinking water. Concentrations as high as 1450 ± 110 ng/L (iomeprol TP629) were detected in groundwater that is influenced by wastewater infiltration, and as high as 289 ± 41 ng/L (iomeprol TP643) in drinking water.

2.1 Introduction

It has been well documented that pharmaceuticals and personal care products (PPCPs) are present in the environment (Kolpin *et al.* 2002; Loos *et al.* 2009). In recent years, most of the research has focused on the development of sensitive analytical methods to be able to detect low concentrations in complex matrices, and treatment technologies to reduce or eliminate the compounds from entering the aquatic environment (Ternes, 1998; Gros *et al.* 2006). The use of liquid chromatography (LC)/tandem mass spectrometry (MS) has become the instrument of choice for analyzing and quantifying target polar pollutants in different environmental matrices. Recently, more research has focused on the environmental fate of these emerging pollutants with

regards to their degradation potential via abiotic or biotic processes, and sorption capabilities (Doll and Frimmel, 2003; Drilla *et al.* 2005; Löffler *et al.* 2005; Schulz *et al.* 2008). However, there is still a major lack of information with regard to the formation of biotransformation products (TPs) in wastewater treatment plants (WWTPs) as well as in the environment.

Some research has focused on the development of analytical techniques for structural identification of TPs of environmental contaminants. Hybrid triple quadrupole-linear ion trap mass spectrometers (Qq-LIT-MS) as well as a quadrupole time-of-flight mass spectrometers (Qq-TOF-MS) have been applied to a limited extent for structural identification of new drugs and their excreted metabolites, and TPs of various pollutants (i.e. pesticides, pharmaceuticals) (Martínez Bueno *et al.* 2007; Pérez *et al.* 2007; Radjenović *et al.* 2008; Seitz *et al.* 2008; Trautwein *et al.* 2008). However, the information obtained from MS fragmentation pathways and elemental compositions is frequently insufficient to confirm the chemical structures. The application of MS techniques and NMR has been widely used for the identification of drug metabolites during pharmacokinetics and metabolism studies, but minimal research has investigated the use of this combination for identification of TPs of environmental contaminants (Schulz *et al.* 2008). The application of on-line LC-NMR-ESI-MS is a possible option for structural identification (Corcoran *et al.* 2003). However, the challenge would be to establish optimal conditions (e.g., compatible mobile phases) appropriate for both NMR and electrospray ionization (ESI) MS as well as to obtain sufficient quantities for NMR. Another option is the combined use of Qq-LIT-MS and off-line NMR for structural identification. This combination has been applied in the current study.

One group of emerging pollutants which are commonly detected at relatively high concentrations (i.e., micro per liter range) in environmental matrices are iodinated X-ray contrast media (ICM)

Hirsch *et al.* 2000; Pérez and Barceló, 2007). ICM are used in human medicine for distinguishing between different organs and blood vessels. Most ICM are derivatives of 2,4,6-triiodobenzoic acid. ICM can be referred to as ionic (e.g., diatrizoate) and nonionic (e.g., iohexol, iomeprol and iopamidol) compounds. The ionic ICM contain carboxylic moieties at their side chains, while the nonionic ICM are amide derivatives with hydroxyl functional groups (Pérez and Barceló, 2007). The global consumption of ICM is close to 3.5×10^6 kg/year, and a single application can be as high as 200 g/application. The ICM are designed to be inert substances, and are eliminated in the urine and feces unmetabolized within 24 hours (Pérez and Barceló, 2007). Therefore, most of what is consumed enters the domestic sewage system unchanged. The ICM are not completely eliminated by conventional and advanced treatment processes of WWTPs (Ternes and Hirsch, 2000; Carballa *et al.* 2004; Putschew *et al.* 2007; Ternes *et al.* 2007; Busetti *et al.* 2008) and therefore enter receiving waters and soil when WWTP effluent is irrigated on agricultural fields. The biotransformation of ICM in contact with irrigated soil and during bank filtration is likely due to the enhanced biological activity and the residence time. Nevertheless, only limited research has investigated the environmental fate of ICM, but some results indicate that iopromide and diatrizoate are biodegradable under certain conditions (Kalsch, 1999; Steger-Hartmann *et al.* 2002; Haiβ and Kümmerer, 2006; Schulz *et al.* 2008). However, there is a lack of information for iomeprol, iopamidol and iohexol regarding the identification of TPs.

The aim of this study was to investigate the biotransformation of iomeprol, iopamidol and iohexol under aerobic conditions in contact with soil, with emphasis on the identification and characterization of the TPs formed. Advanced analytical instrumentation involved the use of Qq-LIT-MS for determining the MS fragmentation pathways (i.e., cleaved moieties), and ^{1}H- and ^{13}C-NMR for structural confirmation (Figure 2.1). This is one of the first studies to provide a

comprehensive examination of the combination of Qq-LIT-MS and NMR for the structural
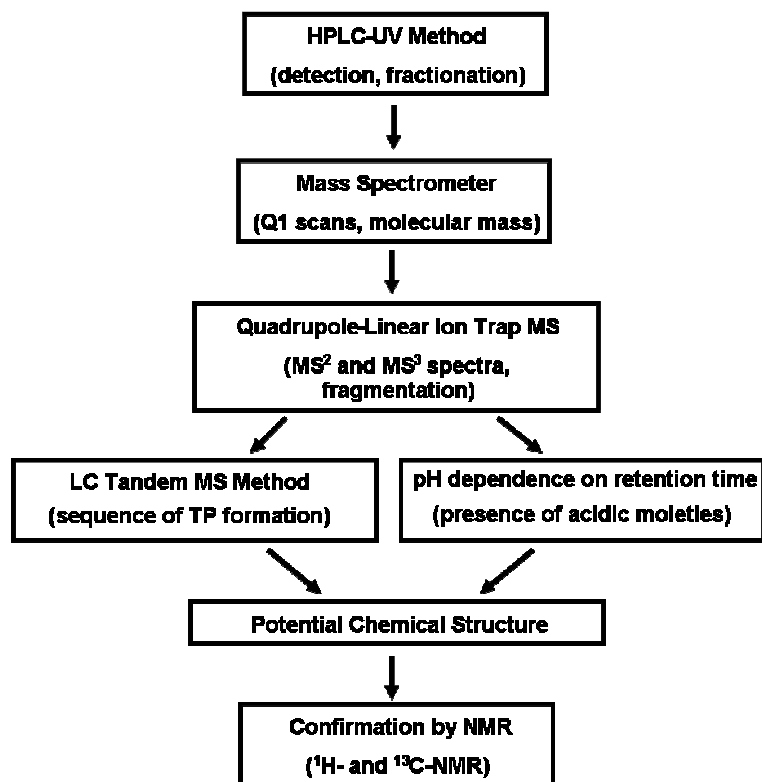
elucidation of TPs of environmental micropollutants.

```
┌─────────────────────────────┐
│      HPLC-UV Method         │
│   (detection, fractionation)│
└─────────────────────────────┘
              │
              ▼
┌─────────────────────────────┐
│     Mass Spectrometer       │
│  (Q1 scans, molecular mass) │
└─────────────────────────────┘
              │
              ▼
┌─────────────────────────────┐
│  Quadrupole-Linear Ion Trap MS│
│     (MS² and MS³ spectra,   │
│         fragmentation)      │
└─────────────────────────────┘
        ↙              ↘
┌──────────────────┐  ┌──────────────────────────┐
│ LC Tandem MS Method│  │pH dependence on retention time│
│(sequence of TP     │  │ (presence of acidic moieties)│
│  formation)        │  │                          │
└──────────────────┘  └──────────────────────────┘
        ↘              ↙
┌─────────────────────────────┐
│  Potential Chemical Structure│
└─────────────────────────────┘
              │
              ▼
┌─────────────────────────────┐
│     Confirmation by NMR     │
│     (¹H- and ¹³C-NMR)       │
└─────────────────────────────┘
```

Figure 2.1: Multistep approach for the identification of biotransformation products of selected iodinated X-ray contrast media

2.2 Experimental Section

2.2.1 Chemicals and Standards

Iohexol, iomeprol and iopamidol were supplied by Bayer Schering Pharma (Berlin, Germany),

and had a purity of >95%. All solvents (n-heptane, acetone, methanol and acetonitrile) were

picograde and purchased from Merck (Darmstadt, Germany). Formic acid (98-100%) was ACS

grade and purchased from Merck (Darmstadt, Germany).

2.2.2 Aerobic Water-Soil Systems

Water-soil systems were prepared for each of the selected ICM. Approximately 100 g of a low organic soil was placed into a 1 L amber bottle, and 500 mL of groundwater (with an ICM concentration of up to 1 g/L) was added. The elevated spiking concentration was used to detect and obtain sufficient quantities of the TPs in the water-soil systems. The batch systems were placed in the dark at room temperature (approx. 24 °C). The soil used for the batch systems was collected from an agricultural area which had been irrigated with secondary wastewater effluent for approximately 50 years. A detailed summary of the soil characteristics is provided elsewhere (Ternes *et al.* 2007). The experiment was conducted under aerobic conditions by measuring redox potential throughout the experimental period. Water-soil systems (2 g of soil and 20 mL of 1g/L of ICM) were also prepared with 2 mL of formaldehyde (37%, v/v) to determine if the transformation observed was the result of microbial activity. In addition, a blank water-soil system was prepared with 25 g of the soil and 125 mL of groundwater. The groundwater was collected from a deep well in Arenberg, a district of Koblenz, Germany.

2.2.3 Liquid Chromatography

An analytical method was developed, using an Agilent Series 1100 chromatography system with an ultraviolet (UV) detector (Agilent Technologies, Santa Clara, USA), to detect the parent compounds as well as potential TPs in batch water-soil systems during the experimental period. The chromatographic system consisted of an autosampler, column oven, quaternary pump and solvent degasser. Separation was achieved by coupling two reversed-phase Synergi Polar RP columns of 4 µm particle size, 150 mm in length and 3 mm i.d. (Phenomenex®, Aschaffenburg, Germany). For the detection of iomeprol TPs and iopamidol TPs, the elution was isocratic and the eluent consisted of 90% Milli-Q water and 10% acetonitrile plus the addition of 0.1%

aqueous formic acid. The composition of the eluent for detection of iohexol TPs was 95% Milli-Q water and 5% acetonitrile plus 0.1% aqueous formic acid. The UV detector was operated at two wavelengths, 245 nm and 254 nm, for iomeprol and iopamidol, and one wavelength of 242 nm for iohexol. The injection volume was 50 µL, column oven temperature was 50°C, run time was 20 min, and flow rate was 0.4 mL/min. The Milli-Q water was obtained with a USF ELGA PURELAB Plus water purification system (conductivity of 0.055µS/cm).

2.2.4 Isolation via Semipreparative HPLC-UV

A Waters HPLC-UV system, with Waters 717 plus autosampler, column oven, Waters 600 controller with quaternary pump, in-line degasser and Waters 2487 dual wavelength absorbance detector was used to fractionate and collect TPs. A semi-preparative column, Synergi Polar RP column 10 mm i.d., 250 mm, 4 µm, (Phenomenex®, Aschaffenburg, Germany), was used to separate the TPs, and fractions of the eluent were collected using an automated sample collector based on the retention time of the peaks in the chromatogram (Advantec SF-2120 Super Fraction Collector, Techlab GmbH, Erkerode, Germany). The eluent composition was the same as described above, however the flow rate was increased to 1.5 mL/min. An aliquot of each fraction collected was analyzed by LC/tandem MS to determine the composition and the purity of the fraction. If the fraction contained only one TP, the remaining amount of the fraction was freeze-dried. A pure solid material was obtained which could be used for NMR and as a standard for quantitative method development.

2.2.5 Mass Spectrometry

Mass spectrometry was performed on an Applied Biosystems/MDS Sciex 4000 Q Trap Qq-LIT-MS (Applied Biosystems, Langen, Germany). The system consisted of a hybrid triple quadrupole

and linear ion trap mass spectrometer equipped with an ESI source. Nitrogen was used as the drying, nebulizing and collision gas.

Q1 scans were performed on the fractions collected to determine the nominal masses. The ESI source was operated in both positive and negative modes to determine the dominant precursor ions at both polarities. The fractions were directly infused into the mass spectrometer at a flow rate of 5 to 10 µL/min. The parameter settings used for Q1 scans included curtain gas at 1.4×10^5 Pa, ion source gas 1 and gas 2 at 2.8×10^5 Pa, IonSpray voltage at 4500 V, temperature at 450 °C, declustering potential at 50 V, entrance potential at 10 V and a scan range of m/z 100 up to m/z 900.

The predominant product ions in the fractions collected were determined from the MS^2 spectra obtained during MS fragmentation. The parameter settings used for the MS^2 spectra were the same as for the Q1 scans with additional parameters set for collision energy at 30 eV and collision cell exit potential at 10 V. Infusion optimization was also conducted on the fractions collected to determine the optimal source and compound-dependent parameters for each dominant precursor-product ion mass transition. MS^3 spectra were completed for a selected number of fractions, in which there was a high enough intensity to obtain MS^3 scans. Additional parameter values were required for MS^3 spectra with the excitation energy, collision energy spread and scan rate set at 100 V, 5 eV, and 100 amu/s, respectively. For MS^2 and MS^3 spectra, the sample was directly infused into the mass spectrometer at a flow of 10 to 15 µL/min.

2.2.6 Nuclear Magnetic Resonance (NMR) Analyses

Approximately 15 mg of iomeprol, iopamidol and iohexol, and 2 to 12 mg of their TPs isolated from the water-soil batch systems were dissolved into 0.8 mL of DMSO-d$_6$. ^{1}H-NMR and ^{13}C-

NMR spectra were determined for the parent compounds and selected TPs. NMR analyses were carried out on a Bruker NMR DRX 700 Avance and DRX 500 instrument (Rheinstetten, Germany). ^{1}H-NMR spectra were measured at 700 MHz with a temperature of 298.3 K, and ^{13}C-NMR spectra were measured at 176 MHz as a spin-echo at a temperature of 298.3 K or at 125 MHz with a temperature of 293.1 K.

2.2.7 Sample Preparation and Analysis of ICM and TPs in Aqueous Samples

Surface water, groundwater and drinking water were monitored to determine if TPs of ICM identified in the batch systems by Qq-LIT-MS and NMR were also found under environmental conditions. Grab samples were taken of surface water as well as groundwater and drinking water. Sample preparation and detection by LC/tandem MS in MRM mode are already described in Schulz *et al.* (2008). However, MRM transitions were determined for the newly identified TPs.. In brief, the samples were adjusted to pH 2.8 with 3.5M of sulfuric acid, and spiked with 10 µL of the two surrogate standards, desmethoxyiopromide (DMI) and N-(2,3-dihydroxypropyl)-2,4,6-triiodo-5-methoxyacetyl-amino-N'-methylisoph-thalamide (DDPHI) provided by Bayer Schering Pharma (Berlin, Germany). Aqueous samples (1 L) were enriched via Isolute® ENV+ SPE cartridges (200 mg, 3mL, IST, Hengoed, UK) and were eluted with 10 mL of methanol. The extracts were evaporated to 100 µL and reconstituted up to 500 µL with Milli-Q water.

The samples were analyzed by LC/tandem MS equipped with an ESI source. A Synergi Polar RP column (Phenomenex®, Aschaffenburg, Germany) with a guard column was used for separation. The column oven was set to 50 °C, flow rate at 0.4 mL/min and injection volume was 20µL. A gradient was used with mobile phases consisting of Milli-Q water plus 0.1% aqueous formic acid (mobile phase A) and acetonitrile plus 0.1% aqueous formic acid (mobile phase B). The gradient

was as follows: after 4 min of 95% mobile phase A, the percentage of A was decreased to 75% within 11 minutes, and then returned to the initial conditions for the duration of the 20 min run time. Due to insufficient reference quantities for most TPs (isolated by LC fractionation), presently only the following TPs could be quantified in environmental samples: iomeprol TP629, TP643, TP701; iopamidol TP745, TP761, TP791; and iohexol TP599, TP657, and TP687A.

2.3 Results and Discussion

The results from this study confirm that the selected non-ionic ICM were biotransformed under aerobic conditions in the water-soil batch systems, with close to 100% of the parent ICM being transformed into a variety of TPs. Twenty-seven ICM TPs were identified with the combination of the elucidation of the MS fragmentation pathways and NMR analyses. The absence of TPs in batch systems with addition of formaldehyde (37%) as well as in blank batch system suggests that transformation of ICM in the soil-water systems was the result of microbial activity.

The proposed chemical structures of the TPs are listed in Table 2.1a and 2.1b, with all TPs resulting from modifications to the side chains of the parent ICM. In general, oxidation of the primary and secondary hydroxyl groups was the initial biological process to occur followed by oxidative decarboxylation, deacetylation, and the cleavage at the amide moieties of the side chains of the ICM.

Table 2.1a: Proposed chemical structures of transformation products of iohexol and iomeprol
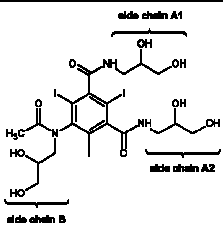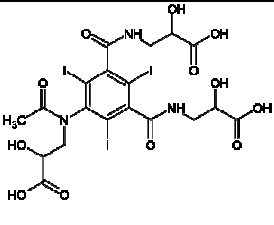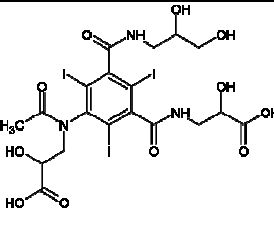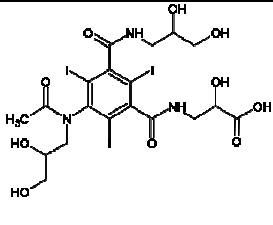
Chemical Structure Name	Chemical Structure Name	Chemical Structure Name	Chemical Structure Name
Iohexol	Iohexol TP863	Iohexol TP849	Iohexol TP835
Iohexol TP833	Iohexol TP775	Iohexol TP745	Iohexol TP687A
Iohexol TP687B	Iohexol TP657	Iohexol TP629	Iohexol TP599
Iomeprol	Iomeprol TP819	Iomeprol TP805	Iomeprol TP789
Iomeprol TP731	Iomeprol TP717	Iomeprol TP701	Iomeprol TP687
Iomeprol TP643	Iomeprol TP629		
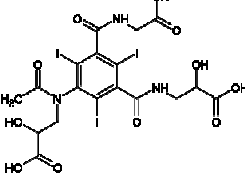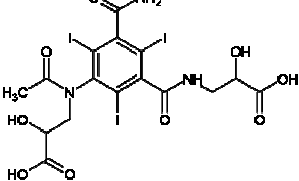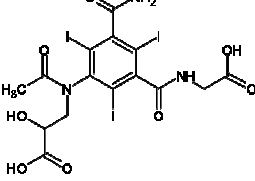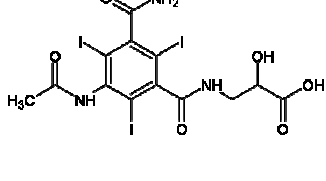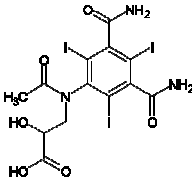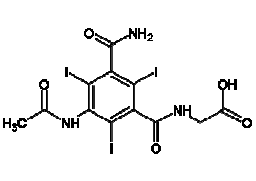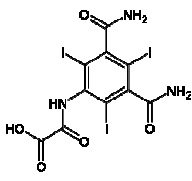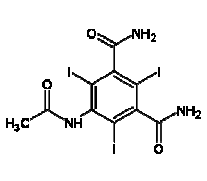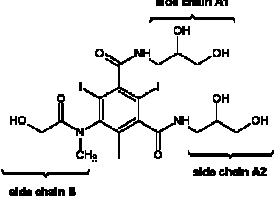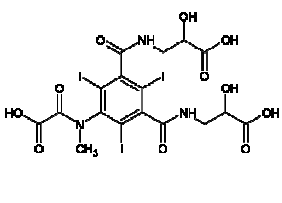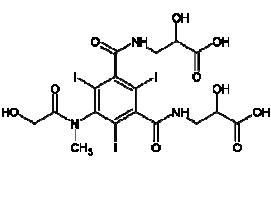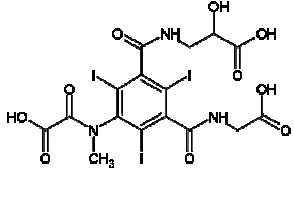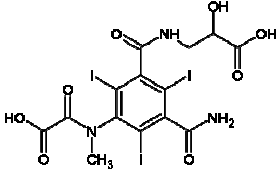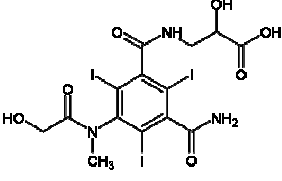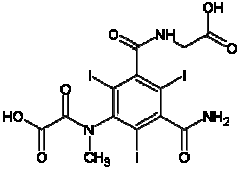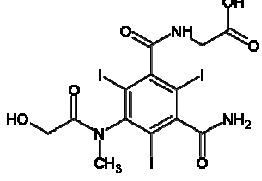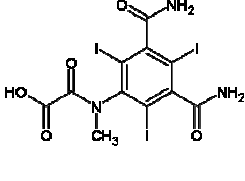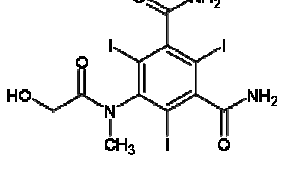
59

Table 2.1b: Proposed chemical structures of transformation products of iopamidol
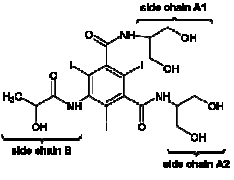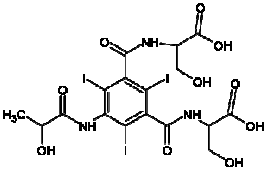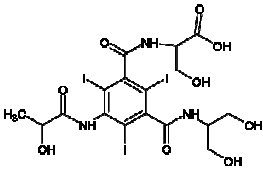
Chemical Structure	Name	Chemical Structure	Name
	Iopamidol		Iopamidol TP805
	Iopamidol TP791		Iopamidol TP775
	Iopamidol TP773		Iopamidol TP761
	Iopamidol TP745		Iopamidol TP687
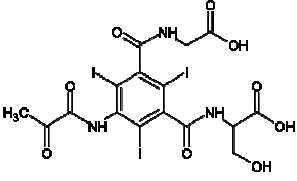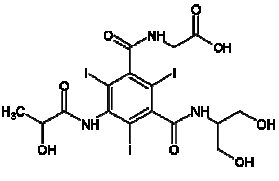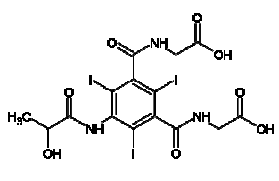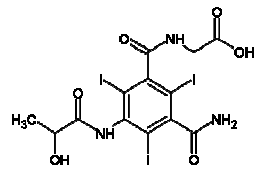
2.3.1 Determination of Molecular Weights via Q1 Scans

The nominal masses of the TPs in the fractions collected were determined by Q1 scans in both positive and negative ionization modes. In total, 27 TPs were determined via Q1 scanning, with 11 TPs detected for iohexol, nine TPs for iomeprol, and seven TPs for iopamidol. The molecular weights of all TPs were odd numbered, suggesting that an odd number of nitrogen atoms were present. This is based on the nitrogen principle that states a neutral molecule will have an uneven molecular mass, when there is an odd number of nitrogen atoms. The odd molecular mass of the TPs suggests that the nitrogen atoms were not cleaved during transformation, since the cleavage of two nitrogen atoms would result in a much lower molecular weight. A similar result was reported for iopromide by Schulz *et al.* (2008), Batt *et al.* (2006), and Pérez *et al.* (2006) in which the molecular weights of iopromide TPs were uneven.

Determination of the molecular weight and therefore the mass difference between the TP and parent compound indicated possible reactions for the formation of the TP. In some cases, the mass difference could be explained by a common reaction. For example, the mass difference of 14 Da between iohexol and iohexol TP835 suggested that oxidation of a primary alcohol to a carboxylic moiety occurred. However, a large mass difference between the parent compound and lower molecular weight TPs (i.e. iomeprol TP629, iohexol TP599) was difficult to explain, since different reactions had taken place. For example, the mass difference of iomeprol and iomeprol TP643 was 148 Da, which resulted in a several reactions (i.e. oxidation and cleavage of certain moieties on the side chains) to obtain the correct mass difference.

2.3.2 Fragmentation Pathways via Qq-LIT-MS

The MS^2 and MS^3 spectra and the proposed MS fragmentation pathways for the parent ICM and TPs are provided in the Supporting Information for collision energy of 30eV. In general, the fragmentation pathways of iomeprol TPs and iopamidol TPs were found to be similar to each other, while the fragmentation of iohexol and its TPs were different. One possible explanation is the distinct difference in the functional moieties of side chain B of iohexol (Table 2.1a). This particular ICM has a propane-1,2-diol and a N-acetyl moiety on side chain B which is not present for iomeprol or iopamidol.

The fragmentation of iohexol, as well as for most iohexol TPs (e.g. iohexol TP849, TP833, and TP745), showed the cleavage of an iodine radical in combination with the cleavage of the acetyl group (loss of 42 Da) on side chain B. Other common cleaved moieties for iohexol TPs included

the loss of two iodine radicals in combination with a CO group (28 Da), and a loss of CH_2O (30 Da).

In the MS fragmentation pathways, it was common for one or more side chains at the amide bond to be cleaved as well as the neutral loss of HI (128 Da), the loss of carbonyl groups (28 Da), the loss of water (18 Da) and the loss of iodine radicals (127 Da). In addition, the cleavage of CO_2 and HCOOH suggested oxidation had occurred on the side chains.

The loss of ammonia (17 Da) and removal of CO-NH (43 Da) were common for the lower molecular weight TPs (e.g., iomeprol TP643, iohexol TP657). For the higher molecular weight TPs, the loss of 17 Da could only be explained by the cleavage of a hydroxyl radical (HO·). The loss of a hydroxyl radical was one of the major groups cleaved during fragmentation of the iopamidol TPs.

The MS^2 spectra provided useful information for the determination of the proposed MS fragmentation patterns by locating the site of transformation. For example, the difference in molecular weight of 28 Da between iopamidol and iopamidol TP805 was likely the result of oxidation, but it was unclear if oxidation occurred twice on the same side chain or on two different side chains. The absence of certain fragment ions in the MS^2 spectra indicated which side chains were oxidized.

In addition, the MS^3 spectra indicated which product ions originated from the precursor ions. The MS^3 spectra also suggested if there was more than one major fragmentation pathway for each

TP. For example, the MS^3 spectra of iopamidol TP805 (Figure S2.6.14 in section 2.6) showed that there was only one major fragmentation pathway for this TP, since all dominant fragment ions found in the MS^2 spectrum were present in the MS^3 *m/z* 806 → 701. Hence, both MS^2 and MS^3 spectra were needed for proposing reliable chemical structures.

The MS fragmentation pattern of iomeprol TP805 did not provide sufficient information to propose a chemical structure. Instead two potential structures could be explained from the mass spectra. The mass difference between iomeprol and iomeprol TP805 suggested that oxidation occurred twice, but it was unclear from the mass spectra which side chains were oxidized (Figure S2.6.4 and S2.6.5 in section 2.6). As described in the NMR section, the presence of multiple chemical shifts representing the methyl group on side chain B for iomeprol TP643, and the stabilization of two isomers by hydrogen bonding and tautomerism resulting in two peaks in the LC chromatogram for this TP, was associated with oxidation on side chain B. The presence of one peak in the LC chromatogram suggested that iomeprol TP805 resulted in oxidation occurring on side chain A1 and A2.

In addition, there were TPs (e.g., iopamidol TP791, iopamidol TP761) in which the cleavage of iodine radicals and hydroxyl radicals resulted in the fragment ions observed in the mass spectra. Although, these cleavages were unusual in collision induced dissociation (CID) fragmentation, the NMR data confirmed the chemical structures.

2.3.3 Determination of TPs with acidic moieties

Samples collected from the batch system were analyzed via LC/tandem MS using an acidic pH 2.8 and then a neutral eluent to indicate which TPs contained acidic moieties such as carboxylic groups. There were only two TPs, iohexol TP599 and iomeprol TP629, in which retention time was not influenced by changes from acidic to neutral pH, and therefore obviously did not have acidic moieties (Figure S2.6.1; Chapter 2.6). This procedure only provided additional information about the presence of acidic functional groups.

2.3.4 Nuclear Magnetic Resonance Analysis

The NMR data was used in combination with the information obtained from the MS fragmentation data and pH-dependent experiments described above to confirm the chemical structures of the TPs. Iohexol, iomeprol, iopamidol and selected TPs (i.e. iomeprol TP629, TP643 and TP701; iohexol TP599 and TP657; iopamidol TP745, TP761 and TP791) were analyzed by ^{1}H-NMR and ^{13}C-NMR (Tables S2.6.1-S2.6.5 and Figures S2.6.33-S2.6.53). The NMR spectra confirmed that the benzene ring, and the methyl group present on side chain B were not modified. The differences in the chemical shifts between the parent ICM and TPs were the result of changes to the side chains, and this correlated well with the proposed structures from the MS fragmentation experiments.

It has to be noted that many NMR signals were split for the ICM and ICM TPs because diasteromers and *cis-trans* isomers were simultaneously occurring, due to the presence of chiral carbon atoms and C=N double bonds (tautomeric structures of the amide moieties), in the chemical structure, respectively. In the current manuscript the NMR spectra were used to

confirm the proposed chemical structures derived from the MS fragmentation pathways. Therefore, the splitting of many NMR signals was not further discussed as long as it was not crucial for the confirmation of the chemical structures.

The presence of a chemical shift at approximately 9.93 ppm in the ^{1}H-NMR spectra for the iohexol TPs and its absence in the spectrum for iohexol indicated the formation of a secondary amide group on side chain B. In addition, many singlets were present between 7.6 ppm and 8.0 ppm for the iohexol TPs as well as the iomeprol TPs, confirming the formation of primary amide functional groups due to the cleavage of propanol-1,2-diol moieties. For iohexol TP599 (Figures S2.6.35 and S2.6.36 in chapet 2.6) the integration resulted in four hydrogens, indicating that two NH_2 groups were present, and for iohexol TP657 Figure S2.6.34), integration resulted in two hydrogens or one NH_2 group. The possible formation of C-N double bonds by tautomerism of the amide structures, causing a hindered rotation of the C-N bonds and formation of *cis-trans* isomers, is an explanation for the multiplet detected in ^{1}H-NMR (Gutowsky and Holm, 1956; Quintanilla-Licea *et al.* 2002).

The presence of more than one distinct peak for the methyl group on side chain B in ^{1}H-NMR spectra of iomeprol TP701 and TP643 (Figure 2.2a), and ^{13}C-NMR spin-echo spectrum of iomeprol TP643 (Figure 2.2b) confirmed once again the presence of structural isomers. Already in 1956 Gutowsky and Holm reported two distinguished singlets for the two N-CH_3 groups of *N*,*N*-dimethylformamide due to the formation of a C=N double bond by the tautomerism of the amide moiety. This might also explain the two peaks observed for the methyl groups in the NMR spectra of the iomeprol TPs.
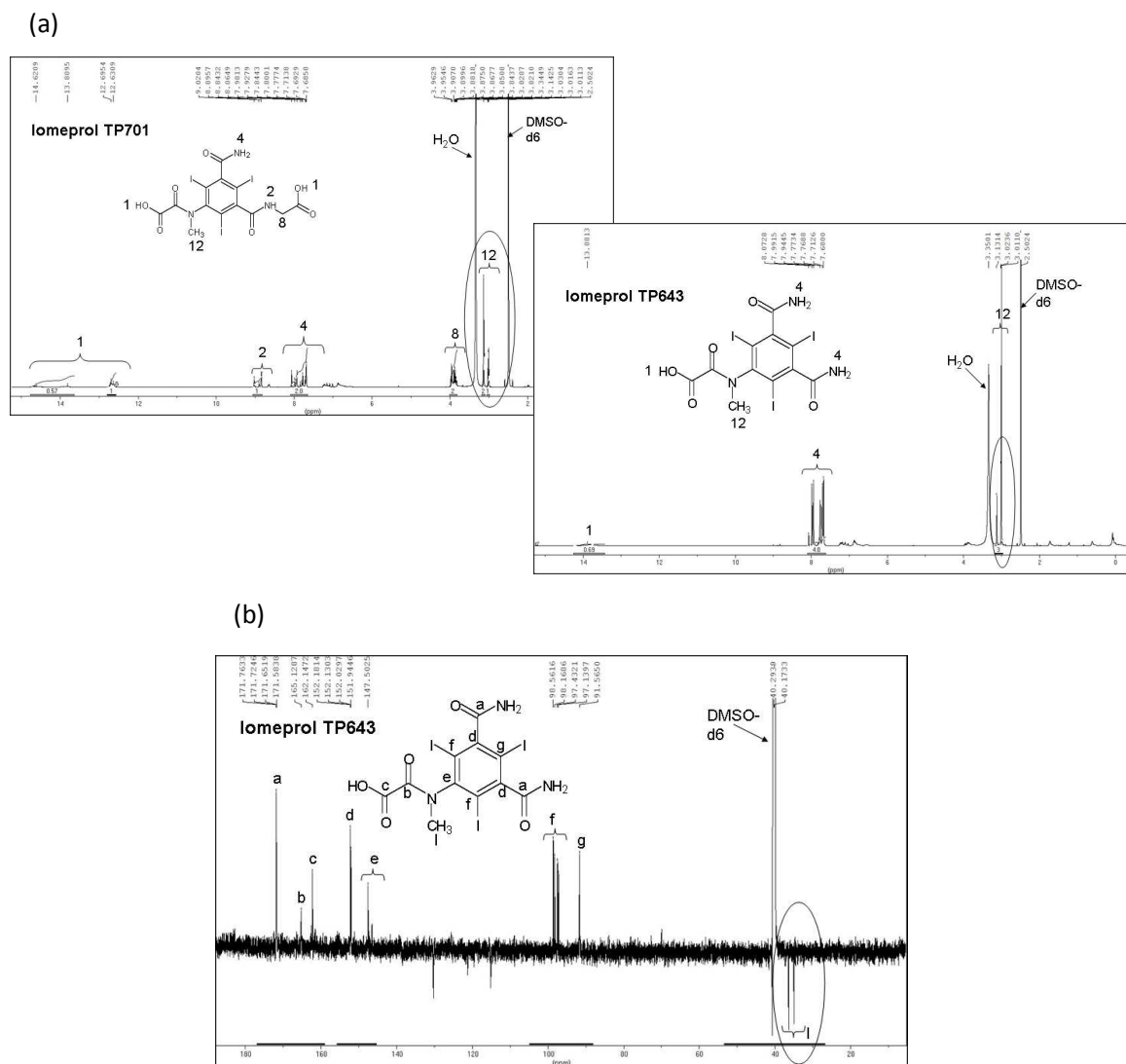
Figure 2.2: ^{1}H-NMR spectra of iomeprol TP701 and iomeprol TP643 (a) measured at 700MHz and temperature of 298.3K, and ^{13}C-NMR spin-echo spectrum for iomeprol TP643 (b) measured at 176MHz and temperature of 298.3K

In the NMR spectra of TP701 and TP643 (Figure 2.2), two distinct peaks for the methyl group on side chain B could be identified, while for compounds such as iomeprol TP629 without the carboxylic moiety at side chain B only one NMR singlet was found for the methyl moiety. It should be noted that the TPs were isolated at an acidic pH, and thus the protonated form of the

compounds were present. In the LC tandem MS chromatograms (Figure 2.3) two separate peaks were also identified at pH 2.8 for iomeprol TPs with a carboxylic moiety on side chain B, while at pH 7 only one peak occurred. Based on the NMR spectra and LC/tandem MS chromatograms, it can be assumed that the intramolecular hydrogen bond (i.e., proton on the carboxylic acid) in conjunction with tautomerism keeps the amide bond from rotating and stabilizes the formation of two *cis-trans* isomers.

The ^{13}C-NMR spectrum (refer to Figure 2.3, ^{13}C-NMR spin-echo spectrum for iomeprol TP643) confirmed that the benzene ring remained unchanged with three iodine atoms and three amide moieties attached. The chemical shifts of approximately 170 ppm (presence of carbonyl groups), 151 ppm (carbon atoms in the benzene ring attached to carbonyl groups), 143 to 148 ppm (carbon atoms in the benzene ring attached to side chain B), and approximately 100 ppm and 91 ppm (carbon atoms in the benzene ring attached to iodine atoms) were present for the parent ICM as well as all selected TPs.
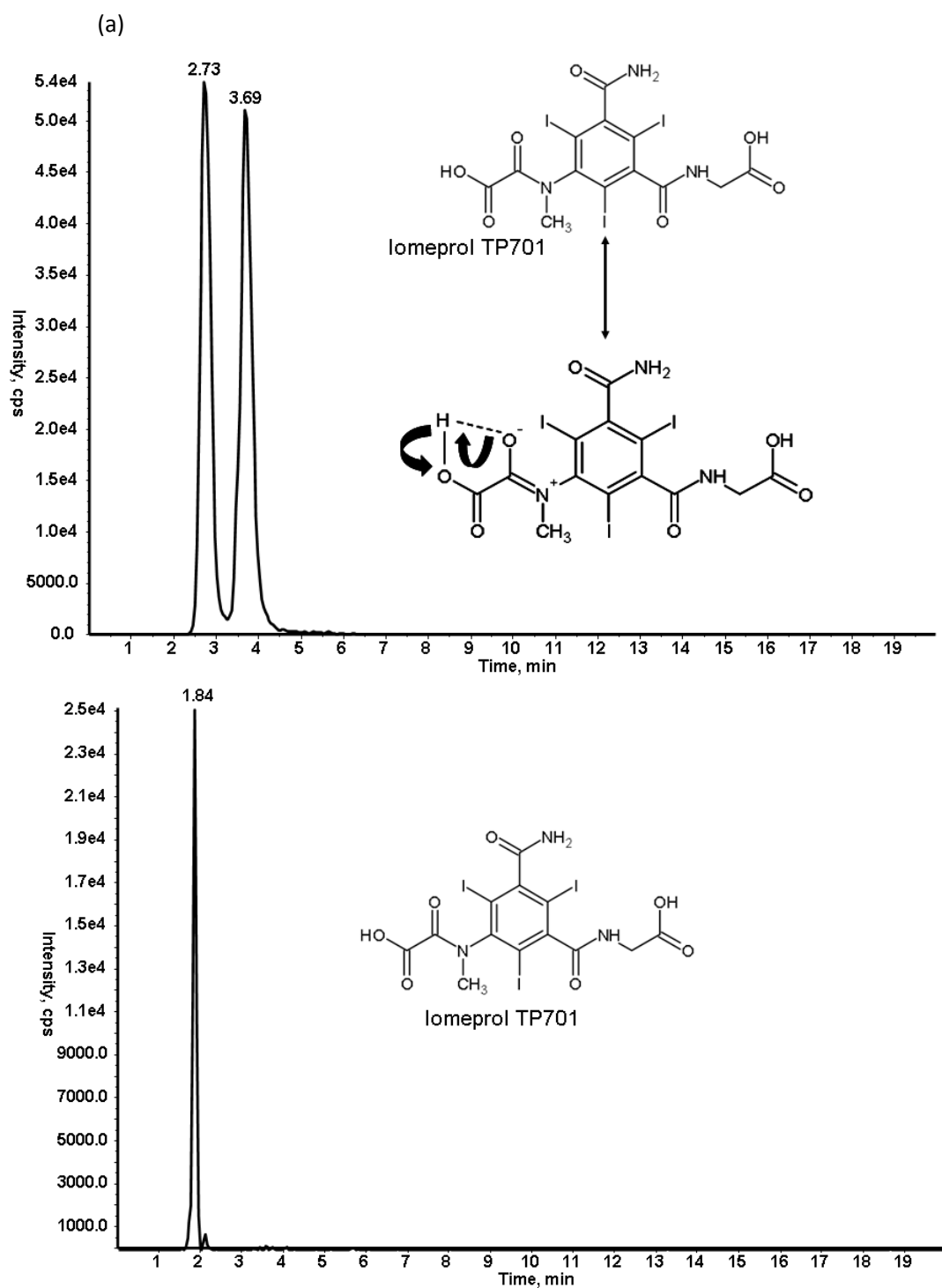
Figure 2.3: LC tandem MS chromatograms showing the presence of structural isomers of iomeprol TP701 via tautomerization at acidic pH of 2.8 (a) and absence of structural isomers at a neutral pH (b)

Although, the NMR confirmed the proposed structures from the MS techniques, the use of NMR alone would not be sufficient to elucidate the chemical structure of TPs. This can be explained since the chemical shifts cannot always be allocated to the chemical groups, and that certain signals maybe hidden by the water peak observed in ^{1}H-NMR spectra. This water peak was still observed in the NMR spectra despite the isolated TPs being dried several times before analysis. In addition, the presence of structural isomers as well as the presence of tautomerism makes interpretation of the NMR spectra quite complicated if this was the only technique being used for structural identification. Thus, MS fragmentation was crucial for TP identification as well.

2.3.5 Presence of ICM TPs in Aqueous Environmental Samples

Some of the newly identified ICM TPs were detected in surface water, groundwater and drinking water using the described LC/tandem MS method. The LC tandem MS chromatograms (MRM mode) are shown in Figure 2.4. Iohexol TP599, iomeprol TP629, TP643, TP717 and iopamidol TP687, TP745, TP791 were identified in surface water, groundwater and even drinking water. In Table 2.2 measured concentrations are listed for five TPs (iohexol TP599, iomeprol TP629, TP643 and iopamidol TP745 and TP791) with a sufficient quantity isolated by LC fractionation as well as the target ICM. Concentrations of iomeprol TP629 were greater than 1 µg/L in a groundwater influenced by wastewater infiltration, and as high as 289±41 ng/L for iomeprol TP643 in finished drinking water. Obviously, the results obtained with the water-soil batch systems can be transferred to real environmental conditions. However, in order to achieve an exact quantification for all TPs, reference standards of more TPs need to be synthesized or isolated in sufficient quantities. Future initiatives will involve a higher number of TPs as well as

a comprehensive sampling campaign to elucidate the biotransformation of ICM and the occurrence of the ICM TPs in the aquatic environment.
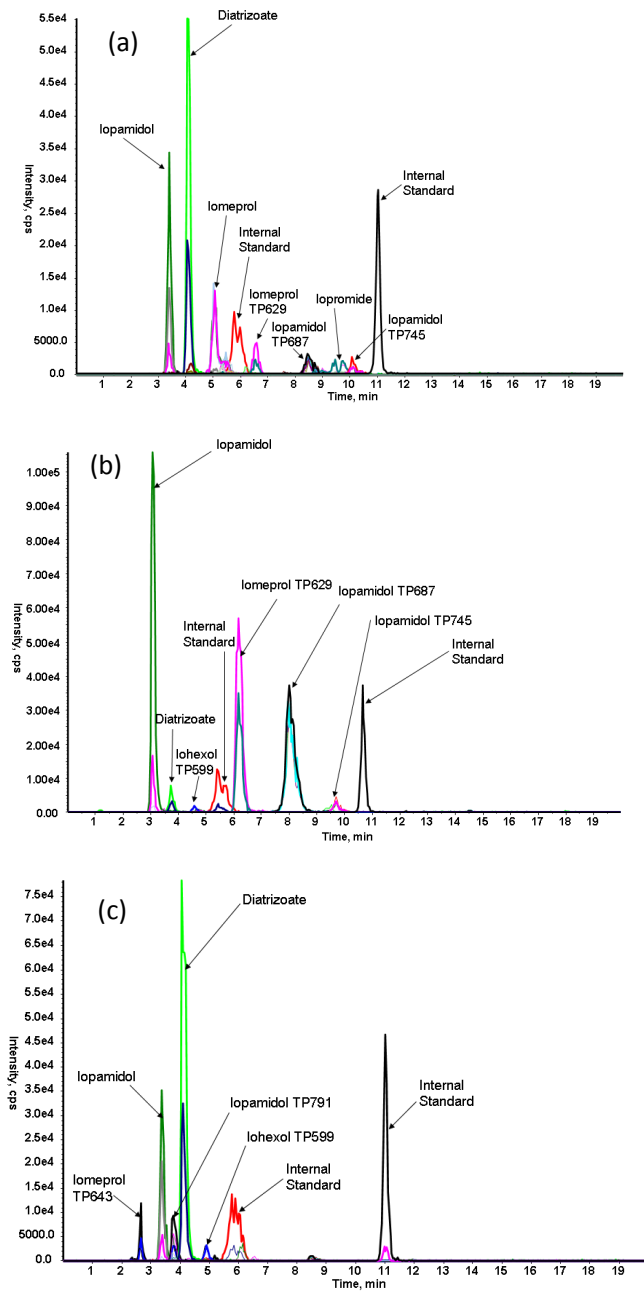
Figure 2.4: LC tandem MS chromatograms showing the presence of selected ICM and TPs in surface water (a), groundwater (b), and drinking water (c)

Table 2.2: Concentrations and 95% confidence intervals (n = 3) of selected ICM and TPs in surface water, groundwater and drinking water

ICM and TPs	Surface Water	Groundwater (influenced by infiltration of WWTP effluent)	Drinking Water
Iohexol	96 ± 26	< LOQ	< LOQ
	(LOQ = 1 ng/L)	(LOQ = 4 ng/L)	(LOQ = 2 ng/L)
Iohexol TP599	< LOQ	28 ± 6	83 ± 11
	(LOQ = 1 ng/L)	(LOQ = 10 ng/L)	(LOQ = 2 ng/L)
Iomeprol	280 ± 23	10 ± 3	< LOQ
	(LOQ = 4 ng/L)	(LOQ = 4 ng/L)	(LOQ = 1 ng/L)
Iomeprol TP629	100 ± 19	1450 ± 110	18 ± 2
	(LOQ = 2.5 ng/L)	(LOQ = 10 ng/L)	(LOQ = 2 ng/L)
Iomeprol TP643	< LOQ	< LOQ	289 ± 41
	(LOQ = 2.5 ng/L)	(LOQ = 10 ng/L)	(LOQ = 1 ng/L)
Iopamidol	180 ± 39	470 ± 65	244 ± 44
	(LOQ = 20 ng/L)	(LOQ = 20 ng/L)	(LOQ = 1 ng/L)
Iopamidol TP745	42 ± 9	76 ± 24	< LOQ
	(LOQ = 2.5 ng/L)	(LOQ = 4 ng/L)	(LOQ = 1 ng/L)
Iopamidol TP791	< LOQ	< LOQ	57 ± 11
	(LOQ = 1 ng/L)	(LOQ = 1 ng/L)	(LOQ = 2 ng/L)

*Concentrations were quantified by use of ICM and isolated TP standards and by applying the described LC/ tandem MS method

2.4 Conclusions

The use of Qq-LIT-MS to elucidate potential structures and NMR for structural confirmation was an effective approach for investigating the biotransformation of ICM. The combination of the fragmentation patterns obtained from the MS^2 and MS^3 spectra with ^{1}H- and ^{13}C-NMR enabled the structural elucidation of 27 previously unidentified ICM TPs. Since some of them were present in aqueous samples, it can be confirmed that nonionic ICM are biotransformed under specific experimental conditions, even though they are resistant to human metabolism and several water treatment processes. Due to the biotransformation, the use of nonionic ICM as ideal wastewater tracers should be carefully considered. The present study provides an example

of how important it is to elucidate the environmental fate of micropollutants because several stable TPs might be formed.

2.5 Acknowledgment

2.6 Supporting Information

2.6.1 Experimental design

The following section contains information on the sample collection and preparation of the samples collected from the batch systems as well as from the environment. In addition, there is information about how the samples were prepared for HPLC-UV analysis, the MS fragmentation experiments, and LC tandem MS method.

Sample Collection: Samples (2 mL aliquots) were collected from the aqueous phase of the batch water-soil systems at repeated intervals for the duration of the 150 d. These samples were frozen to prevent further degradation. In addition, larger volumes were collected from the batch systems at certain experimental days to have a sufficient volume for fractionation and isolation of the TPs. Large volumes were collected on day 67, 94 and 129 for iopamidol, day 67, 94 and 146 for iomeprol, and day 102 and 143 for iohexol.

Sample Preparation and Extraction: For screening and detection of the parent ICM and TPs, samples were prepared by taking 100 µL of the 2 mL aliquot and adding 900 µL of a 90:10 (v/v) Milli-Q water and acetonitrile solution. The samples for fractionation and isolation were prepared by collecting 100 to 150 mL of the aqueous water phase from the batch water-soil systems at the specified days mentioned above. These samples were filtered using folded filters, ø 240 mm (Schleicher & Schüll GmbH, Dassel, Germany), frozen at -25 °C and then freeze dried using a Lyovac GT 2 system (Amsco Finn-Aqua. GmbH, Hürth, Germany) at a pressure of 0.14 mbar. The freeze-dried samples were diluted with 10 to 15 mL of Milli-Q water and sonicated for 10 to 15 min using an ultra-sonication bath. Approximately 2 to 3 mL aliquots of the prepared sample were passed through pre-conditioned solid-phase extraction (SPE) cartridges containing approximately 400 mg of bulk C_{18} sorbent for clean-up purposes. The SPE material was pre-conditioned by using 2 mL n-heptane, 2 mL acetone, 4 x 2 mL methanol and 5 x 2 mL Milli-Q water. The eluate from the cartridges was collected and transferred to HPLC vials for analysis and fractionation via HPLC-UV.

For the real environmental samples, the sample preparation procedure and analytical method applied were similar to what was reported previously by Schulz et al., 2008. All samples were acidified to pH 3 with 3.5M of sulfuric acid to prevent further degradation, and filtered through glass fiber filters (GF 6, Schleicher and Schuell, Dassel, Germany). The sample volumes used for enrichment were 1L for groundwater, surface water and drinking water samples. All samples were adjusted to pH 2.8 with 3.5M of sulfuric acid and spiked with 10 µL (20µg/mL) of the two surrogate standards, desmethoxyiopromide (DMI) and N-(2,3-dihydroxypropyl)-2,4,6-triiodo-5-methoxyacetylamino-N'-methylisophthalamide (DDPHI). The samples were enriched with Isolute® ENV+ SPE cartridges (200mg, 3mL, IST, Hengoed, UK). The cartridges were

conditioned with 2mL of n-heptane, 2mL of acetone, 8mL of methanol and 8mL of groundwater adjusted to pH 2.8. The cartridges were dried by a gentle stream of nitrogen and then eluted with 10mL of methanol. The eluted sample was evaporated to 100µL and reconstituted up to 500µL with Milli-Q water.

The samples were analyzed by LC tandem MS using an Applied Biosystems/MDS Sciex 4000 QTrap system with an electrospray ionization (ESI) source in MRM mode. At least two mass transitions were optimized for each TP as well as for the parent ICM. The mass transitions with selected compound-dependent parameters are summarized in Chapter 3, section 3.6.

Stock solutions were prepared for all nine isolated TPs (i.e. iohexol TP687A, TP657 and TP599, iomeprol TP701, TP643 and TP629, as well as iopamidol TP791, TP761 and TP745) and the parent ICM by dissolving approximately 1mg of standard into 10mL of Milli-Q water. External calibration standards were prepared by diluting the stock solutions with Milli-Q water and spiking 10µL (20µg/mL solution) of the two surrogate standards. The calibration samples ranged from 1ng/mL to 2000ng/mL.

A Synergi Polar RP column (Phenomenex®, Aschaffenburg, Germany) with a guard column was used for separation. The column oven was set to 50 °C, flow rate at 0.4 mL/min and injection volume was 20µL. A gradient was used with mobile phases consisting of Milli-Q water with 0.1% aqueous formic acid (mobile phase A) and acetonitrile with 0.1% aqueous formic acid (mobile phase B). The gradient was as follows: after 4 min of 95% mobile phase A, the

percentage of A was decreased to 75% within 11 minutes, and then returned to the initial conditions for the duration of the 20 min run time.

2.6.2 Identification of TPs with acidic moieties

This section provides further details about the influence of pH on the retention time of the ICM TPs when measured via LC tandem MS. The absence and presence of acid (formic acid) in the eluents during LC tandem MS analysis provided information about the acidic properties of the TPs. Samples collected from the aerobic water-soil systems were prepared as described above and were analyzed by LC tandem MS. The samples were measured with 0.1% formic acid in Milli-Q water (pH 2.8) and acetonitrile, and then the samples were analyzed again at a neutral pH. Comparisons were made between the retention times of the different TPs with and without the addition of formic acid. There were only two TPs (iohexol TP599 and iomeprol TP629) which were not influenced by pH changes. Figure S2.6.1 shows an example of the presence of iomeprol TP626 when analyzed with the addition of formic acid and without. The retention time for iomeprol TP629 remained the same whether measured at a neutral or acid pH. Similar results were found for iohexol TP599. This gave a strong indication that these two TPs did not have acidic moieties in their structures. This was in agreement with the structures proposed from the MS fragmentation experiments and NMR data.

(a)

(b)
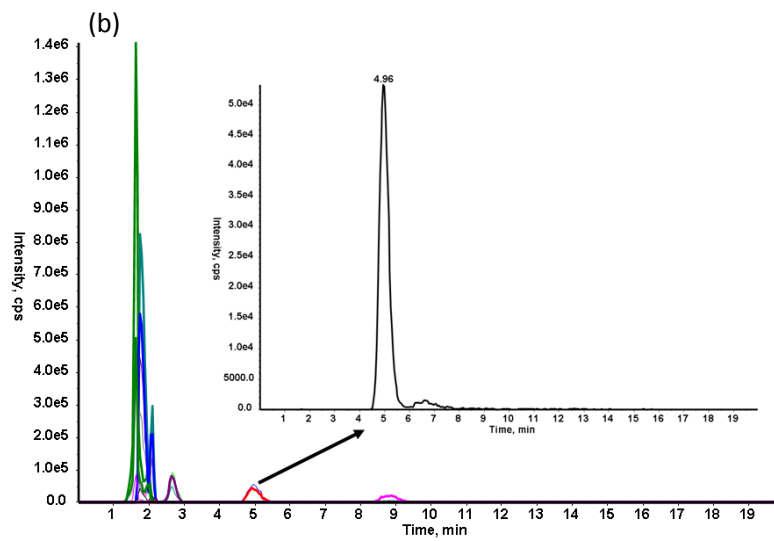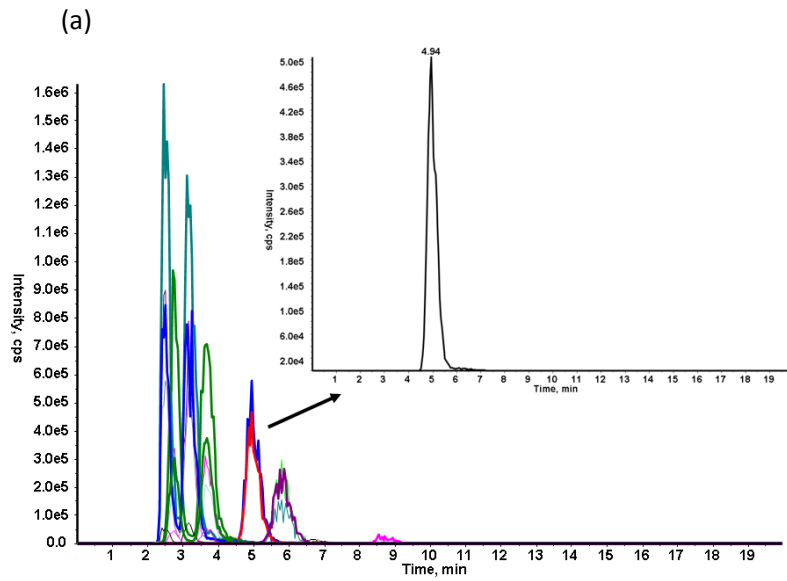
Figure S2.6.1: The presence of iomeprol TP629 in water-soil batch samples when analyzed at an acidic pH (a) and a neutral pH (b) via LC ESI tandem MS

2.6.3 MS Fragmentation Experiments

The following figures contain the MS^2 and MS^3 spectra for the parent non-ionic ICM and their TPs, as well as the proposed fragmentation pathways.
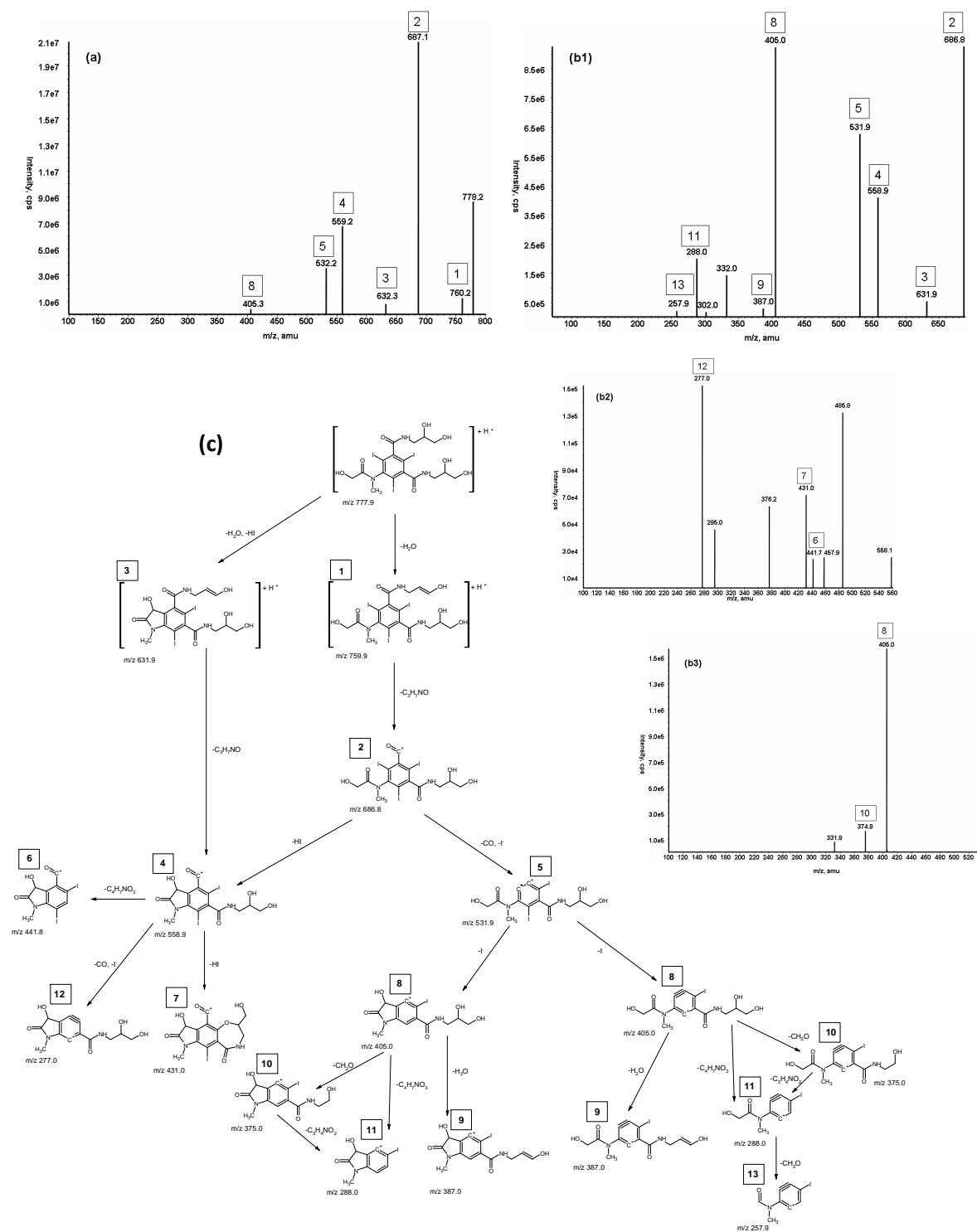
Figure S2.6.2:MS^2 and MS^3 spectra for iomeprol: (a) MS^2 *m/z* 778; (b1) MS^3 *m/z* 778 → 687; (b2) MS^3 *m/z* 778 → 559; (b3) MS^3 *m/z* 778 → 532; (c) proposed fragmentation pathway of iomeprol. The mass spectra were determined at a collision energy of 30 eV.
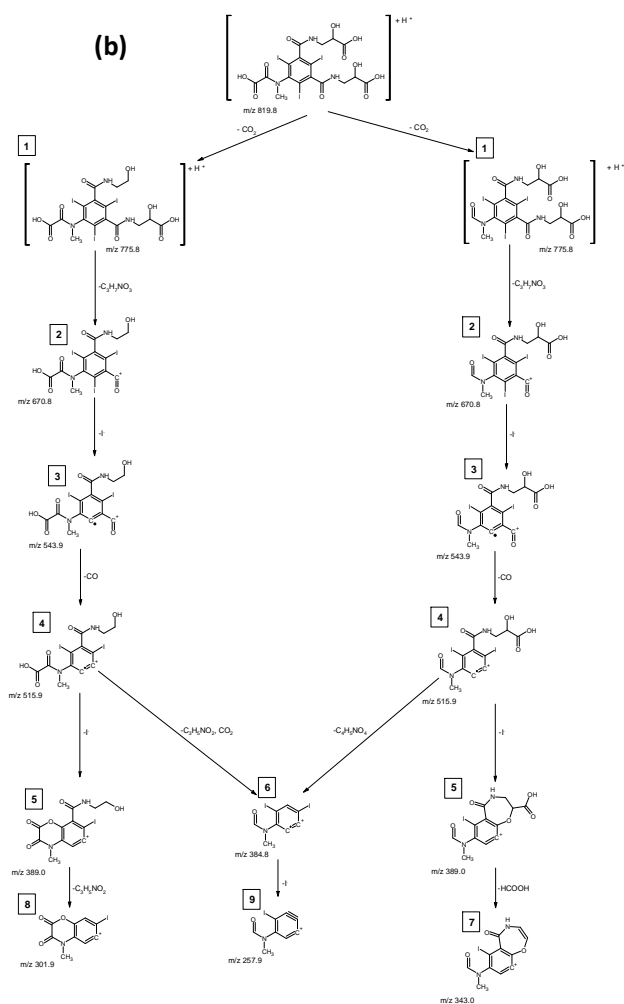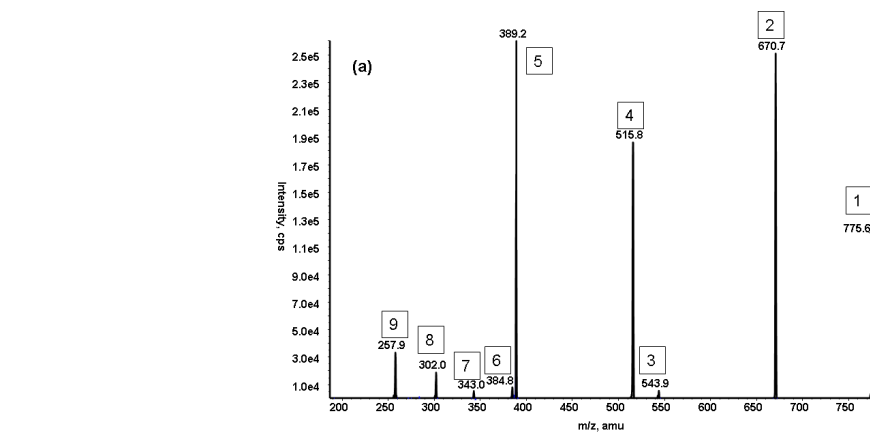
Figure S2.6.3: MS^2 spectrum for iomeprol TP819: (a) MS^2 *m/z* 820; (b) proposed fragmentation pathway of iomeprol TP819. The mass spectrum was determined at a collision energy of 30 eV.
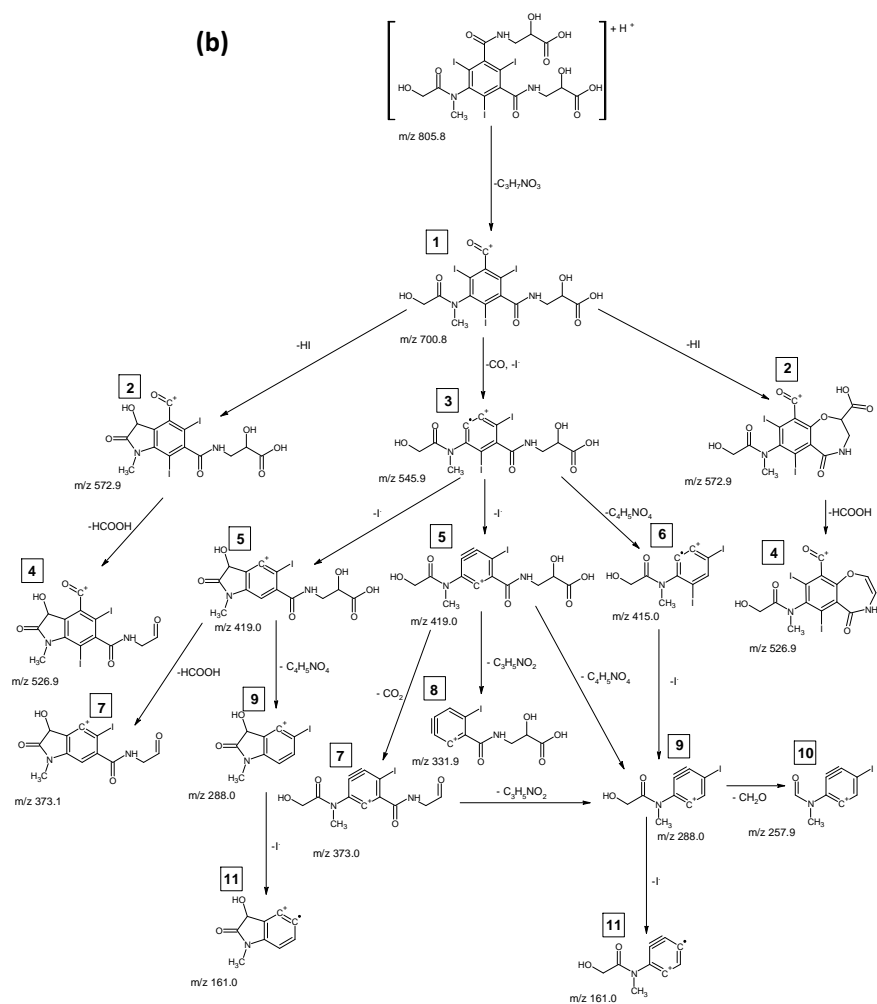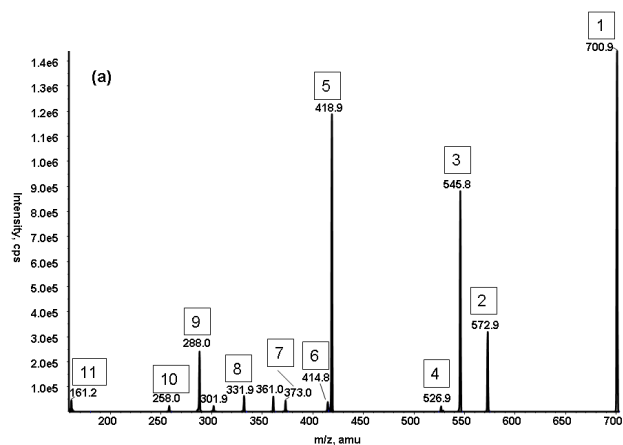
Figure S2.6.4: MS^2 spectrum for iomeprol TP805A: (a) MS^2 *m/z* 806; (b) proposed fragmentation pathway of iomeprol TP805A. The mass spectrum was determined at a collision energy of 30 eV.

Figure S2.6.5: MS² spectrum for iomeprol TP805B: (a) MS² *m/z* 806; (b) proposed fragmentation pathway of iomeprol TP805B. The mass spectrum was determined at a collision energy of 30 eV.

81
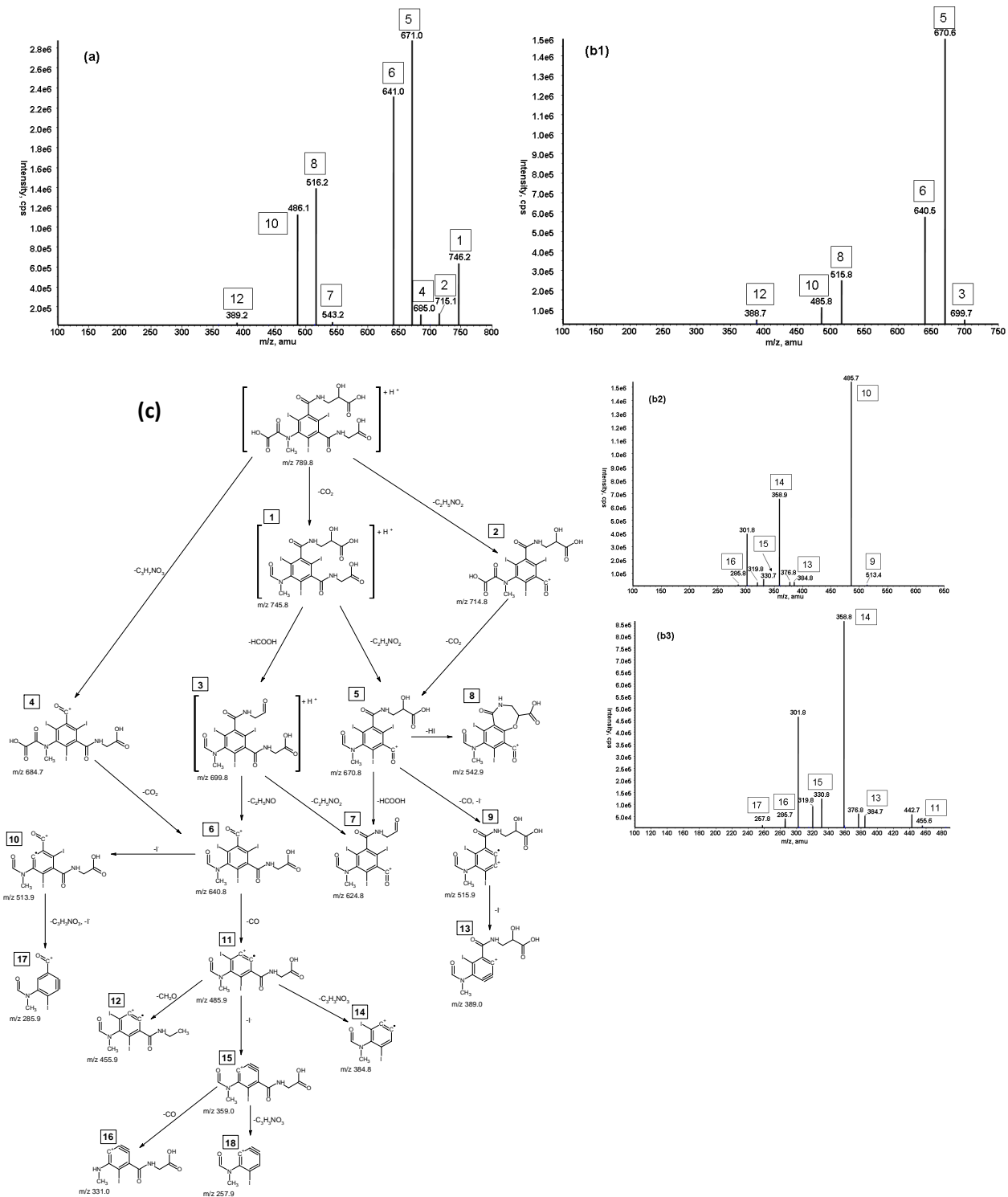
Figure S2.6.6: MS^2 and MS^3 spectra for iomeprol TP789: (a) MS^2 m/z 790; (b1) MS^3 m/z 790 → 746; (b2) MS^3 m/z 790 → 641; (b3) MS^3 m/z 790 → 486; (c) proposed fragmentation pathway of iomeprol TP789. The mass spectra were determined at a collision energy of 30 eV.

82

Figure S2.6.7: MS^2 spectrum for iomeprol TP731: (a) MS^2 *m/z* 732; (b) proposed fragmentation pathway of iomeprol TP731. The mass spectrum was determined at a collision energy of 30 eV.
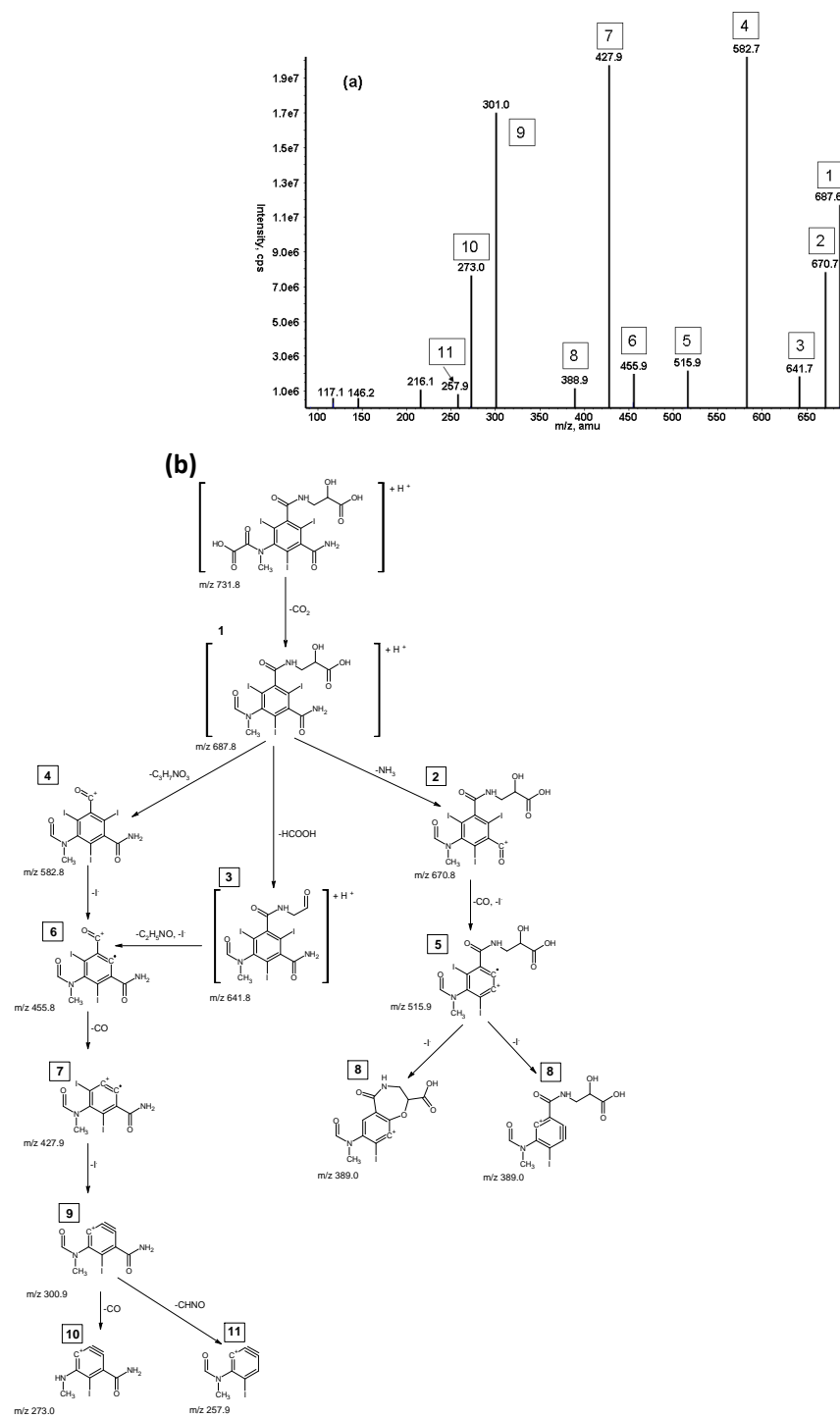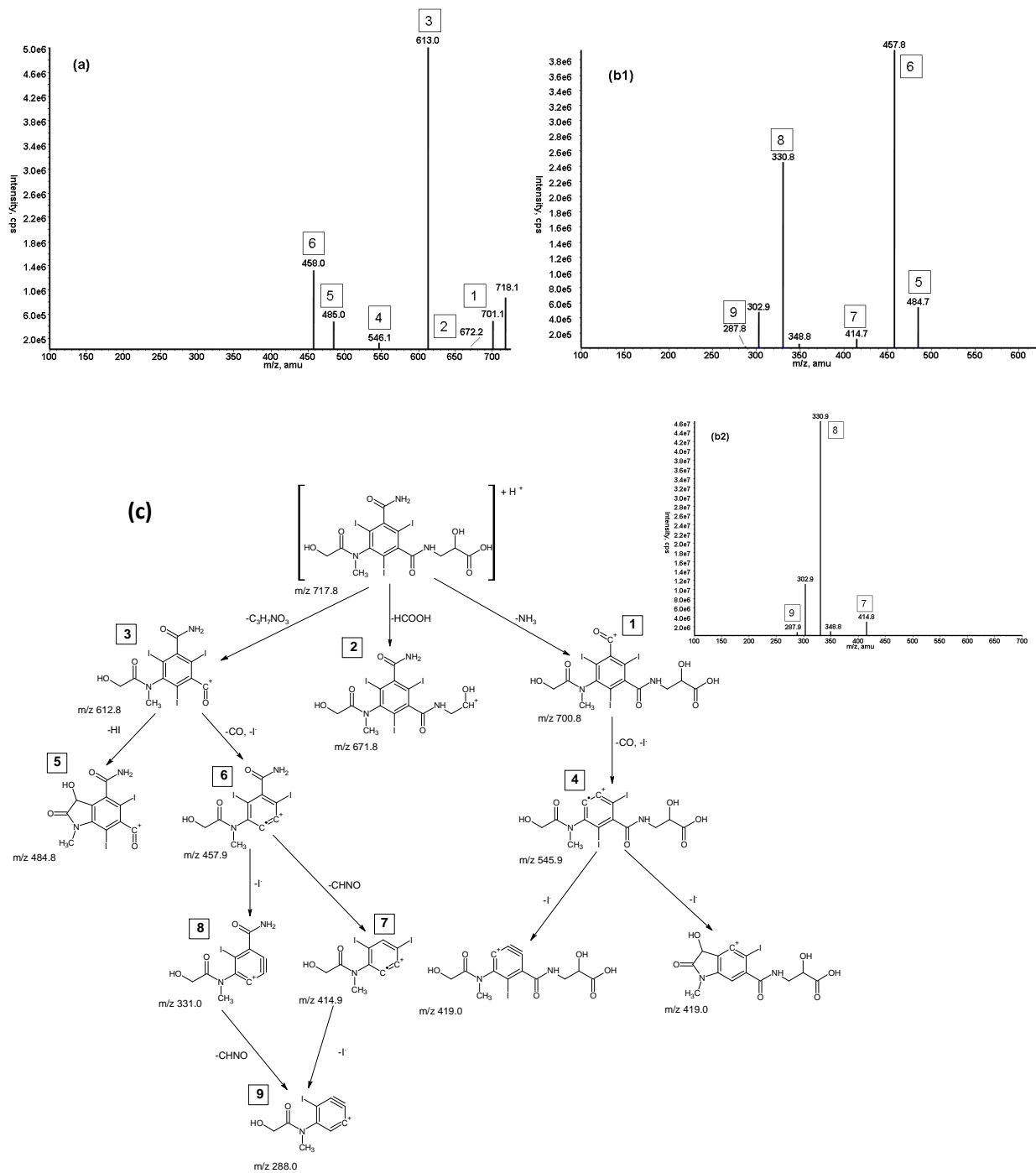
Figure S2.6.8: MS^2 and MS^3 spectra for iomeprol TP717: (a) MS^2 *m/z* 718; (b1) MS^3 *m/z* 718 → 613; (b2) MS^3 *m/z* 718 → 458; (c) proposed fragmentation pathway of iomeprol TP717. The mass spectra were determined at a collision energy of 30 eV.
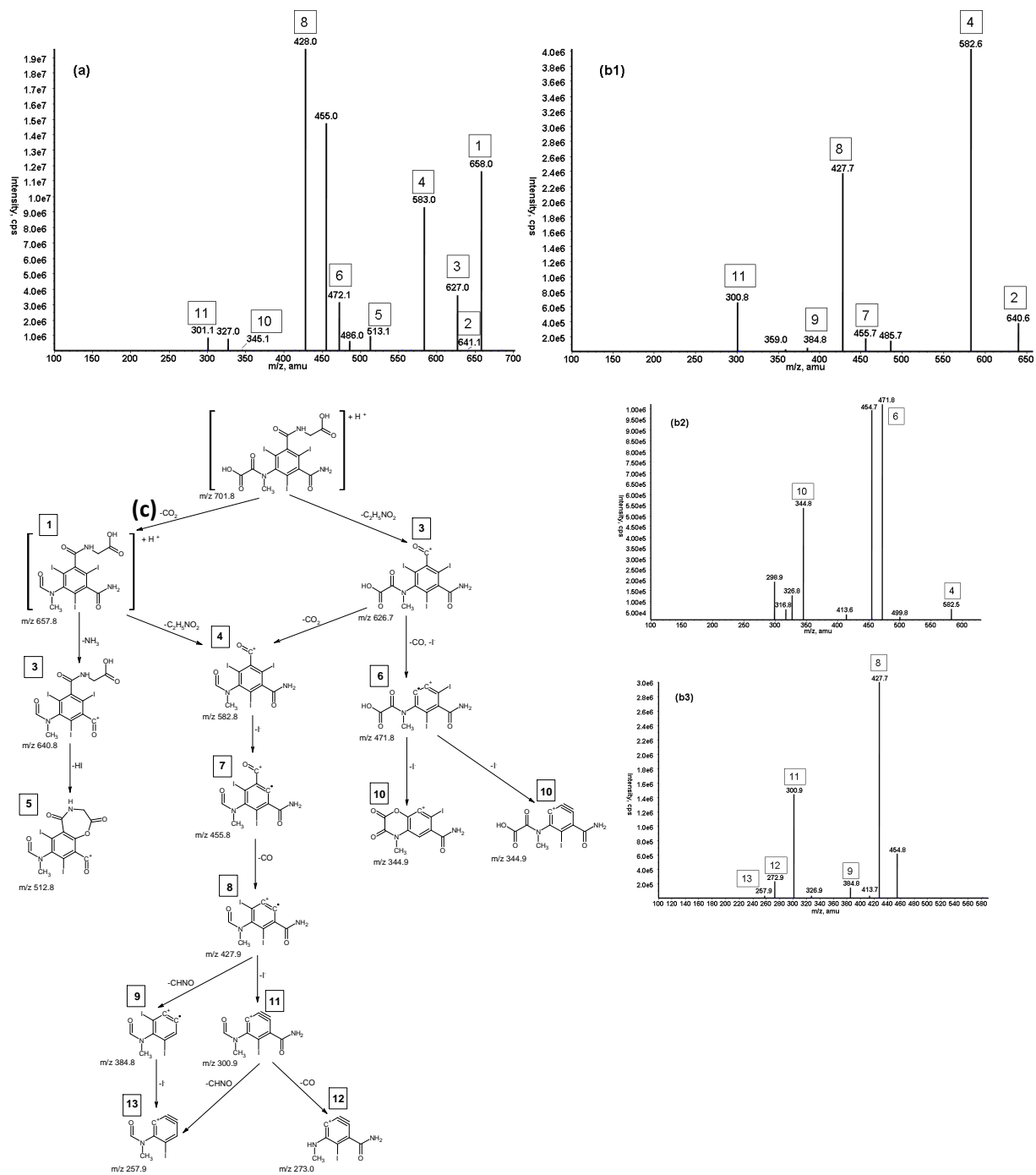
Figure S2.6.9: MS^2 and MS^3 spectra for iomeprol TP701: (a) MS^2 m/z 702; (b1) MS^3 m/z 702 → 658; (b2) MS^3 m/z 702 → 627; (b3) MS^3 m/z 702 → 583; (c) proposed fragmentation pathway of iomeprol TP701. The mass spectra were determined at a collision energy of 30 eV.

Figure S2.6.10: MS^2 spectrum for iomeprol TP687: (a) MS^2 *m/z* 688; (b) proposed fragmentation pathway of iomeprol TP687. The mass spectrum was determined at a collision energy of 30 eV.

86

Figure S2.6.11: MS^2 and MS^3 spectra for iomeprol TP643: (a) MS^2 m/z 644; (b1) MS^3 m/z 644 → 600; (b2) MS^3 m/z 644 → 583; (b3) MS^3 m/z 644 → 428; (c) proposed fragmentation pathway of iomeprol TP643. The mass spectra were determined at a collision energy of 30 eV.
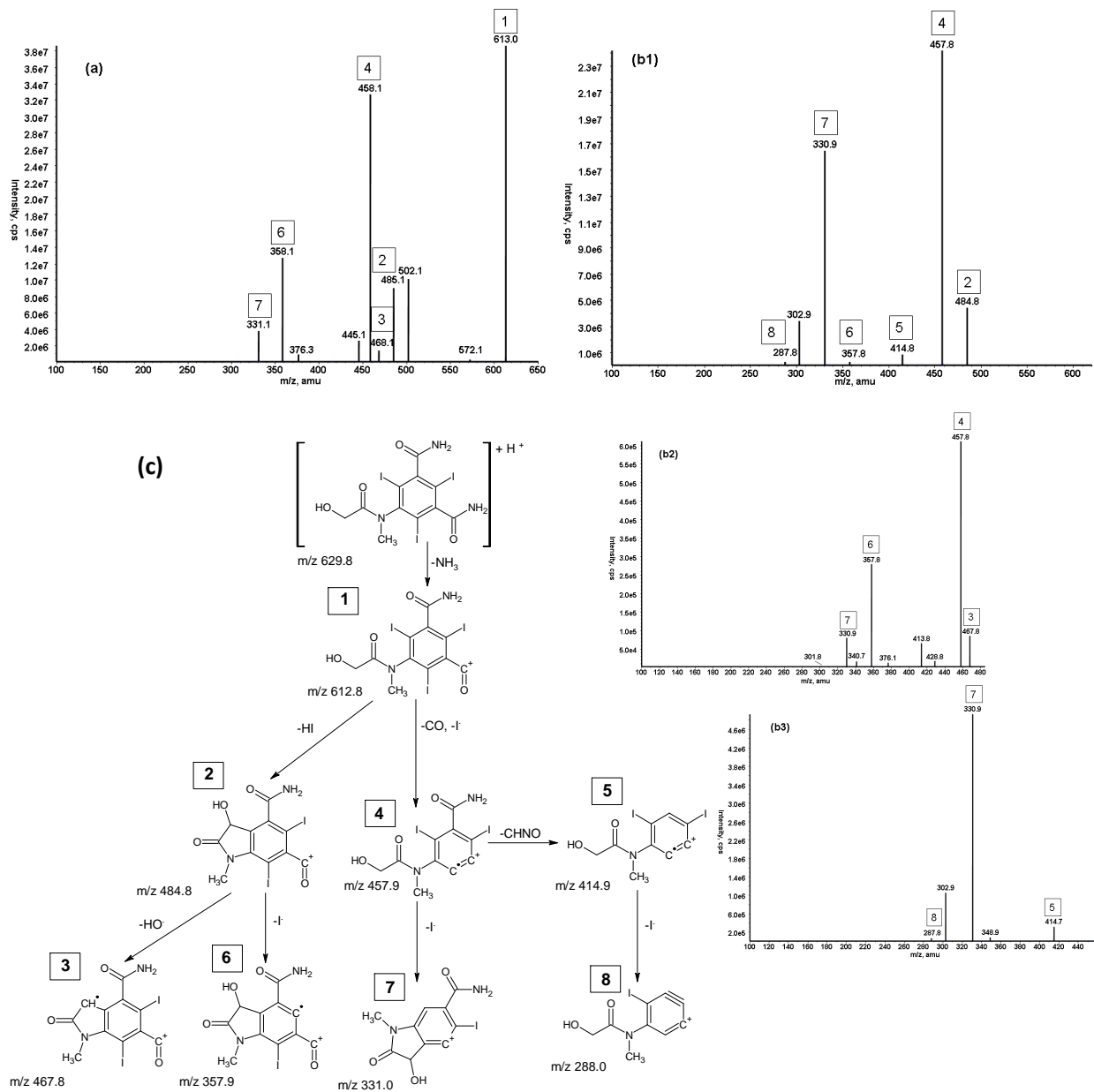
Figure S2.6 12: MS^2 and MS^3 spectra for iomeprol TP629: (a) MS^2 *m/z* 630; (b1) MS^3 *m/z* 630 → 613; (b2) MS^3 *m/z* 630 → 485; (b3) MS^3 *m/z* 630 → 458; (c) proposed fragmentation pathway of iomeprol TP629. The mass spectra were determined at a collision energy of 30 eV.
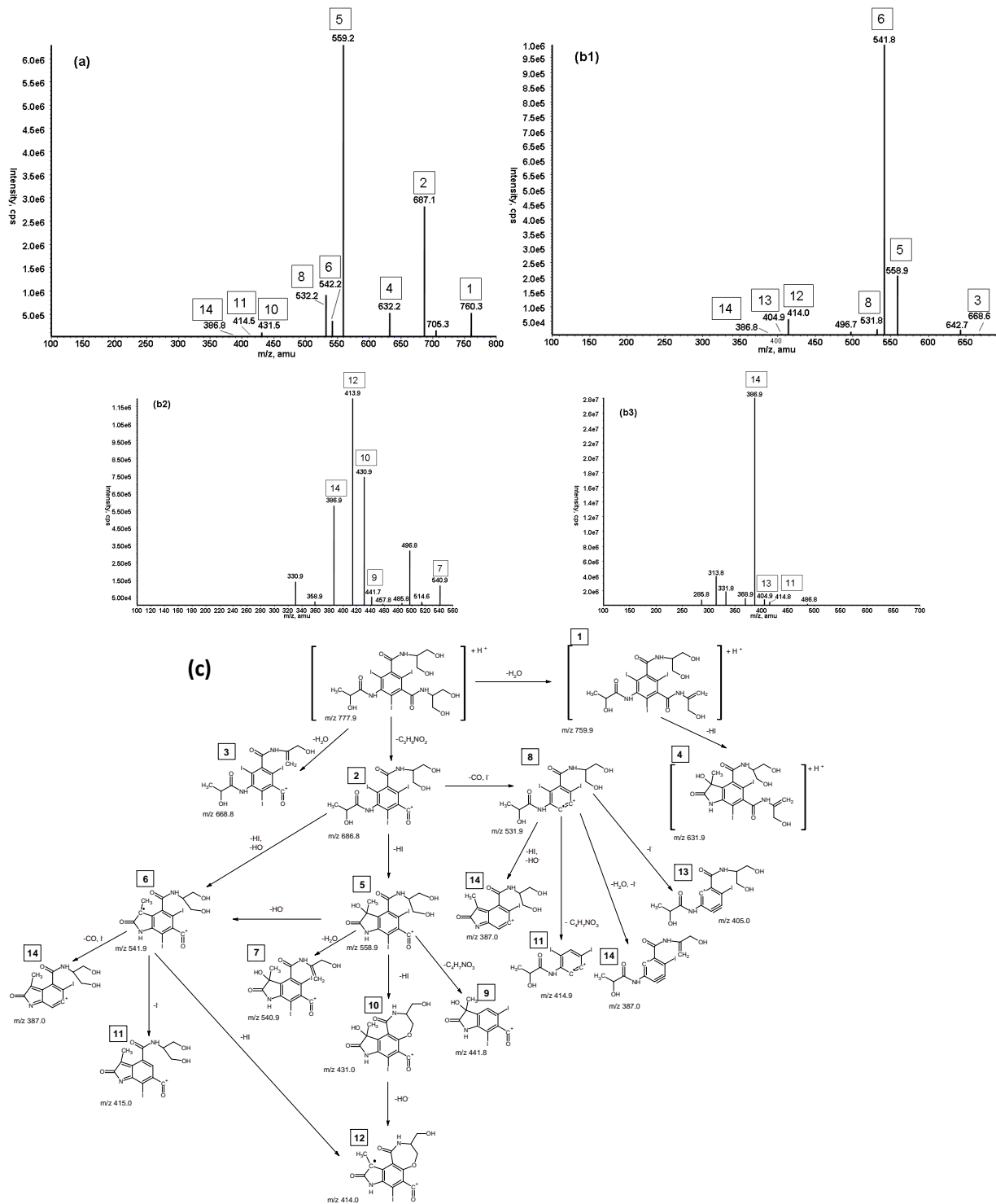
Figure S2.6 13: MS^2 and MS^3 spectra for iopamidol: (a) MS^2 *m/z* 778; (b1) MS^3 *m/z* 778 → 687; (b2) MS^3 *m/z* 778 → 559; (b3) MS^3 *m/z* 778 → 532; (c) proposed fragmentation pathway of iopamidol. The mass spectra were determined at a collision energy of 30 eV.
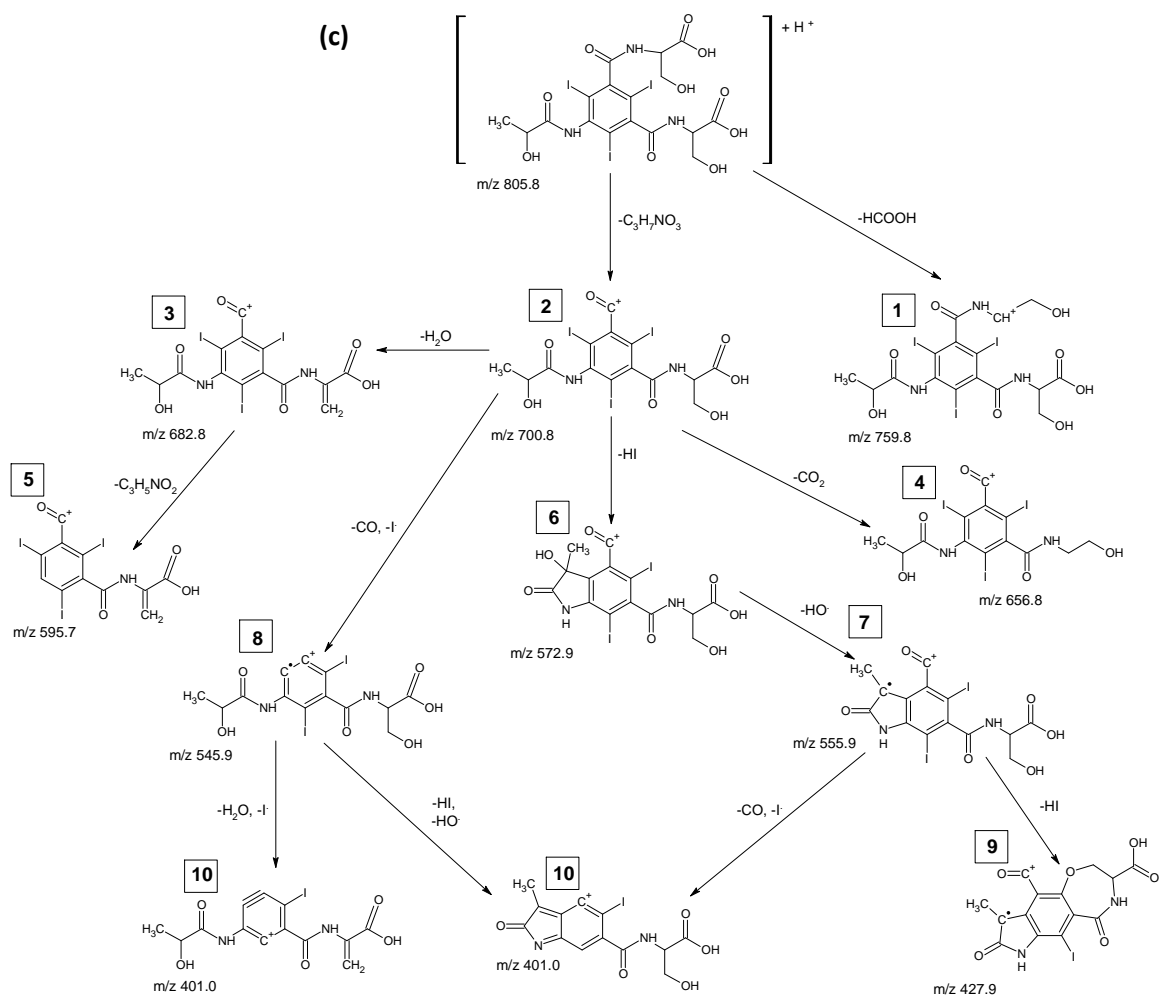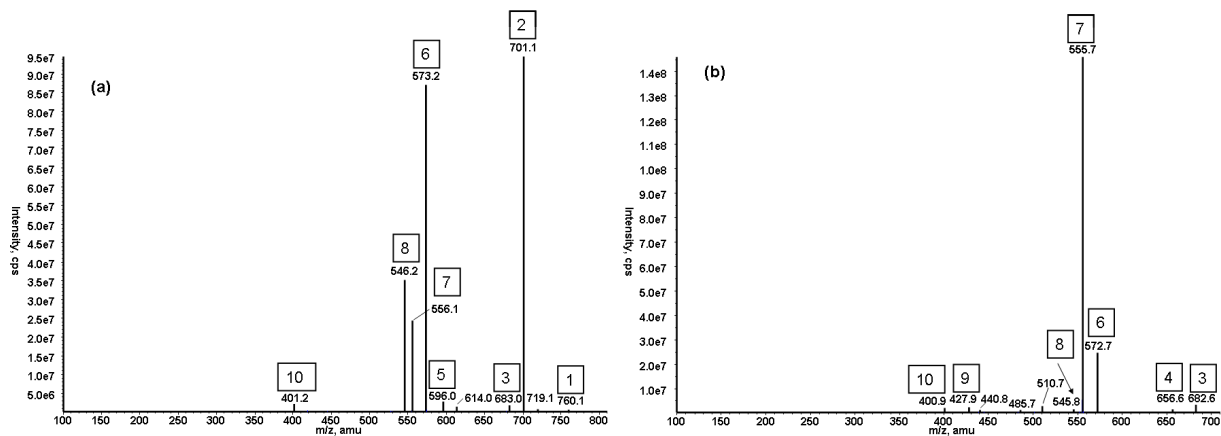
Figure S2.6.14: MS^2 and MS^3 spectra for iopamidol TP805: (a) MS^2 m/z 806; (b) MS^3 m/z 806 → 701; (c) proposed fragmentation pathway of iopamidol TP805. The mass spectra were determined at a collision energy of 30 eV.
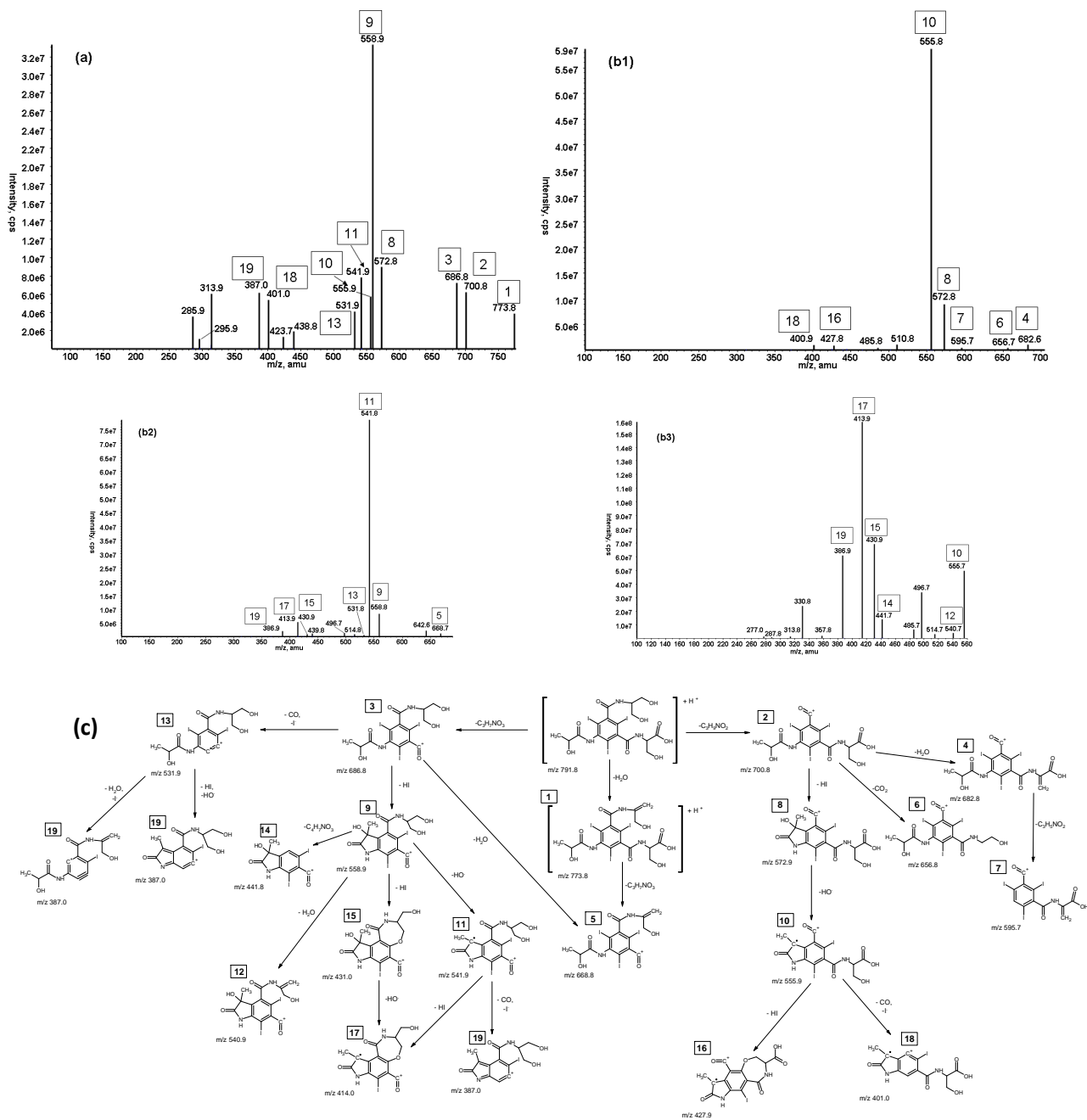
Figure S2.6.15: MS^2 and MS^3 spectra for iopamidol TP791: (a) MS^2 m/z 792; (b1) MS^3 m/z 792 → 701; (b2) MS^3 m/z 792 → 687; (b3) MS^3 m/z 792 → 559; (c) proposed fragmentation pathway of iopamidol TP791. The mass spectra were determined at a collision energy of 30 eV.
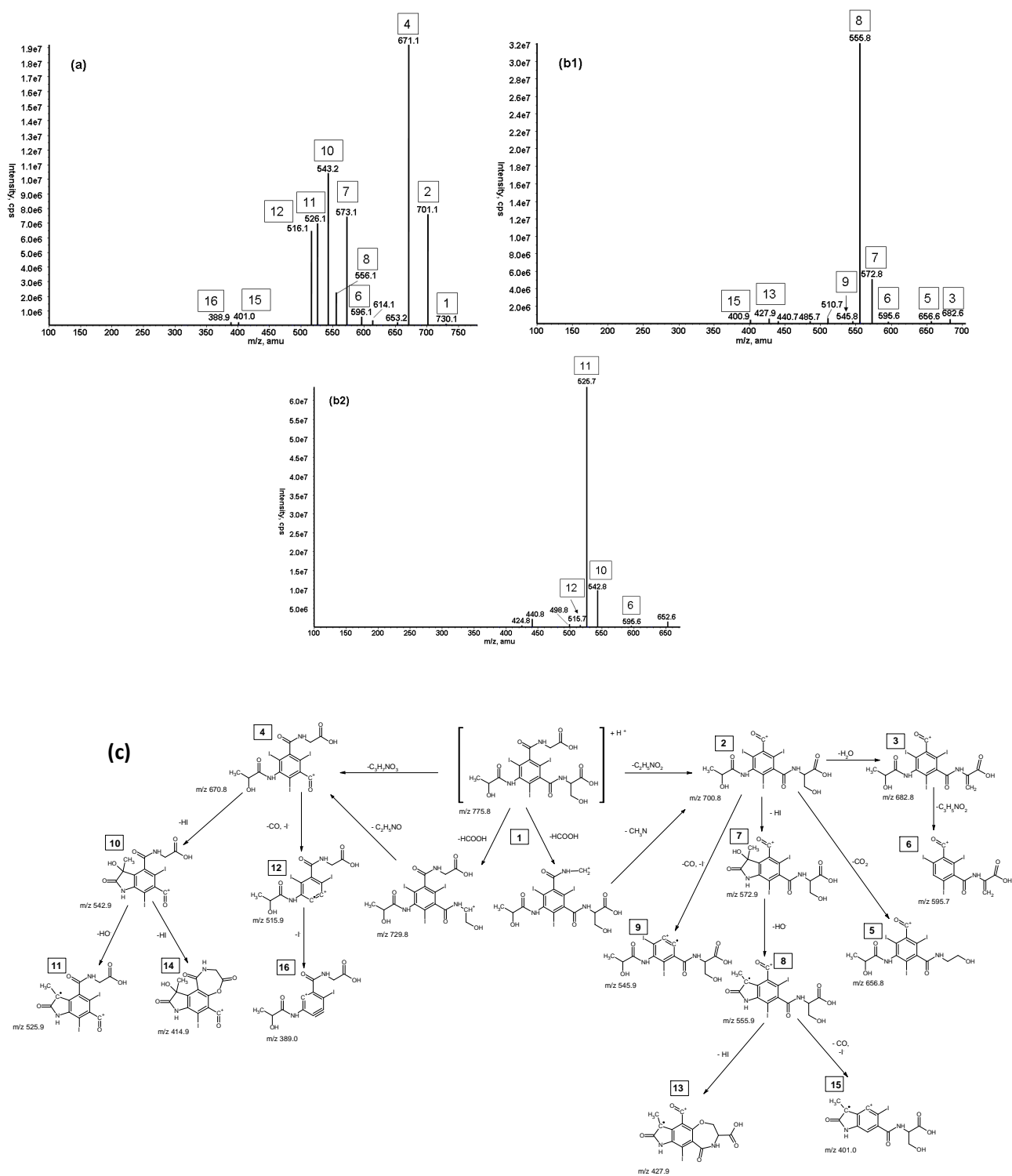
Figure S2.6.16: MS^2 and MS^3 spectra for iopamidol TP775: (a) MS^2 m/z 776; (b1) MS^3 m/z 776 → 701; (b2) MS^3 m/z 776 → 671; (c) proposed fragmentation pathway of iopamidol TP775. The mass spectra were determined at a collision energy of 30 eV.
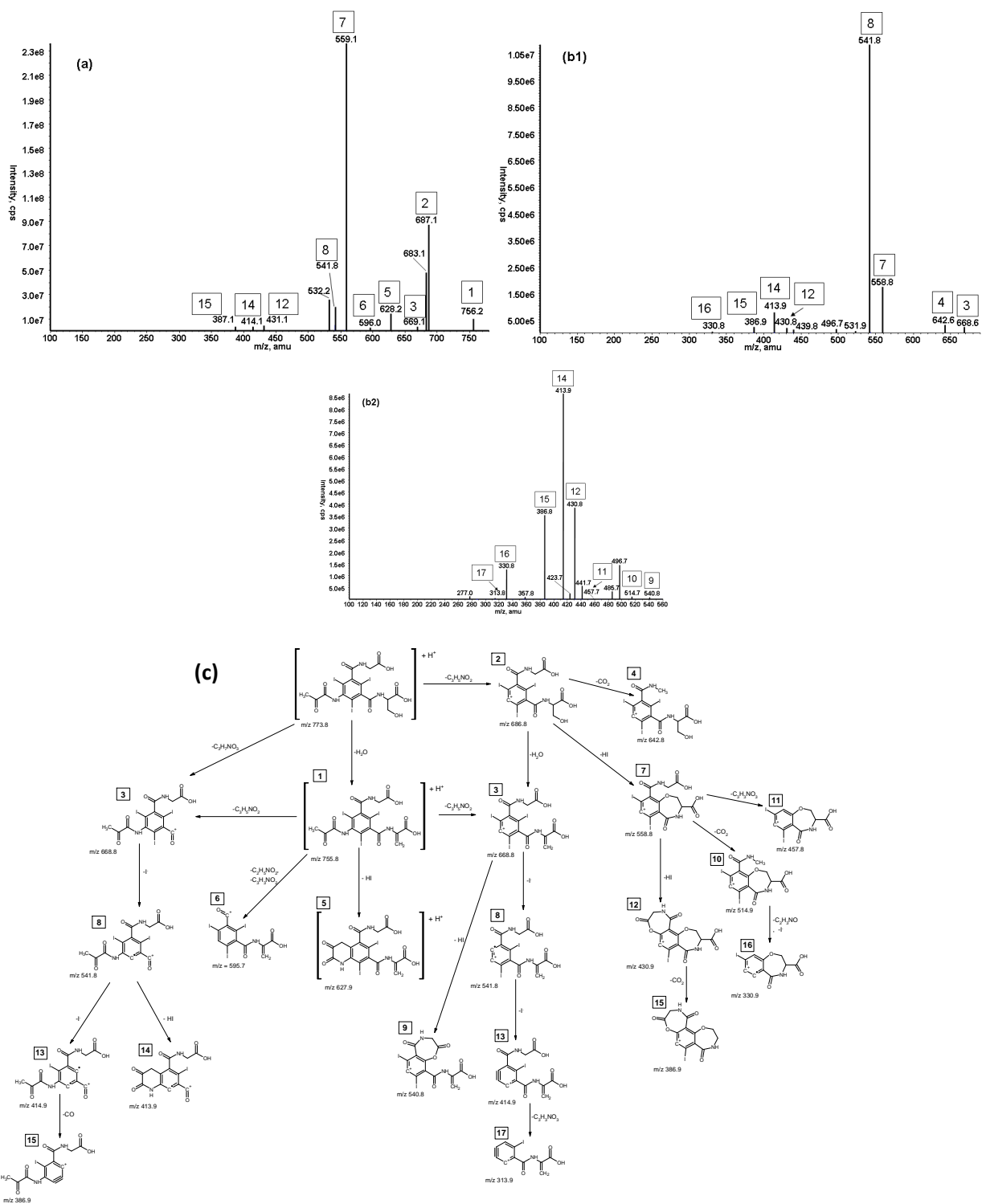
Figure S2.6.17: MS^2 and MS^3 spectra for iopamidol TP773: (a) MS^2 m/z 774; (b1) MS^3 m/z 774 → 687; (b2) MS^3 m/z 774 → 559; (c) proposed fragmentation pathway of iopamidol TP773. The mass spectra were determined at a collision energy of 30 eV.
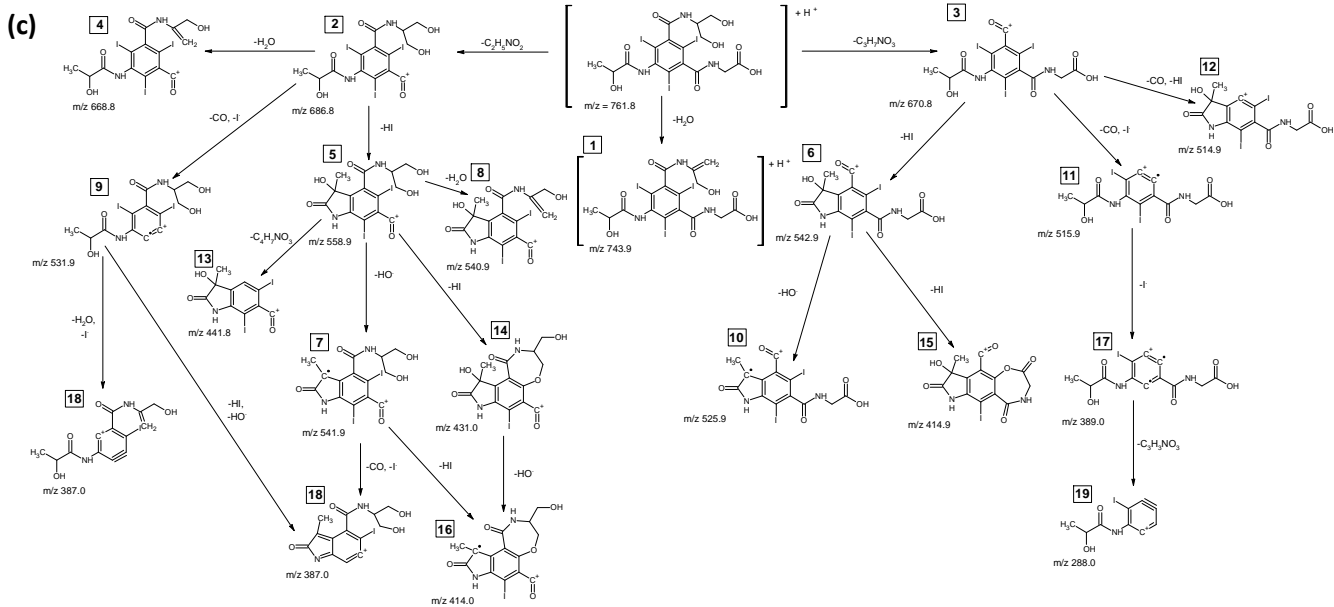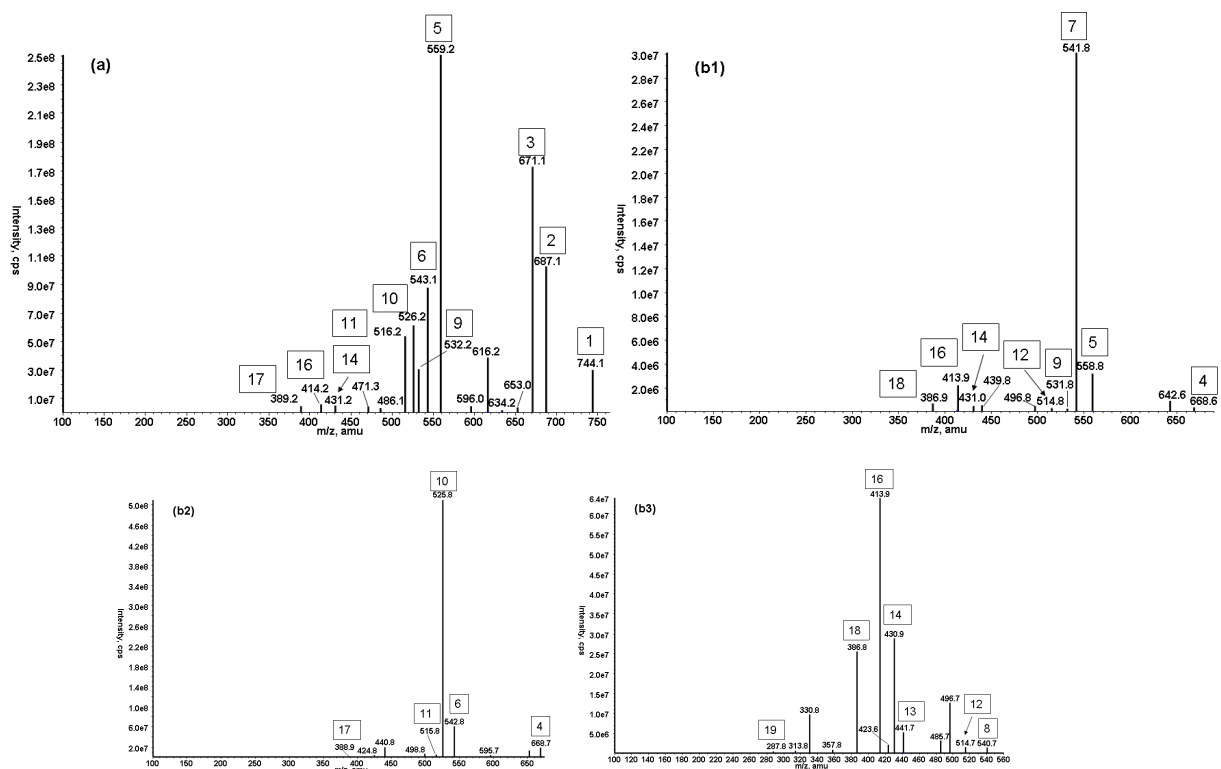
Figure S2.6.18: MS^2 and MS^3 spectra for iopamidol TP761: (a) MS^2 m/z 762; (b1) MS^3 m/z 762 → 687; (b2) MS^3 m/z 762 → 671; (b3) MS^3 m/z 762 → 559; (c) proposed fragmentation pathway of iopamidol TP761. The mass spectra were determined at a collision energy of 30 eV.

94
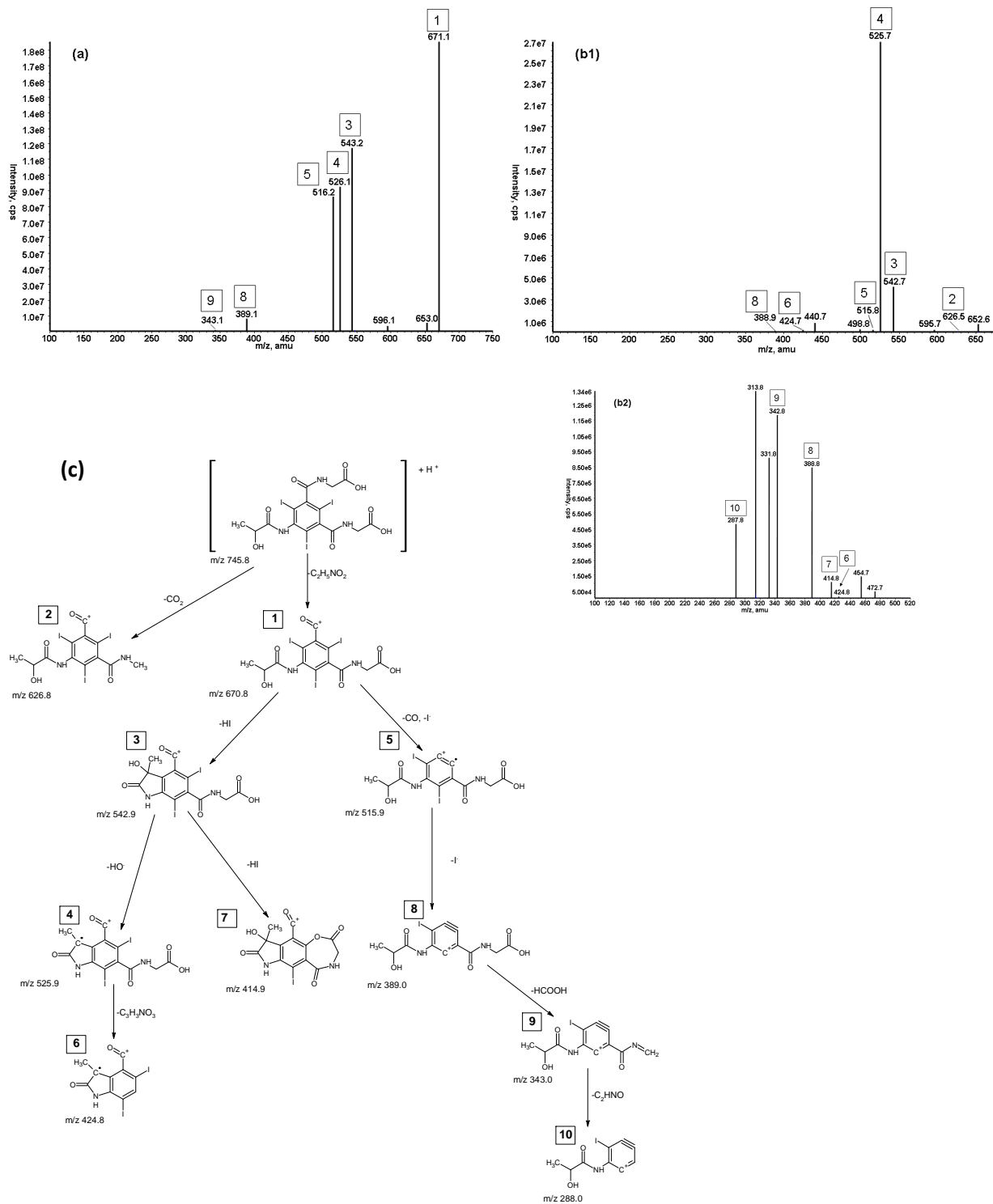
Figure S2.6.19: MS^2 and MS^3 spectra for iopamidol TP745: (a) MS^2 *m/z* 746; (b1) MS^3 *m/z* 746 → 671; (b2) MS^3 *m/z* 746 → 516; (c) proposed fragmentation pathway of iopamidol TP745. The mass spectra were determined at a collision energy of 30 eV.

95
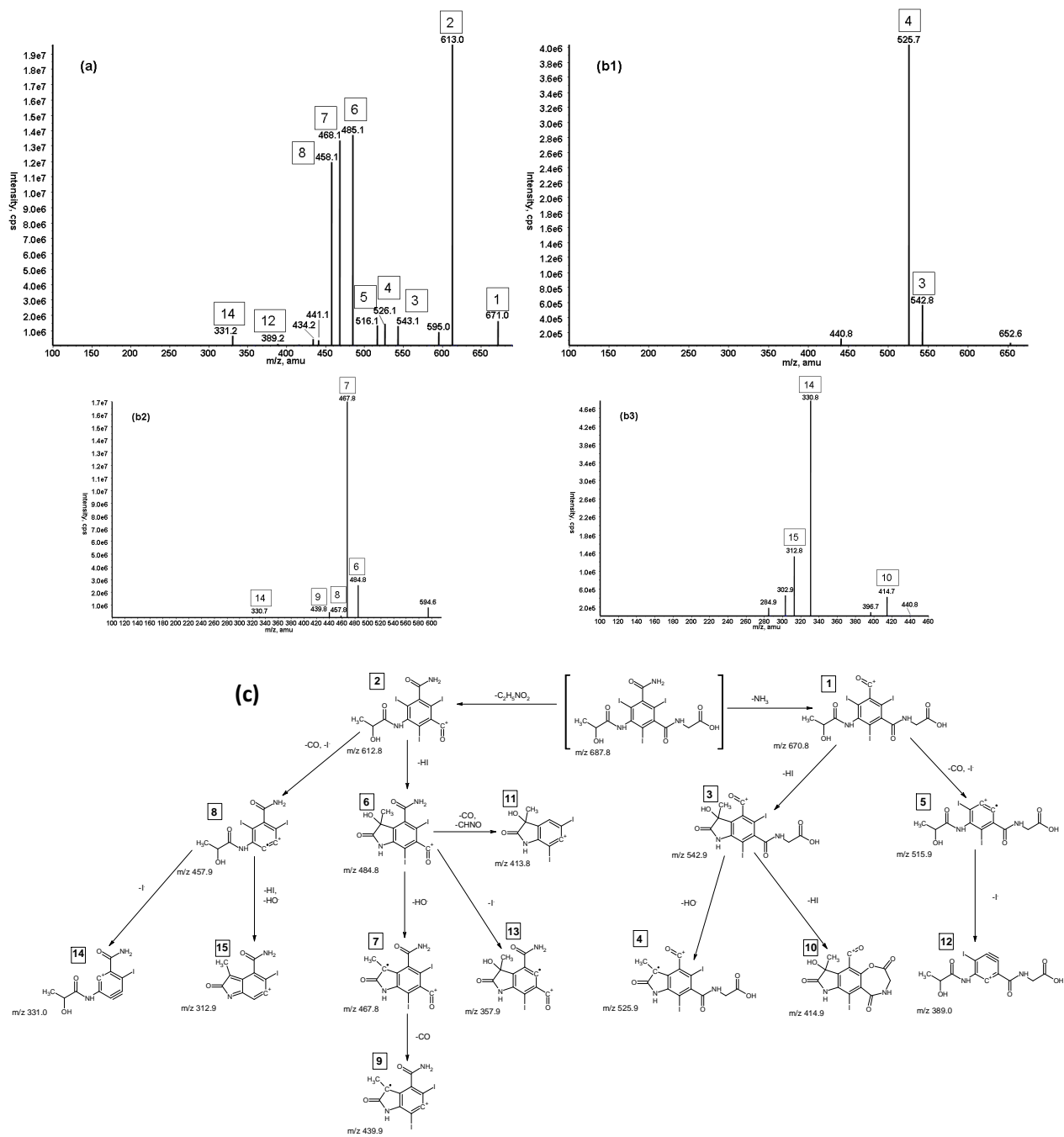
Figure S2.6.20: MS^2 and MS^3 spectra for iopamidol TP687: (a) MS^2 m/z 688; (b1) MS^3 m/z 688 → 671; (b2) MS^3 m/z 688 → 613; (b3) MS^3 m/z 688 → 458; (c) proposed fragmentation pathway of iopamidol TP687. The mass spectra were determined at a collision energy of 30 eV.
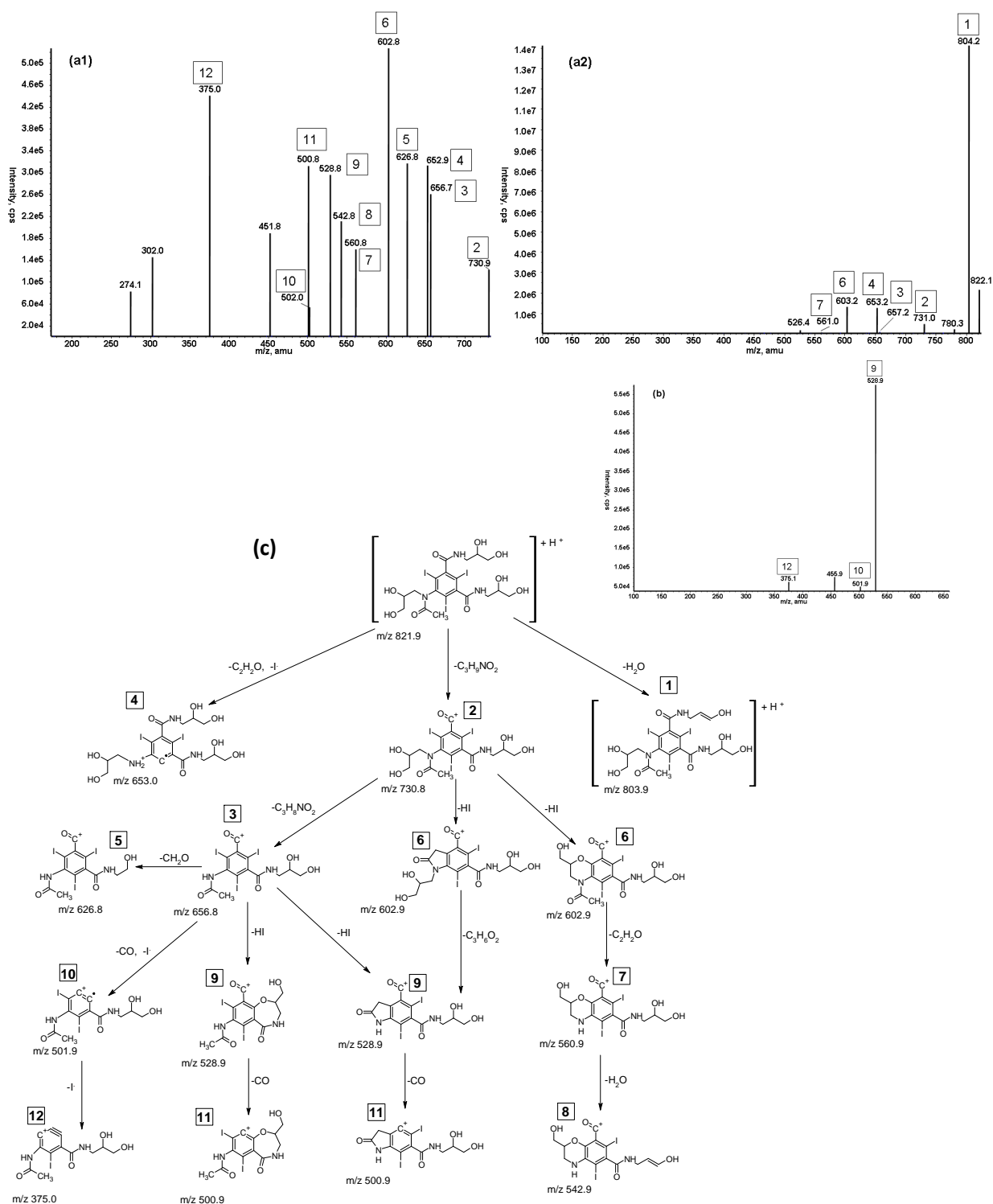
Figure S2.6.21: MS^2 and MS^3 spectra for iohexol: (a1) MS^2 m/z 822; (a2) MS^2 m/z 822; (b) MS^3 m/z 822 → 657; (c) proposed fragmentation pathway of iohexol. The mass spectra were determined at a collision energy of 30 eV.

97
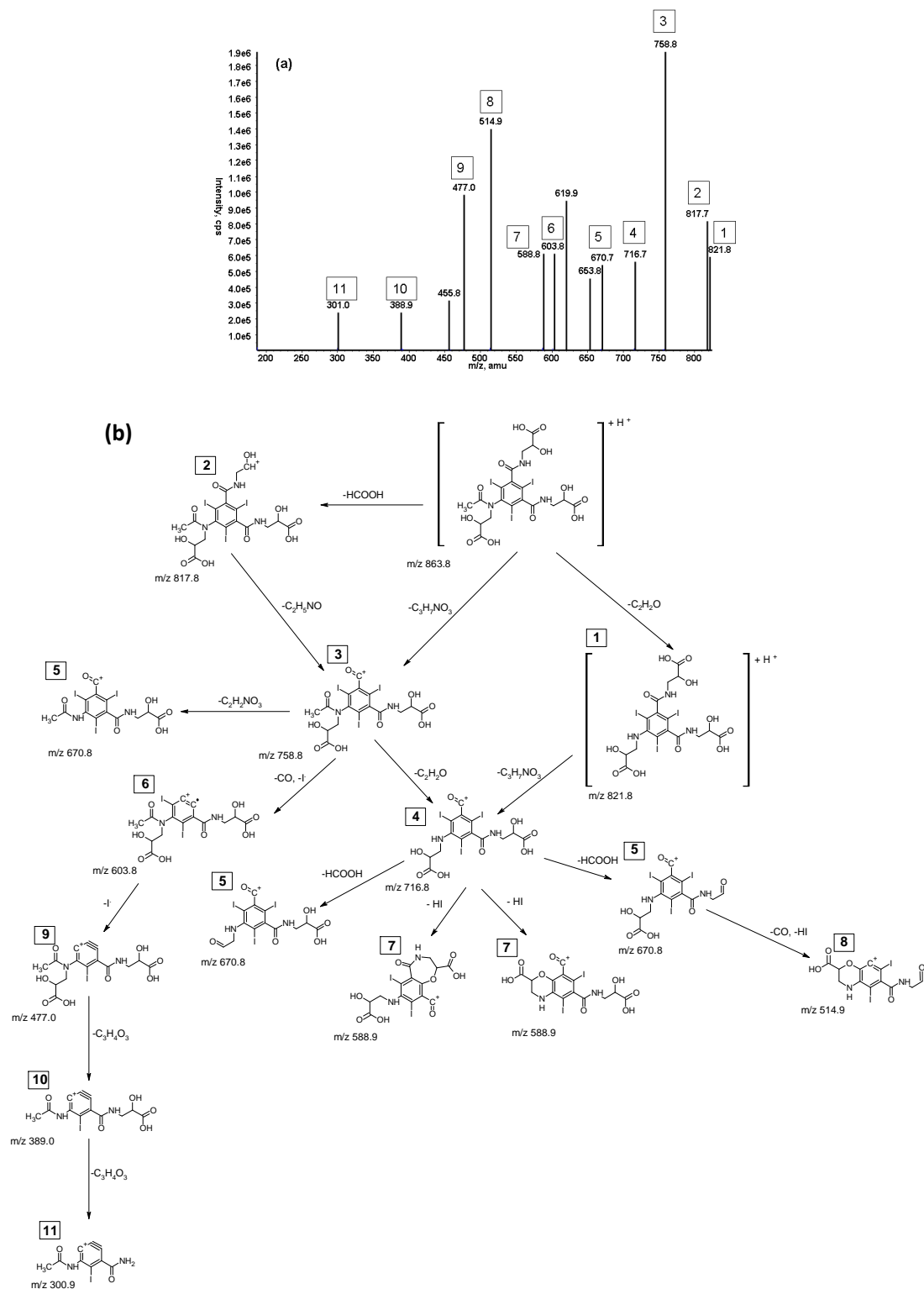
Figure S2.6.22: MS^2 spectrum for iohexol TP863: (a) MS^2 *m/z* 864; (b) proposed fragmentation pathway of iohexol TP863. The mass spectrum was determined at a collision energy of 30 eV.
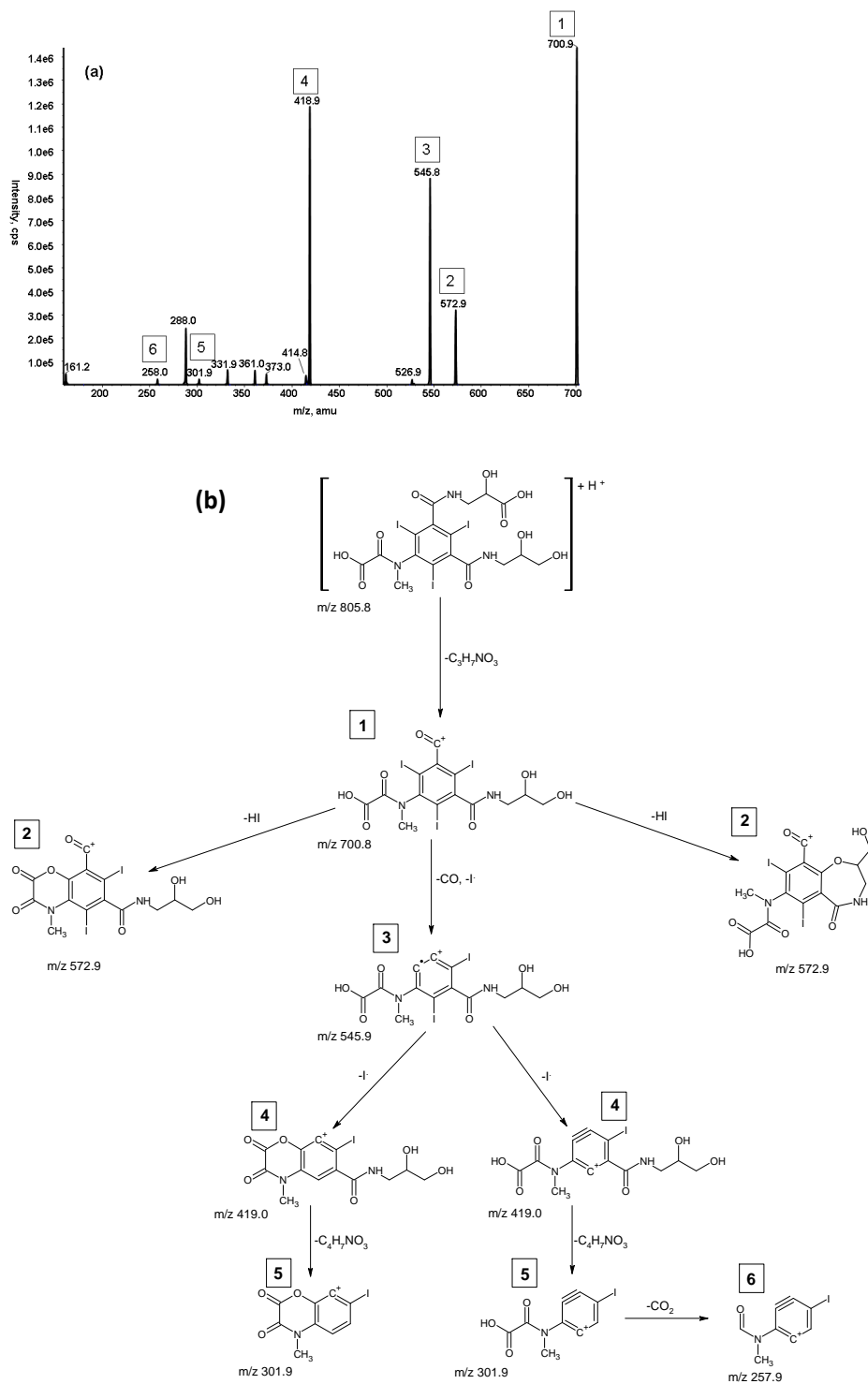
98
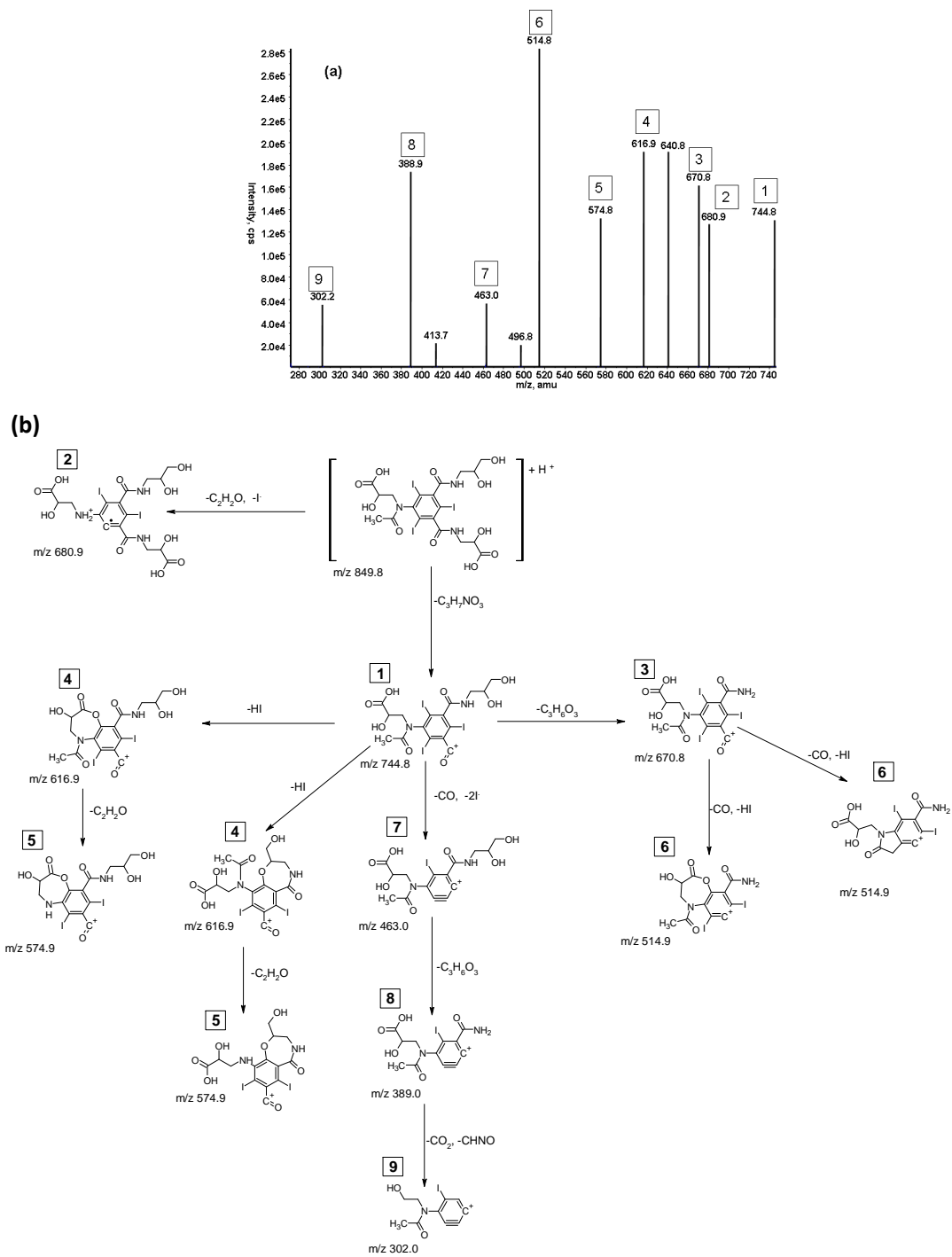
Figure S2.6.23: MS^2 spectrum for iohexol TP849: (a) MS^2 m/z 850; (b) proposed fragmentation pathway of iohexol TP849. The mass spectrum was determined at a collision energy of 30 eV.
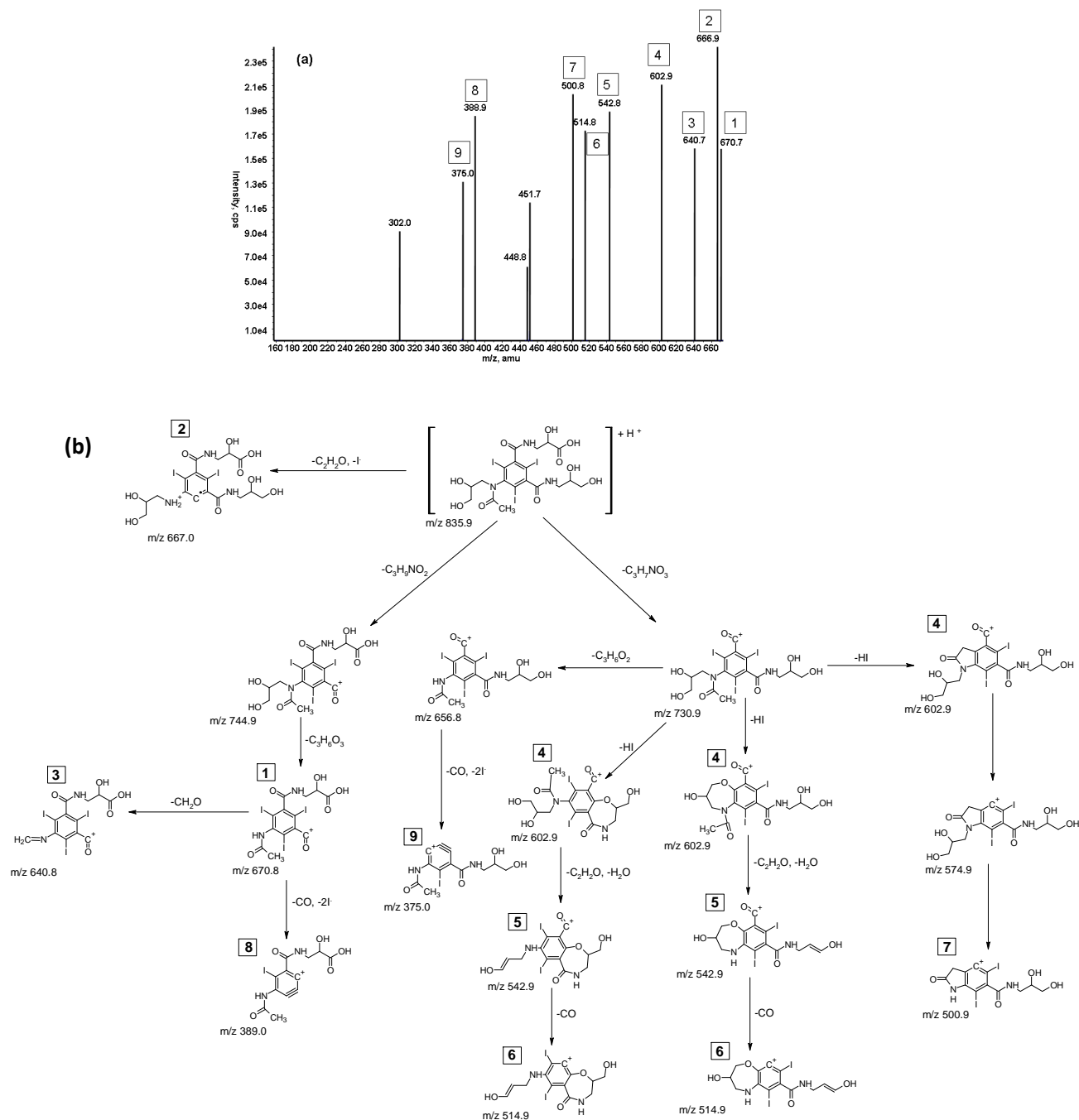
Figure S2.6.24: MS^2 spectrum for iohexol TP835: (a) MS^2 *m/z* 836; (b) proposed fragmentation pathway of iohexol TP835. The mass spectrum was determined at a collision energy of 30 eV.

100
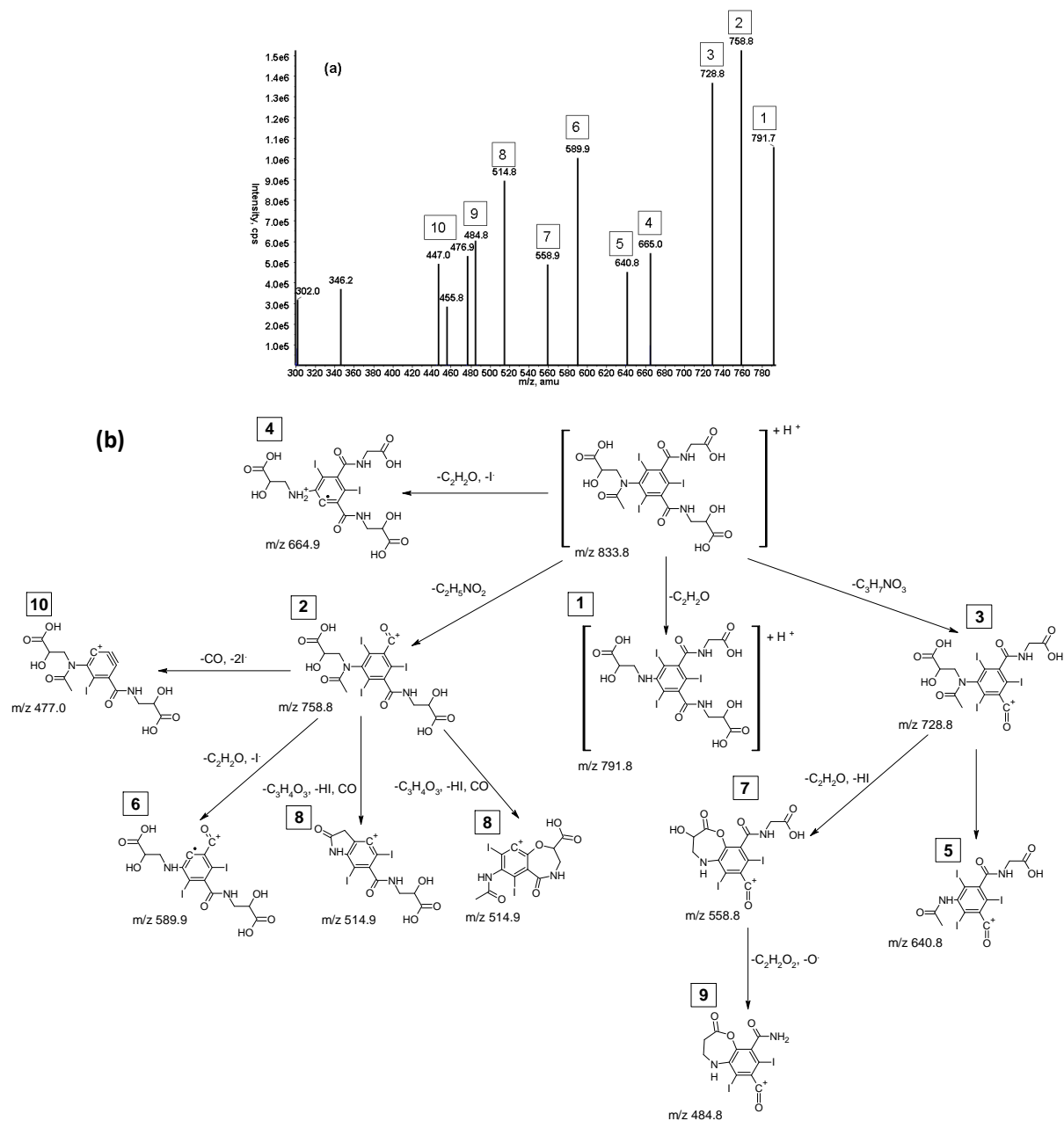
Figure S2.6.25: MS^2 spectrum for iohexol TP833: (a) MS^2 *m/z* 834; (b) proposed fragmentation pathway of iohexol TP833. The mass spectrum was determined at a collision energy of 30 eV.

101
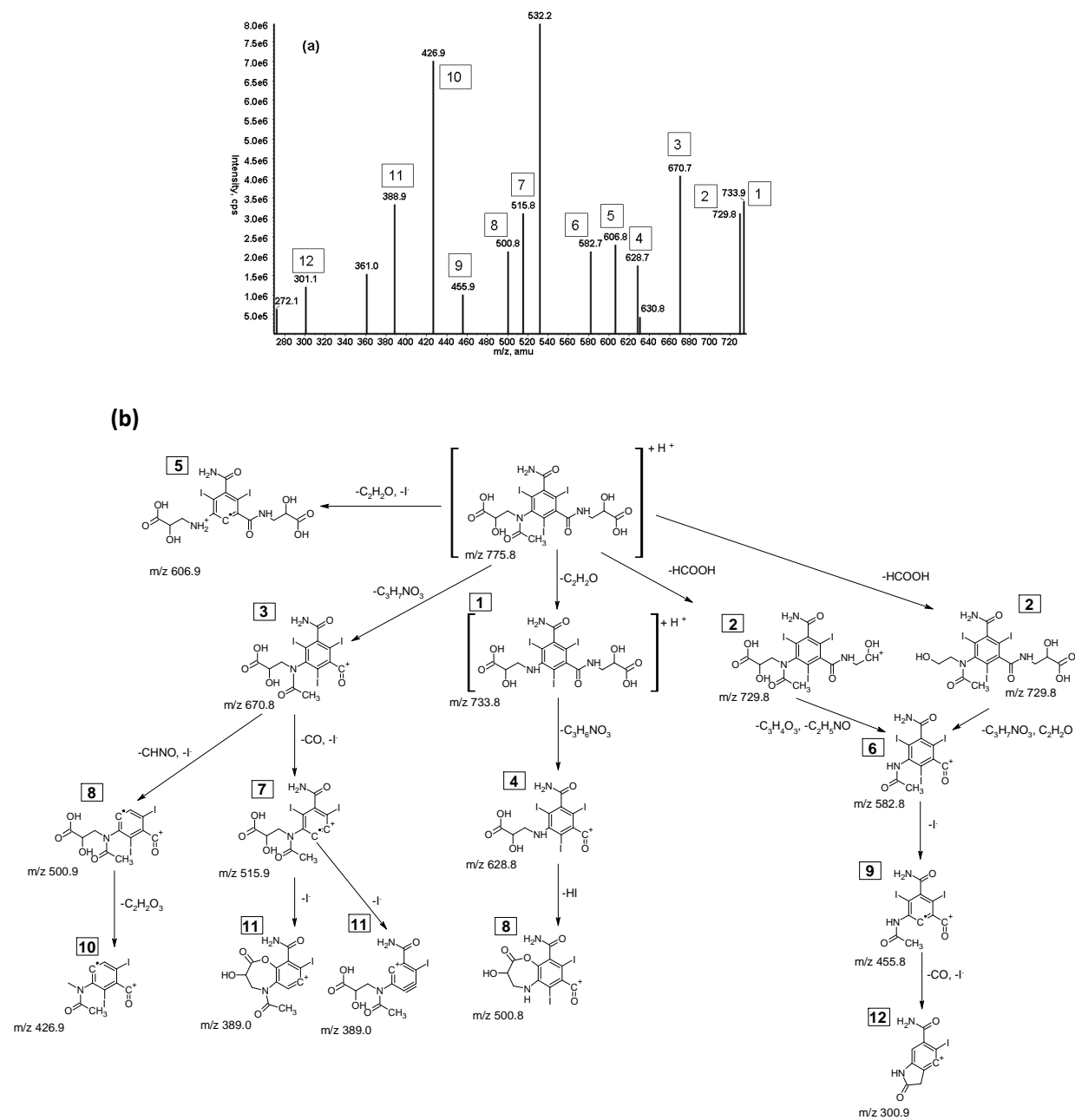
Figure S2.6.26: MS² spectrum for iohexol TP775: (a) MS² *m/z* 776; (b) proposed fragmentation pathway of iohexol TP775. The mass spectrum was determined at a collision energy of 30 eV.
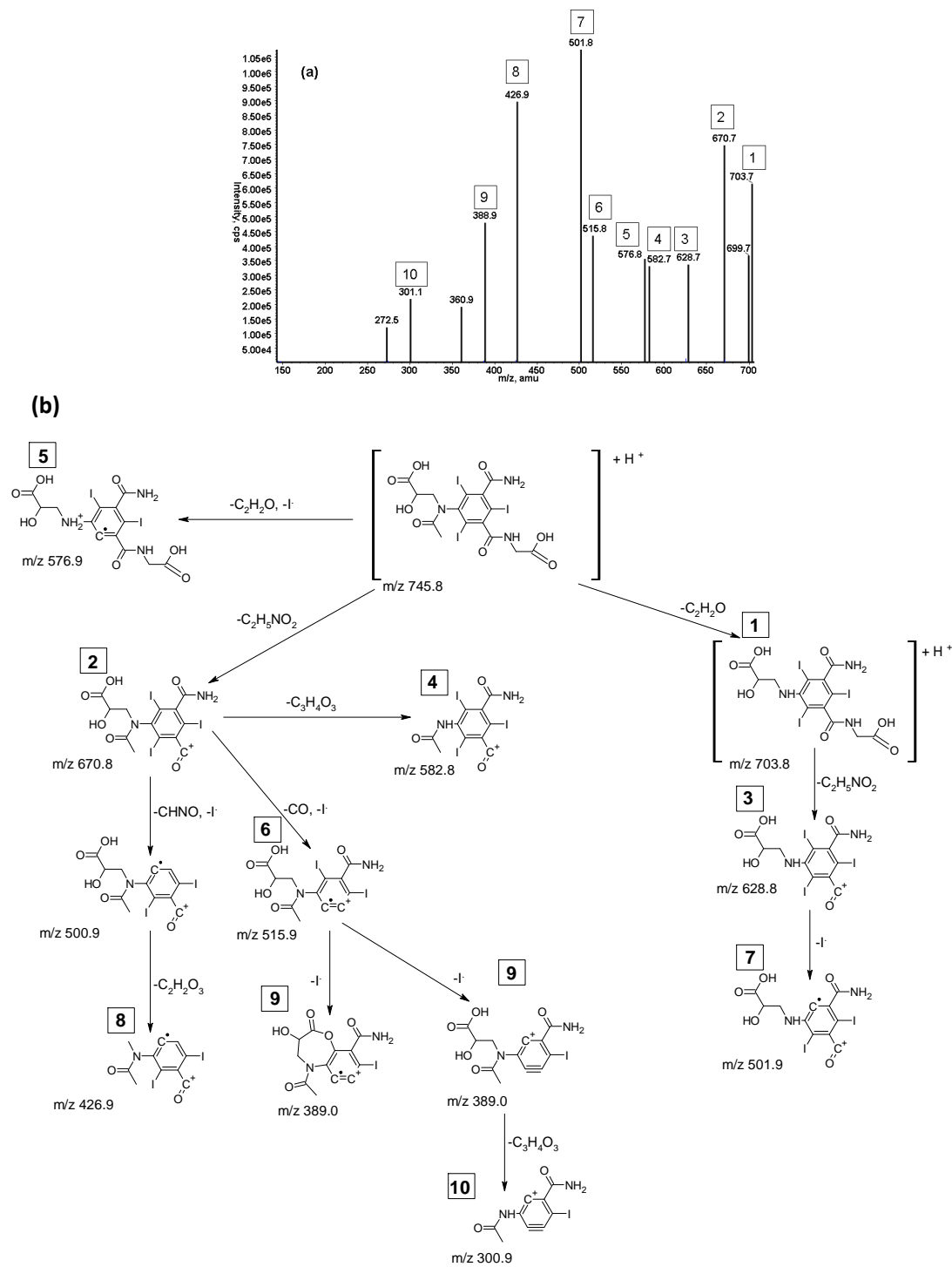
Figure S2.6.27: MS^2 spectrum for iohexol TP745: (a) MS^2 m/z 746; (b) proposed fragmentation pathway of iohexol TP745. The mass spectrum was determined at a collision energy of 30 eV.
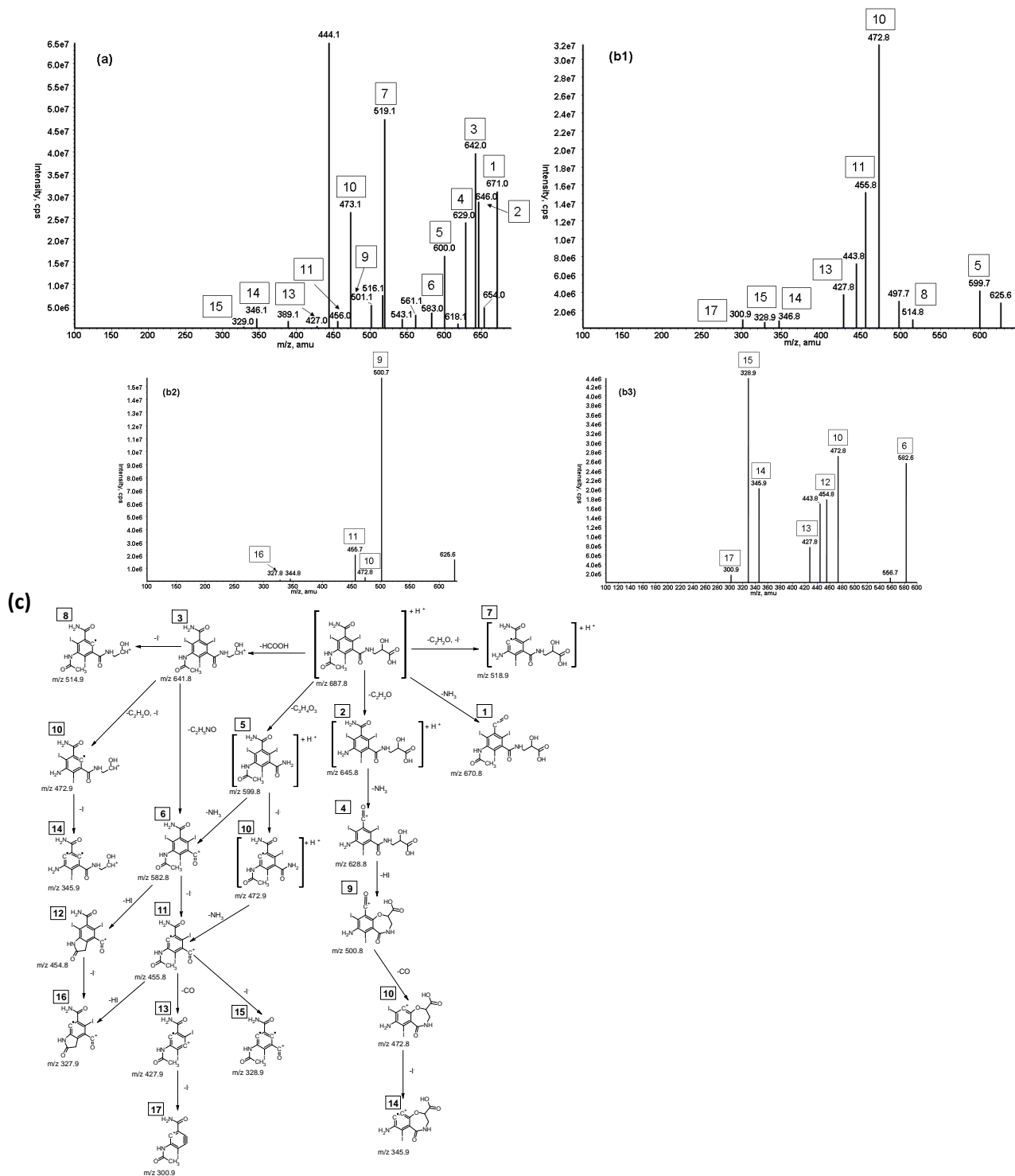
Figure S2.6.28: MS^2 and MS^3 spectra for iohexol TP687A: (a) MS^2 m/z 688A; (b1) MS^3 m/z 688A → 642; (b2) MS^3 m/z 688A → 629; (b3) MS^3 m/z 688A → 600; (c) proposed fragmentation pathway of iohexol TP687A. The mass spectra were determined at a collision energy of 30 eV.

Figure S2.6.29: MS^2 and MS^3 spectra for iohexol TP687B: (a) MS^2 m/z 688B; (b) proposed fragmentation pathway of iohexol TP687B. The mass spectra were determined at a collision energy of 30 eV.
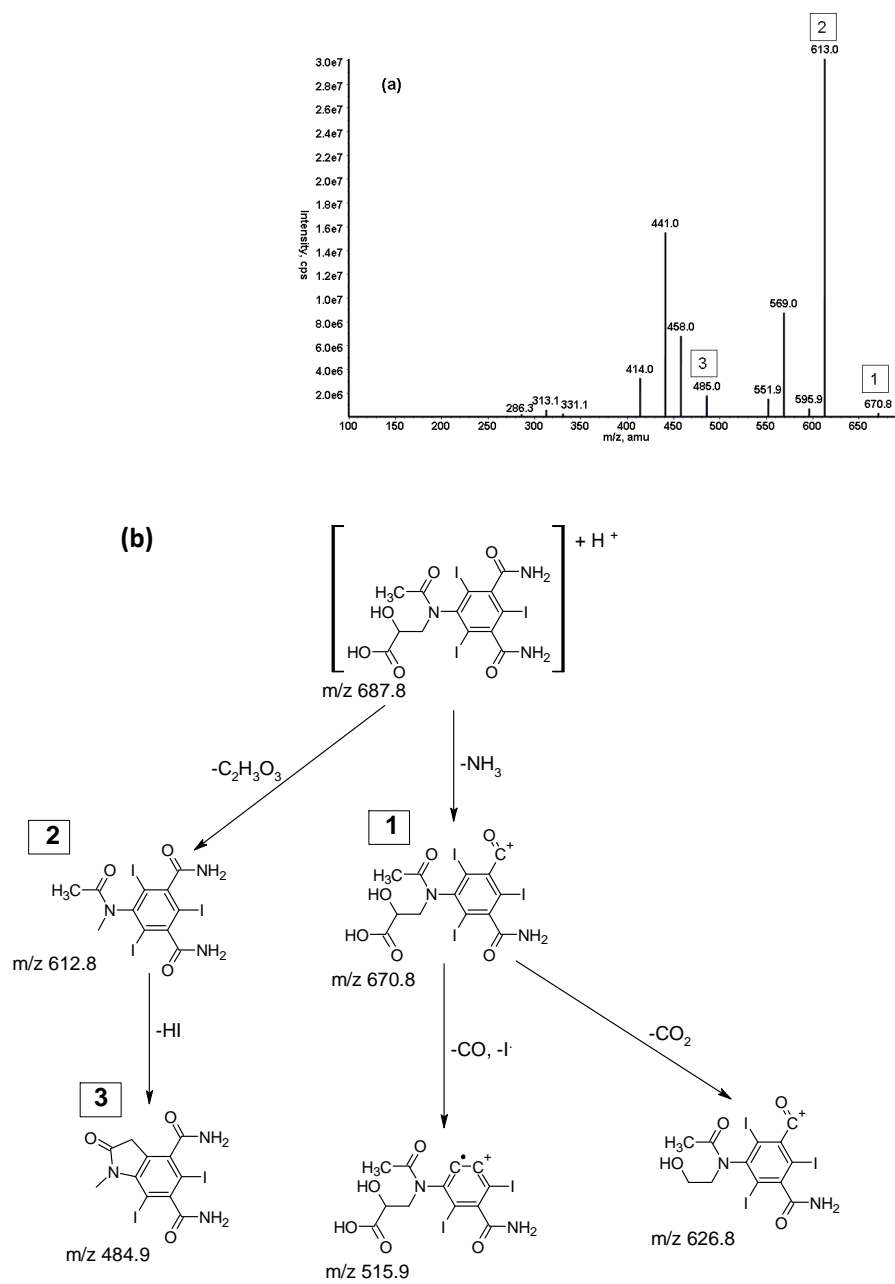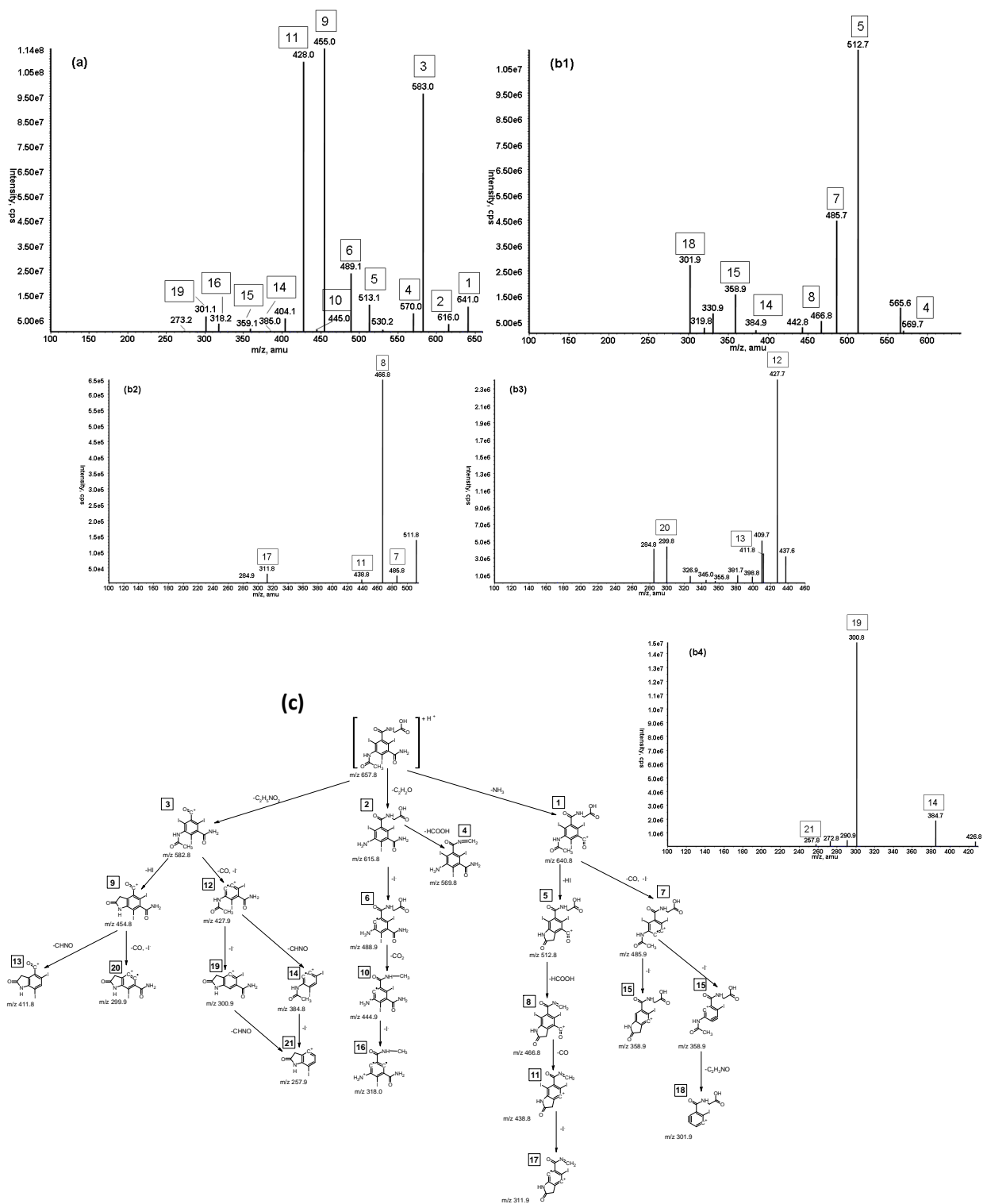
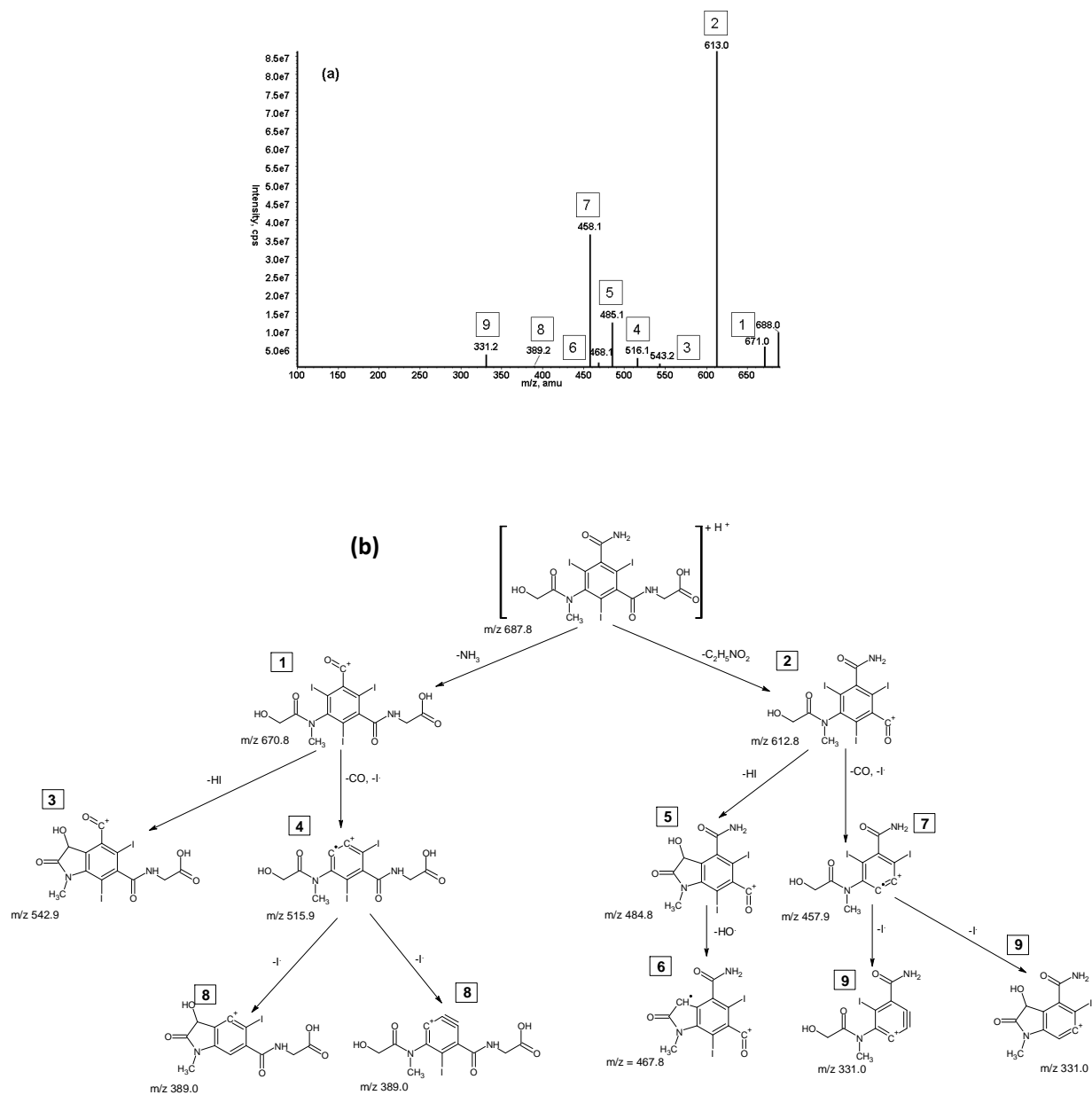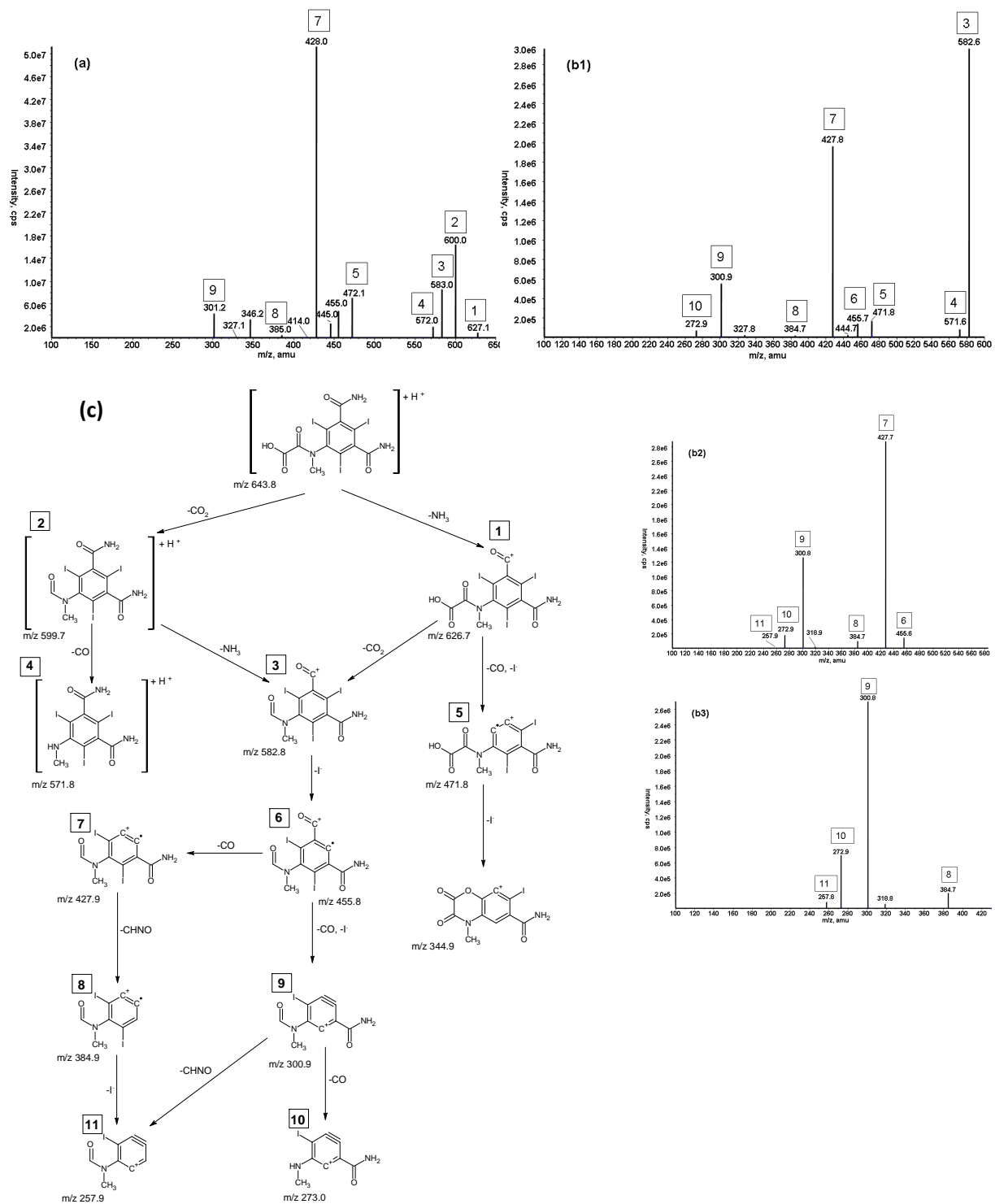Figure S2.6.30: MS^2 and MS^3 spectra for iohexol TP657: (a) MS^2 *m/z* 658; (b1) MS^3 *m/z* 658 → 641; (b2) MS^3 *m/z* 658 → 513; (b3) MS^3 *m/z* 658 → 455; (b4) MS^3 *m/z* 658 → 428; (c) proposed fragmentation pathway of iohexol TP657. The mass spectra were determined at a collision energy of 30 eV.

106
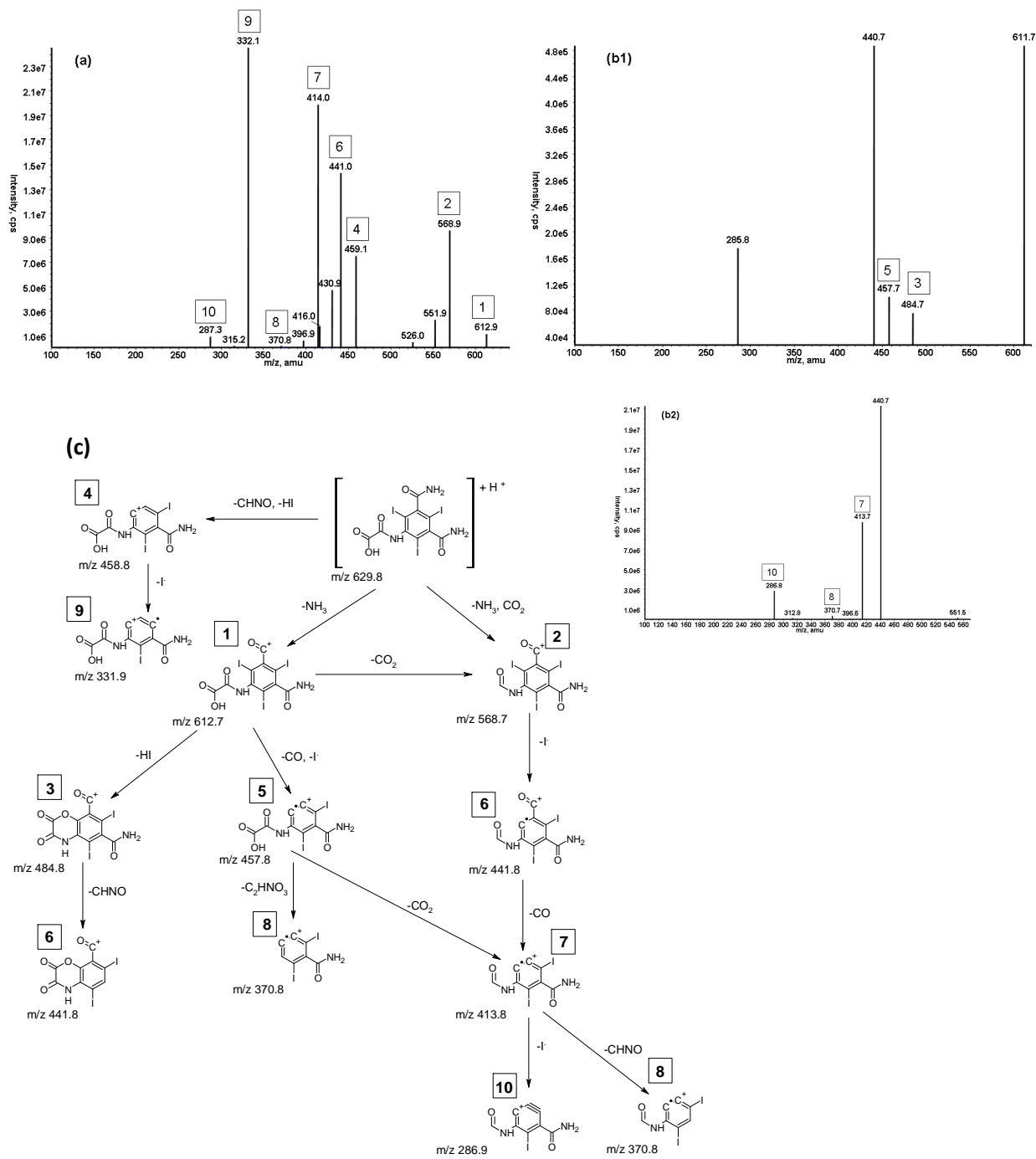
Figure S2.6.31: MS^2 and MS^3 spectra for iohexol TP629: (a) MS^2 *m/z* 630; (b1) MS^3 *m/z* 630 → 613; (b2) MS^3 *m/z* 630 → 569; (c) proposed fragmentation pathway of iohexol TP629. The mass spectra were determined at a collision energy of 30 eV.
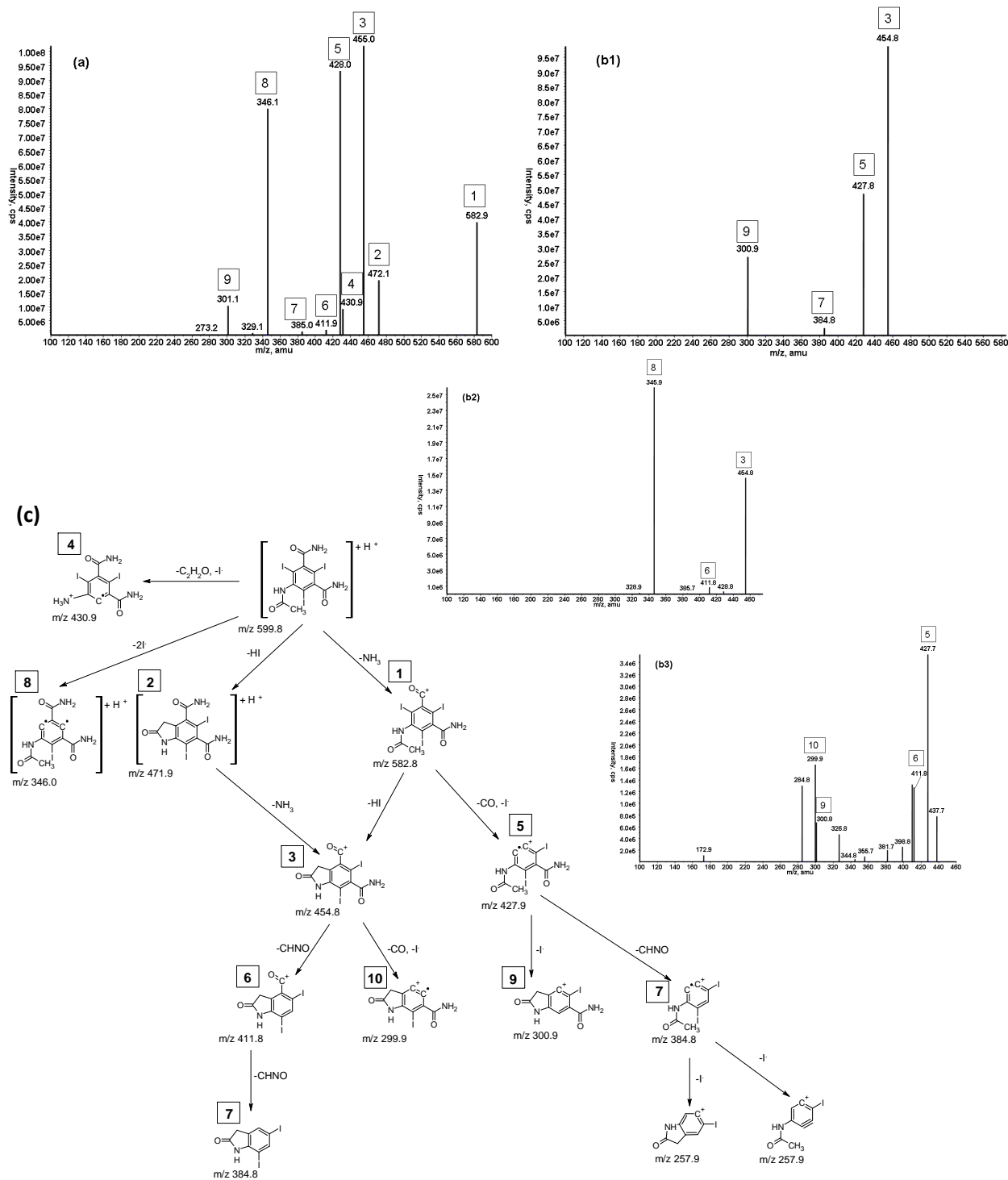
Figure S2.6.32: MS^2 and MS^3 spectra for iohexol TP599: (a) MS^2 *m/z* 600; (b1) MS^3 *m/z* 600 → 583; (b2) MS^3 *m/z* 600 → 472; (b3) MS^3 *m/z* 600 → 455; (c) proposed fragmentation pathway of iohexol TP599. The mass spectra were determined at a collision energy of 30 eV.

108

2.6.4 Nuclear Magnetic Resonance (NMR) Analyses

The non-ionic ICM and selected TPs were analyzed by NMR for structural confirmation of the structures proposed from the MS fragmentation experiments. The selection of DMSO as the solvent for dissolving ICM and ICM TPs is obvious because one can observe acidic protons in functional groups, like NH, COOH or OH, during ^{1}H NMR experiments without the exchange of the protons. Spin-echo experiments ("attached proton test") were also completed for a selected number of ICM TPs and provided additional information about whether an odd or even number of protons were attached to the carbon atom. If the chemical shift was above the baseline an even number of protons were attached to the carbon atom, and an odd number of protons were attached if the chemical shift was below the baseline in the NMR spectrum. The following tables (Table S2.6.1-S2.6.6) provide a summary of the details from the ^{1}H- and ^{13}C-NMR spectra (i.e. chemical shifts, integrated values). In addition, the NMR spectra are provided.

Table S2.6.1: Summary of the ^{1}H-NMR analysis completed for iohexol and selected iohexol TPs

Compound	Corresponding Number in Figure	Chemical Shift (ppm)	Peak Description	Integrated Value	Structure
Iohexol	4	8.50 to 8.59	Two multiplet peaks	2.33	-CO-N**H**-CH$_2$-
	6	4.76 to 4.77 4.53 to 4.63	Two groups of multiplet peaks	2.96 for first group and 5.01 for second group	-CH$_2$-O**H**, -CH$_2$-CH(O**H**)-CH$_2$OH
	7	3.68 to 3.91	Multiplet peak	5.33	-CH$_2$-C**H**(OH)-CH$_2$-
	8	3.39 to 3.48	Multiplet peak	8.28	-C**H$_2$**-OH
	9	3.00 to 3.31	Multiplet peak	5.65	-Ar-N(CO-)-C**H$_2$**-CH(OH)- - NH-C**H$_2$**-CH(OH)-CH$_2$
	10	1.78 to 1.79	Doublet peak (split peak)	3.00 (set value)	-CO-C**H$_3$**
Iohexol TP657	1	12.70	Singlet peak	0.6	-COO**H**
	2	9.93 to 9.97	Triplet peak	0.90	-Ar-N**H**-CO- CH$_3$
	3	8.80 to 8.86	Two singlet peaks (doublet peak)	0.65	-Ar-CO-N**H**-CH$_2$-COOH
	5	7.63 to 8.01	Combination of singlet and doublet peaks	2.05	-Ar-CO-N**H$_2$**
	7	3.84 to 3.91	Wide doublet or triplet peaks	2.26	-NH-C**H$_2$**-COOH -N(CO-)-C**H$_2$**-COOH
	10	2.02	Singlet peak	3.00 (set value)	-CO-C**H$_3$**
Iohexol TP599	2	9.91 to 9.95	Triplet peak	0.86	-Ar-N**H**-CO-CH$_3$
	5	7.63 to 8.02	Combination of singlet and doublet peaks	4.00 (set value)	-Ar-CO-N**H$_2$**
	10	2.02	Singlet peak	2.7	-CO-C**H$_3$**
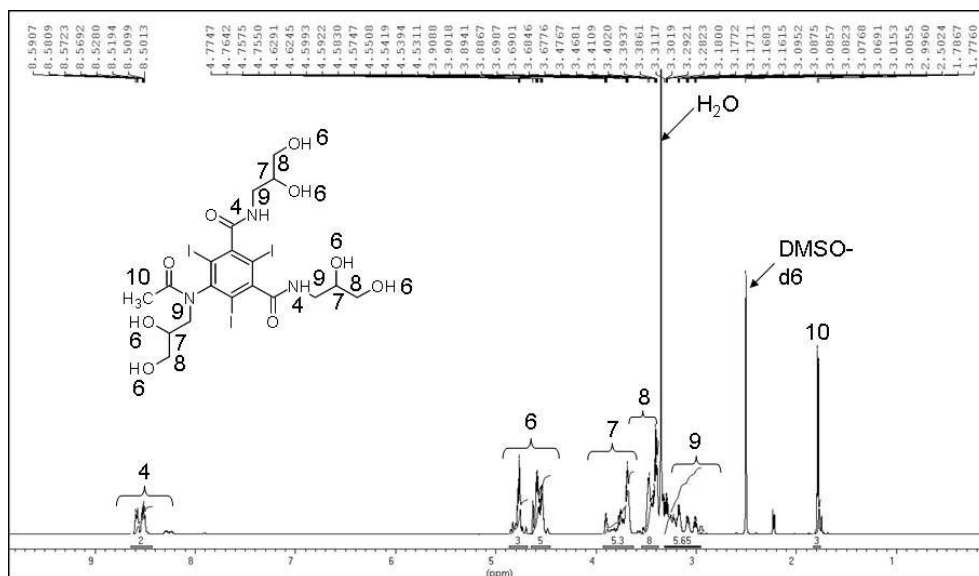
Figure S2.6.33: ^{1}H-NMR spectrum for iohexol at 700MHz and temperature of 298.3K
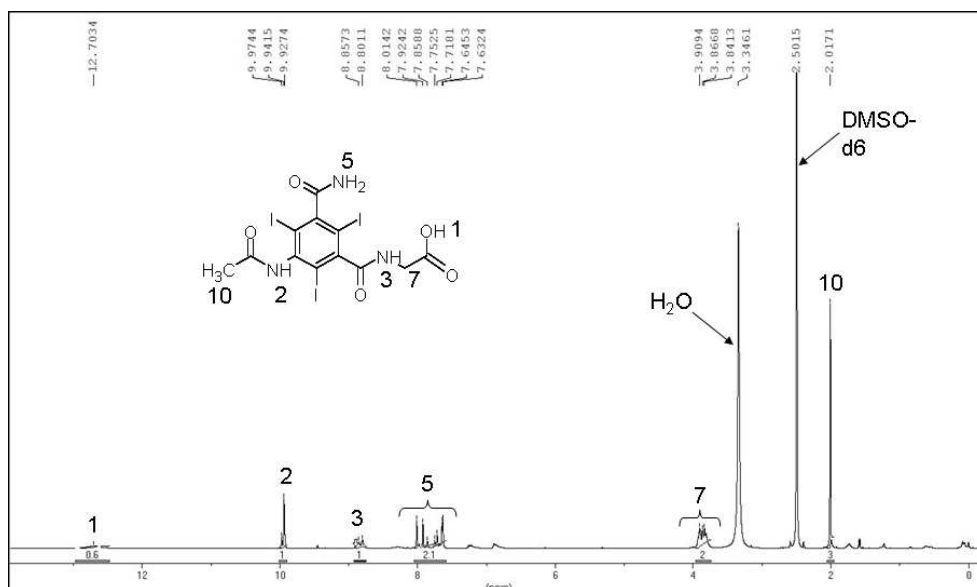
Figure S2.6.34: ^{1}H-NMR spectrum for iohexol TP657 at 700MHz and temperature of 298.3K

Figure S2.6.35: ^{1}H-NMR spectrum for iohexol TP599 at 700MHz and temperature of 298.3K
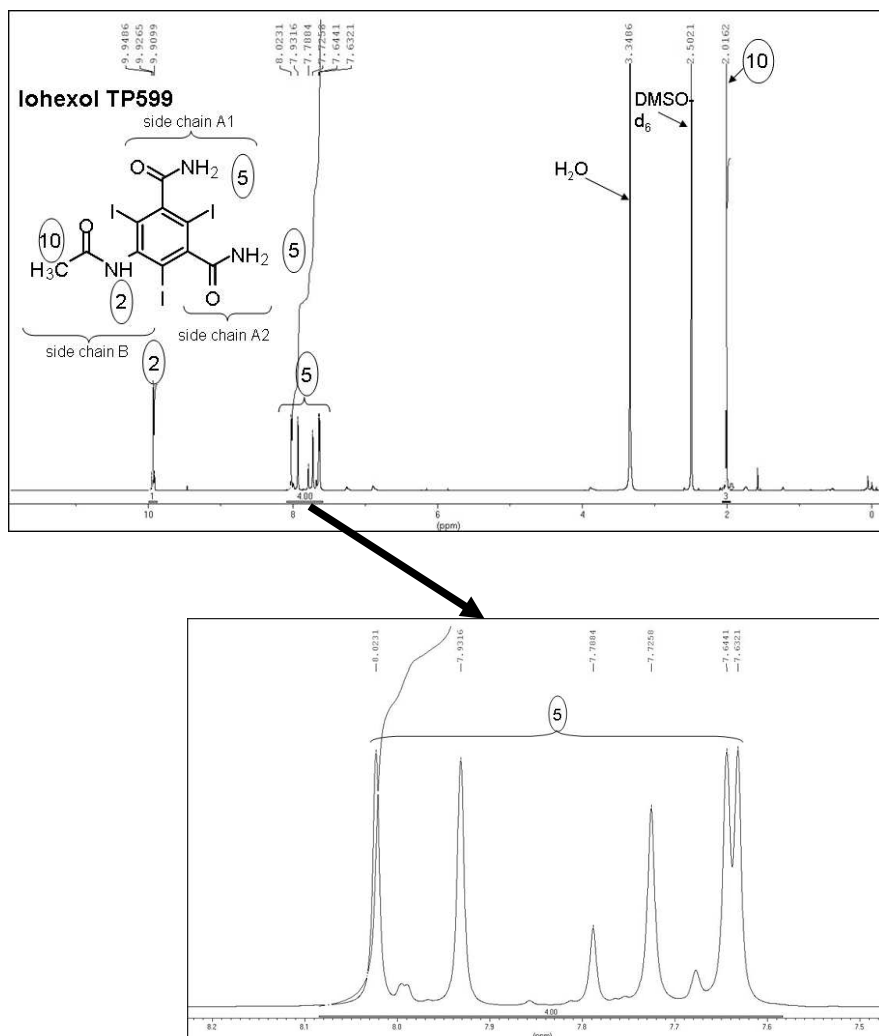
Figure 2.6.36: ^{1}H-NMR spectrum for iohexol TP599 showing the presence of a multiplet signal for NH_2 functional groups

Table S2.6.2: Summary of the ^{13}C-NMR analysis completed for iohexol and selected iohexol TPs

Compound	Corresponding Letter in Figure	Chemical Shift (ppm)	Structure
Iohexol	a	169.54 to 170.74	-Ar-**C**O-NH- -Ar-N(CH$_2$-)-**C**O-CH$_3$
	b	151.02	**C**-CO-NH-CH$_2$-
	c	147.74	**C**-N(CH$_2$-)-CO-CH$_3$
	d	100.05 to 100.91	**C**-I
	e	91.51 to 91.60	**C**-I
	f	70.06 (negative signal)	-CH$_2$-**C**H(OH)-CH$_2$-OH
	g	63.83 to 64.52	-**C**H$_2$-OH
	h	52.96 to 53.56	-Ar-N(CO-)-**C**H$_2$-
	i	42.48	-NH-**C**H$_2$-CH(OH)-
	k	22.78 (negative signal)	-CO-**C**H$_3$
Iohexol TP657	a	168.47 to 171.90	-Ar-NH-**C**O-CH$_3$ -Ar-CO-NH-CH$_2$-**C**OOH -Ar-**C**O-NH$_2$
	b	150.46 to 151.47	**C**-CO-NH- **C**-CO-NH$_2$
	c	144.11	**C**-NH-CO-CH$_3$
	d	99.73 to 99.89	**C**-I
	e	90.36	**C**-I
	i	42.08	-Ar-CO-NH-**C**H$_2$-COOH
	k	23.82	-CO-**C**H$_3$
Iohexol TP599	a	167.62 to 171.11	-Ar-**C**O-NH$_2$ -Ar-NH-**C**O-CH$_3$
	b	150.57	**C**-CO-NH$_2$
	c	143.24	**C**-NH-CO-CH$_3$
	d	98.31 to 98.41	**C**-I
	e	88.87	**C**-I
	k	22.96	-CO-**C**H$_3$
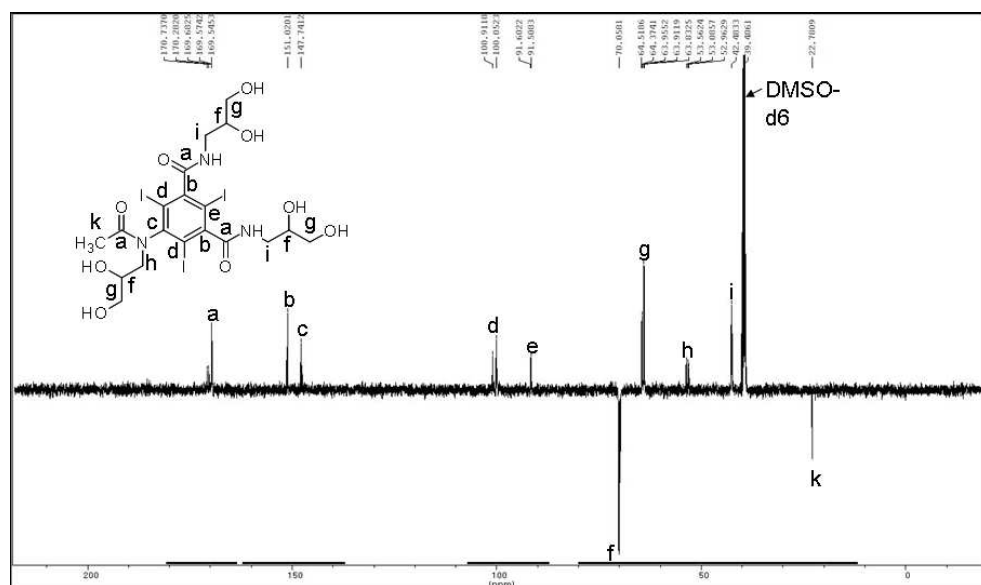
Figure S2.6.37: ^{13}C-NMR spin-echo spectrum for iohexol at 125MHz and temperature of 293.1K
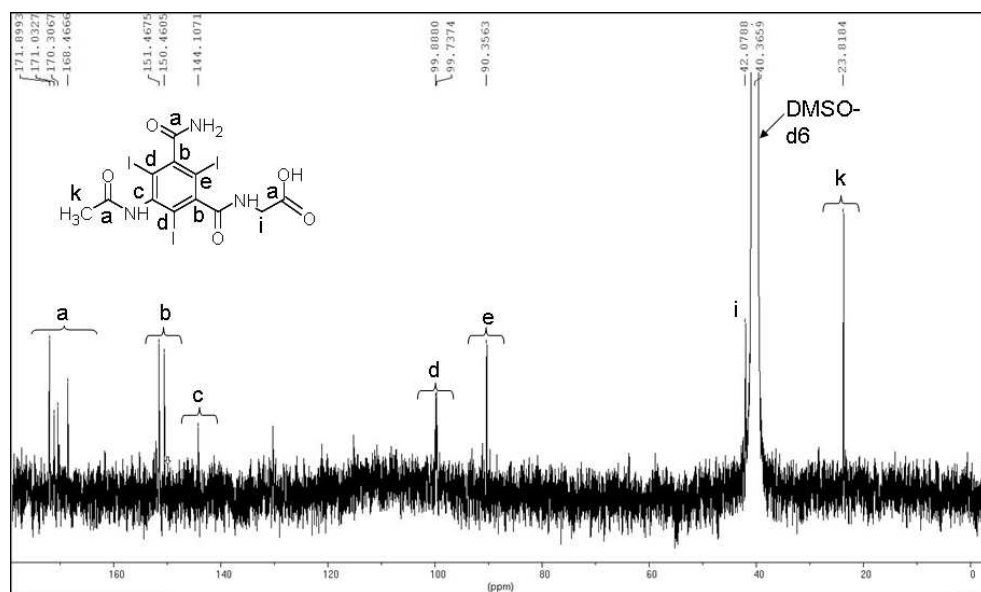
Figure S2.6.38: ^{13}C-NMR spectrum for iohexol TP657 at 125MHz and temperature of 293.1K
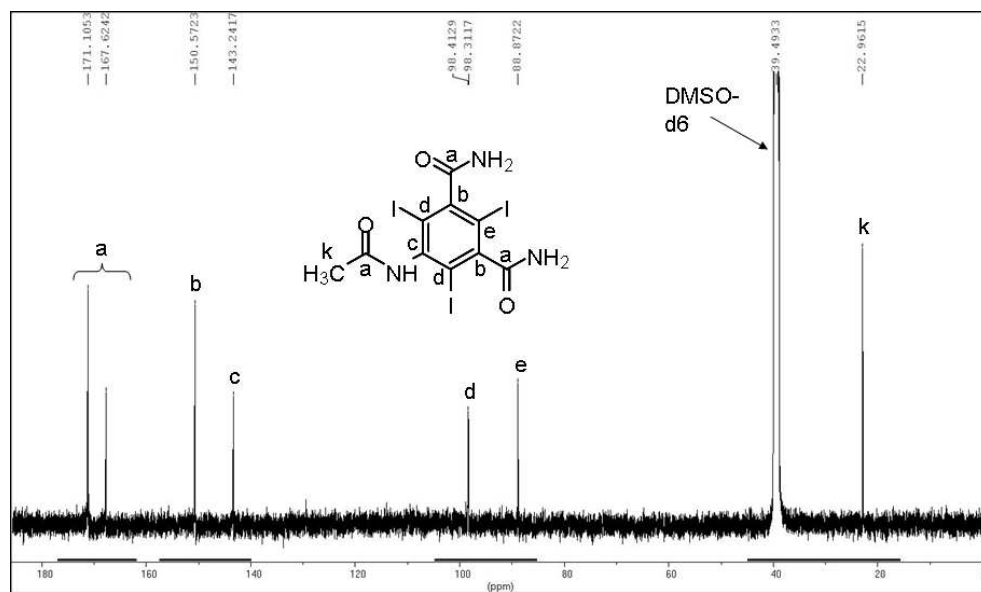
Figure S2.6.39: ^{13}C-NMR spectrum for iohexol TP599 at 125MHz and at a temperature of 293.1K.

Table S2.6.3: Summary of the ^{1}H-NMR analysis completed for iomeprol and selected iomeprol TPs

Compound	Corresponding Number in Figure	Chemical Shift (ppm)	Peak Description	Integrated Value	Structure
Iomeprol	3	8.50 to 8.63	Two groups both as doublet peaks	2.00	-CO-N**H**-CH$_2$-
	5	4.93 to 4.95	Multiplet peak	0.80	-CO-CH$_2$-O**H**
	6	4.74 to 4.79	Two groups both as doublet peaks	2.07	-CH$_2$-O**H**
	7	4.54 to 4.58	Multiplet peak	2.12	-CH$_2$-CH(-O**H**)-CH$_2$-
	9	3.67 to 3.69	Multiplet peaks	2.30	-CO-C**H$_2$**-OH
	10	3.39 to 3.48	Multiplet peaks	3.65 for first group and 2.61 for second group	-C**H$_2$**-OH -NH-C**H$_2$**-CH(-OH)-CH$_2$-
	11	3.00 to 3.18	Multiplet peaks	0.96 and 1.43	-CH$_2$-C**H**(-OH)-CH$_2$-
	12	2.96	Singlet peak	Value of 1.00	-Ar-N(-CO-)-C**H$_3$**
Iomeprol TP701	1	12.63 to 14.62	Three groups, two singlet peaks and then a doublet peak	1.57 (total)	-COO**H**
	2	8.84 to 9.02	Three triplet peaks	0.82	-CO-N**H**-CH$_2$-
	4	7.69 to 8.06	Group of multiplet peaks	2.00 (set value)	-CO-N**H$_2$**
	8	3.82 to 3.96	Group of multiplet peaks	1.94	-NH-C**H$_2$**-COOH
	12	3.01 to 3.14	Singlet peak and triplet peak	1.75 for singlet peak and 0.91 for triplet peak	-Ar-N(-CO-)-C**H$_3$**
Iomeprol TP643	1	13.88	Singlet peak	0.69	-COO**H**
	4	7.68 to 8.07	Combination of singlet and doublet peaks	4.00 (set value)	-CO-N**H$_2$**
	12	3.01 to 3.13	Singlet peak and triplet peak	3.01	-Ar-N(-CO-)-C**H$_3$**
Iomeprol TP629	4	7.73 to 8.03	Combination of singlet and doublet peaks	4.00 (set value)	-CO-N**H$_2$**
	5	4.97 to 4.99	Triplet peak	0.96	-CO-CH$_2$-O**H**
	9	3.49 to 3.71	Two groups both two doublet peaks	First is 1.06 and second is 1.11	-CO-C**H$_2$**-OH
	12	2.97	Singlet peak	2.77	-Ar-N(-CO-)-C**H$_3$**

Figure S2.6.40: ^{1}H-NMR spectrum for iomeprol at 700MHz and temperature of 298.3K

Figure S2.6.41: ^{1}H-NMR spectrum for iomeprol TP701 at 700MHz and temperature of 298.3K

118
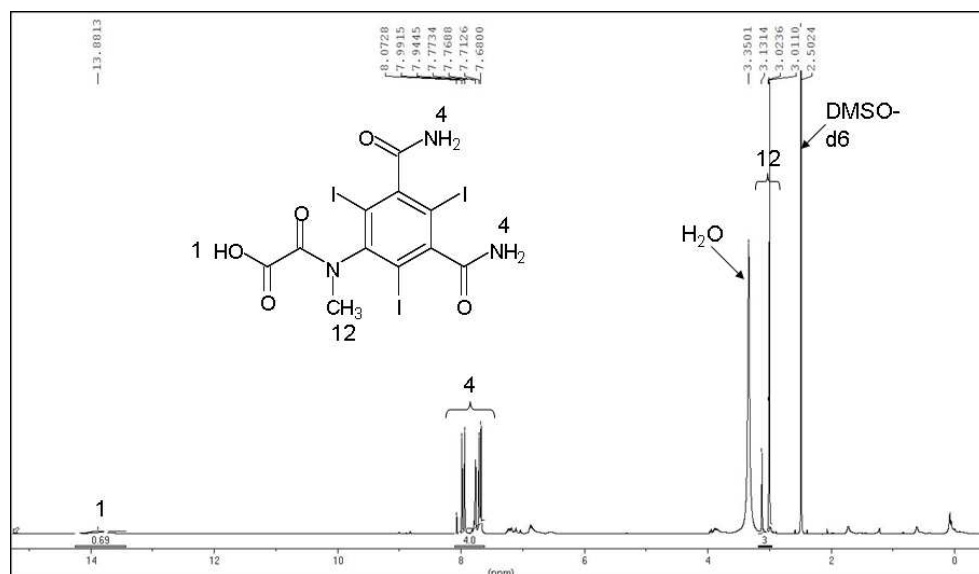
Figure S2.6.42: ^{1}H-NMR spectrum for iomeprol TP643 at 700MHz and at a temperature of 298.3K
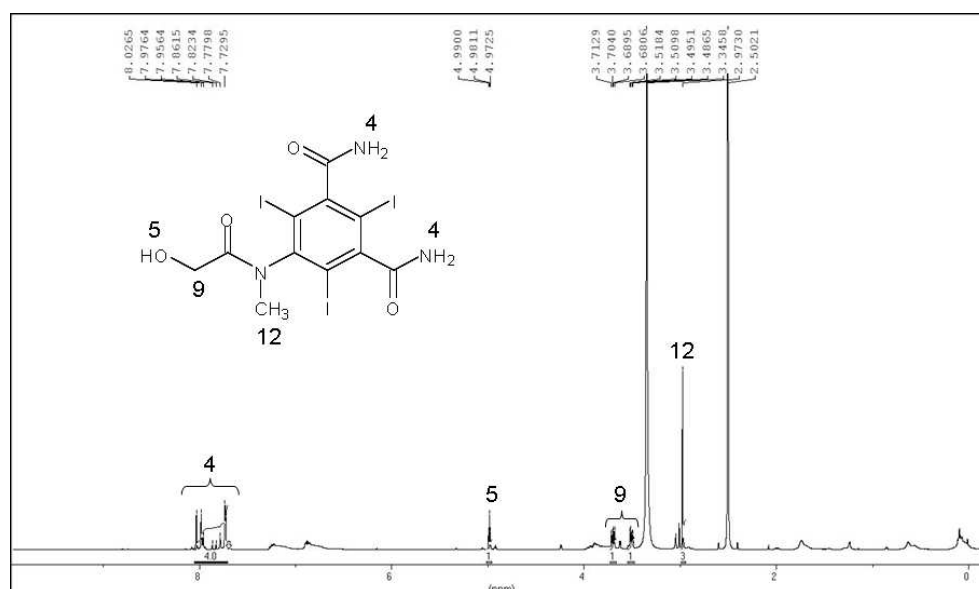
Figure S2.6.43: ^{1}H-NMR spectrum for iomeprol TP629 at 700MHz and temperature of 298.3K

Table 2.6.4: Summary of the ^{13}C-NMR analysis completed for iomeprol and selected iomeprol TPs

Compound	Corresponding Letter in Figure	Chemical Shift (ppm)	Structure
Iomeprol	a	169.34 to 170.69	-Ar-**CO**-NH- -Ar-N(-CH$_3$)-**CO**-
	d	151.03 to 151.14	**C**-CO-NH-
	e	145.34	**C**-N(-CH$_3$)-CO
	f	98.59 to 98.87	**C**-I
	g	92.28	**C**-I
	h	69.89 to 70.17 (negative signal)	-CH$_2$-**CH**-(OH)-CH$_2$-
	i	63.83 to 63.92	-**CH$_2$**-OH
	j	61.38	-CO-**CH$_2$**-OH
	k	42.36 to 42.51	-NH-**CH$_2$**-CH(-OH)-
	l	33.30 (negative signal)	-Ar-N(-CO-)-**CH$_3$**
Iomeprol TP643	a	171.58 to 171.76	-Ar-**CO**-NH$_2$
	b	165.13	-Ar-N(-CH$_3$)-**CO**- COOH
	c	162.15	-CO-**C**OOH
	d	151.94 to 152.18	**C**-CO-NH$_2$
	e	146.43 to 147.50	**C**-N(-CH$_3$)-CO-
	f	97.14 to 98.56	**C**-I
	g	91.57	**C**-I
	l	34.98 to 36.44 (negative signal)	-Ar-N(-CO-)-**CH$_3$**
Iomeprol TP629	a	171.06 to 171.74	-Ar-**CO**-NH$_2$ -Ar-N(-CH$_3$)-**CO**-
	d	152.55	**C**-CO-NH-
	e	146.24	**C**-N(-CH$_3$)-CO-
	f	98.62 to 98.85	**C**-I
	g	91.96	**C**-I
	j	62.20	-CO-**CH$_2$**-OH
	l	34.13 (negative signal)	-Ar-N(-CO-)-**CH$_3$**

Figure S2.6.44: ^{13}C-NMR spin-echo spectrum for iomeprol at 125MHz and temperature of 293.1K

Figure S2.6.45: ^{13}C-NMR spin-echo spectrum for iomeprol TP643 at 176MHz and temperature of 298.3K
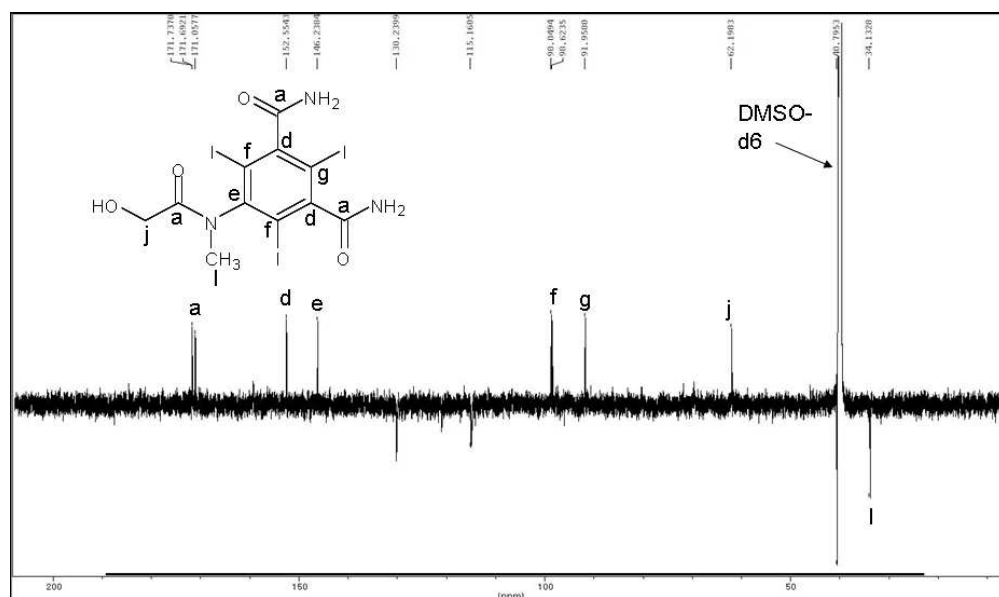
Figure S2.6.46: ^{13}C-NMR spin-echo spectrum for iomeprol TP629 at 176MHz and temperature of 298.3K

Table S2.6.5: Summary of the ^{1}H-NMR analysis completed for iopamidol and selected iopamidol TPs

Compound	Corresponding Number in Figure	Chemical Shift (ppm)	Peak Description	Integrated Value	Structure
Iopamidol	2	9.69- 9.70	Triplet peak	1.00 (set value)	-Ar-N**H**-CO-
	4	8.19- 8.24 7.54-7.63	Two groups of doublet peaks	1.54 for first group, and 0.49 for second group	-CO-N**H**-CH(-CH$_2$OH)- CH$_2$OH
	5	5.61-5.72	Three groups of doublet peaks	1.00	-CO-CH(-O**H**)-CH$_3$
	7	4.66-4.69 4.48-4.53	Two groups, two doublet peaks then doublet and triplet peaks for second group	1.07 for first group, and 3.16 for second group	-CH$_2$-O**H**
	8	4.15-4.17	Triplet peak	1.04	-CO-C**H**(-OH)-CH$_3$
	10	3.82	Singlet peak	2.16	-NH-C**H**(-CH$_2$OH)-CH$_2$OH
	12	3.63-3.65 3.50-3.53	Two groups of multiplet peaks	4.36 for first group and 4.34 for second group	-NH-CH(-C**H$_2$**OH)-C**H$_2$**OH
	13	1.38-1.39	Doublet peak	3.31	-CO-CH(-OH)-C**H$_3$**
Iopamidol TP791	1	12.65	Singlet peak	0.85	-COO**H**
	2	9.67-9.75	Triplet peak	1.00 (set value)	-Ar-N**H**-CO-
	3	8.66-8.75 8.00-8.20 7.53-7.76	Three groups of multiplet peaks	0.79 for the first group, 0.95 for second group and 0.25 for third group (total of approx. 2)	-CO-N**H**-CH(-CH$_2$OH)- COOH -CO- N**H**-CH(-CH$_2$OH)-CH$_2$OH
	5	5.62-5.67	Triplet peak	1.02	-CO-CH(-O**H**)-CH$_3$
	6	4.88	Singlet peak	0.77	-NH-C**H**(-CH$_2$OH)-COOH
	7	4.68-4.71 4.47-4.53	Two groups of doublet peaks	2.94	-CH$_2$-O**H**
	8	4.16	Singlet peak	1.02	-CO-C**H**(-OH)-CH$_3$

Compound	Corresponding Number in Figure	Chemical Shift (ppm)	Peak Description	Integrated Value	Structure
	10	3.82	Two groups with triplet and doublet peaks	5.18 for the first group and 1.89 for the second group (total of approx. 7)	-NH-C**H**(-CH₂OH)-CH₂OH
	11	3.76 to 3.77			-NH-CH(-C**H₂**OH)-COOH
	12	3.51 to 3.64			-NH-CH(-C**H₂**OH)-C**H₂**OH
	13	1.38 to 1.39	Doublet peak	3.15	-CO-CH(-OH)-C**H₃**
Iopamidol TP761	1	12.69	Singlet peak	0.85	-COO**H**
	2	9.69 to 9.72	Multiplet peak	1.02	-Ar-N**H**-CO-
	3	8.82 to 8.91	Three groups of multiplet peaks	0.69 for the first group, 0.95 for second group and 0.23 for third group (total of approx. 2)	-CO-N**H**-CH₂-COOH
		8.20 to 8.25			-CO-N**H**-CH(-CH₂OH)-CH₂OH
		7.73 to 7.81			
	5	5.62 to 5.71	Triplet peak	1.00 (set value)	-CO-CH(-O**H**)-CH₃
	7	4.49 to 4.66	Multiplet peak	1.98	-CH₂-O**H**
	8	4.17	Singlet peak	1.07	-CO-C**H**(-OH)-CH₃
	9 and 10	3.90 to 3.91	Two groups with multiplet peaks	2.99	-NH-C**H₂**-COOH
		3.82 to 3.83			-NH-C**H**(-CH₂OH)-CH₂OH
	12	3.63 to 3.64	Two groups with triplet and doublet peaks	2.21 for the first group and 2.16 for the second group	-NH-CH(-C**H₂**OH)-C**H₂**OH
		3.52			
	13	1.38 to 1.39	Doublet peak	3.34	-CO-CH(-OH)-C**H₃**
Iopamidol TP745	1	12.69	Singlet peak	1.81	-COO**H**
	2	9.71 to 9.77	Multiplet peak	1.00 (set value)	-Ar-N**H**-CO-
	3	8.82 to 8.92	Two groups of multiplet peaks	1.45 for the first group and 0.48 for second group (total of approx. 2)	-CO-N**H**-CH₂-COOH
		8.42 to 8.50			
	5	5.62 to 5.71	Triplet peak	0.95	-CO-CH(-O**H**)-CH₃
	8	4.16 to 4.17	Singlet peak	1.08	-CO-C**H**(-OH)-CH₃
	9	3.82 to 3.91	One multiplet peak and then two groups of doublet peaks	4.22	-NH-C**H₂**-COOH
	13	1.38 to 1.39	Doublet peak	3.32	-CO-CH(-OH)-C**H₃**
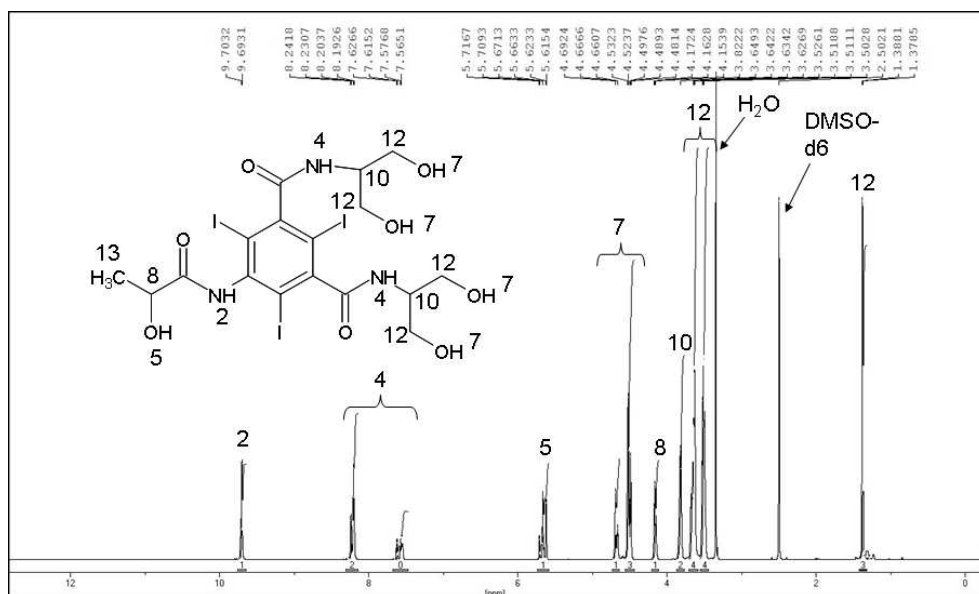
Figure S2.6.47: ^{1}H-NMR spectrum for iopamidol at 700MHz and temperature of 298.3K
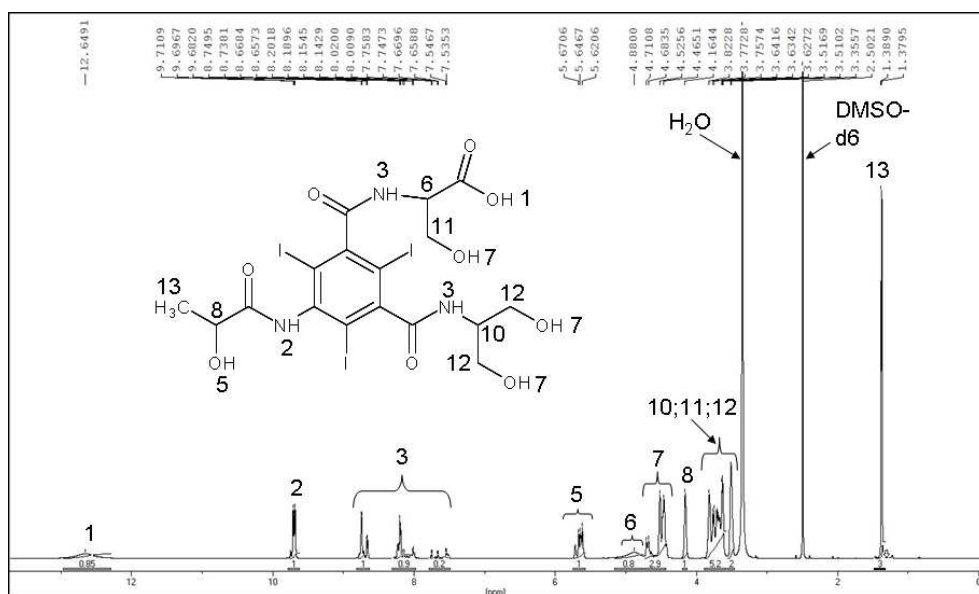
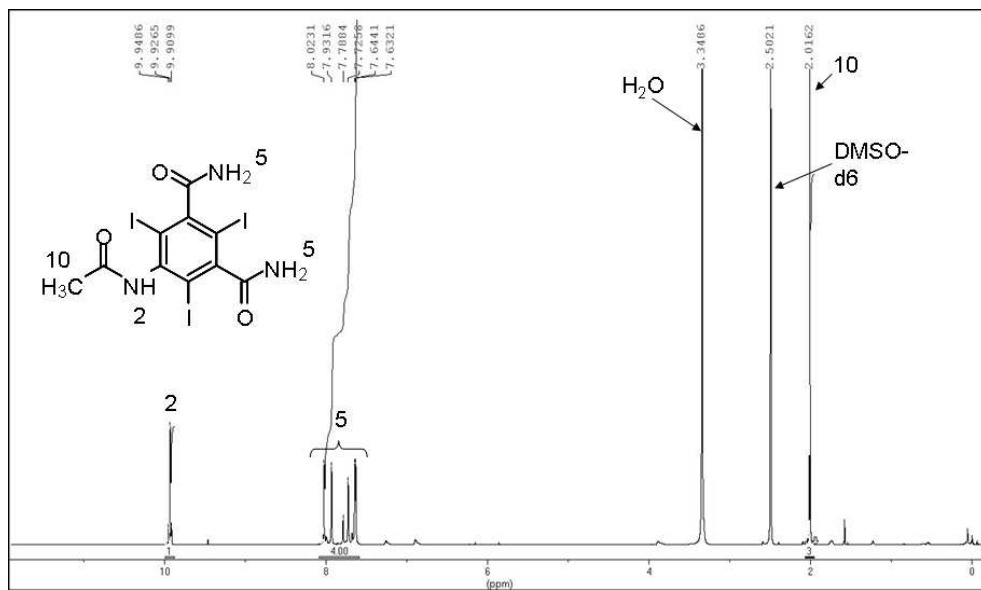Figure S2.6.48: ^{1}H-NMR spectrum for iopamidol TP791 at 700MHz and temperature of 298.3K
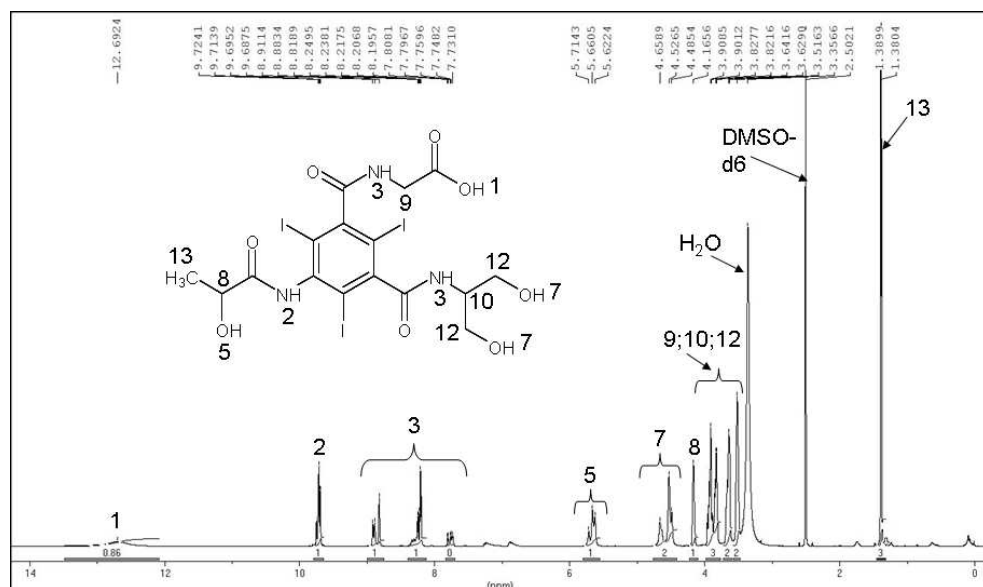
Figure S2.6.49: ^{1}H-NMR spectrum for iopamidol TP761 at 700MHz and temperature of 298.3K
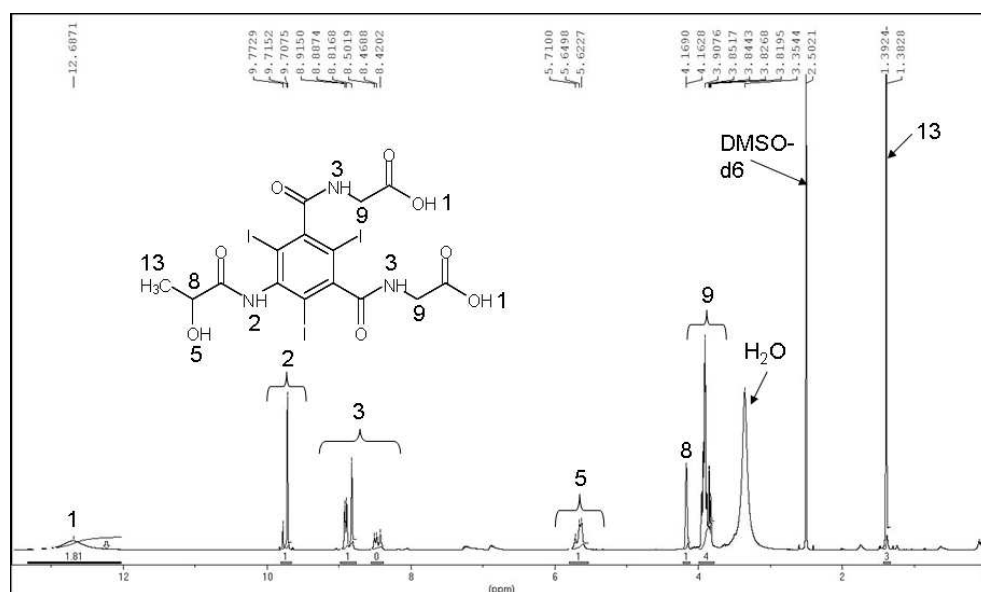
Figure S2.6.50: ^{1}H-NMR spectrum for iopamidol TP745 at 700MHz and temperature of 298.3K

Table S2.6.6: Summary of the ^{13}C-NMR analysis completed for iopamidol and selected iopamidol TPs

Compound	Corresponding Letter in Figure	Chemical Shift (ppm)	Structure
Iopamidol	a	169.02 to 172.63	-Ar-**CO**-NH- -Ar-NH-**CO**-
	b	149.78	**C**-CO-NH-
	c	142.76	**C**-NH-CO-
	d	98.96	**C**-I
	e	90.04	**C**-I
	f	67.54 (negative signal)	-CO-**C**H(-OH)-CH$_3$
	h	58.78 to 59.21	-CH(-**C**H$_2$OH)-**C**H$_2$OH
	j	53.06 to 53.16 (negative signal)	-NH-**C**H(-CH$_2$OH)-CH$_2$OH
	l	21.07 (negative signal)	-CH(-OH)-**C**H$_3$
Iopamidol TP791	a	168.87 to 172.64	Ar-**CO**-NH- -Ar-NH-**CO**- -CH(-**C**OOH)-CH$_2$OH
	b	149.33 to 149.82	**C**-CO-NH-
	c	142.75	**C**-NH-CO-
	d	99.14	**C**-I
	e	90.48	**C**-I
	f	67.54	-CO-**C**H(-OH)-CH$_3$
	g	61.30	-NH-CH(-COOH)-**C**H$_2$OH
	h	59.22	-CH(-**C**H$_2$OH)-**C**H$_2$OH
	i	54.48	-NH-**C**H(-COOH)-CH$_2$OH
	j	53.04 to 53.15	-NH-**C**H(-CH$_2$OH)-CH$_2$OH
	l	21.06	-CH(-OH)-**C**H$_3$

Compound	Corresponding Letter in Figure	Chemical Shift (ppm)	Structure
Iopamidol TP761	a	169.03 to 172.61	-Ar-**C**O-NH-
			-Ar-NH-**C**O-CH(-OH)-CH$_3$
			-CH$_2$-**C**OOH
	b	149.50 to 149.84	**C**-CO-NH-
	c	142.81	**C**-NH-CO-
	d	98.89 to 99.32	**C**-I
	e	90.03	**C**-I
	f	67.54	-CO-**C**H(-OH)-CH$_3$
	h	58.89 to 59.22	-CH(-**C**H$_2$OH)-**C**H$_2$OH
	j	52.84 to 53.16	-NH-**C**H(-CH$_2$OH)-CH$_2$OH
	k	41.13	-NH-**C**H$_2$-COOH
	l	21.06	-CH-(-OH)-**C**H$_3$

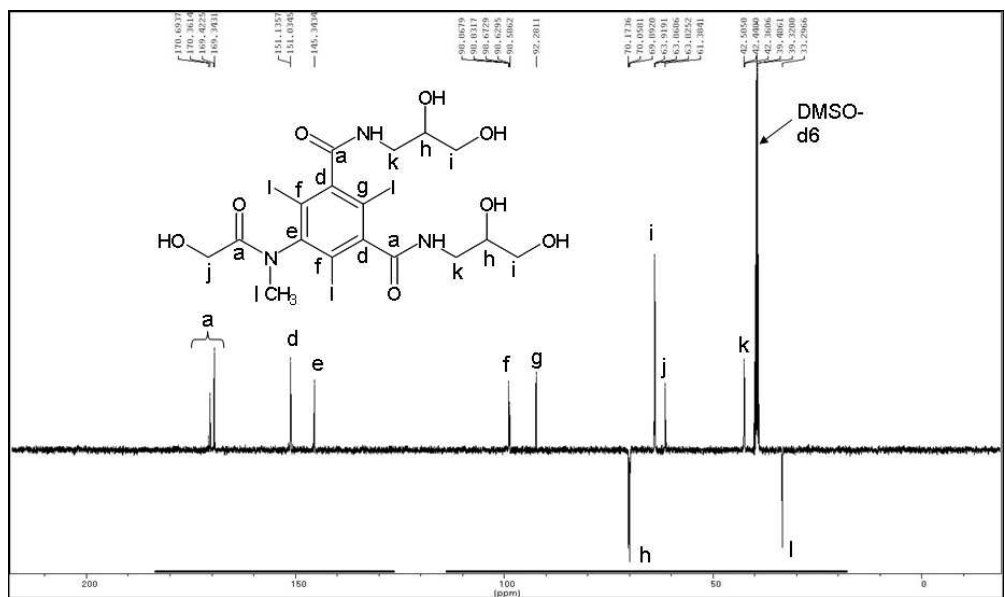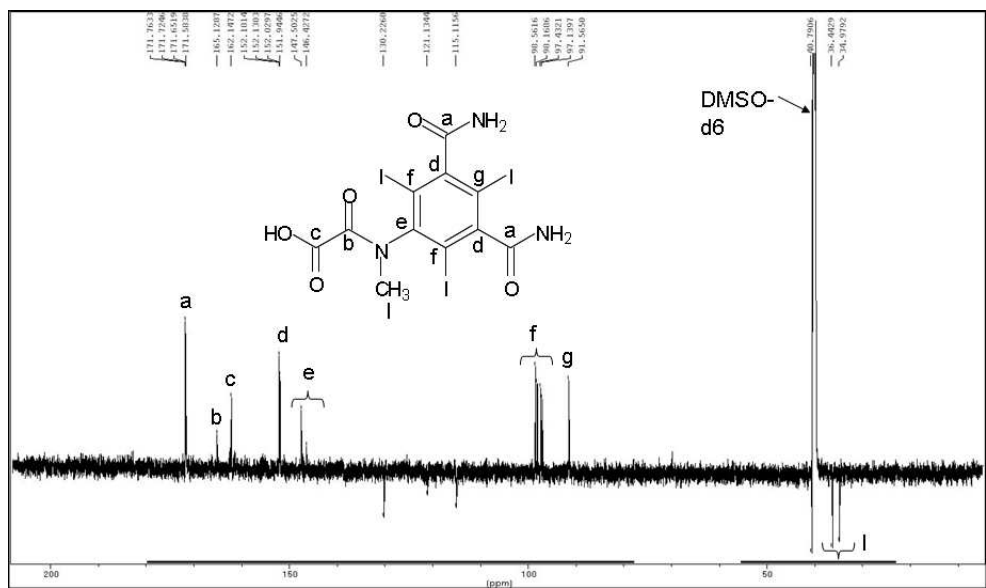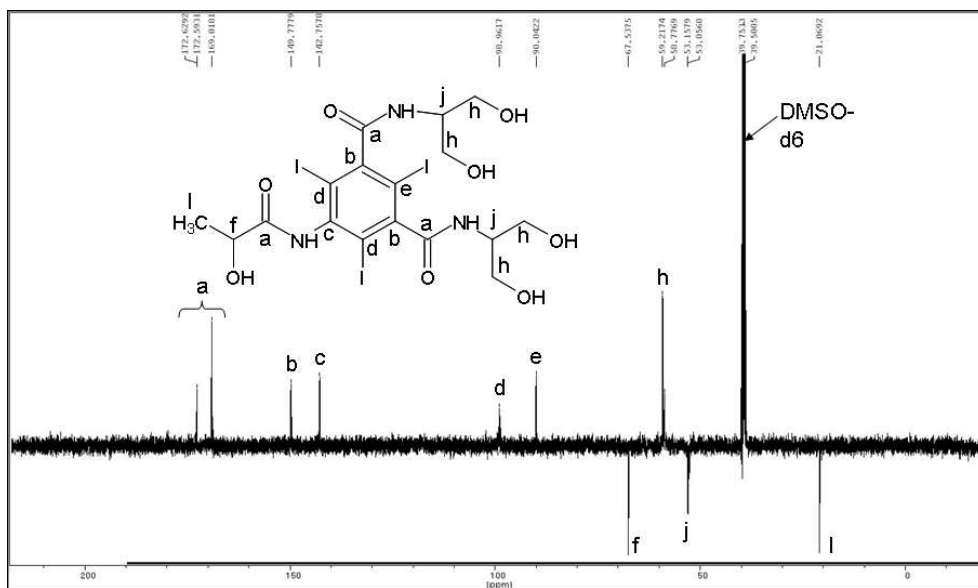Figure S2.6.51: ^{13}C-NMR spin-echo spectrum for iopamidol at 125MHz and temperature of 293.1K
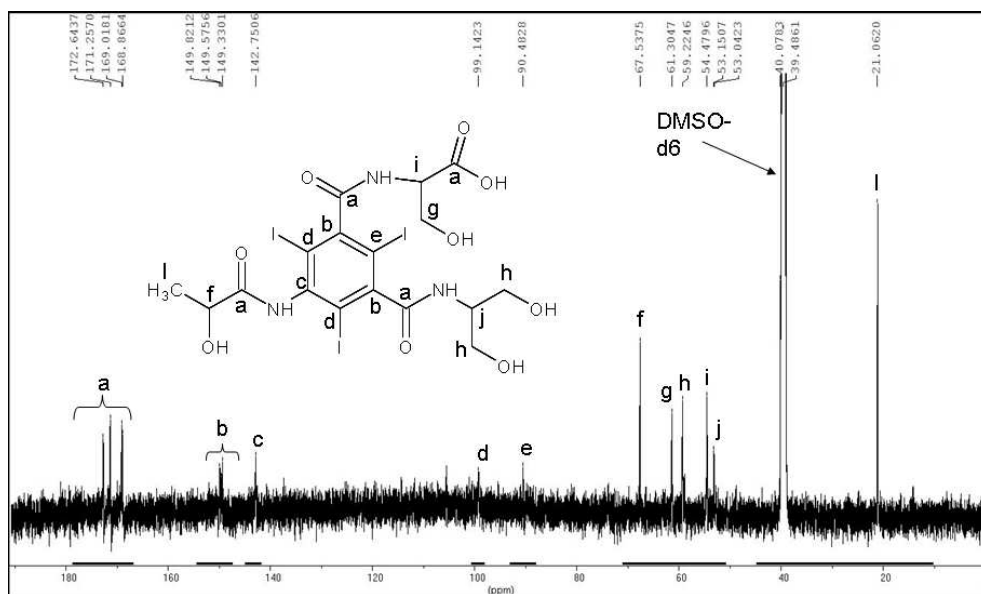
Figure S2.6.52: ^{13}C-NMR spectrum for iopamidol TP791 at 125MHz and at a temperature of 293.1K
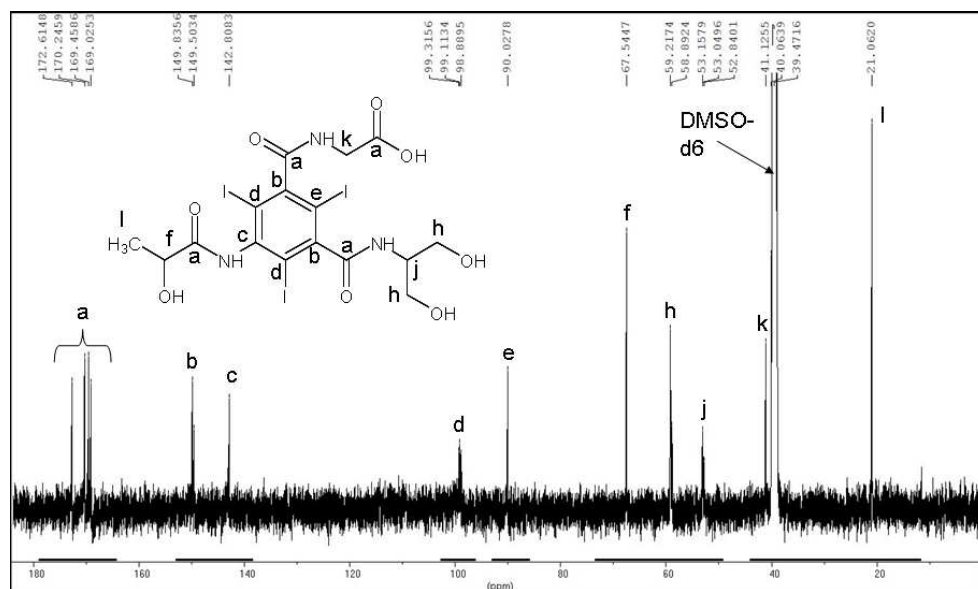
Figure S2.6.53: ^{13}C-NMR spectrum for iopamidol TP761 at 125MHz and temperature of 293.1K

2.7 Literature Cited

Batt, A. L.; Kim, S.; Aga, D. Enhanced biodegradation of iopromide and trimethoprim in nitrifying sludge. *Environ. Sci. Technol.* **2006**, *40* (23), 7367-7373.

Busetti, F.; Linge K. L.; Blythe, J. W.; Heitz, A. Rapid analysis of iodinated X-ray contrast media in secondary and tertiary wastewater by direct injection liquid chromatography-tandem mass spectrometry. *J Chromatogr A*. **2008**, *1213* (2), 200-208.

Carballa, M.; Omil, F.; Lema, J. M.; Llompart, M.; García-Jares, C.; Rodriguez, I.; Gómez, M.; Ternes, T. Behavior of pharmaceuticals, cosmetics and hormones in a sewage treatment plant. *Water Res.* **2004**, *38* (12), 2918-2926.

Corcoran, O.; Spraul, M. LC-NMR-MS in drug discovery. *Drug Discovery Today*. **2003**, *8* (14), 624-631.

Drillia, P.; Stamatelatou, K.; Lyberatos, G. Fate and mobility of pharmaceuticals in solid matrices. *Chemosphere* **2005**, *60* (8), 1034-1044.

Doll, T. E.; Frimmel, F. H. Fate of pharmaceuticals-photodegradation by stimulated solar UV-light. *Chemosphere.* **2003**, *52* (10), 1757-1769.

Gros, M.; Petrović, M.; Barceló, D. Development of a multi-residue analytical methodology based on liquid chromatography–tandem mass spectrometry (LC–MS/MS) for screening and trace level determination of pharmaceuticals in surface and wastewaters. *Talanta.* **2006**, *70* (4), 678-690.

Gutowsky, H. S.; Holm, C. H. Rate processes and nuclear magnetic resonance spectra. II. Hindered internal rotation of amides *J. Chem. Phys.* **1956**, *25*, 1228-1234.

Haiß, A.; Kümmerer, K. Biodegradability of the X-ray contrast compound diatrizoic acid, identification of aerobic degradation products and effects of against sewage sludge micro-organisms. *Chemosphere*. **2006**, *62* (2), 294-302.

Hirsch, R.; Ternes, T. A.; Lindart, A.; Haberer, K.; Wilken, R-D. A sensitive method for the determination of iodine containing diagnostic agents in aqueous matrices using LC-electrospray-tandem-MS detection. *Fresenius J Anal Chem.* **2000**, *366* (8), 835-841.

Kalsch, W. Biodegradation of the iodinated X-ray contrast media diatrizoate and iopromide. *Sci. Total Environ.* **1999**, *225* (1-2), 143-153.

Kolpin, D. W.; Furlong, E. T.; Meyer, M. T.; Thurman, E. M.; Zaugg, S. D.; Barber, L. B.; Buxton, H. T. Pharmaceuticals, hormones, and other organic contaminants in U.S. streams, 1999-2000: A national reconnaissance. *Environ. Sci. Technol.* **2002**, *36* (6), 1202-1211.

Löffler, D.; Römbke, J.; Meller, M.; Ternes, T. A. Environmental fate of pharmaceuticals in water/sediment systems. *Environ. Sci. Technol.* **2005**, *39* (14), 5209-5218.

Loos, R.; Gawlik, B. M.; Locoro, G.; Rimaviciute, E.; Contini, S.; Bidoglio, G. EU-wide survey of polar persistent pollutants in European river waters. *Environ. Pollut.* **2009**, *157* (2), 561-568.

Martínez Bueno, M. J.; Aguera, A.; Gómez, M. J.; Hernando, M. D.; García-Reyes, J. F.; Fernández-Alba, A. R. Application of liquid chromatography/quadrupole-linear ion trap mass spectrometry and time-of-flight mass spectrometry to the determination of pharmaceuticals and related contaminants in wastewater. *Anal. Chem.* **2007**, *79* (24), 9372-9384.

Pérez, S.; Eichhorn, P.; Celiz, M. D.; Aga, D. S. Structural characterization of metabolites of the x-ray contrast agent iopromide in activated sludge using ion trap mass spectrometry. *Anal. Chem.* **2006**, *78* (6), 1866-1874.

Pérez, S.; Barceló, D. Fate and occurrence of X-ray contrast media in the environment. *Anal. Bioanal. Chem.* **2007**, *387* (4), 1235-1246.

Pérez, S.; Eichorn, P.; Barceló, D. Structural characterization of photodegradation products enalapril and its metabolite enalaprilat obtained under stimulated environmental conditions by hybrid quadrupole-linear ion trap-MS and quadrupole-time-of-flight-MS *Anal. Chem.* **2007**, *79* (21), 8293-8300.

Putschew, A.; Miehe, U.; Tellez, A. S.; Jekel, M. Ozonation and reductive deiodination of iopromide to reduce the environmental burden of iodinated X-ray contrast media. *Water Sci. Technol.* **2007**, *56* (11), 159-165.

Quintanilla-Licea, R.; Colunga-Valladares, J.; Caballero-Quintero, A.; Rodríguez-Padilla, C.; Tamez-Guerra, R.; Gómez-Flores, R.; Waksman, N. NMR detection of isomers arising from restricted rotation of the C-N amide bond of N-formyl-o-toluidine and N,N-bis-formyl-o-toluidine. *Molecules* **2002**, *7* (8), 662-673

Radjenović, J.; Pérez, S.; Petrović, M.; Barceló, D. Identification and structural characterization of biodegradation products of atenolol and glibenclamide by liquid chromatography coupled to hybrid quadrupole time-of-flight and quadrupole ion trap mass spectrometry. *J Chromatogr A.* **2008**, *1210* (2), 142-153.

Schulz, M.; Löffler, D.; Wagner, M.; Ternes, T. A. Transformation of the X-ray contrast medium iopromide in soil and biological wastewater treatment. *Environ. Sci. Technol.* **2008**, *42* (19), 7207-7217.

Seitz, W.; Jiang, J.-Q.; Schulz, W.; Weber, W. H.; Maier, D.; Maier, M. Formation of oxidation by-products of the iodinated X-ray contrast medium iomeprol during ozonation. *Chemosphere.* **2008**, *70* (7), 1238-1246.

Steger-Hartmann, T.; Länge, R.; Schweinfurth, H.; Tschampel, M., Rehmann, I. Investigations into the environmental fate and effects of iopromide (ultravist), a widely used iodinated X-ray contrast medium. *Water Res.* **2002**, *36* (1), 266-274.

Ternes, T. A. Occurrence of drugs in German sewage treatment plants and rivers. *Water Res.* **1998**, *32* (11), 3245-3260.

Ternes, T. A.; Hirsch, R. Occurrence and behavior of X-ray contrast media in sewage facilities and the aquatic environment. *Environ. Sci. Technol.* **2000**, *34* (13), 2741-2748.

Ternes, T. A.; Bonerz, M.; Hermann, N.; Teiser, B.; Andersen, H. R. Irrigation of treated wastewater in Braunschweig, Germany: An option to remove pharmaceuticals and musk fragrances. *Chemosphere*. **2007**, *66* (5), 894-904.

Trautwein, C.; Kümmerer, K.; Metzger, J. W. Aerobic biodegradability of the calcium channel antagonist verapamil and identification of microbial dead-end transformation product studied by LC-MS/MS. *Chemosphere*. **2008**, *72* (3), 442-450.

Chapter 3:

Biotransformation of Selected Iodinated X-ray Contrast Media and Characterization of Microbial Transformation Pathways

Jennifer Lynne Kormos,[1] Manoj Schulz,[1] Hans-Peter E. Kohler[2] and Thomas A. Ternes[1]

[1]Federal Institute of Hydrology (BfG), Am Mainzer Tor 1, 56068 Koblenz, Germany

[2]Eawag, Swiss Federal Institute of Aquatic Science and Technology,

Überlandstrasse 133, P.O. Box 611, 8600 Dübendorf, Switzerland

Abstract

Iodinated X-ray contrast media (ICM) are commonly detected in the aquatic environment at concentrations up to the low µg/L range. In this study the biotransformation of selected ICM (diatrizoate, iohexol, iomeprol and iopamidol) in aerobic soil-water and river sediment-water batch systems was investigated. In addition, microbial transformation pathways were proposed. Diatrizoate, an ionic ICM, was not biotransformed, while three nonionic ICM were transformed into several biotransformation products (TPs) at pH 7. Iohexol and iomeprol were biotransformed to eleven TPs and fifteen TPs, respectively, while eight TPs were detected for iopamidol. Since seven of the TPs detected during biotransformation had not been previously identified, mass fragmentation experiments were completed to elucidate the chemical structures. Oxidation of primary alcoholic moieties, cleavage of the N-C bonds (i.e. deacetylation and removal of hydroxylated propanoic acids), and oxidative decarboxylation are potential reactions that can explain the formation of the identified TPs. Iohexol and iomeprol had similar biotransformation rates, while iopamidol was biotransformed slower and to a lesser extent. A LC tandem MS method confirmed the presence of ICM TPs in aqueous environmental samples. Fifteen of the ICM TPs were even detected in drinking water with concentrations up to 120 ng/L.

3.1 Introduction

Iodinated X-ray contrast media (ICM) are used for imaging soft tissues, internal organs and blood vessels, and can be administered to humans at doses up to 200 g per diagnostic session (Pérez and Barceló, 2007). They are designed to be resistant to human metabolism and are excreted mostly unchanged within 24 h (Pérez and Barceló, 2007; Weissbrodt *et al.* 2009). ICM are commonly detected at elevated concentrations in domestic and hospital wastewaters (Ternes, 1998; Hirsch *et al.* 2000; Ternes and Hirsch, 2000; Putschew *et al.*2000; Putschew *et al.* 2007; Busetti *et al.* 2008; Weissbrodt *et al.* 2009), surface waters (Ternes, 1998; Ternes and Hirsch, 2000; Seitz *et al.* 2006a), groundwater and bank infiltrate samples (Sacher *et al.* 2001; Ternes *et al.* 2007; Schulz *et al.* 2008), soil leachates (Oppel *et al.* 2004), and even in drinking water supplies due to their high polarity and persistence (Seitz *et al.* 2006b). ICM are not effectively removed in drinking water treatment plants (DWTPs) and hence are detected in finished water. However, certain advanced processes such as activated carbon filtration and nonselective oxidation reactions have increased removal efficiencies (Joss *et al.* 2006a; Seitz *et al.* 2006b). Soil passage and bank filtration are other possible removal processes for ICM (Oppel *et al.* 2004; Schittko *et al.* 2004). However, the sorption affinity of ICM to sludge and suspended matter is limited (Löffler *et al.* 2005; Ternes *et al.* 2007). The presence of ICM is partly responsible for the high absorbable organic halogen (AOX) content found in hospital wastewaters and effluents from radiographic practices (Putschew *et al.* 2000; Schittko *et al.* 2004).

ICM are only partly transformed in municipal wastewater treatment plants (WWTPs) during nitrification with elevated sludge retention times (SRT) (Batt *et al.* 2006; Carballa *et al.* 2007; Schulz *et al.* 2008). However, mineralization was observed for a precursor of ICM, 5-amino-2,4,6-triiodophthalic acid, in a two-stage anaerobic-aerobic reactor (Lecouturier *et al.* 2003).

Ozonation and advanced oxidation processes (i.e. UV/H$_2$O$_2$) have not been effective for the removal of ICM (Ternes *et al.* 2003; Seitz *et al.* 2006a; Bahr *et al.* 2007; Putschew *et al.* 2007), and the photocatalytic activity of TiO$_2$ did not result in the complete mineralization of iomeprol (Doll and Frimmel, 2005). Although, reductive dehalogenation with zero-valent iron (Putschew *et al.* 2007) and hydrogen dehalogenation in the presence of metal catalysts (Knitt *et al.* 2008) were promising for ICM removal dissolved in pure water, either iodinated by-products were formed or the removal efficiencies were limited in water containing high DOC and natural organic matter. Recent studies have shown that de-iodination of ICM can occur with chemical oxidation (Seitz *et al.* 2006b; Knitt *et al*. 2008), photolysis (Steger-Hartmann *et al.* 2002*)* or biocatalysts, specifically enzymes of white rot fungi (Rode and Müller, 1998).

Transformation of ICM has been investigated in sludge systems as well as in sediment-water systems, however the results have been inconsistent (Kalsch, 1999; Steger-Hartmann *et al.* 1999; Lecouturier *et al.* 2003; Haiβ and Kümmerer, 2006). Nevertheless, in all studies the mineralization of ICM was rare, and biotransformation of ICM was a relative slow process compared to that of other environmental organic pollutants. Recently, Kormos *et al.* (2009) identified a number of TPs of the nonionic ICM, iohexol, iomeprol and iopamidol. However, the biotransformation rates and transformation pathways have not yet been investigated.

The aim of this study was to elucidate the biotransformation of diatrizoate, iohexol, iomeprol and iopamidol in different aerobic soil-water and sediment-water systems, and to propose microbial transformation pathways. In addition, seven unidentified ICM TPs were structurally elucidated. Furthermore, the occurrence of ICM TPs was investigated in the aquatic environment to compare the results obtained in the batch systems to real environmental conditions.

3.2 Experimental Section

3.2.1 Chemicals and Standards

The physical and chemical properties of the selected ICM are described in Table 1.1 (Chapter 1). Desmethoxyiopromide and N-(2,3-dihydroxypropyl)-2,4,6-triiodo-5-methoxyacetylamino-N'-methylisophthalamide were selected as the surrogate standards and used for quantification of the ICM and TPs in the batch systems and environmental samples.

3.2.2 Soils and Sediments

Two different soils were selected for the biotransformation experiments. The LUFA 2.2 soil is a well-known European loamy sand soil which has high organic matter content (organic carbon of 2.3%). The Ap horizon layer (or the upper plowed soil layer) of an agricultural field in Braunschweig, Germany was the other soil selected, which had low organic matter content (approx. 0.9%) and a sand content of more than 90%. This particular soil has been irrigated with secondary treated wastewater effluent and sludge for more than 50 years. Natural river sediment was collected from Unterbach, a tributary of the Lahn River, near Dausenau, Germany. This sediment has a high organic carbon content of 4.36 % and clay/silt content of 47 %, and previously published in Stein *et al.* (2006). The individual parameters of the soils and river sediment are listed in Table S3.6.1.

3.2.3 Soil/Sediment-Water Batch Systems

The groundwater used in the batch systems was collected from a deep well in Arenberg, a district of Koblenz, Germany, and characteristics of this groundwater are found in section 3.6. All batch experiments were conducted under aerobic conditions. The redox potential was measured in the

aqueous phase throughout the experimental period and varied between 100 to 220 mV. In order to determine whether microbial transformation took place, batch systems were prepared by adding 2 mL formaldehyde solution (37%, v/v) to a batch system consisting of 2 g of soil or sediment and 20 mL of 1 g/L of ICM. Experiments at lower concentrations (e.g. 1 mg/L) were not included in the manuscript because similar results were achieved and the transference to environmental concentrations is already confirmed by the detection of the ICM TPs in environmental matrices. Unspiked batch systems with a ratio of 1:5 soil(sediment):groundwater were always run in parallel.

Soil-water batch systems were individually spiked with the four selected ICM. The volume ratio of soil to groundwater was 1:5. The batch systems consisted of 80-100 g of soil and 400-500 mL of groundwater containing a concentration of 1 g/L of the individual ICM. The batch systems were placed at room temperature (20-22°C) in an enclosed cupboard, to prevent transformation of the ICM by natural or artificial light. Previous research has found that selected ICM (i.e. iomeprol) can photodegrade by stimulated sunlight under specific conditions (Doll and Frimmel, 2003). In addition, batch experiments consisting of the Braunschweig soil, were conducted at 30±1°C in a temperature controlled water bath. Samples (2 mL aliquots) were collected from the aqueous phase of the soil-water batch systems at repeated intervals for the duration of the experimental period (up to 159 d).

Sediment-water batch systems were spiked with the three nonionic ICM. The ratio of river sediment to groundwater was 1:5. The batch systems consisted of 4 g of sediment and 25 mL of groundwater containing a concentration of 1 g/L of the individual ICM. The batch systems were placed in an enclosed cupboard at room temperature (20-22°C). Samples (100 µL aliquots) were

138

collected from the aqueous phase of the sediment-water systems at repeated intervals for the duration of the experimental period (up to 155 d).

Prior to analysis, the sample aliquots from the batch systems were prepared by diluting 10 µL of the sample with Milli-Q water (total volume of 1 mL) and spiking with 10 µL of each of the two surrogate standards (20 µg/mL). LC ESI tandem MS was used to measure the ICM and TPs in the prepared samples.

3.2.4 Aqueous Environmental Samples

Grab samples were collected from the influent and effluent of a conventional WWTP in Germany, which consists of mechanical treatment (screens, grit chambers, sedimentation) followed by biological treatment (denitrification and nitrification). The sludge age is approximately 16-20 d, and the WWTP serves 600,000 population equivalents (PE). Grab samples were collected from the Rhine River close to Mainz, Germany. In addition, grab samples were collected from a German DWTP. The treatment processes of the DWTP consisted of flocculation, ozonation and activated carbon filtration. The raw water source for this particular DWTP is river water. The samples were acidified to pH 2.8 after collection, filtered through glass fiber filters, and extracted with Isolute® ENV+ SPE cartridges (200 mg, 3 mL) according to Schulz *et al.* (2008) and Kormos *et al.* (2009). Prior to SPE the two surrogate standards were spiked into a sample volume of 500 mL of surface water and drinking water, 100 mL of WWTP influent, and 200 mL of WWTP effluent. The SPE cartridges were conditioned with 2 mL of n-heptane, 2 mL of acetone, 4×1 mL of methanol and 4×1 mL of groundwater at pH 2.8. The cartridges were dried with a gentle stream of nitrogen, and then eluted with 8 mL of methanol.

The sample extracts were evaporated to 100 µL, and then reconstituted to 1 mL with Milli-Q water.

3.2.5 Detection via LC ESI tandem MS

LC ESI tandem MS (Applied Biosystems/MDS Sciex 4000 Q Trap system) was used for the detection of the parent ICM and identified TPs in the samples collected from the batch experiments as well as environmental samples (Schulz *et al.* 2008; Kormos *et al.* 2009).

The ICM and TPs were separated on a Synergi Polar RP column (Phenomenex®, Aschaffenburg, Germany), with the column oven set at 50 °C. A gradient elution was used and the flow rate was set at 0.4 mL/min. The mobile phases consisted of Milli-Q water with 0.1% aqueous formic acid (mobile phase A) and acetonitrile with 0.1% aqueous formic acid (mobile phase B). The gradient program was as follows: after 4 min of 95% mobile phase A, the percentage of A was decreased to 75% within 11 minutes, and then returned to the initial conditions until the end of the measurement time. The injection volume was 20 µL and the duration of the run was a total of 20 min.

3.2.6 Identification of Transformation Products via MS Fragmentation

The structural elucidation of the seven new ICM TPs (iopamidol TP717, iomeprol TP791, iomeprol TP775, iomeprol TP761, iomeprol TP745, iomeprol TP657 and iomeprol TP599) was completed using the approach described by Kormos *et al.* (2009). This involved determining the fragmentation patterns of the TPs based on MS^2 spectra, as well as applying the information obtained from previous MS fragmentation experiments during structural elucidation of ICM TPs.

3.2.7 Quantification of Parent ICM and TPs via LC ESI tandem MS

Stock solutions were prepared for the nine isolated TPs (i.e. iohexol TP687A, TP657 and TP599, iomeprol TP701, TP643 and TP629, as well as iopamidol TP791, TP761 and TP745) and the four parent ICM. The nine ICM TPs were isolated by a semi-preparative HPLC-UV system coupled to a fraction collector. The fractions collected were infused into a LC tandem MS to determine the purity of the fraction. If only one dominant precursor ion was present in the Q1 scans, the fraction was freeze-dried to obtain a pure substance to be used for preparation of spiking solutions and calibration standards. A more detailed explanation can be found elsewhere (Kormos *et al.* 2009*)*. Approximately 1 mg of standard was dissolved into 10 mL of Milli-Q water. Calibration standards were prepared by diluting the stock solutions with Milli-Q water and spiking 10 µL of each of the two surrogate standards (20 µg/mL). At least two optimized MRM transitions were used for identification and confirmation of the ICM and TPs in the batch system samples as well as the environmental samples. A list of MRM transitions with optimized MS parameters as well as the source-dependent parameters for the ESI source are summarized in Table S3.6.2-S3.6.5. The limit of quantification (LOQ) values for the ICM TPs detected in the environmental samples are provided in Table 3.2.

The concentrations of the parent ICM and nine standard TPs were determined from the linear regression ($r^2 > 0.98$) of the calibration curves. For quantification of the ICM TPs for which standards were not available, either the calibration curve of the parent ICM or a TP with a similar fragmentation pattern and chemical structure was selected.

3.2.8 Determination of biotransformation rate constants and DT_{50} values

Concentrations of the parent ICM detected in the aqueous phases of the batch systems were plotted over the experimental period. In addition, concentrations of the parent ICM were normalized to the measured initial parent ICM concentration and plotted over time (Figure S3.6.7 (a)-(d)). The graphs were used to determine if ICM biotransformation followed zero-order reactions. The biotransformation rate constants, $k_{biol,}$ were estimated from the slope of the concentration vs. time plot if a zero-order reaction were assumed. The rate constants were estimated within the linear range of the graphs.

Disappearance time (DT) is the time in which the initial concentration of the parent ICM is reduced by a certain percentage, usually 50 % (DT_{50}) or 90 % (DT_{90}). For this study, a DT_{50} value ($DT_{50linear}$) was calculated within the linear range of the concentration vs. time graphs, and a $DT_{50total}$ value was estimated for the linear range of biotransformation as well as the initial lag phase. For zero-order kinetics, the DT_{50} values were estimated by using $DT_{50linear} = C_o/(2 \times k_{biol})$, and $DT_{50total} = $ lag phase $+ DT_{50linear}$.

3.3 Results and Discussion

3.3.1 Biotransformation of ICM

The nonionic ICM (iohexol, iomeprol and iopamidol) were biotransformed to several TPs in the aerobic soil- and sediment-water batch systems. The tri-iodinated aromatic ring was not modified, and hence these ICM did not undergo mineralization. The normalized concentration vs. time graphs (Figure S3.6.7 (a)-(d)) illustrate that more than 95% (in most cases close to 100%) of the parent nonionic ICM in the aqueous phase of the batch systems was biotransformed

within a time period of 159 d. The only exception was the biotransformation of iopamidol in the LUFA 2.2 soil-water system, in which close to 50% of the parent ICM was detected. Diatrizoate, an ionic ICM, was not biotransformed in all aerobic batch systems. This is in contrast to the transformation of diatrizoate observed by Kalsch (1999) and Haiß and Kümmerer (2006) who reported the formation of two TPs formed by a deacetylation taking place at the side chains.

The biotransformation rates of the nonionic ICM varied in the different batch systems. Zero-order reactions were always the most appropriate model to describe the ICM biotransformation observed in the batch systems. Lag phases between 15-27 d were observed for iomeprol and iopamidol in the sediment-water systems, the Braunschweig soil-water systems incubated at 30°C and the LUFA 2.2 soil-water systems. This suggests that microbial adaptation was required prior to biotransformation. However, lag phases were absent during the biotransformation of iohexol, iomeprol and iopamidol in the Braunschweig soil incubated at 20-22°C. One explanation could be that the microorganisms were well adapted in the Braunschweig soil after the long-term irrigation of treated wastewater effluent containing X-ray contrast media. Based on previous experimental results, it can be assumed that sorption of ICM is negligible (Löffler *et al.* 2005;Carballa *et al.* 2008). ICM are hydrophilic compounds with reported log K_{ow} values of less than 1.5 (Table 1.1, Chapter 1).

Biotransformation rate constants (k_{biol}) for the nonionic ICM, summarized in Table 3.1, were calculated for the linear portion of the concentration vs. time graphs. The linear section of biotransformation represented a significant portion of the total transformation observed (i.e. greater than 70 % biotransformation of parent ICM) with regression coefficient values of > 0.9. The k_{biol} values ranged from 0.27 to 2.48 μMd^{-1} depending on the nonionic ICM and batch system. Iomeprol and iohexol showed similar biotransformation patterns, while iopamidol was

transformed at a significantly slower rate. For the irrigated Braunschweig soil and the river sediment systems, > 90% of the initial concentration of iohexol and iomeprol was biotransformed within 49 d, while for iopamidol more than 90 d of incubation was needed for > 95% transformation. An exception was the complete elimination of iopamidol after 28 d in the batch systems incubated at 30°C.

DT_{50} values, $DT_{50linear}$ and $DT_{50total}$, are listed in Table 3.1. $DT_{50total}$ values ranged from 12.1 to 42.0 d for iohexol and iomeprol, and 20.0 to 64.0 d for iopamidol. The higher DT_{50} values clearly illustrate the slower rate of iopamidol biotransformation in the Braunschweig soil-water system incubated at room temperature and the sediment-water systems. The lower $DT_{50total}$ values calculated for iomeprol in the LUFA 2.2 soil-water system can be explained by the absence of a lag phase.

Table 3.1: Summary of kinetic analyses for iohexol, iomeprol and iopamidol in the different aerobic batch systems, including lag phases, estimated biotransformation rate constants, k_{biol}, regression coefficients, and disappearance times (DT$_{50linear}$ and DT$_{50total}$)

Batch System	ICM	Lag phase[a]	Linear range[a]	k_{biol}[b] (μMd^{-1})	r^2	DT$_{50linear}$ (d)[c]	DT$_{50total}$ (d)[d]
Braunschweig Soil (20-22°C)	Iohexol		0 d – 51 d	0.46	0.9489	27.6	27.6
	Iomeprol		0 d – 42 d	0.61	0.9515	20.6	20.6
	Iopamidol		0 d – 72 d	0.29	0.9671	41.6	41.6
Braunschweig Soil (30°C)	Iomeprol	0 d – 15 d	15 d – 28 d	1.99	0.9539	6.3	21.3
	Iopamidol	0 d – 15 d	15 d – 28 d	2.48	0.9128	5.0	20.0
LUFA 2.2 Soil	Iomeprol		0 d – 17 d	0.99	0.9252	12.1	12.1
	Iopamidol	0 d – 24 d					
River Sediment	Iohexol	0 d – 21 d	21 d – 39 d	1.15	0.9401	9.3	30.3
	Iomeprol	0 d – 27 d	27 d – 52 d	0.78	0.9849	15.4	42.4
	Iopamidol	0 d – 20 d	20 d – 104 d	0.27	0.9625	44.0	64.0

[a]based on the concentration vs. time graphs; [b]biotransformation rate constants determined for the linear range of the concentration vs. time graphs;

[c]DT$_{50linear}$ value for the linear range; [d]DT$_{50total}$ value is estimated by including the lag phase plus the DT$_{50linear}$ value

Joss *et al.* (2006b) determined higher biotransformation rate constants for ICM in activated sludge systems with k_{biol}=1 to 2 L·gss^{-1}d^{-1} for iohexol and iomeprol, and less than 0.1 L·gss^{-1}d^{-1} for iopamidol (gss·L^{-1} representing the suspended solid concentration). In all matrices (e.g. soil, sediment, and activated sludge) lower k_{biol} values were reported for iopamidol. One explanation might be the branched hydroxylated hydrocarbons attached to the amide moiety which is different for the other nonionic ICM.

3.3.2 Influence of temperature on biotransformation

Two separate batch systems consisting of the Braunschweig soil, one incubated at 20-22°C and the other one incubated at 30°C, were prepared to investigate the influence of temperature on the biotransformation of the selected ICM. The calculated biotransformation rate constants, $k_{biol,}$ for iomeprol and iopamidol were higher in the Braunschweig soil-water systems incubated at 30°C than those at room temperature (20-22°C), increasing from 0.61 to 1.99 µMd^{-1} and 0.29 to 2.48 µMd^{-1}, respectively (Table 3.1).

Previous research has shown that temperature is a parameter which influences the biotransformation rate of organic compounds in contact with activated sludge (Clara *et al.* 2005; Joss *et al.* 2006a). It has been suggested that temperature dependence can be described by the Arrhenius equation (Joss *et al.* 2006a).

$$k_{biol,\ \mathrm{T}ref} = k_{biol,\ \mathrm{T}} \cdot e^{\ \kappa \cdot (\mathrm{T}ref\text{-}\mathrm{T})} \quad \text{Eq (1)}$$

Where, $k_{biol,\ \mathrm{T}ref}$ is the biotransformation rate constant at a reference temperature, $k_{biol,\ \mathrm{T}}$ is the biotransformation rate constant at an observed temperature, κ is the temperature coefficient, T_{ref} is the reference temperature, and T is the experimental temperature. Joss *et al.* (2006b) concluded that a κ value is expected to be between 0.03 to 0.09 for sludge systems.

For iomeprol and iopamidol in contact with the Braunschweig soil, κ values using Eq (1) were calculated to be as high as 0.15 and 0.27 respectively. One explanation might be that the biotransformation rate depends on the growth rate of the bacteria in the batch systems, and therefore temperature dependence does not follow a simple model like the Arrhenius relationship (Heitzer *et al.* 1991).

3.3.3 Formation of Transformation Products (TPs)

Since seven of the TPs detected during biotransformation had not been previously identified, mass fragmentation experiments were completed to elucidate the chemical structures. Figure 3.1 provides the MS spectrum used to propose a fragmentation pathway for iomeprol TP791. The MS spectra and proposed fragmentation pathways for the remaining six ICM TPs are illustrated in Figure S3.6.1 to S3.6.6 of section 3.6.
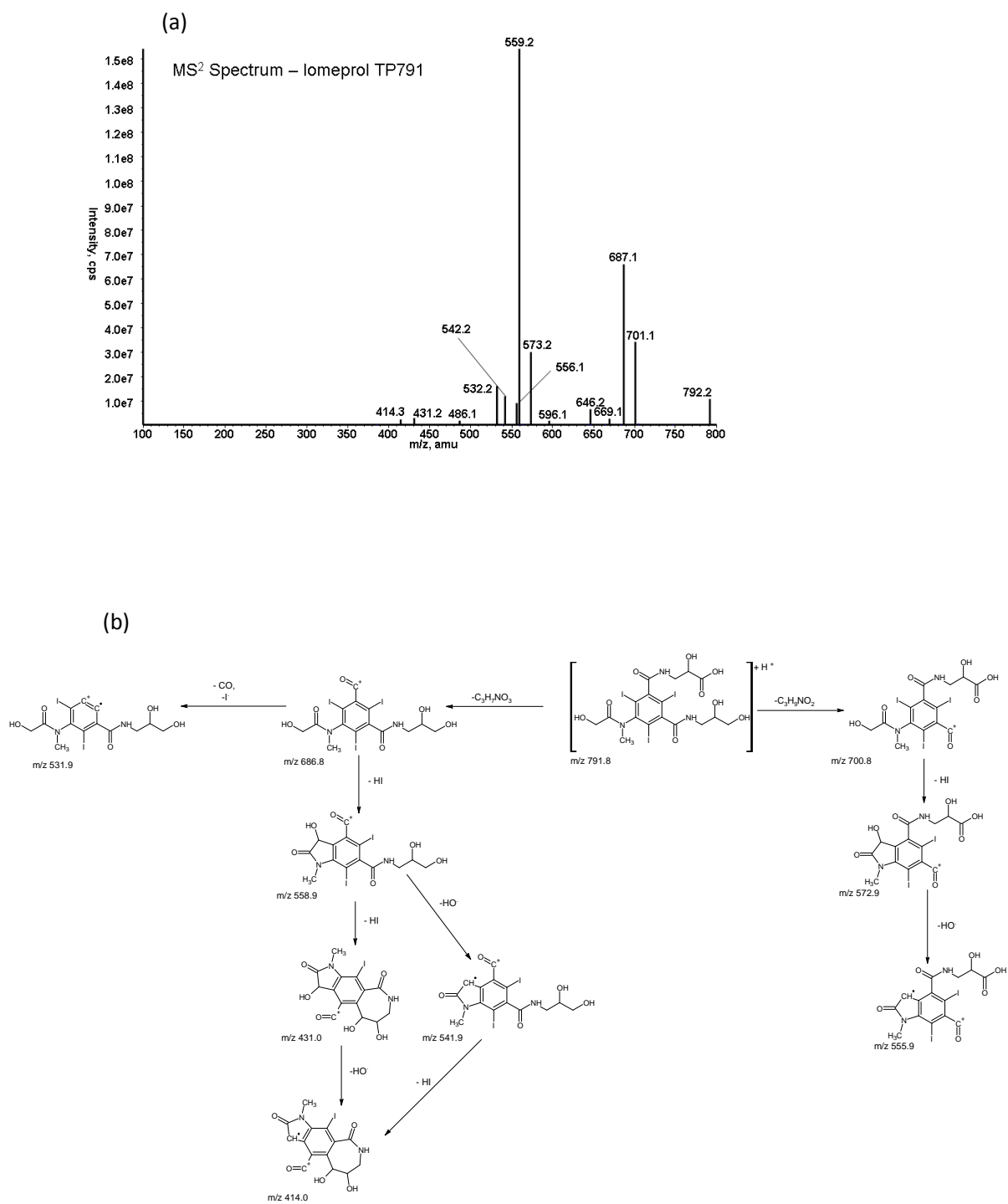
Figure 3.1: MS^2 spectrum for iomeprol TP791: (a) MS^2 *m/z* 792; (b) proposed fragmentation pathway of iomeprol TP791

148

Iohexol: In the sediment-water systems and the Braunschweig soil-water systems, the TPs were formed during two distinct phases, as can be clearly seen in Figure 3.2 (a) and (b). During the first phase, five TPs (TP863, TP849, TP835, TP833 and TP775) emerged and reached their maximal concentrations after 40 d, and in the second phase six more TPs (TP745, TP687A, TP687B, TP657, TP629 and TP599) were formed. After 143 d, five TPs formed during the second phase were still present.
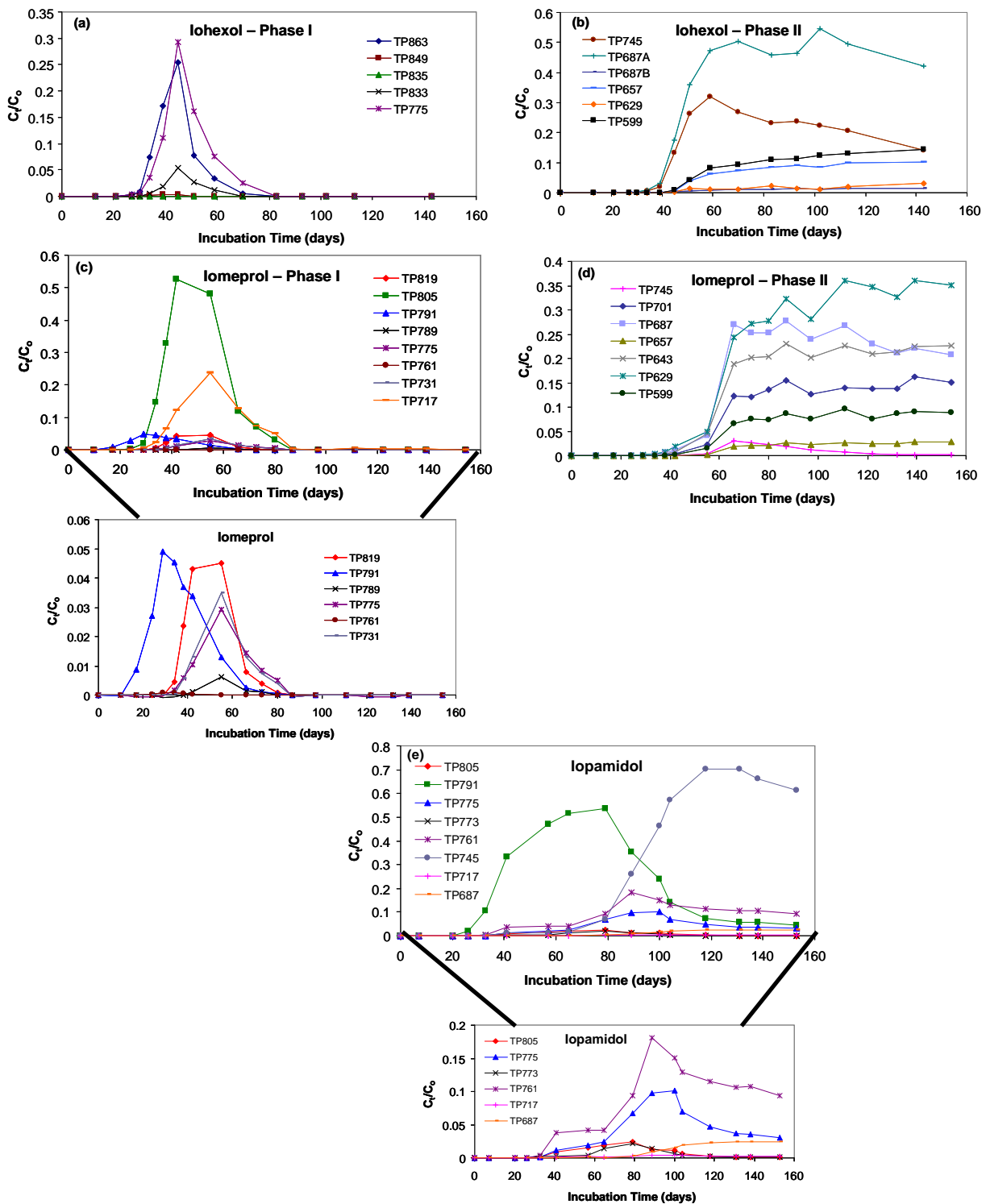
Figure 3.2: The sequence of TP formation of iohexol (a) and (b); iomeprol (c) and (d); and iopamidol (e) and (f); in the river sediment-water batch systems

Iomeprol: In the batch systems, TPs were formed during two distinct phases. Initially TP791 was formed, followed by TP805 and TP819, and five additional TPs (TP717, TP731, TP789, TP761 and TP775) (Figure 3.2 (c)). After 60 d, six more TPs (TP701, TP687, TP657, TP643, TP629 and TP599) were formed in the second phase of iomeprol biotransformation. The TPs detected in the second phase appeared simultaneously and remained at relatively constant concentrations until the end of the experimental period (Figure 3.2 (d)).

Iopamidol: In contrast to iohexol and iomeprol, there were no distinct phases during TP formation. Iopamidol TP791 was the initial TP formed and was dominant during the first half of the experimental period (Figure 3.2 (e)). Four other TPs (TP805, TP775, TP773 and TP761) appeared shortly after the appearance of TP791. At approximately 80 d the last iopamidol TP (TP687) appeared in the batch systems, and remained until the end of the experiment (Figure 3.2 (e)). TP745 was the dominant TP present during the second half of the incubation period.

3.3.4 Mass Balance

Eleven TPs of iohexol, fifteen TPs of iomeprol and eight TPs of iopamidol were detected in the samples collected from the aqueous phase of batch systems. Kormos *et al.* (2009) elucidated the structures of 27 TPs found in soil-water batch systems by means of NMR analyses or MS fragmentation experiments. The structures of the additional seven ICM TPs have been identified in this study and are reported in Figure 3.1 and the section 3.6.

With a few exceptions, the mass balance (sum of parent ICM and identified TPs over time) ranged between 80 to 120% suggesting that the major TPs of the parent ICM were identified in the respective batch systems (Figure 3.3 (a)-(f)). In two cases, a significant reduction from 100% (e.g. 40 to 60% after 120 d; Figure 3.3 (c) and (e)) was observed for iomeprol and iopamidol in

151

the Braunschweig soil-water batch systems after 100 d of incubation. It can be assumed that in those cases further TPs were formed, which were not detected. In either case, it appears that the most relevant TPs were identified.
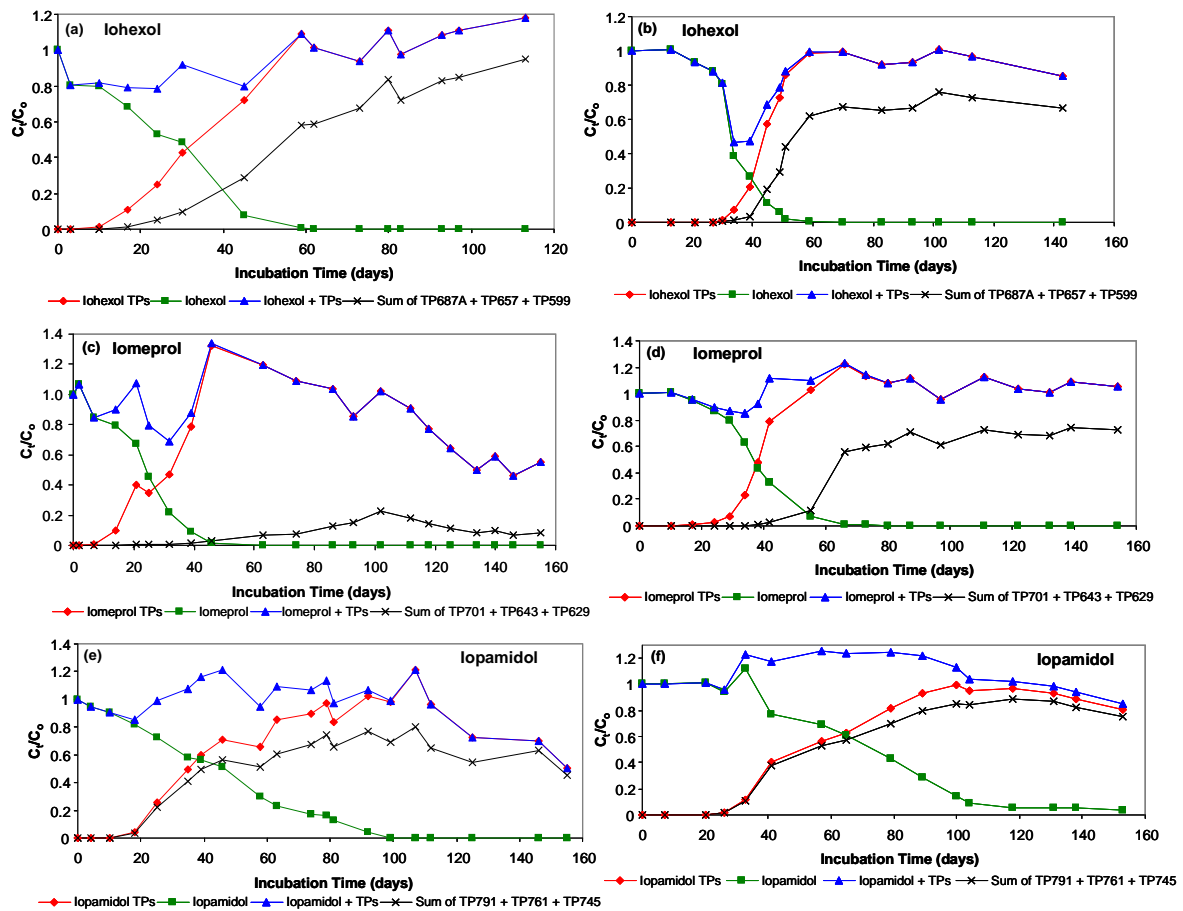
Figure 3.3: Mass balance (parent ICM and TPs) of the iohexol (a), iomeprol (c) and iopamidol (e) in the Braunschweig soil-water systems as well as iohexol (b), iomeprol (d) and iopamidol (f) in the river sediment-water systems

3.3.5 Microbial Transformation Pathways and Biochemical Reactions

The proposed microbial transformation pathways for the three nonionic ICM are shown in Figure 3.4 to 3.6. The pathways are based on the structures of the TPs, fundamental metabolic logic, and the time sequence of their appearance. All identified TPs seem to be the result of modifications to the side chains of the parent compound, in particular changes to the hydroxylated carbon side chains attached to the nitrogen atoms.

I – Oxidation of primary alcohol groups

II – Cleavage of N-C bond

IIa – Cleavage of 2-hydroxyl propanoic acid

IIb – Cleavage of an acetyl group

III – Decarboxylation

IV – Oxidation of methylene group
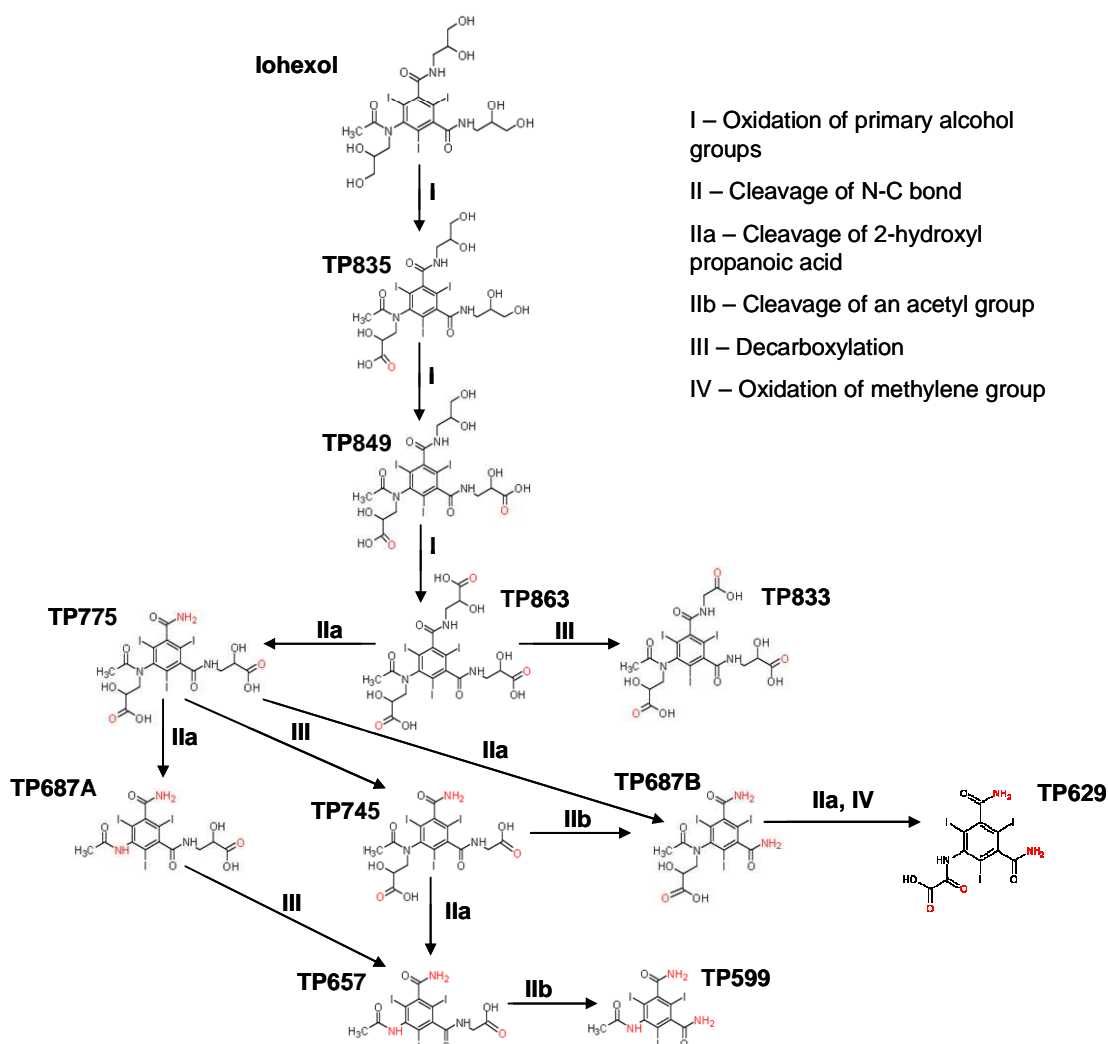
Figure 3.4: Proposed Microbial Transformation Pathway of Iohexol
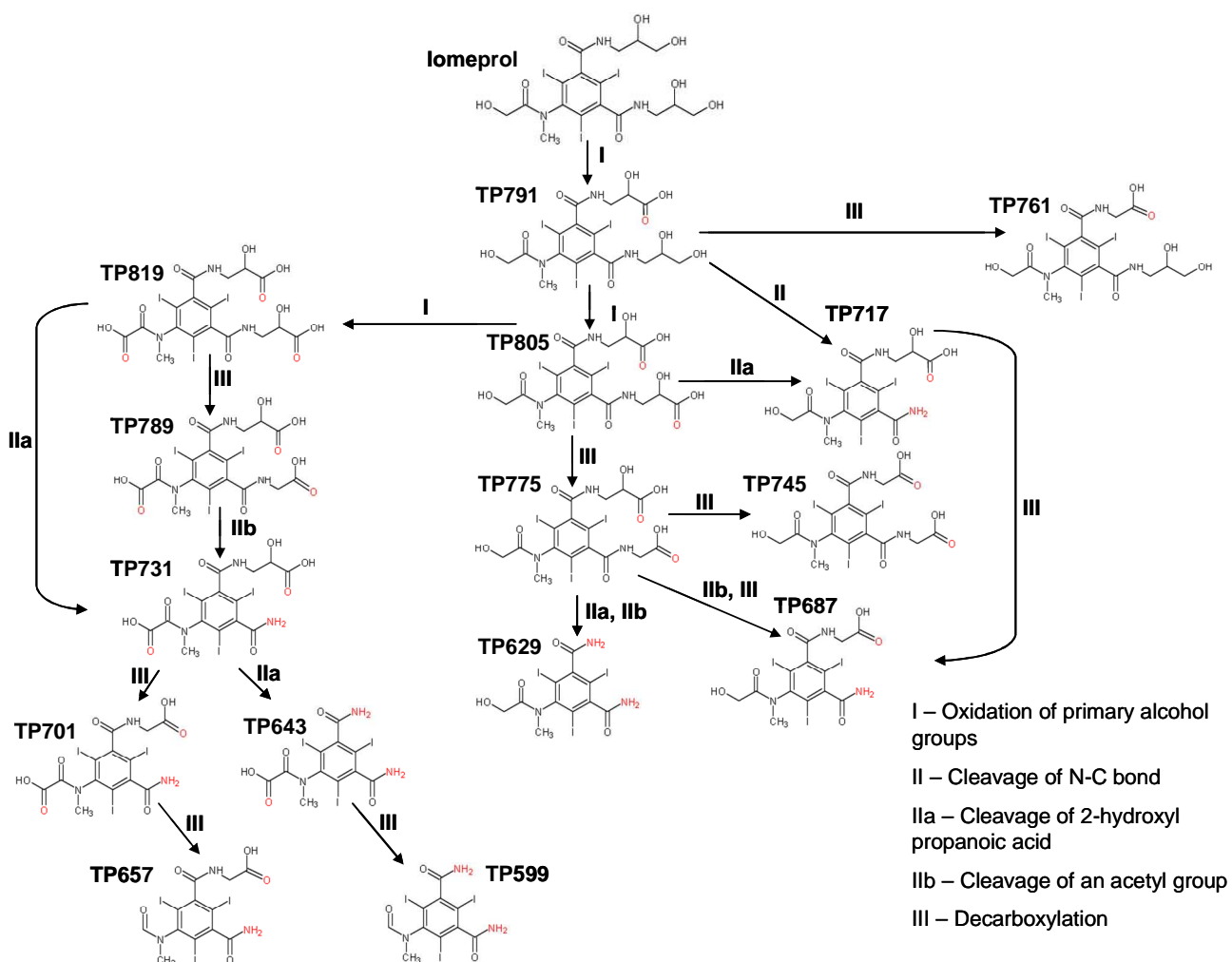
Figure 3.5: Proposed Microbial Transformation Pathway of Iomeprol
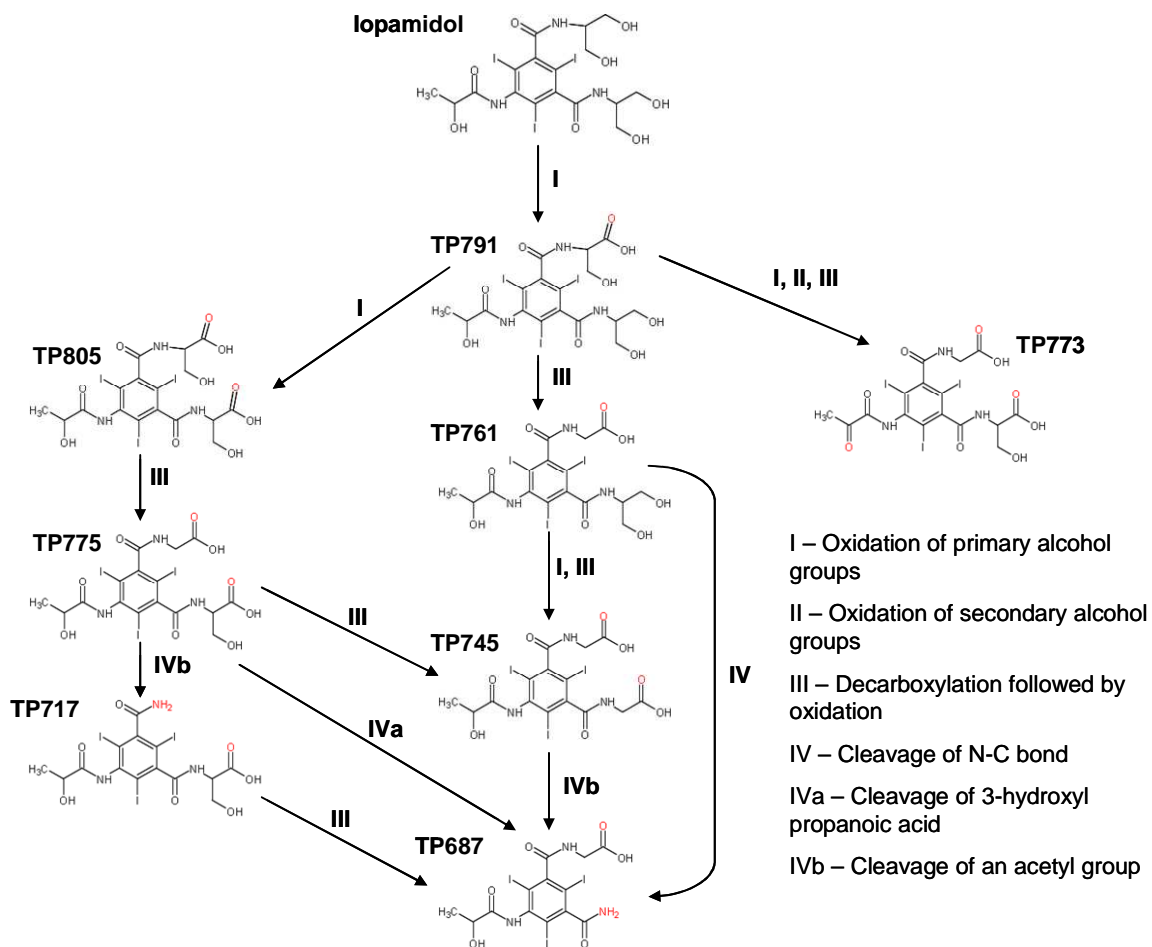
Figure 3.6: Proposed Microbial Transformation Pathway of Iopamidol

Control experiments, in which formaldehyde was added, clearly indicate that the observed transformations were the result of microbial activity. The presence of the same TPs in all batch systems suggests that common microbial reactions occur independent of the matrix composition. However, differences were observed with respect to biotransformation rates. This is not an unexpected result, as the microbial composition in the different batch systems may vary substantially.

The formation of most ICM TPs in the batch systems can be explained by succession of one, two or three of the following biochemical reaction types: i) oxidation of the primary or secondary alcohol groups, ii) decarboxylation, and iii) cleavage of N-C bond.

The formation of the first TPs to appear in the batch systems can be explained in most cases by oxidation of the primary alcohol groups. Oxidation of the hydroxylated hydrocarbon side chains has been observed before for iopromide during biological transformation in soil-water systems as well as in activated sludge systems (Batt *et al.* 2006; Schulz *et al.* 2008). Oxidation of primary alcohol groups to carboxylates has biochemical precedence in alcohol and aldehyde dehydrogenases. There are many different types of such enzymes, including NAD(P)-dependent alcohol dehydrogenases, alcohol oxidases, peroxidases, and monooxygenases (Kroutil *et al.* 2004). Usually carboxylates were the first TPs observed in the batch systems. The absence of detectable amounts of the respective aldehydes suggests that they were quickly oxidized to the corresponding carboxylates in all batch systems.

Decarboxylations are another type of reaction observed. It can be suggested that in the case of iohexol and iomeprol, decarboxylations succeeded the oxidation of the primary alcohol groups. Many different enzymes, such as thiamine pyrophosphate (TPP) dependent enzymes, a group of enzymes consisting of transketolases, α-keto acid decarboxylases, and pyruvate-like decarboxylases *(Sprenger et al. 1999)* are capable of catalyzing such reactions. In case of iopamidol, metabolism might proceed slightly different (Figure 3.6) as the exact sequence of the reactions is not yet clear.

Cleavage of the N-C bond is another common reaction type that was observed in the batch system experiments. In general, this reaction took place at the end of the incubation period and

included the removal of acetyl groups (deacetylation) as well as the removal of hydroxylated propanoic acids. Various enzymes are capable of cleaving N-C bonds, including monooyxgenases (i.e. cytochrome P-450 monooxygenases), α-keto acid-dependent enzymes (Hegg *et al.* 1999) alcohol and aldehyde dehydrogenases, and decarboxylases. Oxidation of the carbon atom attached to the nitrogen is necessary to promote cleavage at the N-C bond. It is unclear, however, whether decarboxylation and oxidation of the hydroxyl groups were required prior to cleavage of the N-C bond or if direct cleavage of the N-C bond could occur.

Although TPs contain amide functionalities, amide hydrolysis was never observed during incubation. The absence of amide hydrolysis during nonionic ICM biotransformation is unexpected. Amide hydrolysis is a very common reaction, especially during the breakdown of proteins to peptides or amino acids, and was the reaction proposed to occur during the transformation of atenolol to atenololic acid (Radjenović *et al.* 2008). One explanation for the absence of amide hydrolysis might be that the presence of the large iodine atoms render the amide bonds inaccessible to enzymatic attack (Kalsch 1999). It has been suggested that the steric hindrance of the iodine atoms may be responsible for the inability of certain enzymes, such as oxygenases, to attack the aromatic rings of the ICM. It appears that the iodine atoms need to be removed before such oxygenases are able to attack the aromatic structure (Kalsch 1999). A similar argument can be used to explain the slow biotransformation of iopamidol. The increase in steric hindrance due to the branched hydroxylated hydrocarbon side chains might be responsible for the low biotransformation rates estimated for iopamidol.

3.4 Environmental Occurrence

The ICM TPs identified in batch systems were found in WWTP effluent, surface water, groundwater (data not shown) and DWTP samples, with a total 19 ICM TPs detected in the environmental samples (Table 3.2). In the effluent of a municipal WWTP, 10 ICM TPs were detected with concentrations as high as 660 ng/L (iomeprol TP791). In the Rhine River, close to Mainz, 15 ICM TPs were detected above the limit of quantification, exhibiting a maximum concentration of 110 ng/L for iomeprol TP629. Since the Rhine River has an average percentage of treated wastewater significantly less than 10 %, the elevated concentrations indicate the high stability of some of these ICM TPs in the aquatic environment. Even in drinking water 15 TPs were identified, with only seven TPs having a concentration above 10 ng/L, but a maximum concentration of 120 ng/L (iomeprol TP629). In general, higher concentrations were detected for those TPs which are formed at the end of the proposed transformation pathways.

Obviously, the ICM TPs are already formed to some extent in municipal WWTPs and are further formed in contact with soil and sediment. Even advanced treatment processes such as ozonation and activated carbon filtration are not capable of completely removing these TPs. Similar results have been found with iopromide (Schulz *et al.* 2008). The incomplete mineralization of ICM and the presence of their TPs in the environment clearly emphasize the need for a comprehensive evaluation of the environmental fate of ICM as well as other emerging organic pollutants. Research needs to focus on techniques and assays to assess the biotransformation of emerging organic pollutants to provide more information on the impact these compounds and their TPs have on ecological and human health.

Currently, there is no toxicological data available for the newly identified ICM TPs. When comparing the chemical structures of the parent ICM to the TPs, it can be assumed that the TPs will probably pose a similar negligible impact to ecosystems and humans as the parent ICM. A potential concern of ICM and their TPs present in drinking water treatment systems is whether low molecular toxic iodine-containing disinfection by-products are formed (Richardson *et al.* 2008) when strong oxidants (i.e. chlorine and chloramines) are used for disinfection.

Table 3.2: Concentrations (ng/L) and the 95 % confidence intervals (n=3) of the nonionic ICM and ICM TPs in wastewater, surface water, and drinking water (LOQ values are given in brackets)

Sample Type	Iomeprol	TP805	TP791	TP775	TP761	TP745	TP717	TP687	TP643	TP629
WWTP effluent	6920±1460 (4)	440±28 (4)	660±170 (4)	73±9 (4)	180±10 (4)	99±19 (4)	360±54 (4)	400±150 (4)	<LOQ (10)	340±59 (10)
Rhine water	150±28 (2.5)	16±7 (5)	<LOQ (5)	9±3 (5)	<LOQ (5)	29±15 (5)	29±7 (5)	71±3 (5)	7±3 (5)	110±33 (2.5)
Drinking water	31±6 (1)	<LOQ (1)	4±1 (1)	<LOQ (1)	4.2; 3.2 (1)	10±5 (1)	5±1 (1)	45±5 (1)	23±5 (2.5)	120±30 (2.5)

	Iohexol	TP775	TP745	TP687A	TP599
WWTP effluent	72±32 (4)	170±21 (4)	310±190 (4)	<LOQ (40)	<LOQ (10)
Rhine water	43±5 (1)	22±9 (1)	82±33 (10)	<LOQ (10)	3±0.8 (1)
Drinking water	6±0.6 (1)	3±0.6 (1)	27±13 (1)	13±1 (10)	7±2 (1)

	Iopamidol	TP805	TP791	TP761	TP745	TP717	TP687
WWTP effluent	1870±520 (20)	<LOQ (20)	<LOQ (1)	<LOQ (4)	<LOQ (4)	<LOQ (20)	<LOQ (20)
Rhine water	160±48 (5)	6.7, 6.3 (5)	38±4 (1)	<LOQ (2)	23±9 (2.5)	13±3 (5)	55±3 (5)
Drinking water	20±7 (1)	<LOQ (2)	<LOQ (1)	7.5; 5.8 (5)	25±3 (1)	3±0.6 (1)	18±7 (1)

3.5 Acknowledgment

3.6 Supporting Information

3.6.1 Experimental Section

Diatrizoate, iohexol, iomeprol and iopamidol were kindly provided by Bayer Schering Pharma (Berlin, Germany), and had a purity of > 95%. The chemical structures of the ICM as well as general physicochemical properties are provided in Table 1.1 (Chapter 1). Desmethoxyiopromide (DMI, CAS no. 76350-28-2) and N-(2,3-dihydroxypropyl)-2,4,6-triiodo-5-methoxyacetylamino-N'-methylisophthalamide (DDPHI) (purity > 95%) were selected as surrogate standards for quantification of the parent ICM and TPs in the samples collected from the batch systems, as well as the environmental samples. The surrogate standards were provided by Bayer Schering Pharma.

The organic solvents (n-heptane, acetone, methanol and acetonitrile) were picograde and purchased from Merck (Darmstadt, Germany). Formic acid (ACS grade, 98-100%) was purchased from Merck (Darmstadt, Germany).

Aerobic batch systems were prepared for each of the selected ICM. Two different soils were used as well as natural river sediment for the biotransformation experiments. Table S3.6.1 provides detailed characteristics of the different soils and sediment used.

The groundwater used for the preparation of the batch systems was collected from a well in Koblenz-Arenberg, Germany. This groundwater is considered pristine, and free of the target analytes based on measurements of blank groundwater samples. The groundwater has a pH of 6.70, conductivity of 522 µS/cm, TOC level of 0.59 mg/L, redox potential of 156 mV, and dissolved oxygen content of 1.4 mg/L.

3.6.2 Identification of Seven New ICM TPs

In addition to the 27 ICM TPs previously identified by Kormos et al. (2009), seven new TPs were found in the aerobic batch systems which had not previously been structurally identified. One additional iopamidol TP (TP717) and six additional iomeprol TPs (TP791, TP775, TP761, TP745, TP657 and TP599) were detected in the batch systems. In general, these additional TPs were not dominant in the Braunschweig soil-water systems, and therefore structural identification of these new TPs was based on MS^2 spectra, as well as the fragmentation patterns previously reported for the other ICM TPs. Figure S3.6.1-S3.6.6 display the MS spectra and proposed fragmentation pathways for six ICM TPs. The MS spectra and fragmentation pathway for the seventh new TP (iomeprol TP791) is shown in Figure 3.6.1 of the manuscript.
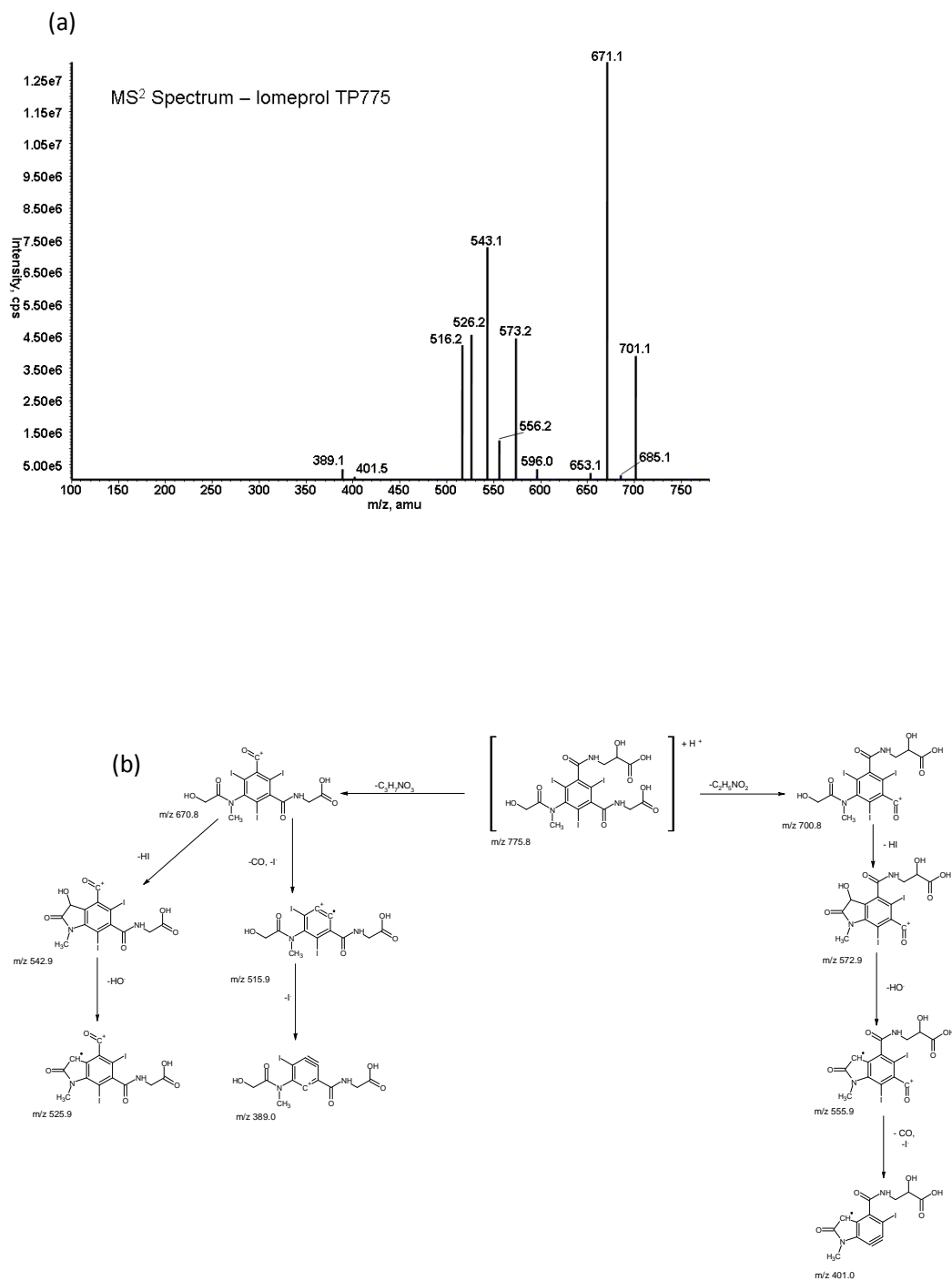
Figure S3.6.1: MS^2 spectrum for iomeprol TP775: (a) MS^2 *m/z* 776; (b) proposed fragmentation pathway of iomeprol TP775

(a)

MS^2 Spectrum – Iomeprol TP761
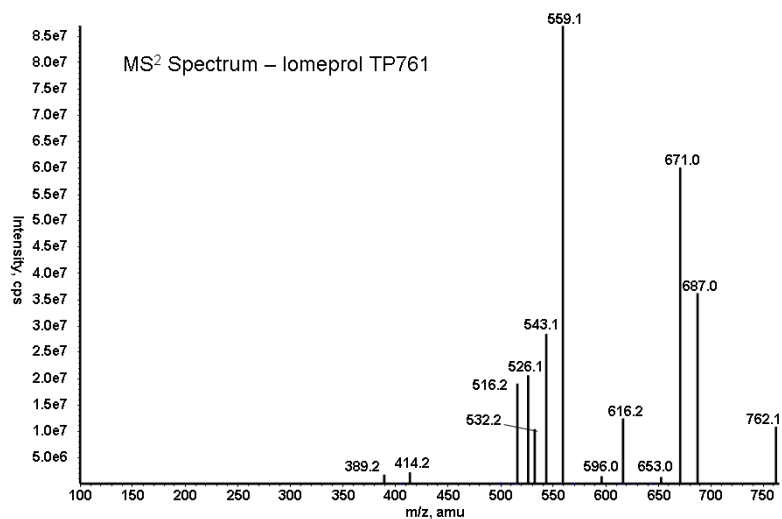
(b)
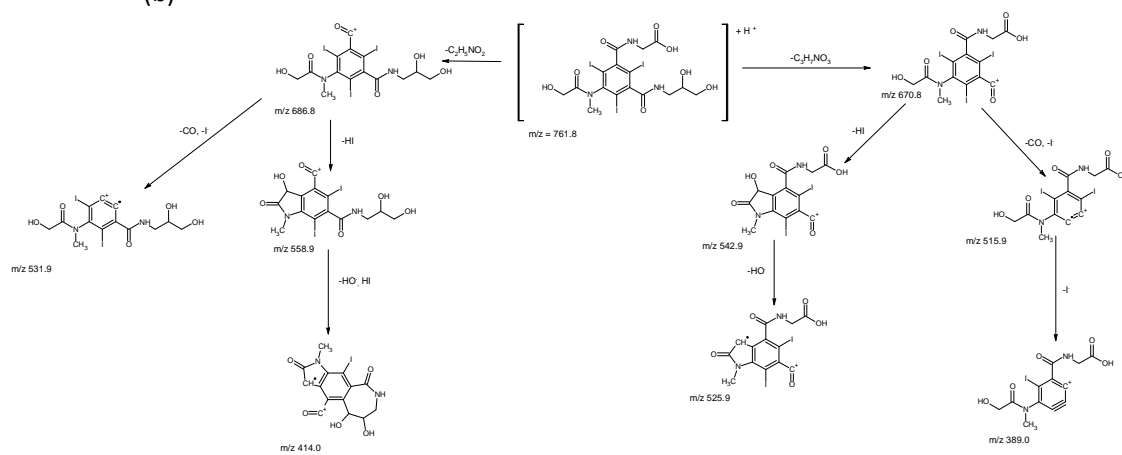
Figure S3.6.2: MS^2 spectrum for iomeprol TP761: (a) MS^2 m/z 762; (b) proposed fragmentation pathway of iomeprol TP761

(a)

(b)
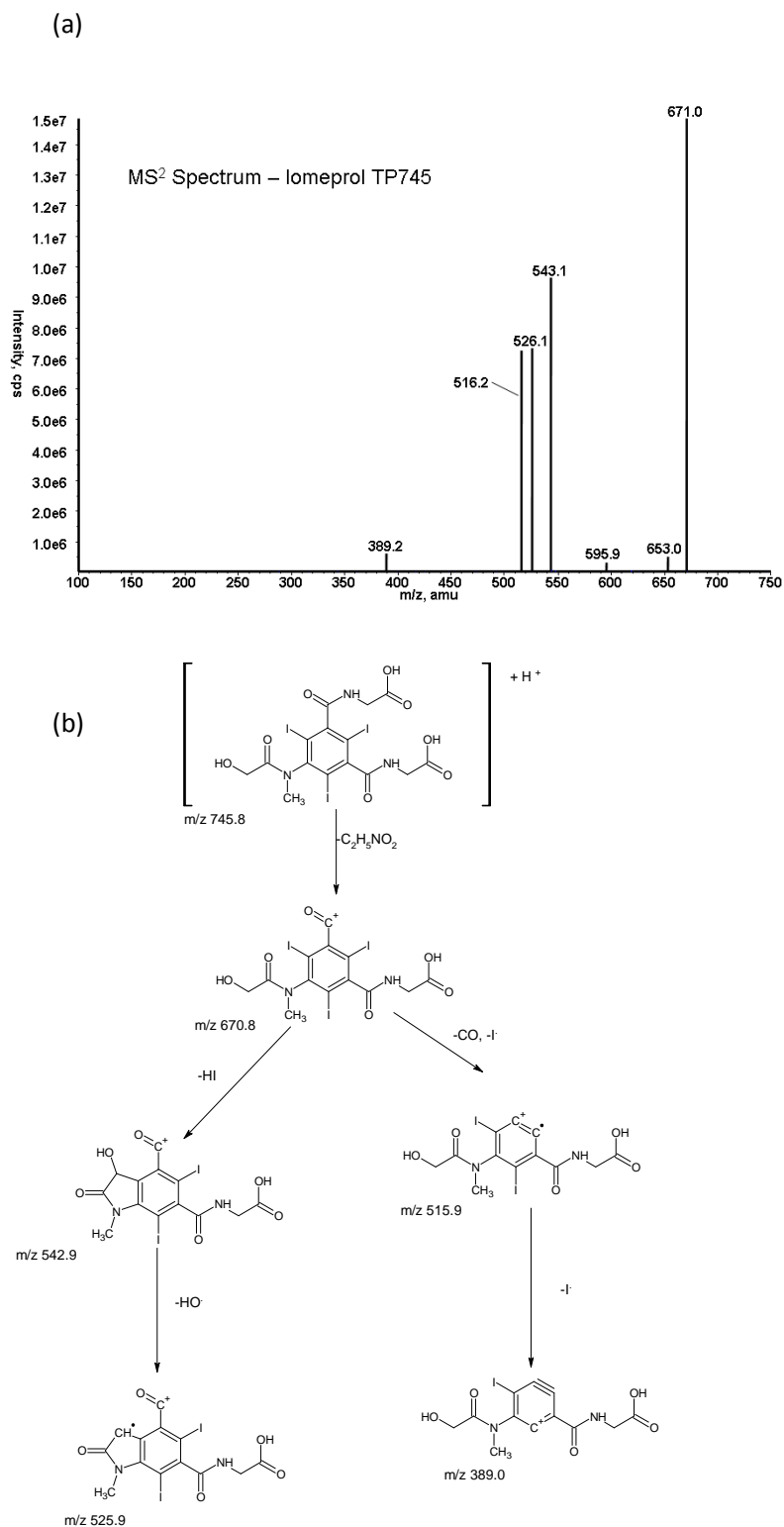
Figure S3.6.3: MS^2 spectrum for iomeprol TP745: (a) MS^2 m/z 746; (b) proposed fragmentation pathway of iomeprol TP745

165

(a)

(b)
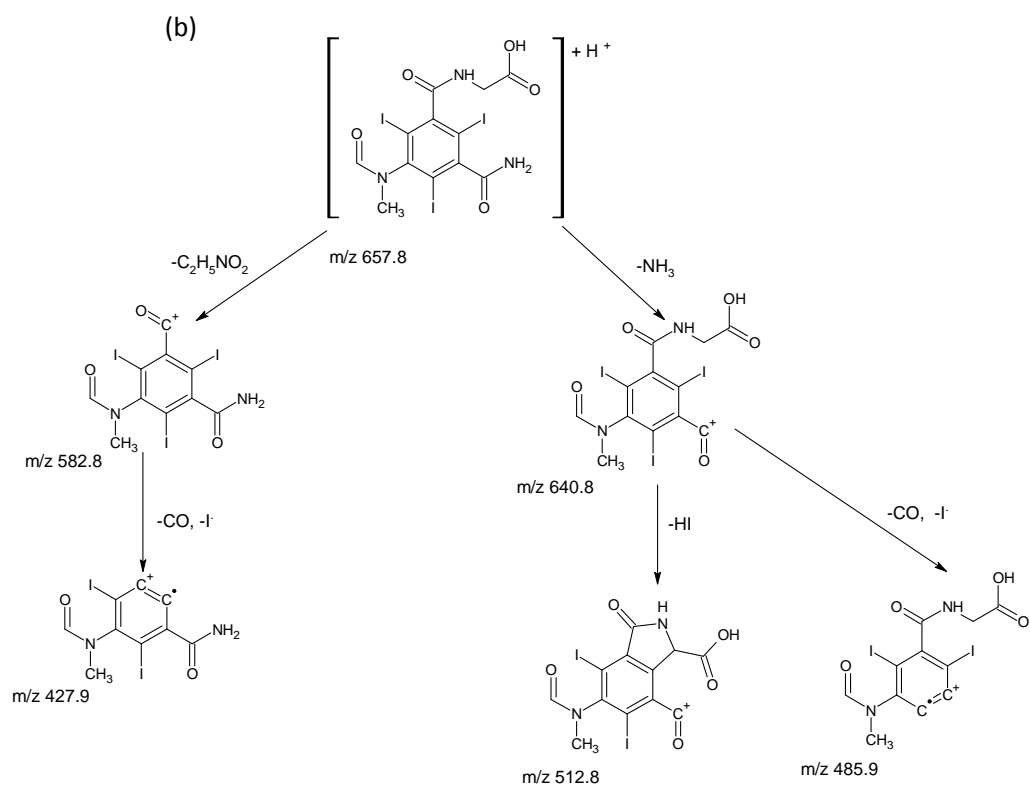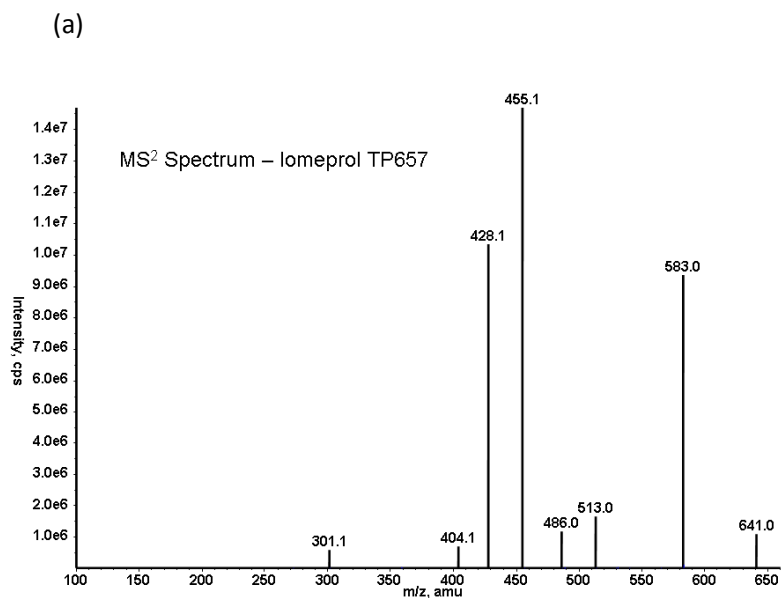
Figure S3.6.4: MS^2 spectrum for iomeprol TP657: (a) MS^2 m/z 658; (b) proposed fragmentation pathway of iomeprol TP657

(a)

(b)
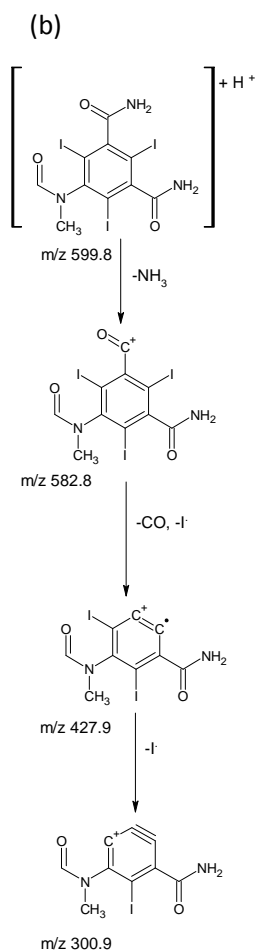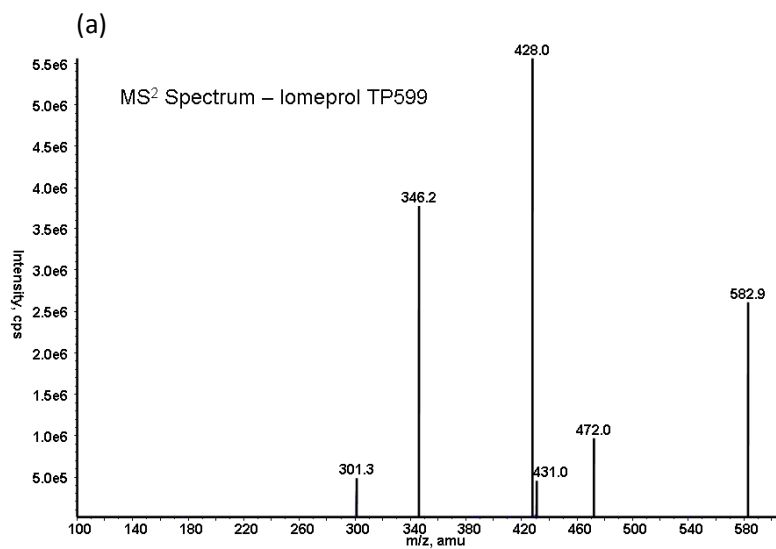
Figure S3.6.5: MS^2 spectrum for iomeprol TP599: (a) MS^2 *m/z* 600; (b) proposed fragmentation pathway of iomeprol TP599

(a)

MS^2 Spectrum – Iopamidol TP717

(b)
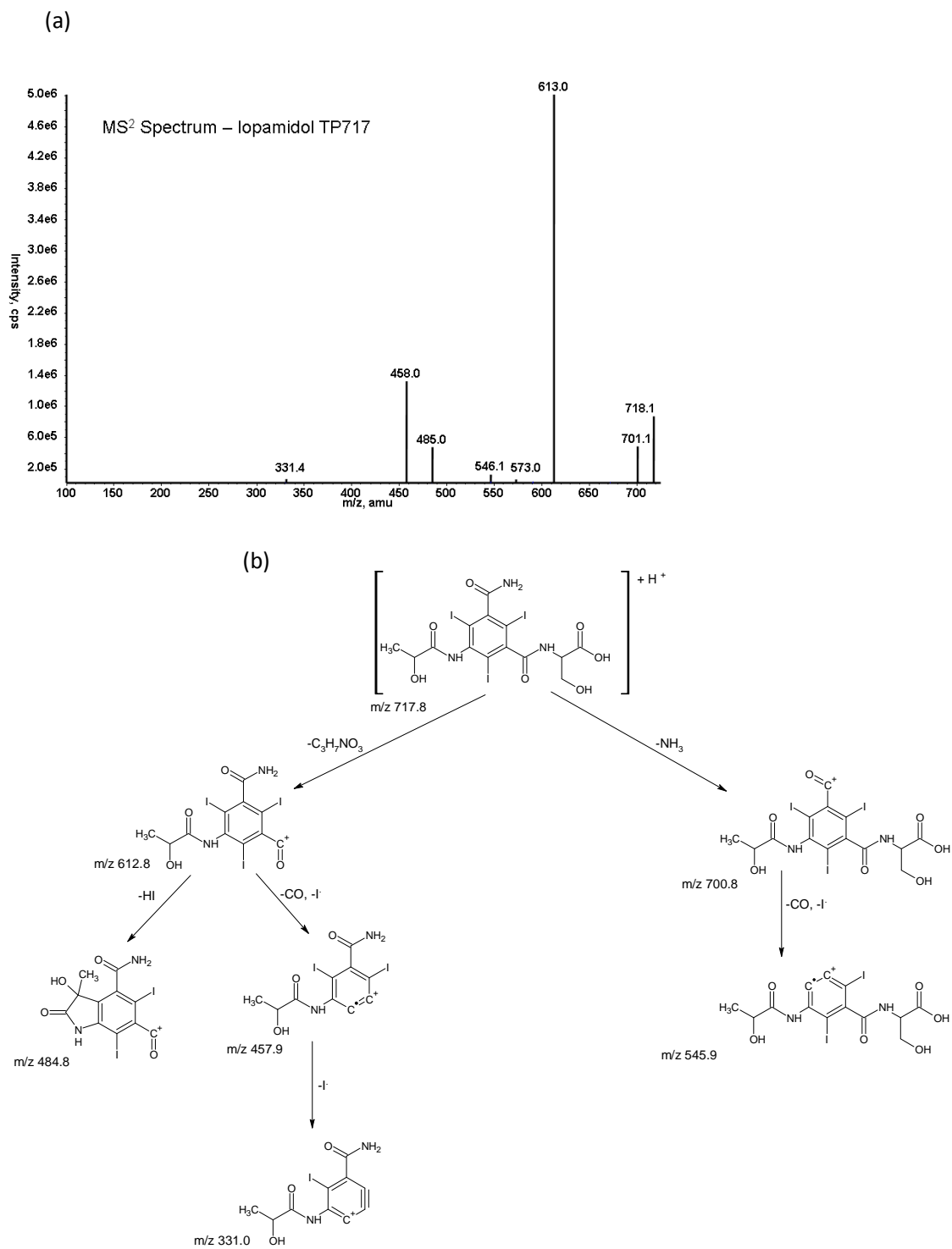
Figure S3.6.6: MS^2 spectrum for iopamidol TP717: (a) MS^2 *m/z* 718; (b) proposed fragmentation pathway of iopamidol TP717
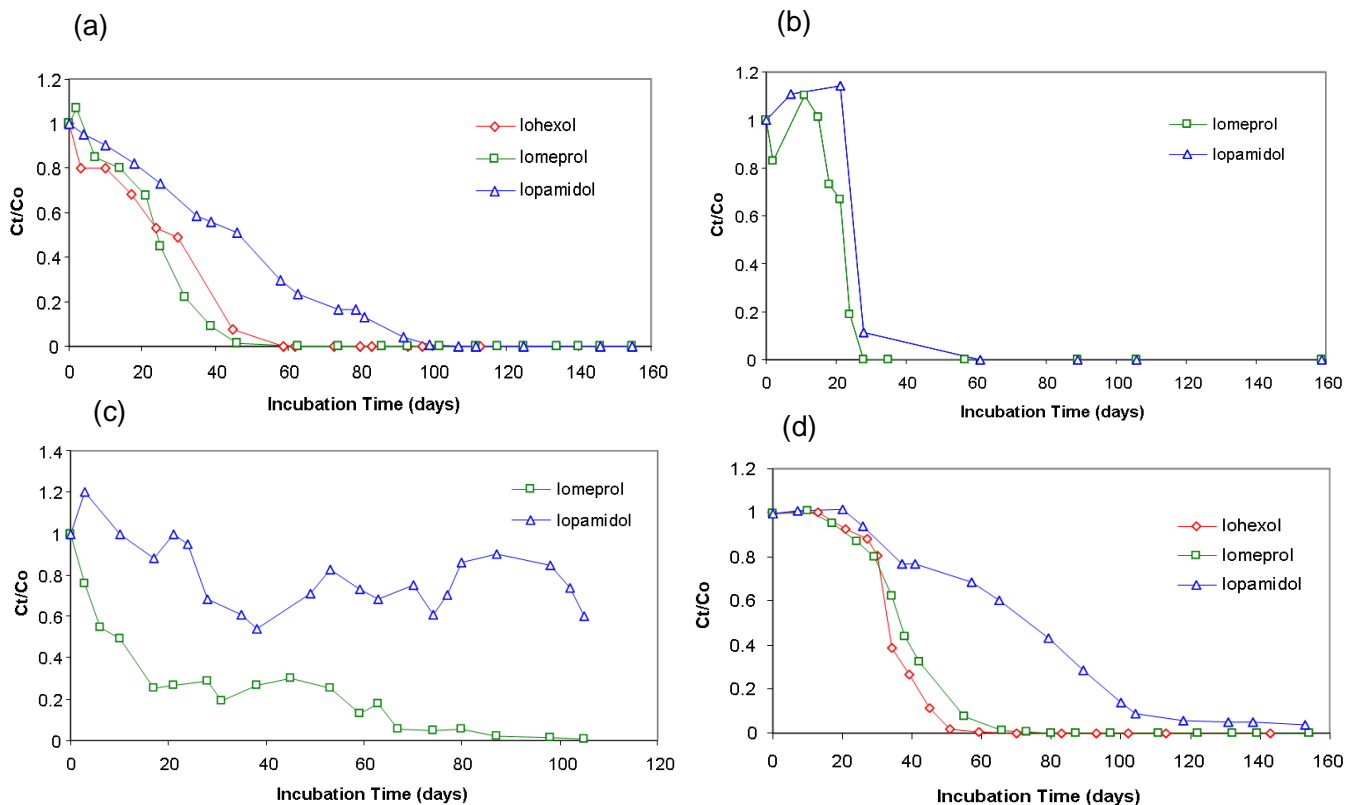
Figure S3.6.7: The normalized concentrations vs. time graphs for selected ICM in the Braunschweig soil-water batch system incubated at 20-22°C (a); Braunschweig soil-water system incubated at 30°C (b); LUFA 2.2 soil-water system (c); River sediment-water system (d). C_o is the initial concentration of the parent ICM when time = 0. C_t is the concentration of the parent ICM at time = t.

169

Table S3.6.1: Characteristics of the river sediment and soils used for the biotransformation experiments

Characteristic/Parameter	Braunschweig Soil[a, b]	LUFA 2.2 Soil[c]	River Sediment[d]
C_{org} (%)	0.61	2.3	4.36
Organic matter content (%)	0.9	4.0	4.9
Texture	cambisol, sand	loamy sand	fine grain (< 2mm)
Clay (%)	2.9	8.2	18
Silt (%)	6.1	17.0	29
Sand (%)	91.3	74.8	53
Sampling depth	0-5 cm	0-10 cm	0-10 cm

[a]Ternes et al. (2007); [b]Schulz et al. (2008); [c]Yu, L.; Fink, G.; Wintgens, T.; Melin, T.; Ternes, T. A. Sorption behavior of potential organic wastewater indicators with soil. *Water Res.* **2009**, *43*, 951-960.; [d]Stein et al. (2008).

Table S3.6.2: Source-Dependent Parameters for LC-ESI Tandem MS

Source-Dependent Parameter	Parameter Value
CAD	10
Curtain gas	138 kPa
Gas 1	276 kPa
Gas 2	276 kPa
Temperature	600°C
IonSpray Voltage	4500 V
Entrance Potential	10 V

Table S3.6.3: MRM Transitions and Optimized MS Parameters for Diatrizoate, Iohexol and Iohexol TPs

Compound	Precursor Ion (*m/z*)	Product Ion (*m/z*)	Declustering Potential (V)	Collision Energy (eV)	Cell Exit Potential (V)
Diatrizoate	614.8	233.1	51	63	8
		147.9	91	79	4
Iohexol	821.9	602.9	111	35	18
		500.7	111	67	30
Iohexol TP863	863.8	515.1	71	57	40
		476.9	71	31	18
Iohexol TP849	849.8	616.9	56	67	24
		514.8	56	49	26
Iohexol TP835	835.9	667.1	66	73	28
		514.8	66	41	42
Iohexol TP833	833.9	758.9	71	29	20
		728.7	71	29	18
Iohexol TP775	775.8	531.9	71	67	20
		426.7	71	35	16
Iohexol TP745	745.7	501.9	61	43	46
		703.9	61	25	20
Iohexol TP687A	687.8	645.6	66	23	20
		444.0	66	49	8
Iohexol TP687B	687.8	440.7	71	39	34
		568.7	86	19	34
Iohexol TP657	657.8	454.8	121	33	24
	657.9	582.6	71	19	32
Iohexol TP629	629.8	458.9	86	21	12
		568.7	71	15	18
Iohexol TP599	599.8	582.7	101	17	36
		454.9	76	33	12

Table S3.6.4: MRM Transitions and Optimized MS Parameters for Iomeprol and TPs

Compound	Precursor Ion (*m/z*)	Product Ion (*m/z*)	Declustering Potential (V)	Collision Energy (eV)	Cell Exit Potential (V)
Iomeprol	777.9	405.0	106	39	14
		531.9	71	37	12
Iomeprol TP819	819.9	775.9	101	19	18
		670.7	101	23	22
Iomeprol TP805	805.8	700.9	116	31	22
		418.9	116	61	6
Iomeprol TP791	791.9	558.9	81	29	20
		572.6	81	35	14
Iomeprol TP789	789.8	670.7	66	21	22
		640.6	66	23	22
Iomeprol TP775	775.9	670.7	86	21	24
		700.7	81	23	24
Iomeprol TP761	761.9	558.9	91	31	30
		670.8	91	27	10
Iomeprol TP745	745.9	670.7	61	21	22
		515.8	61	37	14
Iomeprol TP731	731.9	427.9	66	39	36
		582.7	66	23	16
Iomeprol TP717	717.8	330.9	81	69	20
		457.7	81	39	24
Iomeprol TP701	701.8	428.0	61	35	24
		657.7	61	15	12
Iomeprol TP687	687.8	612.8	81	27	18
		457.9	76	41	22
Iomeprol TP657	657.8	427.9	121	39	28
		582.6	71	19	32
Iomeprol TP643	643.7	599.7	61	15	20
		300.9	61	51	22
Iomeprol TP629	629.9	330.8	41	53	8
		457.8	41	41	36
Iomeprol TP599	599.8	582.7	101	17	36
		427.8	101	35	30

Table S3.6.5: MRM Transitions and Optimized MS Parameters for Iopamidol and TPs

Compound	Precursor Ion (*m/z*)	Product Ion (*m/z*)	Declustering Potential (V)	Collision Energy (eV)	Cell Exit Potential (V)
Iopamidol	777.9	558.8	91	33	18
		387.0	91	55	12
Iopamidol TP805	805.8	700.9	116	31	22
		418.9	116	61	6
Iopamidol TP791	791.9	558.9	81	29	20
		686.7	81	19	38
Iopamidol TP775	775.9	670.7	86	21	24
		700.7	81	23	24
Iopamidol TP773	773.9	559.0	56	25	16
		670.8	56	17	30
Iopamidol TP761	761.9	558.9	91	31	30
		670.8	91	27	10
Iopamidol TP745	745.9	670.7	61	21	22
		515.8	61	37	14
Iopamidol TP717	717.8	330.9	81	69	20
		457.7	81	39	24
Iopamidol TP687	687.8	612.8	81	27	18
		457.9	76	41	22

3.7 Literature Cited

Bahr, C.; Schumacher, J.; Ernst, M.; Luck, F.; Heinzmann, B.; Jekel, M. SUVA as a control parameter for the effective ozonation of organic pollutants in secondary effluent. *Water Sci Technol.* **2007**, *55* (12), 267-274.

Batt, A. L.; Kim, S.; Aga, D. Enhanced biodegradation of iopromide and trimethoprim in nitrifying sludge. *Environ. Sci. Technol.* **2006**, *40* (23), 7367-7373.

Busetti, F.; Linge K. L.; Blythe, J. W.; Heitz, A. Rapid analysis of iodinated X-ray contrast media in secondary and tertiary wastewater by direct injection liquid chromatography-tandem mass spectrometry. *J Chromatogr A.* **2008**, *1213* (2), 200-208.

Carballa, M.; Omil, F.; Ternes, T. A.; Lema, J. M. Fate of pharmaceuticals and personal care products (PPCPs) during anaerobic digestion of sewage sludge. *Water Res.* **2007**, *41* (10), 2139-2150.

Carballa, M.; Fink, G.; Omil, F.; Lema, J. M.; Ternes, T. A. Determination of the solid-water distribution coefficient (K_d) for pharmaceuticals, estrogens and musk fragrances in digested sludge. *Water Res.* **2008**, *42* (1-2), 287-295.

Clara, M.; Strenn, B.; Gans, O.; Martinez, E.; Kreuzinger, N.; Kroiss, H. Removal of selected pharmaceuticals, fragrances and endocrine disrupting compounds in a membrane bioreactor and conventional wastewater treatment plants. *Water Res.* **2005**, *39* (19), 4797-4807.

Doll, T. E.; Frimmel, F. H. Fate of pharmaceuticals-photodegradation by stimulated solar UV-light. *Chemosphere.* **2003**, *52* (10), 1757-1769.

Doll, T. E.; Frimmel, F. H. Cross-flow microfiltration with periodical back-washing for photocatalyic degradation of pharmaceuticals and diagnostic residues-evaluation of the long-term stability of the photocatalyic activity of TiO_2. *Water Res.* **2005**, *39* (5), 847-854.

Haiß, A.; Kümmerer, K. Biodegradability of the X-ray contrast compound diatrizoic acid, identification of aerobic degradation products and effects of against sewage sludge micro-organisms. *Chemosphere.* **2006**, *62* (2), 294-302.

Hegg, E. L.; Whiting, A. K.; Saari, R. E.; McCracken, J.; Hausinger, R. P.; Que Jr., L. Herbicide-degrading α-keto acid-dependent enzyme TfdA: Metal coordination environment and mechanistic insights. *Biochemistry.* **1999**, *38* (50), 16714-16726.

Heitzer, A.; Kohler, H-P. E.; Reichert, P.; Hamer, G. Utility of phenomenological models for describing temperature dependence of bacterial growth. *Appl Environ Microbiol.* **1991**, *57* (9), 2656-2665.

Hirsch, R.; Ternes, T. A.; Lindart, A.; Haberer, K.; Wilken, R-D. A sensitive method for the determination of iodine containing diagnostic agents in aqueous matrices using LC-electrospray-tandem-MS detection. *Fresenius J Anal Chem.* **2000**, *366* (8), 835-841.

Joss, A.; Carballa, M.; Kreuzinger, N.; Siegrist, H.; Zabczynski, S. In *Human Pharmaceuticals, Hormones and Fragrances: The challenge of micropollutants in urban water management*; Ternes, T. A., Joss, A., Eds.; IWA Publishing: London, 2006a.

Joss, A.; Zabczynski, S.; Göbel, A.; Hoffmann, B.; Löffler, D.; McArdell, C. S.; Ternes, T. A.; Thomsen, A.; Siegrist, H. Biological degradation of pharmaceuticals in municipal wastewater treatment: proposing a classification scheme. *Water Res.* **2006b**, *40* (8), 1686-1696.

Kalsch, W. Biodegradation of the iodinated X-ray contrast media diatrizoate and iopromide. *Sci. Total Environ.* **1999**, *225* (1-2), 143-153.

Knitt, L. E.; Sharply, J. R.; Strathmann, T. J. Rapid metal-catalyzed hydrodehalogenation of iodinated X-ray contrast media. *Environ. Sci. Technol.* **2008**, *42* (2), 577-583.

Kormos, J. L.; Schulz, M.; Wagner, M.; Ternes, T. A. Multistep approach for the structural identification of biotransformation products of iodinated X-ray contrast media by liquid chromatography/hybrid triple quadrupole linear ion trap mass spectrometry and ^{1}H and ^{13}C nuclear magnetic resonance. *Anal. Chem.* **2009**, *81* (22), 9216-9224.

Kroutil, W.; Mang, H.; Edegger, K.; Faber, K. Biocatalyic oxidation of primary and secondary alcohols. *Adv Synth Catal.* **2004**, *346* (2-3), 125-142.

Lecouturier, D.; Rochex, A.; Lebeault, J.-M. The mineralization of 5-amino-2,4,6-triiodoisophthalic acid by a two-stage fixed-bed reactor. *Water Res.* **2008**, *42* (10-11), 2491-2498.

Löffler, D.; Römbke, J.; Meller, M.; Ternes, T. A. Environmental fate of pharmaceuticals in water/sediment systems. *Environ. Sci. Technol.* **2005**, *39* (14), 5209-5218.

Oppel, J.; Broll, G.; Löffler, D.; Meller, M.; Römbke, J.; Ternes, Th. Leaching behaviour of pharmaceuticals in soil-testing-systems: a part of an environmental risk assessment for groundwater protection. *Sci. Total Environ.* **2004**, *328* (1-3), 265-273.

Pérez, S.; Barceló, D. Fate and occurrence of X-ray contrast media in the environment. *Anal Bioanal Chem.* **2007**, *387* (4), 1235-1246.

Putschew, A.; Wischnack, S.; Jekel, M. Occurrence of triiodoinated X-ray contrast agents in the aquatic environment. *Sci. Total Environ.* **2000**, *255* (1), 129-134.

Putschew, A.; Miehe, U.; Tellez, A. S.; Jekel, M. Ozonation and reductive deiodination of iopromide to reduce the environmental burden of iodinated X-ray contrast media. *Water Sci Technol.* **2007**, *56* (11), 159-165.

Radjenović, J.; Pérez, S.; Petrović, M.; Barceló, D. Identification and structural characterization of biodegradation products of atenolol and glibenclamide by liquid chromatography coupled to hybrid quadrupole time-of-flight and quadrupole ion trap mass spectrometry. *J Chromatogr A.* **2008**, *1210* (2), 142-153.

Richardson, S. D.; Fasano, F.; Ellington, J. J.; Crumley, F. G.; Buettner, K. M.; Evans, J. J.; Blount, B. C.; Silva, L. K.; Waite, T. J.; Luther, G. W.; McKague, A. B.; Miltner, R. J.; Wagner, E. D.; Plewa, M. J. Occurrence and mammalian cell toxicity of iodinated disinfection byproducts in drinking water. *Environ. Sci. Technol.* **2008**, *42* (22), 8330-8338.

Rode, U.; Müller, R. Transformation of the ionic X-ray contrast agent diatrizoate and related triiodinated benzoates by *Trametes versicolor. Appl Environ Microbiol.* **1998**, *64* (8), 3114-3117.

Sacher, F.; Lange, F. T.; Brauch, H.-J.; Blankenhorn, I. Pharmaceuticals in groundwaters Analytical methods and results of a monitoring program in Baden-Württemberg, Germany. *J Chromatogr A.* **2001**, *938* (1-2), 199-210.

Schittko, S.; Putschew, A.; Jekel, M. Bank filtration: a suitable process for the removal of iodinated X-ray contrast media? *Water Sci Technol.* **2004**, *50* (5), 261-268.

Schulz, M.; Löffler, D.; Wagner, M.; Ternes, T. A. Transformation of the X-ray contrast medium iopromide in soil and biological wastewater treatment. *Environ. Sci. Technol.* **2008**, *42* (19), 7207-7217.

Seitz, W.; Weber, W. H.; Jiang, J.-Q.; Lloyd B. J.; Maier, M.; Maier, D.; Schulz, W. Monitoring of iodinated X-ray contrast media in surface water. *Chemosphere*. **2006a**, *64* (8), 1318-1324.

Seitz, W.; Jiang, J.-Q.; Weber, W. H.; Lloyd B. J.; Maier, M.; Maier, D. Removal of iodinated X-ray contrast media during drinking water treatment. *Environ Chem.* **2006b**, *3* (1), 35-39.

Sprenger, G. A.; Pohl, M. Synthetic potential of thiamin diphosphate-dependent enzymes. *J. Mol Catal B: Enzym.* **1999**, *6* (3), 145-159.

Steger-Hartmann, T.; Länge, R.; Schweinfurth, H. Environmental risk assessment for the widely used iodinated X-ray contrast agent iopromide (Ultravist). *Ecotoxicol Environ Saf.* **1999**, *42* (3), 274-281.

Steger-Hartmann, T.; Länge, R.; Schweinfurth, H.; Tschampel, M., Rehmann, I. Investigations into the environmental fate and effects of iopromide (ultravist), a widely used iodinated X-ray contrast medium. *Water Res.* **2002**, *36* (1), 266-274.

Stein, S.; Ramil, M.; Fink, G.; Sander, M.; Ternes, T. A. Analysis and sorption of psychoactive drugs onto sediment. *Environ. Sci. Technol.* **2008**, *42* (17), 6415-6423.

Ternes, T. A. Occurrence of drugs in German sewage treatment plants and rivers. *Water Res.* **1998**, *32* (11), 3245-3260.

Ternes, T. A.; Hirsch, R. Occurrence and behavior of X-ray contrast media in sewage facilities and the aquatic environment. *Environ. Sci. Technol.* **2000**, *34* (13), 2741-2748.

Ternes, T. A.; Stüber, J.; Herrman, N.; McDowell, D.; Ried, A.; Kampmann, M.; Teiser, B. Ozonation: a tool for removal of pharmaceuticals, contrast media and musk fragrances from wastewater? *Water Res.* **2003**, *37* (8), 1976-1982.

Ternes, T. A.; Bonerz, M.; Hermann, N.; Teiser, B.; Andersen, H. R. Irrigation of treated wastewater in Braunschweig, Germany: An option to remove pharmaceuticals and musk fragrances. *Chemosphere*. **2007**, *66* (5), 894-904.

Weissbrodt, D.; Kovalova, L.; Ort, C.; Pazhepurackel, V.; Moser, R.; Hollender, J.; Siegrist, H.; McArdell, C. S. Mass flows of X-ray contrast media and cytostatics in hospital wastewater. *Environ. Sci. Technol.* **2009**, *43* (13), 4810-4817.

Chapter 4:

Occurrence of Iodinated X-ray Contrast Media and their Biotransformation Products in the Urban Water Cycle

Jennifer Lynne Kormos,[1] Dominic A. Urban,[1] Manoj Schulz,[1] and Thomas A. Ternes[1]

[1]*Federal Institute of Hydrology (BfG), Am Mainzer Tor 1, D-56068, Koblenz, Germany*

Abstract

A LC tandem MS method was developed for the simultaneous determination of five iodinated X-ray contrast media (ICM) and 46 biotransformation products (TPs) in raw and treated wastewater, surface water, groundwater and drinking water. Recoveries ranged from 70% to 130%, and limits of quantification (LOQ) were between 1 ng/L to 3 ng/L for groundwater and drinking water, and 10 ng/L to 30 ng/L for wastewater. Iohexol, iomeprol, and iopromide were transformed to > 80% in a conventional wastewater treatment plant, while for iopamidol it was only 30%. The loads in WWTP effluent of the ICM TPs formed under aerobic conditions could account for up to 45% of iopromide and 16% iomeprol transformation, while for iohexol and iopamidol only 3% and 1% could be found. A significant change in the pattern of ICM TPs was found after bank filtration and groundwater recharge leading to TPs formed at the end of the aerobic transformation pathway. Therefore, several ICM TPs such as iohexol TP599, iomeprol TP643, and iopromide TP701A and TP643 were formed during soil passage, and were even not removed by granular activated carbon (GAC) filtration or ozonation during drinking water treatment. Seven ICM TPs, such as iomeprol TP687 and TP643, and iopromide TP701A, were detected at concentrations > 100 ng/L in groundwater and drinking water, with most of these TPs formed during groundwater recharge or bank filtration.

4.1 Introduction

Iodinated X-ray contrast media (ICM) are used for the imaging of internal body structures (i.e. organs, blood vessels and soft tissues) during diagnostic examinations (Christiansen, 2005). ICM have been reported to be the most widely used pharmaceuticals for intravascular administration, and most frequently used in hospitals (Hirsch *et al.* 2000; Christiansen, 2005). They are applied

at high doses (i.e. up to 200 g/application), and are eliminated unmetabolized in the urine within 24 h (Steger-Hartmann *et al.* 2002). Most ICM are derivatives of 2,4,6-triiodobenzoic acid, and are classified as ionic or non-ionic depending on the functional groups at their side chains. For instance, the ionic ICM, diatrizoate, is negatively charged at neutral pH due to its carboxylic moiety (pKa = 3.4), while the non-ionic ICM (i.e. iohexol, iopamidol and iomeprol) are uncharged at neutral pH because they contain only hydroxyl groups which become deprotonated at pH> 10 (Pérez and Barceló, 2007; Busetti *et al.* 2008).

Several studies have shown that these hydrophilic and biologically stable ICM are not effectively removed during treatment in wastewater treatment plants (WWTPs) (Ternes and Hirsch 2000; Carballa *et al.* 2004; Clara *et al.* 2005). The elevated concentrations of ICM in surface water, groundwater, and even water of drinking water treatment plants (DWTPs) indicate their persistence (Hirsch *et al.* 2000, Putschew *et al.* 2000; Schittko *et al.* 2004; Joss *et al.* 2006; Seitz *et al.* 2006; Ternes *et al.* 2007).

Recent research has shown that certain oxidation processes (i.e. ozonation, advanced oxidation processes) as well as biological processes in WWTPs with elevated sludge retention times (SRT) of > 12 d are capable of removing non-ionic ICM (Doll and Frimmel, 2004; Pérez *et al.* 2006; Seitz *et al.* 2008; Zwiener *et al.* 2009;). However, the elimination did not result in mineralization of the parent ICM. In most cases, oxidation products or biotransformation products (TPs) were formed (Kalsch 1999; Batt *et al.* 2006; Seitz *et al.* 2008; Schulz *et al.* 2008; Kormos *et al.* 2010). Aerobic biological transformation results in a shorting of the side chains of the parent ICM, while chemical oxidation processes might lead to deiodinated organic products (Pérez *et al.* 2009; Zwiener *et al.* 2009). Recently, a total of 46 TPs for four non-ionic ICM have been

identified (Schulz *et al.* 2008; Kormos *et al.* 2009 and 2010). However so far minimal effort has focused on the occurrence and the fate of these newly identified TPs in the aquatic environment.

The main objective of this study was to investigate the occurrence and fate of the newly identified TPs of four nonionic ICM (iohexol, iomeprol, iopamidol and iopromide) in different aqueous matrices using an optimized LC ESI tandem MS method. In particular, this study is aiming at changes occurring in the composition and patterns of the TPs in water which is following the urban water cycle from WWTPs via surface water to groundwater and drinking water.

4.2 Experimental Section

4.2.1 Description of Sampling Locations

4.2.1.1 Sampling of wastewater treatment plants (WWTPs)

Weekly composite samples were collected from a conventional German WWTP (WWTP1) during a dry weather period in December 2009 (December 14th to 18th 2009). This WWTP serves 285,000 population equivalents (PEs), and has a SRT and hydraulic retention time (HRT) of 16 d and 60 h, respectively. The average wastewater inflow is approximately 35,500 m^3/d. WWTP1 receives two different wastewater streams from the surrounding area. The composition of wastewater consists of domestic sewage from various districts of the city as well as hospital wastewaters. WWTP1 consists of mechanical treatment, biological phosphate removal, denitrification, nitrification, secondary sedimentation and filtration (Figure 4.1). The mechanical treatment consists of different sized screens, a grit removal tank (sand filtration tank) and a primary sedimentation tank. After primary sedimentation, the wastewater enters a biological

phosphate elimination tank, followed by an activated sludge tank consisting of a denitrification compartment and a nitrification compartment. The effluent enters a secondary sedimentation tank and a filtration system before being discharged into the receiving water body. Figure 4.1 provides a schematic diagram of WWTP1, and where the samples were collected. Samples were taken from both influent streams (sampling point 1 and 2), prior to biological treatment (sampling point 3), after secondary sedimentation (sampling point 4), and after filtration (sampling point 5).
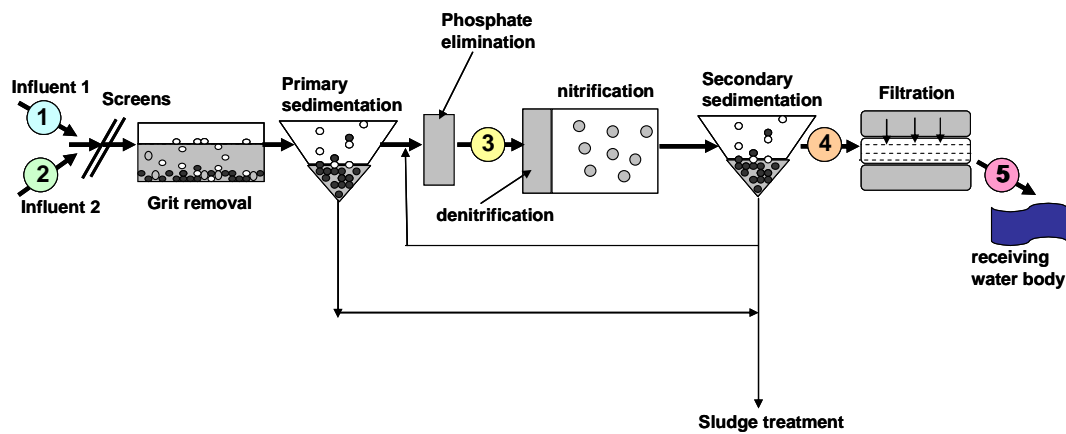
Figure 4.1: Flow scheme of a conventional German WWTP (WWTP1) consisting of mechanical and biological treatment. The numbers indicate the locations where samples were taken.

Grab effluent samples were also collected from two municipal WWTPs in Germany to obtain more information on the composition of ICM and ICM TPs being discharged into surface waters. A detailed description of the two WWTPs, (i.e.WWTP2 and WWTP3), can be found in the section 4.5. In brief, WWTP2 is a medium-sized facility with approximately 300,000 inhabitant equivalent values, and has a HRT of 36 h and a SRT of 12 d. WWTP3 has a SRT of 20 d and a HRT of 36 h, and with a capacity of 600,000 PEs. The two WWTPs apply similar treatment

processes, including screens, grit removal/sand filtration, primary sedimentation, biological treatment (nitrification and denitrification), phosphate elimination, and secondary sedimentation.

4.2.1.2 Sampling of Surface Waters

Ruhr Watershed. Samples were collected along the Ruhr River and its tributaries in September 2009 during dry weather conditions (Figure 4.2). A detailed description of the sampling campaign can be found elsewhere (Prasse *et al.* 2010). In brief, water samples were collected from 23 locations along the Ruhr River, six locations along its tributaries, two sites at Rhine River close to its confluence with the Ruhr, and one site at the mouth of the Emscher River entering the Rhine.
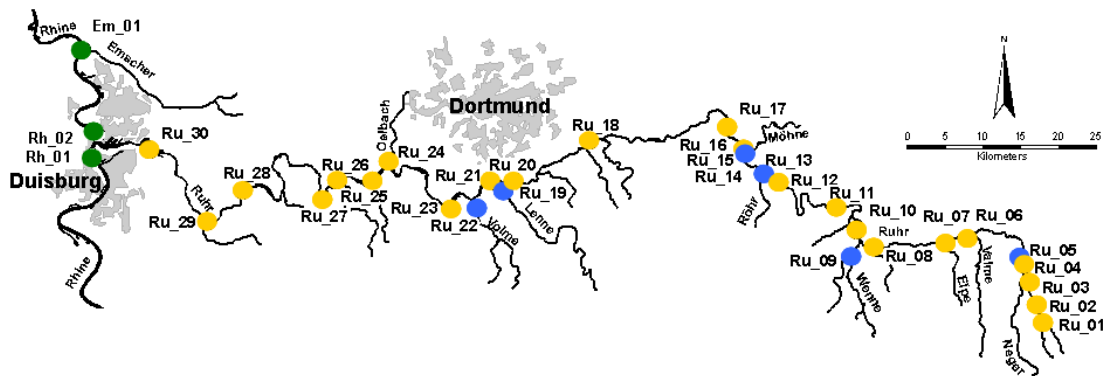
Figure 4.2: Diagram of the Ruhr Watershed showing the sites where water samples were collected during a sampling campaign in September 2009 (Sampling points Ru_01 to Ru_30 were taken along the Ruhr and its tributaries; Rh_01 and Rh_02 refer to samples taken before and after joining the Rhine, and Em_01 is the sampling point at the mouth of the Emscher River). The blue circles represent the sampling spots of the tributaries of the Ruhr, the yellow circles are the sampling spots along the Ruhr, and the green circles are samples taken from the Rhine and Emscher.

The Ruhr River is a medium-size river with a length of 217 km, located in the Western part of Germany. The headwaters of the Ruhr begin in the Rothaar Mountains and flow through a moderately populated area. The river enters the Ruhr Valley, which is the most densely

182

populated region within Germany, prior to joining the Rhine River at Duisburg. There are 28 WWTPs located within the Ruhr Watershed, which discharge wastewater of close to two million inhabitants into the Ruhr or its tributaries (i.e. Wenne, Lenne, Valme, Volme, Möhne, and Röhr). The Ruhr and its tributaries serve as a main source for drinking water production for millions of people.

4.2.1.3 Sampling of Groundwater and Bank Filtration Sites

Four locations were selected in which infiltration of surface water, in particular river water, into groundwater is known or could be possible based on the close proximity of the river to the groundwater wells.

At sampling location 1, samples were collected from the river and three groundwater wells located close to the river. The water level depth (varying between 8.3 m to 9.3 m), pH, water temperature, dissolved oxygen content and conductivity were measured at the different groundwater sampling locations, and are summarized in Table S4.5.1 of section 4.5. River water, groundwater and bank filtrate were collected from sampling location 2. Sampling location 3 and 4 are located within the same watershed. The samples were collected from a river, groundwater recharge area located close to the river, and groundwater influenced the river. Information about the hydrogeology for sampling location 3 and 4 is provided in the section 4.5.

4.2.1.4 Sampling of water after certain DWTP processes

Samples were collected from five German DWTPs. The main treatment processes are summarized in Table 4.1. Samples were taken before and after certain treatment processes at the five selected DWTPs (referred to as DWTP1 to DWTP5). The raw water source for DWTP1 is a mixture of groundwater and bank filtrate, which is then treated by GAC filtration before being

distributed. DWTP2 receives its raw water from bank filtration, artificial groundwater recharge and natural groundwater. Afterwards, only physical treatment processes are applied such as aeration, and sand filtration. DWTP3 receives its raw water from a reservoir and groundwater and uses flocculation, multi-layer filtration, and UV disinfection. DWTP4 and DWTP5 direct use river water to produce drinking water, and hence a multi-barrier approach is used to prevent the breakthrough of pathogens and pollutants by applying processes such as flocculation, ozonation, and filtration (i.e. sand filtration and GAC filtration).

Table 4.1: Summary of the different treatment processes applied at the five selected German DWTPs

Treatment Process	DWTP1	DWTP2	DWTP3	DWTP4	DWTP5
Bank filtration	X	X			X
Flocculation			X	X	X
Sedimentation				X	X
Aeration		X			X
Multi-layer filtration			X	X	
Sand filtration		X			X
GAC filtration	X			X	X
UV disinfection			X		
Ozonation				X	
Chlorine disinfection					X

4.2.2 Sample Preparation and Extraction for ICM TPs

The aqueous samples were filtered through glass fiber filters (Schleicher and Schuell, Dassel, Germany), acidified to pH 3 with sulfuric acid (H_2O_4, 3.5 M), and stored at 4 °C prior to

184

extraction. Two solid phase extraction (SPE) cartridges, C_{18} cartridge (3 mL, 200 mg, J.T. Baker) coupled with Bakerbond^{TM} SDB-1 (3 mL, 200 mg, J.T. Baker), were used simultaneously for clean-up and extraction, respectively. Both SPE cartridges were conditioned with 4×1 mL of methanol and 4×1 mL groundwater adjusted to pH 3 with 3.5M H_2SO_4. For raw and treated wastewater, 100 mL and 200 mL were extracted, respectively, and 500 mL or 1 L was extracted for surface water, groundwater and drinking water. Prior to extraction, all samples were spiked with 10 µL of a surrogate solution (20 ng/µL). The surrogate standard solution consisted of iohexol-d_5, iomeprol-d_3, iopamidol-d_3, diatrizoate-d_6, desmethoxyiopromide (DMI), and N-(2,3-dihydroxypropyl)-2,4,6-triiodo-5-methoxyacetylamino-N'-methylisophthalamide (DDPHI). DMI and DDPHI were kindly provided by Bayer Schering Pharma (Berlin, Germany), diatrizoate-d_6 was purchased from Compro Scientific (Berlin, Germany), and iohexol-d_5, iomeprol-d_3 and iopamidol-d_3 were purchased from Toronto Research Chemicals (North York, Canada). After enrichment by SPE, the cartridges were washed with 4 mL of Milli-Q water adjusted to pH 3 with 3.5M H_2SO_4. The SDB-1 cartridges were then dried under a gentle stream of nitrogen gas. The analytes were eluted with 4×2 mL of methanol, evaporated to 100 µL using nitrogen gas and reconstituted to 1 mL with Milli-Q water (depending on the volume extracted during SPE). The extracted samples were stored at 4° C until measured by LC tandem MS.

4.2.3 LC ESI(+) Tandem MS detection of ICM and TPs

An Agilent 1200 Series HPLC system, consisting of an autosampler, binary pump and degasser (Waldbronn, Germany), was coupled to a column oven (MayLab Analytical Instruments, Austria). Chromatographic separation of the analytes was achieved on two coupled Chromolith® Performance RP-18e columns (4.6 mm × 100 mm, Merck, Darmstadt, Germany) with a Chromolith® RP-18e guard column (4.6 mm × 5 mm, Merck, Darmstadt, Germany). A sample

aliquot of 50 µL was injected into the LC ESI tandem MS, and the analytes were eluted from the column using two mobile phases, 95% Milli-Q water, 5% methanol and 0.5% formic acid (A), and 99.5% Milli-Q water and 0.5% formic acid (B). The gradient elution program was as follows: 0-2 min, 100% A; 17 min 90% A; 17.1-20 min; 100% A. Iopromide and its TPs were measured in a different HPLC run using an isocratic elution program which consisted of 90% A and 10% B for 20 min. A flow rate of 0.8 mL/min and column oven temperature of 50 °C was used for the measurements of all ICM and TPs.

The HPLC system was coupled to a 4000 Q Trap[TM] MS system (Applied Biosystems/MDS Sciex, Darmstadt, Germany) consisting of an electrospray ionization (ESI) source (operated in positive ionization mode). The source-dependent parameters were optimized for the ICM and their TPs. These parameters are summarized in Table S4.5.2 of the section 4.5. Two mass transitions were optimized for the parent ICM and each TP for identification and confirmation purposes in MRM mode. The MRM transitions and compound-dependent parameters for the parent ICM and TPs as well as the surrogate standards are summarized in Table S4.5.3-S4.5.6 of section 4.5.

4.2.4 Method Validation

4.2.4.1 Recoveries

Recoveries for the analytical method were determined by spiking the analytes and surrogate standards into samples of raw and treated wastewater, surface water, groundwater and drinking water. The spiking concentrations were different between the wastewater samples (i.e. spiking concentration of 0.1 and 1 µg/L) and the other aqueous samples (i.e. 0.05, 0.1 and 0.2 µg/L), and based on background concentrations of parent ICM previously detected in the different matrix

types. Recoveries were also carried out in the wastewater samples at higher concentrations (i.e. 10 µg/L and 50 µg/L) for direct injection into the LC tandem MS.

The recoveries were calculated by subtracting the mean concentration (n=3) of the analyte in the spiked enriched samples (C_{spiked}) by the mean concentration (n=3) in the non-spiked enriched samples ($C_{non-spiked}$), and dividing it by the initial spiking concentration ($C_{initial}$) (refer to Eq 4.1).

$$\text{Recovery } [\%] = (C_{spiked} - C_{non-spiked}) \div (C_{initial}) \times 100 \qquad \text{Eq (4.1)}$$

Variations from the mean values (n=3) were given as 95% confidence intervals.

4.2.4.2 Quantification and LOQs

The calibration was prepared by spiking standard solutions of diatrizoate, iohexol, iomeprol and iopamidol and nine isolated TP standards (iohexol TP687A, TP657, TP599; iomeprol TP701, TP643, TP629; iopamidol TP791, TP761, TP745) as well as iopromide and its seven isolated TPs (TP819, TP759, TP731B, TP729A, TP701A, TP701B, TP643) into a final volume of 1 mL Milli-Q water. A detail explanation of how the TPs were isolated and the preparation of the standard solutions can be found elsewhere (Schulz et al. 2008; Kormos et al. 2010). In addition, 10 µL of a surrogate standard solution (20 ng/µL) was spiked into each calibration sample. The 12 point calibration curve ranged from 1 to 3000 ng/L. Linear and quadratic regressions were applied to the calibration curves with a weighing factor of 1/x.

For remaining ICM TPs, which could not be isolated in sufficient quantities, the concentrations were determined using either the calibration curve of the parent compound or a TP which had the same detected fragment ions. These TPs are marked with an asterisk because the concentrations have been semi-quantified due to insufficient quantities of the standards. A summary of the

analytes as well as the surrogate standards used for quantification (semi-quantification) of each analyte are summarized in Table S4.5.7-S4.5.8 of section 4.5.

Samples from the soil-water batch systems with spiked ICM (i.e. 1 g/L) were analyzed to verify the correct retention times of different ICM TPs having similar MRM transitions. The experimental set-up of the batch systems are described in Schulz *et al.* (2008) and Kormos *et al*. (2009). At specific time intervals, samples (10 µL) were taken, spiked with 10 µL of the surrogate standard (20 ng/µL) solution, and diluted to 1 mL with Milli-Q water prior to LC tandem MS detection.

The limits of quantification (LOQ) were defined as a signal/noise ratio of > 10, which was individually determined in each environmental sample and calibration sample for each analyte. In any case, the LOQ was always higher than the lowest calibration point in the linear or quadratic regression.

4.2.5 Diatrizoate and carbamazepine as municipal wastewater indicators

Diatrizoate and carbamazepine were simultaneously monitored as indicators of wastewater contamination because these compounds are known to be persistent during wastewater treatment (Ternes and Hirsch, 2000; Ternes et al., 2007; Hummel et al. 2006). Diatrizoate was measured and quantified using the described LC tandem MS method. Carbamazepine was detected using a LC tandem MS method described previously by Hummel et al. 2006.

4.3 Results and Discussion

4.3.1 Method Validation for ICM and TPs in Aqueous Matrices

An analytical method using LC tandem MS instrumentation was developed to determine the occurrence of diatrizoate, four nonionic ICM (iohexol, iomeprol, iopamidol and iopromide), and 46 ICM TPs in various aqueous matrices. The recoveries for the parent ICM, selected TPs, and the wastewater indicators, diatrizoate and carbamazepine, are summarized in Table 4.2. In general, the recoveries were between 70% to 130% with 95% confidence intervals (n=3) of less than 30%. The LOQs for analytes detected in surface water, ground and drinking water ranged from 1 ng/L to 3 ng/L. The LOQs for the raw and treated wastewater samples were significantly higher due to the elevated matrix background and ranged from 10 ng/L to 30 ng/L. The analytical method developed was able to quantify ICM and their 46 TPs in a variety of aqueous matrices with sufficient accuracy and sensitivity.

Table 4.2: Recoveries (%) and 95% confidence intervals (n=3) for ICM and selected TPs, and the wastewater indicators (carbamazepine and diatrizoate) in the investigated environmental matrices

Analyte	WWTP influent[a]	WWTP effluent[a]	River water[b]	Groundwater[b]	Drinking water[c]
Iohexol	91 ± 25	120 ± 21	71,89 n=2	106 ± 14	96 ± 31
Iohexol TP687A	95 ± 11	119 ± 6	78 ± 12	75 ± 12	84 ± 10
Iohexol TP657	106 ± 21	117 ± 15	90 ± 10	105 ± 4	120 ± 7
Iohexol TP599	83 ± 49	123 ± 36	82 ± 5	85 ± 2	136 ± 18
Iomeprol	123 ± 158*	92 ± 21	80 ± 9	113 ± 14	89 ± 41
Iomeprol TP701	94 ± 29	108 ± 22	121 ± 26	106 ± 29	96 ± 27
Iomeprol TP643	90 ± 27	104 ± 15	84 ± 27	104 ± 46	120 ± 40
Iomeprol TP629	105 ± 17	112 ± 9	74 ± 8	82 ± 16	83 ± 26
Iopamidol	111 ± 13	100 ± 9	117	113 ± 20	128 ± 38
Iopamidol TP791	87 ± 4	93 ± 6	93 ± 5	90 ± 17	87;86 (n=2)
Iopamidol TP761	112 ± 19	97 ± 10	93 ± 21	88 ± 14	141 ± 29
Iopamidol TP745	94 ± 4	99 ± 3	88 ± 14	78 ± 6	109 ± 25
Iopromide	79 ± 13	89 ± 14	119 ± 33	105 ± 1	111 ± 15
Iopromide TP759	82 ± 10	95 ± 10	102 ± 3	93 ± 15	123 ± 18
Iopromide 701A	81 ± 4	92 ± 3	100 ± 15	94 ± 13	111 ± 16
Iopromide TP643	83 ± 11	99 ± 10	76 ± 13	72 ± 18	71 ± 13
Wastewater Indicators					
Carbamazepine	92 ± 9	105 ± 6	111;105 n=2	100 ± 8	105 ± 14
Diatrizoate	77 ± 8	95 ± 15	106 ± 5	112 ± 20	77;81 (n=2)

[a]spiking concentration of 50 µg/L (direct injection); [b]spiking concentration of 0.1 µg/L; [c]spiking concentration of 0.05 µg/L; *spiking concentration was too low (background concentrations were high compared to spiking concentration)

4.3.2 Transformation of ICM and TPs in a municipal WWTP

Five-day composite samples were collected from WWTP1 at five sampling locations, as illustrated in Figure 4.1. Influent concentrations of the more contaminated wastewater stream (Influent 1) ranged from 18 µg/L (iohexol) to 131 µg/L (iomeprol), and from 3.7 µg/L (iohexol) to 6.6 µg/L (iomeprol) in the other influent stream (Influent 2) (Table 4.3 and 4.4). Transformation of the parent nonionic ICM mainly occurred during biological treatment. The other processes (i.e. filtration) were of minor importance for the transformation of the selected ICM. The transformation efficiencies of iohexol, iomeprol and iopromide were > 80% indicating the extremely high biological efficiency for WWTP1 (Table 4.3 and 4.4). This is probably the result of the high SRT of 16 d and HRT of 60 h at this WWTP. In the literature, the removal rates for ICM have varied from no removal (Ternes and Hirsch 2000; Carballa *et al.* 2004; Clara *et al.* 2005) to greater than 80% (Ternes *et al.* 2007) indicating that a minimal SRT of > 8 d is required (Joss *et al.* 2006). Batt *et al.* 2006 reported that a SRT of 12 to 14 d was responsible for the high removal efficiency of iopromide during activated sludge treatment.

Iopamidol was transformed to a minor extent with a calculated transformation rate of 35% during biological treatment. This lower removal rate in biological wastewater treatment is consistent with its slow biotransformation rates observed in aerobic soil-water and sediment-water batch experiments (Kormos *et al.* 2010). In the effluent of WWTP1 only one iopamidol TP (TP791) could be detected, while in the same effluent 10 iomeprol TPs and all 12 iopromide TPs were detected. Obviously, iopamidol is more reluctant towards biotransformation in municipal WWTPs than other non-ionic ICM.

Table 4.3: Concentrations [µg/L] and loads [g/d] of iopromide and TPs, and iomeprol and TPs at specific sampling locations, and mass balance based on loads of iopromide and iomeprol during treatment at WWTP1

Sampling Point	Iopromide					Iomeprol			
	Conc. [µg/L] (Load [g/d])	Sum of phase I TPs[a] [µg/L] [g/d]	Sum of phase II TPs[b] [µg/L] [g/d]	Sum of phase III TPs[c] [µg/L] [g/d]	Mass balance [%][f] [[g/d]	Conc. [µg/L] (Load [g/d])	Sum of phase I TPs[d] [µg/L] [g/d]	Sum of phase II TPs[e] [µg/L] [g/d]	Mass balance [%][f] [g/d]
Influent 1 (1)	60 ± 6 (1100 ± 120)	0.31 ± 0.08 (6 ± 1)	0.03 ± 0.01 (0.5 ± 0.1)	0.17 ± 0.05 (4.2 ± 0.8)	---	131 ± 12 (2400 ± 230)	0.6 ± 0.2 (11 ± 4)	0.7 ± 0.2 (13 ± 4)	
Influent 2 (2)	1.7 ± 0.2 (28 ± 4)	0.6 ± 0.2 (9 ± 4)	0.10 ± 0.04 (1.7 ± 0.7)	0.18 ± 0.02 (3.2 ± 0.3)	---	5.7 ± 0.2 (95 ± 3)	0.21 ± 0.02 (3.6 ± 0.2)	0.5 ± 0.2 (9 ± 4)	
Pre-biological treatment (3)	31 ± 2 (1200 ± 80)	1.6 ± 0.2 (62 ± 8)	0.82 ± 0.07 (32 ± 3)	0.58 ± 0.08 (12 ± 3)	---	71 ± 2 (2700 ± 60)	1.2 ± 0.6 (45 ± 11)	1.0 ± 0.3 (40 ± 11)	
Post-biological treatment (4)	3.7; 3.8 (130; 130) (n=2)	7.5; 8.4 (260; 290) (n=2)	7.3; 7.4 (250; 250) (n=2)	3.4; 1.3 (26; 43) (n=2)	39%; 44%	12 ± 0.4 (410 ± 10)	3 ± 2 (73 ± 61) (n=2)	5 ± 2 (170 ± 82)	9%
Effluent (5)	3.4; 3.4 (120; 120) (n=2)	7.6; 7.9 (260; 270) (n=2)	6.7; 8.8 (230; 290) (n=2)	4.3; 2.1 (66; 41) (n=2)	42%, 49%	13 ± 3 (450 ± 110)	3.3; 2.8 (96; 110) (n=2)	10; 7.6 (260; 350) (n=2)	14%; 19%

[a]phase I iopromide TPs are TP819, TP805A, TP805B, and TP817; [b] phase II iopromide TPs are TP787, TP731A, TP731B and TP729; [c]phase III iopromide TPs are TP759, TP701A, TP701B and TP643;[d]phase I iomeprol TPs are TP819, TP805, TP791, TP789, TP775, TP761, TP731 and TP717; [e]phase II iomeprol TPs are TP745, TP701, TP687, TP657, TP643, TP629 and TP599; [f]Mass balance is the ratio of the sum of TPs divided by the transformation of the parent ICM in loads [g/d]

Table 4.4: Concentrations [µg/L] and loads [g/d] of iohexol and TPs, and iopamidol and TPs, carbamazepine and diatrizoate at specific sampling locations, and mass balance based on loads of iohexol and iopamidol during treatment at WWTP1

Sampling Point	Iohexol			Iopamidol			Diatrizoate	Carbamazepine
	Conc. [µg/L] (Load [g/d])	Phase II TPs[a] [µg/L] [g/d]	Mass balance [%][b] [g/d]	Conc. [µg/L] (Load [g/d])	TP791 [µg/L] [g/d]	Mass balance [%][b] [g/d]	Conc. [µg/L] (Load [g/d])	Conc. [µg/L] (Load [g/d])
Influent 1 (1)	18 ± 2 (330 ± 30)	0.13 ± 0.04 (2.3 ± 0.8)	---	35 ± 3 (640 ± 60)	---	---	27 ± 3 (500 ± 50)	1 ± 0.00 (19 ± 2)
Influent 2 (2)	3.7 ± 0.4 (62 ± 6)	(0.46 ± 0.01) (7.9 ± 0.2)	---	6.6 ± 0.5 (120 ± 8)	---	---	1.3; 1.2 (24; 22) (n=2)	1.4 ± 0.5 (24 ± 8)
Pre-biological treatment (3)	11 ± 0.3 (410 ± 10)	0.11 ± 0.03 (4 ± 1)	---	21 ± 1 (380 ± 30)	---	---	18 ± 2.6 (680 ± 100)	1.0 ± 0.1 (41 ± 6)
Post-biological treatment (4)	0.9 ± 0.2 (31 ± 7)	0.2 ± 0.1 (8 ± 4)	1%	13 ± 1 (250 ± 10)	0.07 ± 0.02	0.6%	13 ± 0.8 (440 ± 30)	0.9 ± 0.04 (32 ± 2)
Effluent (5)	1.2 ± 0.1 (40 ± 3)	0.4 ± 0.1 (13 ± 5)	3%	16 ± 3 (280 ± 50)	0.07; 0.08 (n=2)	0.9%	14; 13 (440; 470) (n=2)	1.1 ± 0.2 (37 ± 7)

[a] phase II iohexol TPs are TP745, TP687A, TP687B , TP657, TP629, and TP599; [b]Mass balance is the ratio of the sum of TPs divided by the transformation of the parent ICM in loads [g/d]

4.3.3 Mass Balances

The mass balances, calculated in percent, were the ratio of the sum of the respective ICM TPs concentrations [nmol/L] divided by the transformation of the parent ICM [nmol/L], or the ICM TP loads [g/d] divided by the transformation of the parent ICM load. The TPs of iopromide accounts for about 45% of iopromide transformed during biological treatment at WWTP1, while the iomeprol TPs and iohexol TPs account for 16% and 3%, respectively (Table 4.3 and 4.4). It has to be noted that only three TPs of iohexol (i.e. TP687A, TP657 and TP599) have been detected after biological treatment, and were only phase II iohexol TPs. One explanation for the incomplete mass balances might be that other TPs are formed which have not been identified so far.

Figure 4.3 illustrates the dominant TPs of iomeprol and iopromide formed during biological treatment. Concentrations as high as 5.7 µg/L (iomeprol TP629) were detected. In general, TPs formed at the beginning of the proposed transformation pathways were expected. This was true for iomeprol TP805 and TP791, and iopromide TP817A and TP805A. However, additional TPs (i.e. iomeprol TP629 and iopromide TP701A) were detected which were proposed to be formed at the end of the microbial transformation pathways (Schulz *et al*. 2008; Kormos *et al.* 2010). This might be caused by the elevated HRT of 60 h and high SRT of 16 d. The concentration of ICM and ICM TPs found in the effluent samples of WWTP2 and WWTP3 were much lower than those detected in WWTP1 (Figure 4.4). However, the TP patterns were relatively consistent between the three WWTPs, in which ICM TPs such as iomeprol TP629 and TP687, and iopromide TP701A formed at the end of the proposed microbial pathways were detected. This might

be caused by the elevated SRT of > 12 d and the recirculation of the treated sludge during wastewater treatment.
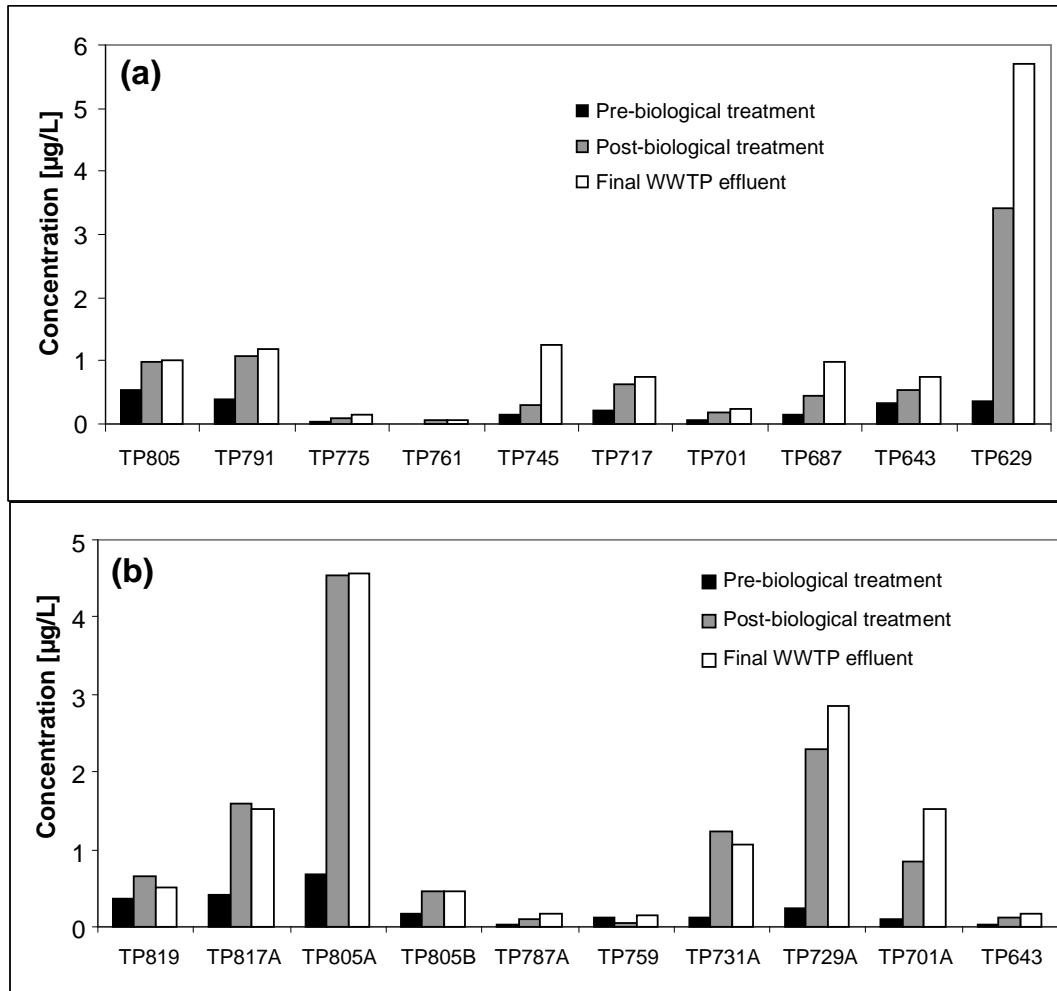
Figure 4.3: Concentrations [µg/L] of iomeprol TPs (a) and iopromide TPs (b) detected prior to biological treatment (sampling point 3), after biological treatment (sampling point 4) and in the final effluent (sampling point 5) at WWTP1 during dry weather conditions in December 2009.
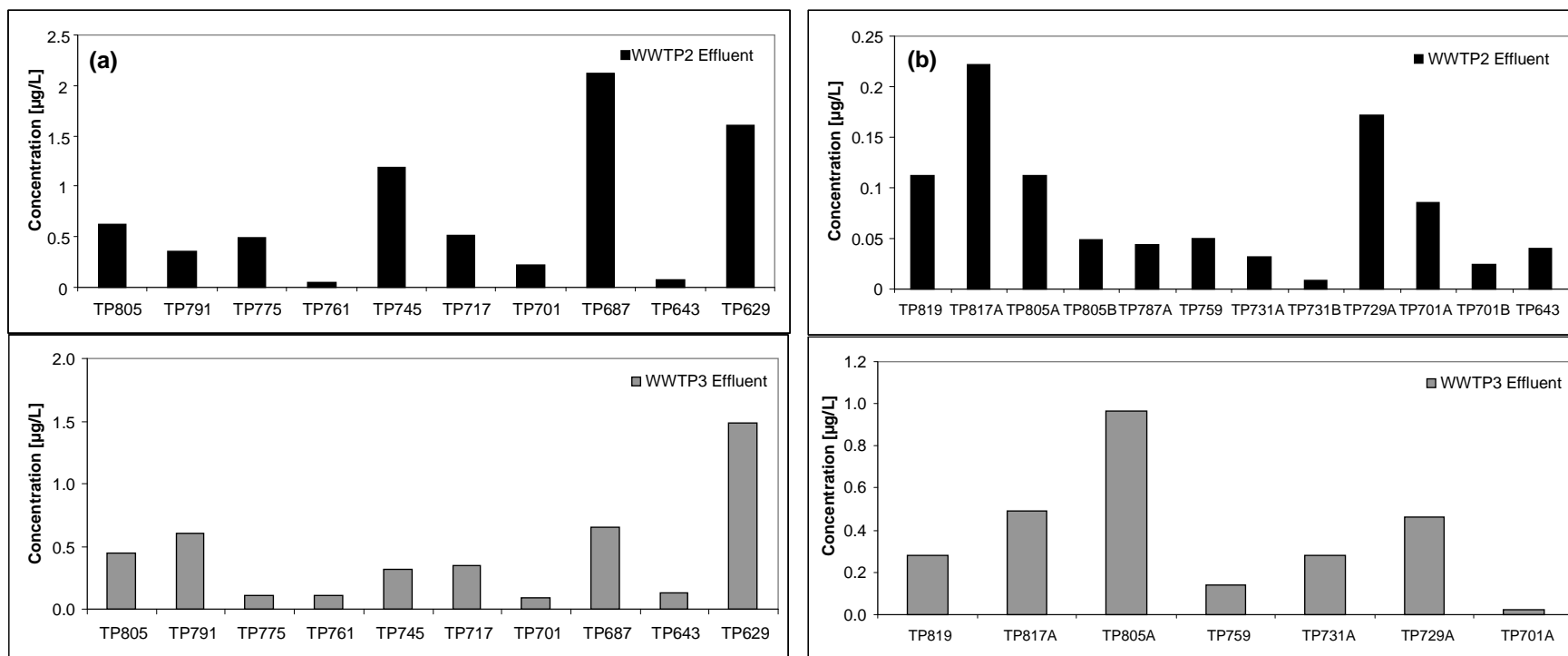
Figure 4.4: Concentrations [µg/L] of the ICM TPs pattern of iomeprol (a) and iopromide (b) detected in the effluent of WWTP2 and WWTP 3.

4.3.4 Occurrence of ICM and TPs in the Ruhr Watershed

With the exception of diatrizoate, the other parent ICM and their TPs were not detected until after the Valme River joined the Ruhr (sampling point Ru_07). The increase in concentrations of the non-ionic ICM and TPs along the Ruhr River followed a similar pattern as the two wastewater indicators, carbamazepine and diatrizoate. This was obvious when comparing the concentration profile of the two wastewater indicators (Figure 4.5), and the concentrations of iomeprol and TPs, and iopromide and TPs from sampling location Ru_18 to Ru_30 (Figure 4.6a and b). As expected, the concentration was correlated to the percentage of treated wastewater in the Ruhr. The concentrations detected at the sampling locations closer to the Rhine remained relatively constant for the ICM as well as the TPs. This suggests that limited biotransformation is occurring at the lower section of the Ruhr (sampling location Ru_18 to Ru_30).
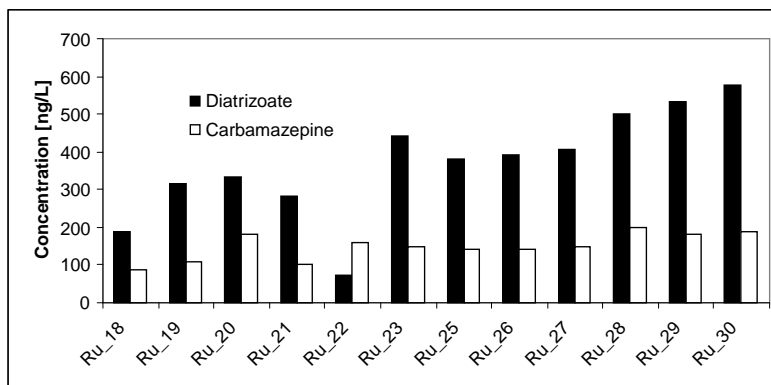
Figure 4.5: Concentrations [ng/L] of the two wastewater indicators along a section of the Ruhr Watershed (sampling points Ru_18 to Ru_30).
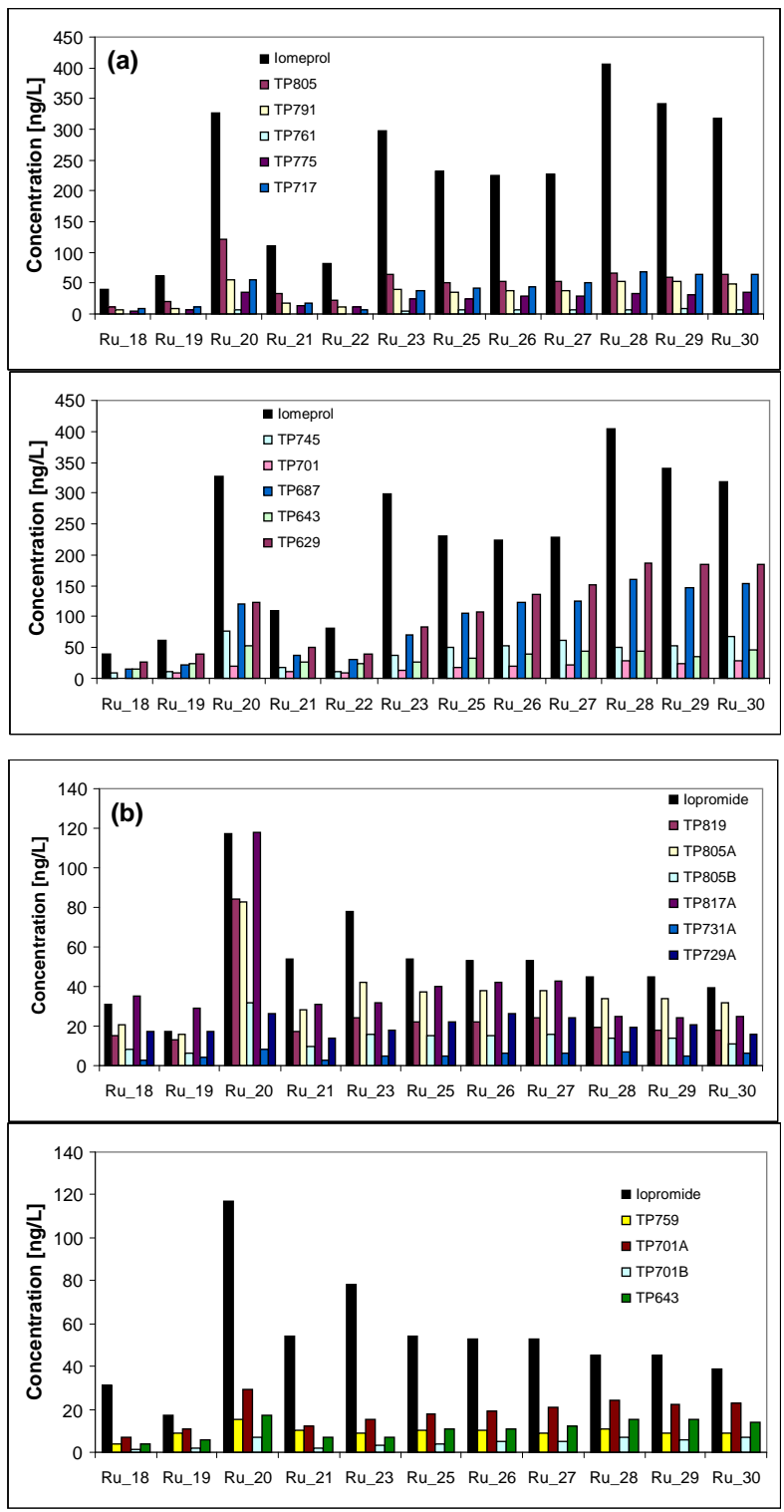
Figure 4.6: Concentrations [ng/L] of iomeprol and TPs (a); and iopromide and TPs (b) along a section of the Ruhr River (sampling points Ru_18 to Ru_30).

In general, higher concentrations were detected for the parent ICM compared to the TPs (Figure 4.3.4), but the ratio between the ICM and different TPs was constant for the lower section of the Ruhr. Figure 4.3.4 illustrates that higher concentrations of iomeprol phase II TPs were detected compared to the iomeprol phase I TPs, however the opposite was observed for iopromide. In either case, the ICM and TP pattern remained relatively constant.

Elevated concentrations of most analytes monitored at sampling location Ru_20 was observed, and indicated that this tributary (the Lenne River) receives either WWTP effluent with higher concentrations of ICM and TPs or there is a higher percentage of WWTP effluent in this tributary. For other tributaries such as the Volume (sampling location Ru_22), minimal contamination of ICM and TPs was observed. The lower concentrations of carbamazepine and diatrizoate detected at sampling location Ru_22 suggested there is a lower percentage of WWTP effluent in this tributary.

4.3.5 Fate of ICM and TPs during different treatment processes

4.3.5.1 Bank filtration and river water infiltration

Four sites were compared according to the composition of ICM TPs before and after surface water infiltration or bank filtration. The results confirmed that i) ICM are further transformed, ii) the pattern of ICM TPs changed significantly, and iii) mineralization is unlikely. The results obtained from most study sites confirmed that certain ICM TPs are formed during surface water infiltration and bank filtration. Iohexol TP657 and TP599; iomeprol TP701 and TP643; iopamidol TP791 and TP773; as well as iopromide TP701A and TP643 were the dominant ICM TPs formed during bank filtration or found in groundwater under the influence of surface water infiltration. Most of these TPs have been proposed to be formed at the end of the transformation

pathways (Schulz *et al.* 2008; Kormos *et al.* 2010). In addition, the concentrations of the parent ICM, including iopamidol, as well as the higher molecular weight TPs found at the beginning of the microbial pathways decreased during bank filtration. Obviously, contact with soil and aquifer material resulted in further transformation until stable TPs are formed where the hydroxylated hydrocarbon side chains were mainly degraded (Schulz *et al*. 2008; Kormos *et al*. 2009).

Figure 4.7 provides an example of the formation of certain iohexol TPs and iopromide TPs during bank filtration and their presence in groundwater influenced by the infiltration of river water at selected sampling sites.
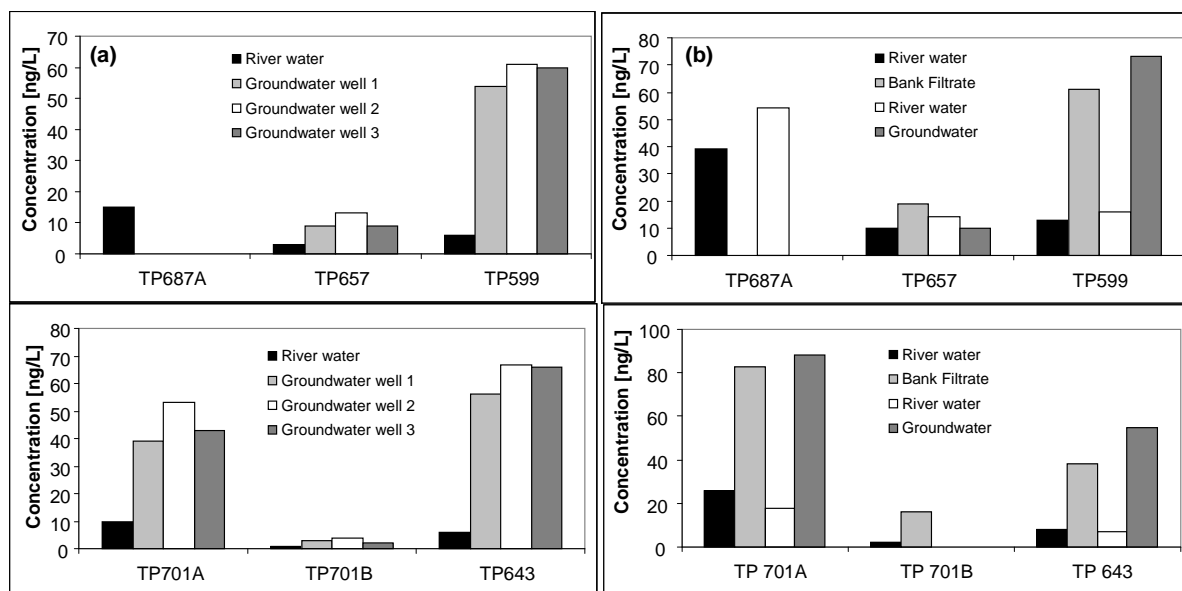
Figure 4.7: Concentrations [ng/L] of iohexol TPs (top graphs) and iopromide TPs (bottom graphs) at sampling location 1 (a) and at sampling locations 3 and 4 (b) showing the formation of TPs during bank filtration and groundwater influenced by surface water infiltration.

4.3.5.2 Granular activated carbon (GAC)

Diatrizoate and iopamidol were the only parent ICM detected in the raw water of DWTP1. No removal by the two GAC filters was observed for diatrizoate, iopamidol TP791 and TP773, iohexol TP657, or iomeprol TP701 and TP643. Similar results were obtained for iopamidol, iopromide TP701A and TP643, as well as iohexol TP599 for GAC filter 1, while the second GAC filter exhibited removal of these compounds. Obviously, GAC filtration is able to partially eliminate ICM and ICM TPs by sorption as long as the filter pre-loading is limited. Previous research has shown that GAC filtration can remove non-ionic ICM. Selected ICM were eliminated up to 85% with a combination of different processes including ozonation and GAC filtration. It was reported that GAC filtration accounted for 50% of the observed removal of the parent non-ionic ICM (Seitz *et al.* 2006). Ternes *et al*. (2002) reported that compared to other DWTP processes, such as sand filtration and flocculation, GAC filtration was a very effective removal techniques for certain pharmaceuticals.

In DWTP 5 the concentrations of the four non-ionic ICM were reduced after GAC filtration, but diatrizoate was not eliminated and some ICM TPs exhibited similar or in a few cases even slightly higher concentrations. Due to the enhanced polarity, the removal of ICM TPs is very limited. However, it cannot be excluded that the removal of the parent ICM was at least partly caused by microbial transformation, since fouling of these filters creates an environment suitable for microbial activities.

With the exception of diatrizoate, the other parent ICM were detected at lower concentrations after GAC filtration at DWTP4. As it was observed in DWTP5, minimal or no removal was observed for some of the ICM TPs. For example, iohexol TP687A and TP599, iomeprol TP643

and iopromide TP731A increased after GAC filtration. In addition, iomeprol TP643 and TP629 as well as iopromide TP701A and TP643 were not removed or showed minimal removal after GAC filtration.

4.3.5.3 Fate of ICM TPs at DWTP5

The four nonionic ICM were removed after a combination of processes; flocculation, sand filtration and GAC filtration (Figure 4.3.6a). Diatrizoate was not removed after GAC filtration, and was detected at concentration of > 50 ng/L (Figure 4.3.6a). A total of 12 ICM TPs were detected in at least one of the samples collected from this DWTP (Figure 4.3.6b). Iomeprol TP745 and TP717, and iopromide TP731A were found in the samples collected in the raw water as well as after GAC filtration. However, the composition of TPs changed when groundwater was mixed with the treated river water. For example, iohexol TP657 and TP599, iomeprol TP643, as well as iopromide TP701A and TP643 were detected at higher concentrations after the treated river water was mixed with groundwater. Most TPs present in the mixture of river water and groundwater are known to be formed at the end of the transformation pathways and have been found in bank filtrates. Hence, groundwater is obviously influenced by infiltration of surface water containing ICM and ICM TPs.
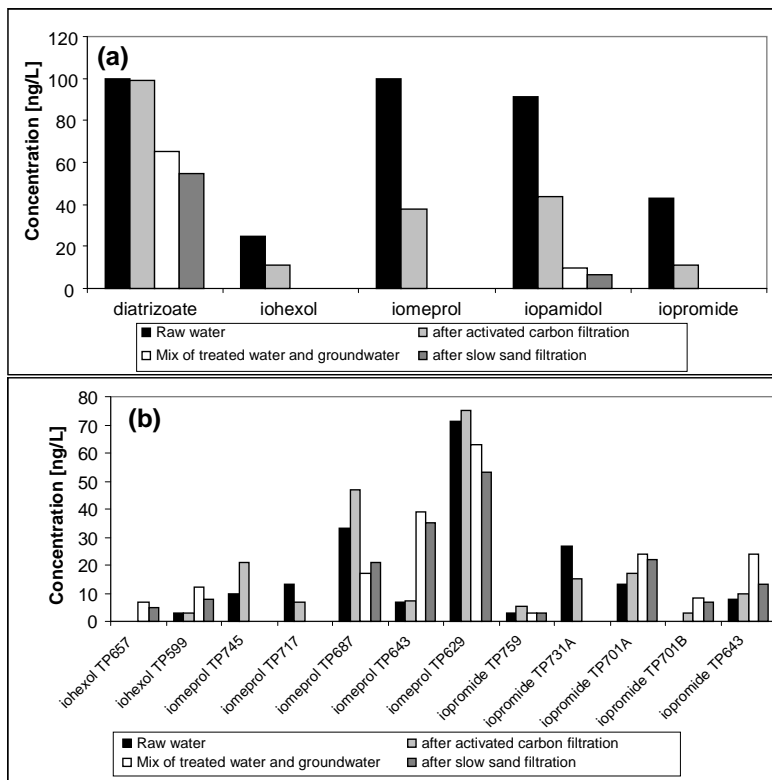
Figure 4.8: Concentrations [ng/L] of the five parent ICM (a); and selected ICM TPs (b) at the four sampling locations at DWTP5

4.3.5.4 UV disinfection

UV disinfection of all four non-ionic ICM showed no significant decrease in concentration. The overall concentrations of the ICM TPs were quite low and therefore transformation of the ICM TPs could not be investigated. Only two ICM TPs (iomeprol P629 and iopamidol TP773) were detected at concentrations above their LOQs.

4.3.6 Occurrence of ICM and TPs in Drinking Water

Diatrizoate, the four nonionic ICM and their TPs were measured and quantified in drinking water at five different waterworks. The concentrations are summarized in Table 4.5a and 4.5b, and in general varied from 1 ng/L to 50 ng/L. However elevated concentrations of up to 500 ng/L

(iomeprol TP687) were detected. DWTP2 was found to have the highest concentrations and number of ICM TPs compared to the other DWTPs.

The concentrations detected for iopamidol in drinking water were higher (>100 ng/L) than for the other nonionic ICM. This confirms the persistence of iopamidol due to its limited biotransformation (Kormos *et al*. 2010).

In general, it was found that the TPs detected with the highest concentrations in drinking water were formed at the end of the proposed microbial transformation pathways. For example, iohexol TP657 and TP599, iomeprol TP687, TP643 and TP629, and iopromide TP701A and TP643 were the dominant ICM TPs present in groundwater and drinking water.

It is unclear whether these ICM TPs have a toxicological impact on human health. However, it cannot be excluded that ICM TPs may react with strong oxidants (i.e. chlorine) during drinking water disinfection. There are some indications that parent ICM react with disinfectants during drinking water production and this could result in the formation of oxidation by-products (Seitz *et al.* 2008) as well as iodinated disinfection by-products (Richardson *et al*. 2008).

Table 4.5a: Concentrations [ng/L] and 95% confidence intervals (n=3) of diatrizoate, iohexol and TPs, and iomeprol and TPs in drinking water collected at four water treatment facilities in Germany (LOQ values are given in brackets)

	Diatrizoate	Iohexol	Iohexol TP657	Iohexol TP599	Iomeprol	Iomeprol TP761*	Iomeprol TP745*	Iomeprol TP701	Iomeprol TP687*	Iomeprol TP643	Iomeprol TP629
DWTP1	130 ± 10	<LOQ (3)	8 ± 1	23 ± 1	<LOQ (3)	<LOQ (1)	<LOQ (3)	7 ± 1	<LOQ (1)	480 ± 40	2 ± 1
DWTP2	91 ± 7	<LOQ (3)	7 ± 1	7 ± 0	11 ± 2	7 ± 4	380 ± 60	120 ± 20	500 ± 60	250 ± 20	400 ± 40
DWTP3	62; 61	8; 8	<LOQ (3)	13; 13	11; 15	<LOQ (3)	<LOQ (1)	4; 5	1; 1	16; 14	1; 2
DWTP5	55 ± 23	<LOQ (1)	13 ± 1	7 ± 2	<LOQ (3)	<LOQ (3)	<LOQ (3)	9.4; 8.1	21 ± 2	35 ± 12	53 ± 12

* no isolated standards available, concentrations are semi-quantified

Table 4.5b: Concentrations [ng/L] and 95% confidence intervals (n=3) of iopromide and TPs, and iopamidol and TPs in drinking water collected at four water treatment facilities in Germany (LOQ values are given in brackets)

	Iopromide	Iopromide TP805A*	Iopromide TP759	Iopromide TP731A*	Iopromide TP729A	Iopromide TP701A	Iopromide TP701B	Iopromide TP643	Iopamidol	Iopamidol TP791	Iopamidol TP773*	Iopamidol TP761
DWTP1	<LOQ (3)	<LOQ (3)	<LOQ (3)	<LOQ (1)	<LOQ (3)	40 ± 11	<LOQ (1)	19 ± 4	20; 15	<LOQ (1)	<LOQ (1)	<LOQ (1)
DWTP2	21 ± 12	18 ± 1	260 ± 11	6 ± 1	12 ± 1	170 ± 4	40 ± 8	40 ± 1	270 ± 30	42 ± 4	30 ± 8	29 ± 9
DWTP3	2; 2	<LOQ (3)	<LOQ (1)	<LOQ (1)	<LOQ (3)	10; 12	<LOQ (1)	9; 9	119; 114	6; 9	1; 1	<LOQ (3)
DWTP5	<LOQ (3)	<LOQ (10)	3 ± 2	<LOQ (10)	<LOQ (10)	22 ± 6	7 ± 2	13 ± 3	7 ± 1	<LOQ (3)	<LOQ (3)	<LOQ (3)

* no isolated standards available, concentrations are semi-quantified

4.4 Acknowledgment

4.5 Supporting Information

4.5.1 Experimental Section

4.5.1.1 Description of Sampling Locations

Sampling of municipal wastewater treatment plants (WWTPs)

Samples were collected from a total of three municipal WWTPs in Germany. Five-day composite samples were collected from one WWTP (WWTP1) at five sampling points along the treatment lane (Figure 1).

Grab effluent samples were collected from an additional three WWTPs (referred to as WWTP2 and WWTP3). WWTP1 is considered a medium-sized facility with approximately 300,000 inhabitant equivalent values. WWTP2 has an average inflow of 38,000 m³/day. This treatment plant consists of an aerated grit chamber, a primary settling tank, two aeration basins, a circular aeration basin and a final settling tank. The plant has an upstream denitrification step and

simultaneous precipitation of phosphate with ferric salt. The solid retention time (SRT) and hydraulic retention time (HRT) are 12 d, and 36 h (during dry weather conditions), respectively.

Effluent samples were also collected from WWTP3 in November 2009. This facility serves 600,000 PE, has a SRT of 20 d and a HRT of 36 h. Preliminary treatment consists of screens, aerated double grit chambers and primary sedimentation tanks. Biological treatment takes place in individual tanks, with eight tanks operated under anaerobic conditions and 14 tanks operating under anoxic and aerobic conditions, which is followed by secondary sedimentation. Biological phosphate elimination is completed in combination with nitrification and denitrification treatment.

Sampling of surface water and groundwater

Sampling location 1. Grab samples were collected from a river, and then three groundwater wells located in close proximately to the river on November 18th, 2009. On February 18th, 2010, grab samples were collected the river as well as groundwater well 3. The river bank and soil surrounding the groundwater wells was found to consist of a crushed rock and gravel mixture. Table S4.5.1 provides some characteristics about the selected three groundwater wells.

Table S4.5.1: Characteristics of the three selected groundwater wells and corresponding water quality parameter values

Groundwater well	Sampling day	Water level depth [m]	Temperature [°C]	Distance from river [m]	Conductivity [µS/cm]	Dissolved oxygen [mg/L]	pH
Groundwater well 1	18.11.2009	9.29	12.1	150	664	4.04	6.71
Groundwater well 2	18.11.2009	8.66	12.0	75	671	3.87	6.94
Groundwater well 3	18.11.2009	8.53	12.1	36	686	3.86	6.63
Groundwater well 3	18.02.2010	8.30	11.6	36	728	5.01	6.48

Sampling location 3 and 4. Groundwater wells described for sampling location 3 were found in an area dominated by mostly gravel from the nearby river. The groundwater level depth was approximately 14 m, and the wells have been reported to be influenced by the river water. For sampling location 4, the area consisted of coarse-grained gravel and sand, and there is an impermeable layer of clay and silt at the bottom (approx. 20 m below the ground). The groundwater in this area is the result of river bank filtration. It has been found that if the Rhine River is high, this river water can enter groundwater area. The content of limestone is high, while iron and manganese is generally low. The groundwater level depth is approximately 9 m.

Table S4.5.2: Optimized Source-Dependent Parameters for Measurement of Iodinated X-ray Contrast Media and ICM TPs using LC Tandem MS in MRM mode

Source Parameter	Iopromide and TPs	Diatrizoate, and Iohexol, Iomeprol, Iopamidol and their TPs
Curtain Gas	10 psi	20 psi
Temperature	600°C	600°C
GS1	70 psi	60 psi
GS2	50 psi	50 psi
CAD (collision gas)	high	medium
IonSpray Voltage	5500 V	5500 V
Entrance Potential	10 V	10 V

Table S4.5.3: MRM Transitions and Optimized Compound-Dependent Parameters for Diatrizoate, Iohexol

and its TPs for LC ESI Tandem MS detection

Analyte	MRM Transitions	Declustering Potential (V)	Collision Energy (eV)	Collision Cell Exit Potential (V)
Diatrizoate	**614.8 → 233.1**	51	63	8
	614.8 → 147.9	91	79	4
Iohexol	**821.9 → 602.9**	111	35	18
	821.9 → 500.7	111	67	30
TP863*	**863.8 → 515.1**	71	57	40
	863.8 → 476.9	71	31	18
TP849*	**849.8 → 514.8**	56	49	26
	849.8 → 616.9	56	67	24
TP835*	**835.9 → 514.8**	66	41	42
	835.9 → 667.1	66	73	28
TP833*	**833.8 → 728.7**	71	29	18
	833.8 → 758.9	71	29	20
TP775*	**775.8 → 531.9**	71	67	20
	775.8 → 426.7	71	35	16
TP745*	**745.7 → 501.9**	61	43	46
	745.7 → 703.9	61	25	20
TP687A	**687.8 → 444.0**	66	49	8
	687.8 → 645.6	66	23	20
TP687B*	**687.8 → 440.7**	71	39	34
	687.8 → 568.7	86	19	34
TP657	**657.9 → 582.6**	71	19	32
	657.8 → 454.8	121	33	24
TP629*	**629.8 → 568.7**	71	15	18
	629.8 → 458.9	86	21	12
TP599	**599.8 → 582.7**	101	17	36
	599.8 → 454.9	76	33	12

*no isolated standards available, concentrations are semi-quantified

Table S4.5.4: MRM Transitions and Optimized Compound-Dependent Parameters for Iomeprol and its TPs for LC ESI Tandem MS detection

Analyte	MRM Transitions	Declustering Potential (V)	Collision Energy (eV)	Collision Cell Exit Potential (V)
Iomeprol	**777.9 → 405.0**	106	39	14
	777.9 → 531.8	71	37	12
TP819*	**819.8 → 775.9**	101	19	18
	819.8 → 670.7	101	23	22
TP805*	**805.8 → 700.9**	116	31	22
	805.8 → 418.9	116	61	6
TP791*	**791.9 → 558.9**	81	29	20
	791.9 → 572.6	81	35	14
TP789*	**789.8 → 670.7**	66	21	22
	789.8 → 640.6	66	23	22
TP775*	**775.9 → 700.7**	81	23	24
	775.8 → 670.7	86	21	24
TP761*	**761.9 → 558.8**	91	31	30
	761.9 → 670.8	91	27	10
TP745*	**745.9 → 515.8**	61	37	14
	745.9 → 670.7	61	21	22
TP731*	**731.8 → 427.9**	66	39	36
	731.8 → 582.7	66	23	16
TP717*	**717.8 → 330.9**	81	69	20
	717.8 → 457.7	81	39	24
TP701	**701.9 → 657.7**	61	15	12
	701.8 → 428.0	61	35	24
TP687*	**687.8 → 612.8**	81	27	18
	687.8 → 331.0	76	61	14
TP657*	**657.8 → 427.9**	121	39	28
TP643	**643.7 → 300.9**	61	51	22
	643.7 → 599.7	61	15	20
TP629	**629.9 → 330.8**	41	53	8
	629.9 → 457.8	41	41	36
TP599*	**599.8 → 427.8**	101	35	30

*no isolated standards available, concentrations are semi-quantified

211

Table S4.5.5: MRM Transitions and Optimized Compound-Dependent Parameters for Iopamidol and its TPs for LC ESI Tandem MS detection

Analyte	MRM Transitions	Declustering Potential (V)	Collision Energy (eV)	Collision Cell Exit Potential (V)
Iopamidol	**777.9 → 558.8**	106	33	18
	777.9 → 387.0	91	55	12
TP805*	**805.8 → 700.9**	116	31	22
	805.8 → 418.9	116	61	6
TP791	**791.9 → 558.9**	81	29	20
	791.9 → 572.6	81	35	14
TP775*	**775.9 → 700.7**	81	23	24
	775.8 → 670.7	86	21	24
TP773*	**773.9 → 559.0**	56	25	16
	773.9 → 686.7	56	17	30
TP761	**761.9 → 558.8**	91	31	30
	761.9 → 670.8	91	27	10
TP745	**745.9 → 670.7**	61	21	22
	745.9 → 515.8	61	37	14
TP717*	**717.8 → 330.9**	81	69	20
	717.8 → 457.7	81	39	24
TP687*	**687.8 → 612.8**	81	27	18
	687.8 → 457.9	76	41	22

*no isolated standards available, concentrations are semi-quantified

Table S4.5.6: MRM Transitions and Optimized Compound-Dependent Parameters for Iopromide

and its TPs for LC ESI Tandem MS detection

Analyte	MRM Transitions	Declustering Potential (V)	Collision Energy (eV)	Collision Cell Exit Potential (V)
Iopromide	**791.9 → 572.7**	101	33	20
	791.9 → 558.7	101	39	18
TP819	**819.8 → 586.6**	101	35	18
	819.8 → 714.3	101	29	24
TP817A*	**817.8 → 700.8**	91	27	24
	817.8 → 712.7	91	27	26
TP805A*	**805.8 → 558.8**	91	39	14
	805.8 → 686.5	91	31	18
TP805B*	**805.8 → 572.7**	101	33	20
	805.9 → 700.9	91	27	24
TP787A*	**787.8 → 670.5**	81	27	22
	787.8 → 712.3	81	25	24
TP759	**759.5 → 670.5**	66	23	18
	759.5 → 684.4	66	23	22
TP731A*	**731.5 → 612.5**	91	27	18
	731.5 → 453.5	91	39	12
TP731B	**731.9 → 626.4**	91	23	22
	731.9 → 467.6	91	41	14
TP729A	**729.5 → 612.5**	76	27	18
	729.5 → 457.5	76	41	30
TP701A	**701.5 → 612.7**	66	25	18
	701.5 → 453.7	66	43	26
TP701B	**701.8 → 626.6**	81	17	14
	701.8 → 467.7	81	37	22
TP643	**643.6 → 516.6**	61	19	16
	643.6 → 612.5	61	21	18

*no isolated standards available, concentrations are semi-quantified

Table S4.5.7: Quantification of the Occurrence of Diatrizoate, Iohexol, Iomeprol and their TPs in Environmental Samples

Analyte	Isolated Standard Available?	Analyte used for Calibration Curve	Surrogate Standard used for Quantification
Diatrizoate	Yes	Diatrizoate	Diatrizoate-d_6
Iohexol	Yes	Iohexol	Iohexol-d_5
TP863*	No	Iohexol	Iohexol-d_5
TP849*	No	Iohexol	Iohexol-d_5
TP835*	No	Iohexol	Iohexol-d_5
TP833*	No	Iohexol	Iohexol-d_5
TP775*	No	Iohexol	Iohexol-d_5
TP745*	No	Iohexol	Iohexol-d_5
TP687A	Yes	Iohexol TP687A	Iohexol-d_5
TP687B*	No	Iohexol TP687A	Iohexol-d_5
TP657	Yes	Iohexol TP657	Iohexol-d_5
TP629*	No	Iomeprol TP629	Iomeprol-d_3
TP599	Yes	Iohexol TP599	Diatrizoate-d_6
Iomeprol	Yes	Iomeprol	Iomeprol-d_3
TP819*	No	Iomeprol	Iomeprol-d_3
TP805*	No	Iopamidol TP791	Iopamidol-d_3
TP791*	No	Iopamidol TP791	Iopamidol-d_3
TP789*	No	Iomeprol TP701	Iopamidol-d_3
TP775*	No	Iopamidol TP791	Iopamidol-d_3
TP761*	No	Iopamidol TP761	Iopamidol-d_3
TP745*	No	Iopamidol TP745	Iopamidol-d_3
TP731*	No	Iomeprol TP701	Iopamidol-d_3
TP717*	No	Iomeprol TP629	Iomeprol-d_3
TP701	Yes	Iomeprol TP701	Iopamidol-d_3
TP687*	No	Iomeprol TP629	Iomeprol-d_3
TP657*	No	Iohexol TP657	Iohexol-d_5
TP643	No	Iomeprol TP643	Iomeprol-d_3
TP629	Yes	Iomeprol TP629	Iomeprol-d_3
TP599*	No	Iohexol TP599	Diatrizoate-d_6

*no isolated standards available, concentrations are semi-quantified

Table S4.5.8: Quantification of the Occurrence of Iopamidol, Iopromide and their TPs in Environmental Samples

Analyte	Isolated Standard Available?	Analyte used for Calibration Curve	Surrogate Standard used for Quantification
Iopamidol	Yes	Iopamidol	Iopamidol-d_3
TP805*	No	Iopamidol TP791	Iopamidol-d_3
TP791	Yes	Iopamidol TP791	Iopamidol-d_3
TP775*	No	Iopamidol TP791	Iopamidol-d_3
TP773*	No	Iopamidol TP791	Iopamidol-d_3
TP761	Yes	Iopamidol TP761	Iopamidol-d_3
TP745	Yes	Iopamidol TP745	Iopamidol-d_3
TP717*	No	Iomeprol TP629	Iomeprol-d_3
TP687*	No	Iomeprol TP629	Iomeprol-d_3
Iopromide	Yes	Iopromide	DMI
TP819	Yes	Iopromide TP819	DMI
TP817A*	No	Iopromide TP819	DMI
TP805A*	No	Iopromide	DMI
TP805B*	No	Iopromide	DMI
TP787A*	No	Iopromide TP759	DMI
TP759	Yes	Iopromide TP759	DMI
TP731A*	No	Iopromide TP701A	DMI
TP731B	Yes	Iopromide TP731A	DMI
TP729A	Yes	Iopromide TP729A	DMI
TP701A	Yes	Iopromide TP701A	DMI
TP701B	Yes	Iopromide TP701B	DMI
TP643	Yes	Iopromide TP643	DMI

*no isolated standards available, concentrations are semi-quantified

4.6 Literature Cited

Batt, A. L.; Kim, S.; Aga, D. Enhanced biodegradation of iopromide and trimethoprim in nitrifying sludge. *Environ. Sci. Technol.* **2006**, *40* (23), 7367-7373.

Carballa, M.; Omil, F.; Lema, J. M.; Llompart, M.; García-Jares, C.; Rodriguez, I.; Gómez, M.; Ternes, T. Behavior of pharmaceuticals, cosmetics and hormones in a sewage treatment plant. *Water Res.* **2004**, *38* (12), 2918-2926.

Clara, M.; Strenn, B.; Gans, O.; Martinez, E.; Kreuzinger, N.; Kroiss, H. Removal of selected pharmaceuticals, fragrances and endocrine disrupting compounds in a membrane bioreactor and conventional wastewater treatment plants. *Water Res.* **2005**, *39* (19), 4797-4807.

Doll, T. E.; Frimmel, F. H. Kinetic study of photocatalytic degradation of carbamazepine, clofibric acid, iomeprol and iopromide assisted by different TiO_2 materials – determination of intermediates and reaction pathways. *Water Res.* **2004,** *38* (4), 955-964.

Hirsch, R.; Ternes, T. A.; Lindart, A.; Haberer, K.; Wilken, R-D. A sensitive method for the determination of iodine containing diagnostic agents in aqueous matrices using LC-electrospray-tandem-MS detection. *Fresenius J Anal Chem.* **2000**, *366* (8), 835-841.

Hummel, D.; Löffler, D.; Fink, G.; Ternes, T. A. Simultaneous determination of psychoactive drugs and their metabolites in aqueous matrices by liquid chromatography mass spectrometry. *Environ. Sci. Technol.* **2006**, *40* (23), 7321-7328.

Joss, A.; Zabczynski, S.; Göbel, A.; Hoffmann, B.; Löffler, D.; McArdell, C. S.; Ternes, T. A.; Thomsen, A.; Siegrist, H. Biological degradation of pharmaceuticals in municipal wastewater treatment: proposing a classification scheme. *Water Res.* **2006**, *40* (8), 1686-1696.

Kalsch, W. Biodegradation of the iodinated X-ray contrast media diatrizoate and iopromide. *Sci. Total Environ.* **1999**, *225* (1-2), 143-153.

Kormos, J. L.; Schulz, M.; Wagner, M.; Ternes, T. A. Multistep approach for the structural identification of biotransformation products of iodinated X-ray contrast media by liquid chromatography/hybrid triple quadrupole linear ion trap mass spectrometry and ^{1}H and ^{13}C nuclear magnetic resonance. *Anal. Chem.* **2009**, *81* (22), 9216-9224.

Kormos, J. L.; Schulz, M.; Kohler, H.-P. E.; Ternes, T. A. Biotransformation of selected iodinates X-ray contrast media and characterization of microbial transformation pathways. *Environ. Sci. Technol.* **2010** *(in press)*

Pérez, S.; Eichhorn, P.; Celiz, M. D.; Aga, D. S. Structural characterization of metabolites of the x-ray contrast agent iopromide in activated sludge using ion trap mass spectrometry. *Anal. Chem.* **2006**, *78* (6), 1866-1874.

Pérez, S.; Barceló, D. Fate and occurrence of X-ray contrast media in the environment. *Anal. Bioanal. Chem.* **2007**, *387* (4), 1235-1246.

Pérez, S.; Eichhorn, P.; Ceballos, V.; Barceló, D. Elucidation of phototransformation reactions of the X-ray contrast medium iopromide under simulated solar radiation using UPLC-ESI-QqTOF-MS. *J. Mass Spectrom.* **2009**, *44* (9), 1308-1317.

Prasse, C.; Schlüsener, M. P.; Schulz, R.; Ternes, T. A. Antiviral drugs in wastewater and surface waters: A new pharmaceutical class of environmental relevance? *Environ. Sci. Technol.* **2010**, *44* (5), 1728-1735.

Putschew, A.; Wischnack, S.; Jekel, M. Occurrence of triiodinated X-ray contrast agents in the aquatic environment. *Sci. Total Environ.* **2000**, *255* (1), 129-134.

Richardson, S. D.; Fasano, F.; Ellington, J. J.; Crumley, F. G.; Buettner, K. M.; Evans, J. J.; Blount, B. C.; Silva, L. K.; Waite, T. J.; Luther, G. W.; McKague, A. B.; Miltner, R. J.; Wagner, E. D.; Plewa, M. J. Occurrence and mammalian cell toxicity of iodinated disinfection byproducts in drinking water. *Environ. Sci. Technol.* **2008**, *42* (22), 8330-8338.

Rode, U.; Müller, R. Transformation of the ionic X-ray contrast agent diatrizoate and related triiodinated benzoates by *Trametes versicolor*. *Appl. Environ. Microbiol.* **1998**, *64* (8), 3114-3117.

Schittko, S.; Putschew, A.; Jekel, M. Bank filtration: a suitable process for the removal of iodinated X-ray contrast media? *Water Sci. Technol.* **2004**, *50* (5), 261-268.

Schulz, M.; Löffler, D.; Wagner, M.; Ternes, T. A. Transformation of the X-ray contrast medium iopromide in soil and biological wastewater treatment. *Environ. Sci. Technol.* **2008**, *42* (19), 7207-7217.

Seitz, W.; Jiang, J.-Q.; Weber, W. H.; Lloyd B. J.; Maier, M.; Maier, D. Removal of iodinated X-ray contrast media during drinking water treatment. *Environ. Chem.* **2006**, *3* (1), 35-39.

Seitz, W.; Jiang, J.-Q.; Schulz, W.; Weber, W. H.; Maier, D.; Maier, M. Formation of oxidation by-products of the iodinated X-ray contrast medium iomeprol during ozonation. *Chemosphere.* **2008**, *70* (7), 1238-1246.

Steger-Hartmann, T.; Länge, R.; Schweinfurth, H.; Tschampel, M., Rehmann, I. Investigations into the environmental fate and effects of iopromide (ultravist), a widely used iodinated X-ray contrast medium. *Water Res.* **2002**, *36* (1), 266-274.

Ternes, T. A. Occurrence of drugs in German sewage treatment plants and rivers. *Water Res.* **1998**, *32* (11), 3245-3260.

Ternes, T. A.; Hirsch, R. Occurrence and behavior of X-ray contrast media in sewage facilities and the aquatic environment. *Environ. Sci. Technol.* **2000**, *34* (13), 2741-2748.

Ternes, T. A.; Meisenheimer, M.; McDowell, D.; Sacher, F.; Brauch, H.-J.; Haist-Gulde, B.; Preuss, G.; Wilme, U.; Zulei-Seibert, N. Removal of pharmaceuticals during drinking water treatment. *Environ. Sci. Technol.* **2002**, *36* (17), 3855-3863.

Ternes, T. A.; Bonerz, M.; Hermann, N.; Teiser, B.; Andersen, H. R. Irrigation of treated wastewater in Braunschweig, Germany: An option to remove pharmaceuticals and musk fragrances. *Chemosphere*. **2007**, *66* (5), 894-904.

Zwiener, C.; Glauner, T.; Sturm, J.; Wörner, M.; Frimmel, F. H. Electrochemical reduction of the iodinated contrast medium iomeprol: iodine mass balance and identification of transformation products. *Anal. Bioanal. Chem.* **2009**, *395* (6), 1885-1892.

5 Conclusions

5.1 Conclusions

This thesis focused on the environmental fate of a group of emerging contaminants, iodinated X-ray contrast media (ICM). In particular, the microbial transformation of selected ICM, diatrizoate, iohexol, iomeprol, and iopamidol, under aerobic conditions.

Diatrizoate, an ionic ICM, was not biotransformed in the aerobic batch systems. This result correlates well with the high concentrations detected in different environmental matrices, and its use as an indicator of wastewater contamination. The three selected non-ionic ICM, iohexol, iomeprol and iopamidol, were biotransformed to several TPs, however did not undergo mineralization. The ICM TPs were formed and detected in different aerobic soil-water and sediment-water batch systems.

In total, 34 previously unknown TPs of three ICM were structurally elucidated. For iohexol and iomeprol, 11 and 15 TPs were identified, and 8 TPs were found for iopamidol. The structural identification of ICM TPs involved the application of a number of analytical techniques. Although, LC tandem MS was shown to be an accurate method for structural identification of TPs, NMR was required for structural confirmation. In addition, an optimized semi-preparative HPLC-UV method was needed for isolation of the TPs formed in the batch systems.

The development of a LC tandem MS method in multiple reaction monitoring (MRM) mode for two optimized mass transitions resulted in the determination of the TPs in the samples collected from the aerobic batch systems. Iohexol and iomeprol were biotransformation at a faster rate compared to iopamidol. One explanation is that the branched hydroxylated side chains of

iopamidol increase the steric hindrance, and therefore restrict enzymes from cleaving the side chains.

Zero-order reactions were used to explain the biotransformation of all three non-ionic ICM. Lag phases were observed for the non-ionic ICM in all batch systems except for the low organic carbon soil system (Braunschweig soil-water system) conducted at room temperature. The lack of a lag phase in this system suggests that the microbes have adapted to the presence of ICM, since this soil had been irrigated with WWTP effluent containing ICM for many years.

In most cases, the mass balance in the aerobic systems was between 80 to 120% suggesting that the most relevant TPs were identified. The formation of iomeprol TPs and iohexol TPs took place in two phases, while no distinct phases were observed during the formation of iopamidol TPs.

Microbial transformation pathways of the three non-ionic ICM were proposed based on the chemical structures as well as the sequence of TP formation in the batch systems. Since the same TPs were detected in all batch systems, it was assumed that common biochemical reactions are involved in ICM biotransformation. However, the biotransformation rate was affected by the composition of the soil and sediment.

The biotransformation of the three non-ionic ICM could be explained by a single reaction or a combination of three reaction types. Oxidation of the primary or secondary alcohol groups, decarboxylation and cleavage of the N-C bond were the dominant reactions proposed. The first TPs to be formed in the batch systems could be explained by oxidation of the primary alcohol moieties, while the TPs formed at the end of the proposed microbial pathways resulted from decarboxylations and cleavage of the N-C bonds. A number of enzymes were proposed for the

observed biochemical reactions, including alcohol and aldehyde dehydrogenases for the oxidation of the primary alcoholic groups, and thiamine pyrophosphate (TPP) dependent enzymes for the decarboxylation reactions. The cleavage of the N-C bond, which included deacetylation and removal of hydroxylated propanoic acid, could be explained by various enzymes including monooxygenases and α-keto acid-dependent enzymes.

Although, these ICM TPs were detected and well characterized in laboratory aerobic batch systems, the environmental relevance of ICM biotransformation remained unclear. A LC tandem MS method was developed for the parent ICM and 46 TPs, including 12 iopromide TPs, to determine the occurrence and fate of these compounds in different environmental matrices.

Results from the occurrence study showed that iohexol, iomeprol and iopromide are effectively biotransformed during biological treatment in WWTPs, especially WWTPs with a sludge retention time of > 12 d. A number of ICM TPs were detected in the WWTP effluents, with concentrations up to a few µg/L for some TPs. Iopamidol was not eliminated during wastewater treatment, and correlates well with the slow biotransformation observed in the aerobic batch systems. High concentrations of the parent ICM and some TPs were also detected in the Ruhr Watershed, with concentrations up to the µg/L range. The increase in concentrations of ICM and TPs were correlated to the percentage of treated wastewater.

Elevated concentrations of TPs formed at the end of the proposed microbial pathways were detected in bank filtrate samples and groundwater influenced by surface water. This suggests even though the parent ICM can be removed by soil passage, the formation of ICM TPs takes place. Certain TPs, such as iohexol TP599, iomeprol TP643 and iopromide TP701A, which are formed during soil passage, were also not effectively removed in DWTPs using GAC filtration,

ozonation, sand filtration and flocculation treatment. The presence of TPs in finished drinking water also illustrates the stability of certain TPs and raises concerns about the impact these TPs have on human health.

The presented research on the biotransformation of ICM is an example of how important it is to investigate the formation of TPs (or oxidation products) during abiotic and biotic processes. When completing an environmental risk assessment for a chemical or product, a comprehensive evaluation of the environmental fate (i.e. sorption and biotransformation) is necessary to obtain a better and more complete understanding of the impact the parent compound and TPs have on ecological and human health.

5.2 Future Research Initiatives

The work presented in this thesis provides a better understanding about the biotransformation of ICM in aerobic batch systems as well as under real environmental conditions. However, there are still many unanswered questions. Below is a list of future research initiatives to consider in understanding the environmental fate of ICM and potential impact on aquatic and human health.

1. Investigate the presence and removal of ICM TPs before and after different wastewater and drinking water treatment processes in full-scale facilities. This would expand the information already present in Chapter 4. In particular to predict and estimate which treatment processes can effectively remove ICM TPs and therefore decrease exposure to aquatic organisms and humans.

2. Continue with the fractionation and isolation of the identified ICM TPs, so high quantities can be used to prepare standard solutions for quantitative analysis by LC tandem MS. These isolated standards can also be used for determining the toxicity of

ICM TPs in acute and chronic ecotoxicity tests. This would lead to answers about the impact the ICM TPs have on aquatic ecosystems.

In particular, focus should be placed on obtaining high amounts of the TPs formed at the end of the microbial transformation pathways. These stable ICM TPs were found at high concentrations in the environment.

3. Correlate hydrogeological parameters to presence and removal of ICM and TPs. For example, the comparison between soil composition and removal efficiency of certain ICM TPs. This also would explore the limitations and impacts of using bank filtered water for drinking water production, when contaminants, such as ICM TPs are present.

4. The enzymes and biochemical reactions involved in the transformation of ICM needs to be further discussed. Experiments should be conducted to investigate if certain enzymes are capable of transforming ICM under various conditions. This information would be helpful to WWTPs for enhancing microbial activity in activated sludge systems for better removal.

5. Research is currently being conducted to investigate the reaction of certain ICM with strong disinfection oxidants commonly applied in DWTPs. The purpose is to investigate whether ICM can lead to the formation of very toxic iodinated disinfection by-products. It is important that this area of research also focuses on the reaction of disinfectants have to stable ICM TPs which are commonly identified in DWTPs.

Curriculum Vitae

Name	Jennifer Lynne Kormos
Birth Date	November 13th 1979
Place of Birth	St. John's, Canada
Nationality	Canadian
Address	Schützenstr. 10, 56068 Koblenz

Education

Sept. 1983 – June 1992	Primary School, Bayview Heights Public School, Pickering, Canada
Sept. 1992 – June 1998	Ontario Secondary School Diploma, Pine Ridge Secondary School, Pickering, Canada
Sept. 1998 – Dec. 2002	Bachelor of Science in Biomedical Toxicology, University of Guelph, Guelph, Canada
Sept. 2004 – Mar. 2007	Master of Science in Biology, University of Waterloo, Waterloo, Canada
	Title of Thesis: Occurrence and Seasonal Variability of Selected Pharmaceuticals in Southern Ontario Drinking Water Supplies
May 2007 – present	Doctorate of Philosophy (PhD), University of Koblenz-Landau and Federal Institute of Hydrology, Koblenz, Germany
	Title of Thesis: Investigating the Environmental Fate of Iodinated X-ray Contrast Media in the Urban Water Cycle: Identification, Characterization and Occurrence of Biotransformation Products
	Funding was provided by the Marie Curie Research Training Network KEYBIOEFFECTS (MRTN-CT-2006-035695)